UNCLASSIFIED

NYO-4696(Del.)

Subject Category: BIOLOGY

UNITED STATES ATOMIC ENERGY COMMISSION

RADIOACTIVE FALLOUT IN NORTH AMERICA FROM OPERATION TEAPOT

By
Robert J. List

February 1956

Weather Bureau
Washington, D. C.

Technical Information Service Extension, Oak Ridge, Tenn.

UNCLASSIFIED

Date Declassified: April 10, 1956.

Printed in USA, Price 65 cents. Available from the Office of Technical Services, Department of Commerce, Washington 25, D. C.

AEC, Oak Ridge, Tenn.

NYO-4696(Del.)

RADIOACTIVE FALLOUT IN NORTH AMERICA FROM OPERATION TEAPOT

by

Robert J. List

U. S. Department of Commerce
Weather Bureau
Washington, D. C.

February 1956

CONTENTS

ACKNOWLEDGEMENTS

The work reported here was under the supervision of Dr. Lester Machta, Chief of the Special Projects Section, Scientific Services Division, U. S. Weather Bureau. Radiological measurements were made by the Health and Safety Laboratory of the U. S. Atomic Energy Commission's New York Operations Office, Merril Eisenbud, Manager. Mr. Daniel E. Lynch of that office coordinated the efforts of the Weather Bureau and the Atomic Energy Commission. Arrangements for special observations at Argonne National Laboratory were made through Mr. Harry Moses of the Radiological Physics Division.

Many helpful suggestions were received from the author's colleagues in the Special Projects Section. The laborious computations, the meticulous plotting of data, the preparation of finished drawings, and the typing of the manuscript were done by the staff of the Special Projects Section.

ABSTRACT

Operation Teapot, in the spring of 1955, consisted of 14 atomic detonations at the Nevada Test Site. Meteorological trajectories were computed for the resulting radioactive debris and related to the fallout observed by the gummed film network of 87 stations in the continental United States, twelve stations in Canada, and six stations elsewhere in North America. Maps showing daily fallout data for the period February 18 - May 20, 1955 are appended.

A series of special gummed film observations near Chicago indicated that on dry days with significant fallout, film exposed in vertical and inverted positions averaged about 40 percent of the activity on a regular horizontal film. On days with precipitation, the values were 4 percent on vertical films and 1 percent on the inverted films.

A radioautograph of individual raindrops during a period when rainout was occurring indicated about three drops in a hundred were radioactive. The radioactive drops contained both particulate and dissolved radioactivity.

CHAPTER 1

INTRODUCTION

1.1 THE ATOMIC CLOUD

The tremendous heat resulting from the detonation of a nuclear device in the atmosphere produces a bouyant bubble of intensely hot gases which serves not only to carry aloft the debris resulting from the fissions and the disintegration of the bomb casing and auxiliary equipment, but also to suck up great amounts of soil and dust, much of which is rendered radioactive. As the bouyant gases rise, they cool by radiation, by adiabatic expansion, and by entrainment of the surrounding air. The resulting atomic cloud apparently consists of an ascending toroidal ring with debris, dirt, and water droplets circulating about this ring, upward in the center and downward at the outer edges. For most tower or relatively low air bursts, the surface material, as a result of the effects of thermal radiation and blast, rises as a column of dust, pulled up by the central updraft. The ascending mass of air and debris continues to rise until it has cooled to equilibrium with its environment and lost its upward velocity, usually within six to eight minutes.

Typically, just after the ascending motion has ceased, the cloud of radioactive debris consists of a long, slender "stem", capped by a broader "mushroom" top. Often, especially in the case of low air bursts, the stem and top are not joined.

Although considerable debris is contained in the stem, the bulk of the radioactive material is in the mushroom cap. The subsequent history of the debris depends on many factors, including the size distribution and fall velocity of the particles, the nature of the wind field, the eddy diffusivity, and the scavenging of particles by precipitation.

1.2 FALLOUT

The problem of fallout of radioactive particles resulting from atomic explosions divides itself into two major categories:

(1) fallout in the vicinity of the burst site ("close-in" fallout), which must be subject to rigid controls because of the possibility of health hazards, and (2) distant fallout, that which occurs beyond about 200 miles. This report is concerned with the latter category only.

The term "fallout" refers to the deposition, on or near the surface of the earth, of radioactive particles resulting from the detonation of a nuclear device. It includes deposition due to the direct gravitational fall, to deposition resulting from vertical currents and eddies in the atmosphere, and to particles scavenged from the atmosphere and deposited by falling precipitation. The latter phenomenon is at times referred to as "rainout."

1.3 CLOUD MOVEMENT

The movement of the atomic cloud is governed by the wind field. At any given level, the trajectory of the primary cloud, i.e., that portion of the initial cloud which moves approximately horizontally with the winds and is unaffected by diffusion or fallout, can be completed by conventional meteorological techniques. The determination of the movement of all the debris is a much more complex problem.

It is, of course, apparent that all of the particles will fall; the larger particles will reach the ground soon after the burst while the smallest may remain airborne almost indefinitely. Knowledge of the size distribution and fall velocity of the particles is so incomplete that only qualitative estimates can be used in studying fallout.

Similarly, the phenomenon of atmospheric diffusion is difficult to handle quantitatively. It is evident that the ever-present turbulent eddies of the atmosphere will diffuse debris both horizontally and vertically at a rate many orders of magnitude greater than ordinary molecular diffusion. The extent of the diffusion depends not only on the characteristics of the eddies, but also on the time and space scale under consideration. As the cloud grows, larger and larger eddies become diffusing elements, so that the rate of growth increases.

Horizontal and vertical wind shears coupled with fallout and diffusion can result in a very rapid spreading of the cloud in many instances. In other cases, where mixing is inhibited by stable stratification or little wind shear exists, relatively concentrated patches of debris can be carried for long distances in the upper troposphere.

1.4 METEOROLOGICAL TRAJECTORIES

The movement and distortion of the primary cloud is computed from routine meteorological reports. In the United States and Canada, more than 150 stations report the direction and speed of the winds aloft every six hours. About half of these stations are equipped with electronic devices enabling soundings to be made at six- or twelve-hour intervals to very high altitudes even in the presence of clouds and also to measure the pressure, temperature, and relative humidity aloft. The results of these observations are normally entered on maps representing standard constant pressure surfaces, which for practical purposes may be considered as surfaces of constant height. The standard meteorological map surfaces and the corresponding approximate heights above sea level are shown in Table 1.1.

TABLE 1.1 - Standard Meteorological Map Surfaces

Pressure	Height (MSL)
850 millibars	5,000 feet
700 millibars	10,000 feet
500 millibars	18,000 feet
*400 millibars	24,000 feet
300 millibars	30,000 feet
200 millibars	40,000 feet
150 millibars	45,000 feet

* Not routinely drawn by National Weather Analysis Center

Meteorological trajectories were prepared from the routine maps of the National Weather Analysis Center (supplemented by additional wind reports from the vicinity of the test site) for each of the standard map surfaces (except 850 millibars) near

which visible debris was observed at the Test Site. If the top of the cloud was not near one of the standard levels, additional series of maps were prepared and trajectories computed.

Since the 850-millibar level is near to, or even below, the surface of the earth in the vicinity of the Nevada Test Site and flow patterns within a few thousand feet of the ground are affected by local terrain, no trajectories were computed at this level.

All trajectories were computed by assuming that the flow patterns on a given map were representative of the flow for a six-hour period centered at map time. As far as possible, actual wind observations were used to determine the flow patterns. On occasion, due to the paucity of wind observations, it became necessary to use the geostropic wind, which is based on the relation of the pressure pattern to the wind field. In some instances when two equally probable paths appeared to exist, the trajectories are shown as branching.

Meteorological trajectories are, of course, subject to error, particularly over regions of sparse data or in areas of rapidly changing or complex flow patterns. In general, over the United States for trajectories of the order of a thousand miles, it has been found that the errors average ten to twenty percent of the length of the trajectory.

CHAPTER 2

FALLOUT MONITORING

2.1 GUMMED FILM NETWORK

The problem of measuring fallout on a continental scale involves an extensive network of monitoring stations (Fig. 2.1). This in turn means that a simple and inexpensive monitoring system must be employed which requires no elaborate equipment or highly trained observers and involves a minimum of time. These considerations led to the adoption of the gummed film technique. This consists of exposing a one-foot square of gummed cellulose-acetate film on a horizontal stand. Duplicate films were exposed at most stations on stands about six feet apart. The film is exposed for a 24-hour period and then mailed, together with a data card, to the Health and Safety Laboratory of the Atomic Energy Commission's New York Operations Office. Here the film is reduced to ash and counted for beta activity by automatic counting equipment. The delay between collection and counting was about three weeks, on the average, for the Teapot Series.

Although a gummed film network is not the ideal monitoring system, it does provide useful information. Major objections to the gummed film concern its efficacy during rain and snow, its representativeness as an indicator of deposition on natural surfaces, and the possibility that it tends to concentrate activity in dusty regions due to redeposition of fallout which has already reached the ground. For the Teapot Series, eighteen northern stations were equipped with heated stands to melt the snow on the gummed film.

From the gummed film results, it is apparent that for debris more than a day or two old, the principal deposition occurs in precipitation areas. Since tests are not conducted when precipitation is expected to occur along the path of fresh debris, high activity in the general area of the test site is confined to dry fallout. Although precipitation is an effective scavenger of debris, the efficiency of the gummed film for collection of this debris is unknown. Results from previous tests have indicated that on the average, with the exception of fresh debris, about

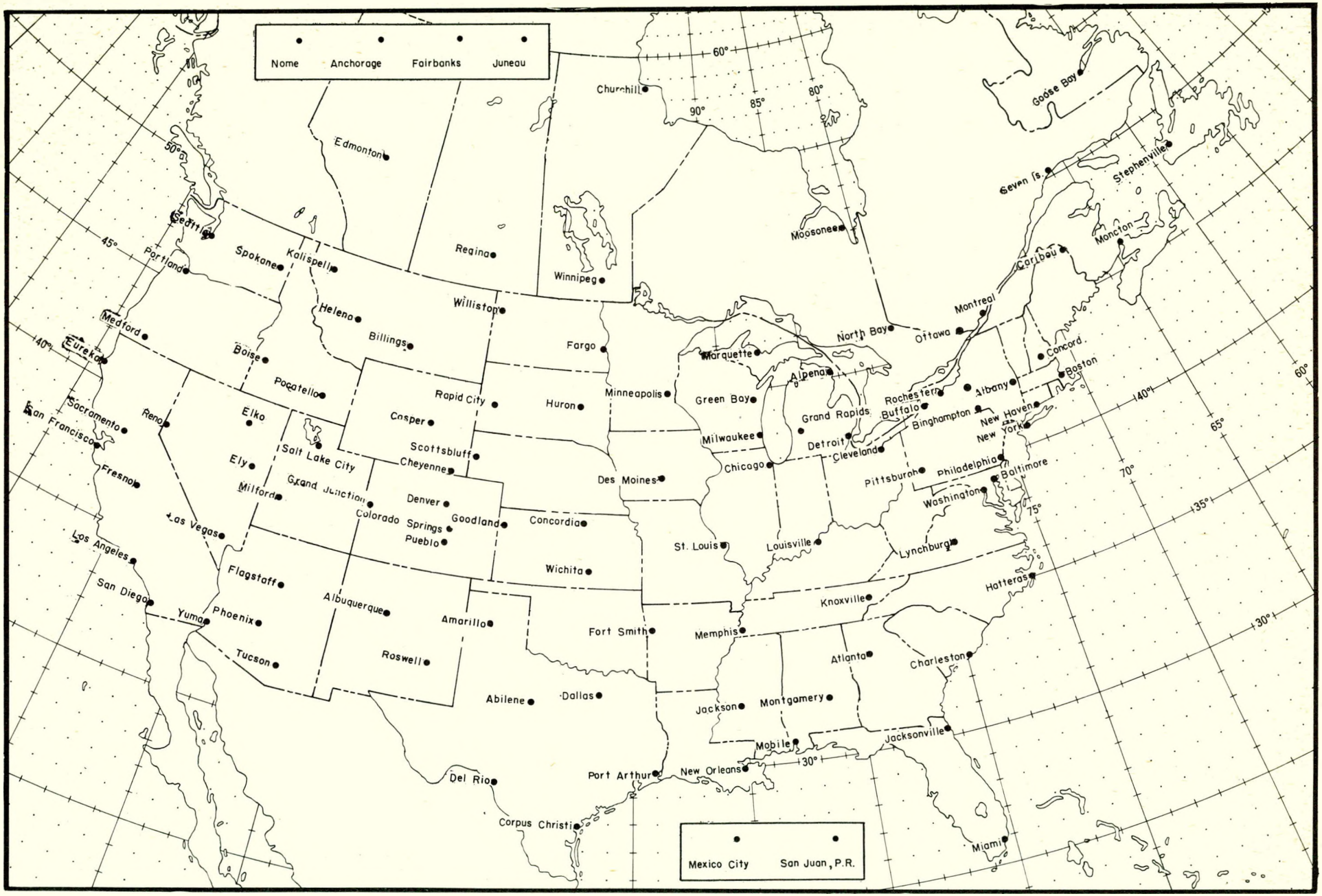

Figure 2.1 Fallout Monitoring Stations in North America

an order of magnitude more activity is found on film exposed during precipitation as is found on dry days. Although in heavy rains an appreciable fraction of the activity must run off the film with the excess water, the evidence shows that, in general, the heavier the rainfall, the more the collection. Figure 2.2 shows the average daily activity on the gummed film for the period February 18 - May 20, 1955 as a function of precipitation intensity for all stations in the United States except those between the Western Rockies and 104° W to eliminate the fair-weather bias in the vicinity of the Test Site.

Machta[1] has summarized the existing evidence concerning the characteristics of the gummed film and the Armour Research Foundation is currently engaged in a laboratory and field investigation of its properties.

2.2 UNITS OF RADIOACTIVITY

The radiological data reported here is β-activity expressed in units of millicuries per 100 square miles extrapolated to January 1, 1956. (This is a departure from previous reports on the New York Operations Office monitoring in the United States following earlier Nevada tests, where activity was extrapolated to sampling day.) Radioactivity was corrected to January 1, 1956 by means of the Way-Wigner decay law:

$$A_t = A_o\, t^{-1.2}$$

where A_t is the activity at time t and A_o is the activity at unit time. All extrapolations were made by assuming that fallout was from the most recent burst. The use of the January 1, 1956 date for extrapolation not only makes computation of accumulated activity simpler, but also tends to minimize errors introduced by assigning debris to the wrong burst. Since the bursts were about a week apart, on the average, and counting was done about three weeks after collection, the error arising from the arbitrary burst assignment scheme was at most about 35 percent and would be applicable to only a few samples with relatively low activities, since high activity is invariably from the most recent burst.

2.3 FALLOUT MAPS

Maps showing the daily fallout data for all stations in North America from February 18 to May 20, 1955 are given in Appendix A. Each map shows the fallout data for the 24-hour period beginning

---

1. Machta, Lester, U. S. Weather Bureau, (To be published).

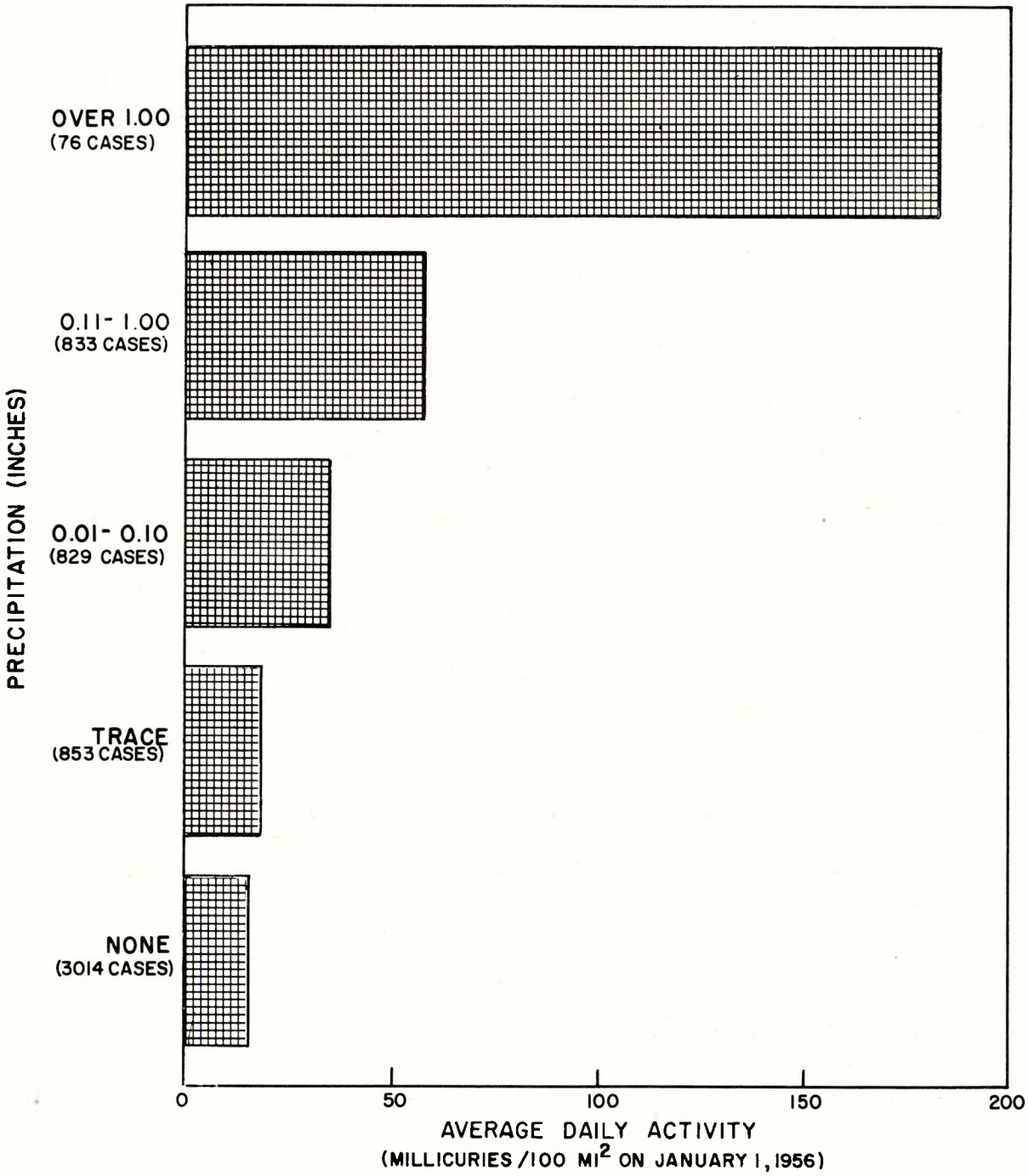

Fig. 2.2 Average Daily Activity as a Function of Precipitation Amount

at 1230 GCT (0730 EST). All references to fallout on specific dates refer to this 24-hour period beginning on the date indicated.

The figures give the activity in millicuries per 100 square miles on January 1, 1956 and the letters indicate the precipitation amounts during the period in the code given on each map. Areas with more than a trace of precipitation are shaded. The solid lines outline areas with more than 200 millicuries per 100 square miles on the most active paper at each station in the area. The dashed lines similarly outline areas of more than 20 millicuries per 100 square miles.

CHAPTER 3

FALLOUT FOLLOWING OPERATION TEAPOT

3.1 OPERATION TEAPOT

Operation Teapot consisted of 14 nuclear tests at the Nevada Test Site during the spring of 1955. The bursts are listed in Table 3.1.

- TABLE 3.1 - Summary of Bursts in Operation Teapot

Burst Number	Date (1955)	Time (GCT)	Type of Burst	Height of Top of Cloud (feet, MSL)
1	18 February	2000	Low Air	20,000
2	22 February	1345	Tower	24,500
3	1 March	1330	Tower	30,000
4	7 March	1320	Tower	45,000
5	12 March	1320	Tower	37,000
6	22 March	1305	Tower	39,500
7	23 March	2030	Underground	12,000
8	29 March	1255	Tower	32,000
9	29 March	1800	Low Air	31,500
10	6 April	1800	High Air	55,000
11	9 April	1230	Tower	15,500
12	15 April	1915	Tower	41,500
13	5 May	1210	Tower	43,000
14	15 May	1200	Tower	36,000

3.2 FALLOUT FROM INDIVIDUAL BURSTS

3.2.1 Burst 1, February 18

Although the cloud resulting from this burst extended to 20,000 feet, virtually no fallout was observed with the meteorological trajectories at the 10,000- and 18,000-foot levels (Fig. 3.1) despite the fact that the cloud at times appeared to be associated with a precipitation area. However, since the trajectories were caught in an intense cyclonic circulation, there is considerable doubt as to their true path. The only appreciable fallout in the United States from this burst occurred to the south of the test site on the day of the burst, undoubtedly a result of the low-level air flow which showed strong northerly winds from the surface to about 8,000 feet, MSL.

3.2.2 Burst 2, February 22

Since almost no visible debris was reported below 15,000 feet in the cloud resulting from this burst, only 18,000- and 24,000-foot trajectories are shown (Fig. 3.2). These moved rapidly eastward and the fallout, which was very light, occurred to the east.

3.2.3 Burst 3, March 1

As in the # 2 burst, virtually no visible debris was reported below about 17,000 feet and the initial cloud top was estimated at about 27,000 feet. Subsequent re-evaluation of the cloud-top data raised this figure to 30,000 feet. At all these levels, rapid west-east flow prevailed, the 18,000-, 24,000- and 30,000-foot trajectories are shown (Fig. 3.3). A small but relatively intense area of dry fallout occurred in the plains states on March 2; but as the cloud continued eastward, most of the fallout occurred in rain. Southerly surface winds carried the debris north of the primary cloud trajectories in the eastern half of the country.

3.2.4 Burst 4, March 7

This test resulted in the deposition of considerable dry fallout in a relatively narrow band in the United States on the 8th and 9th of March. A comparison with the trajectories (Fig. 3.4) indicates that this fallout was associated with the debris which moved at lower levels, 18,000 feet and below, and evidence of surface deposition from the fast moving cloud at 30,000 to 40,000 feet is lacking because of the absence of precipitation in these areas. Although the winds below 10,000 feet may have

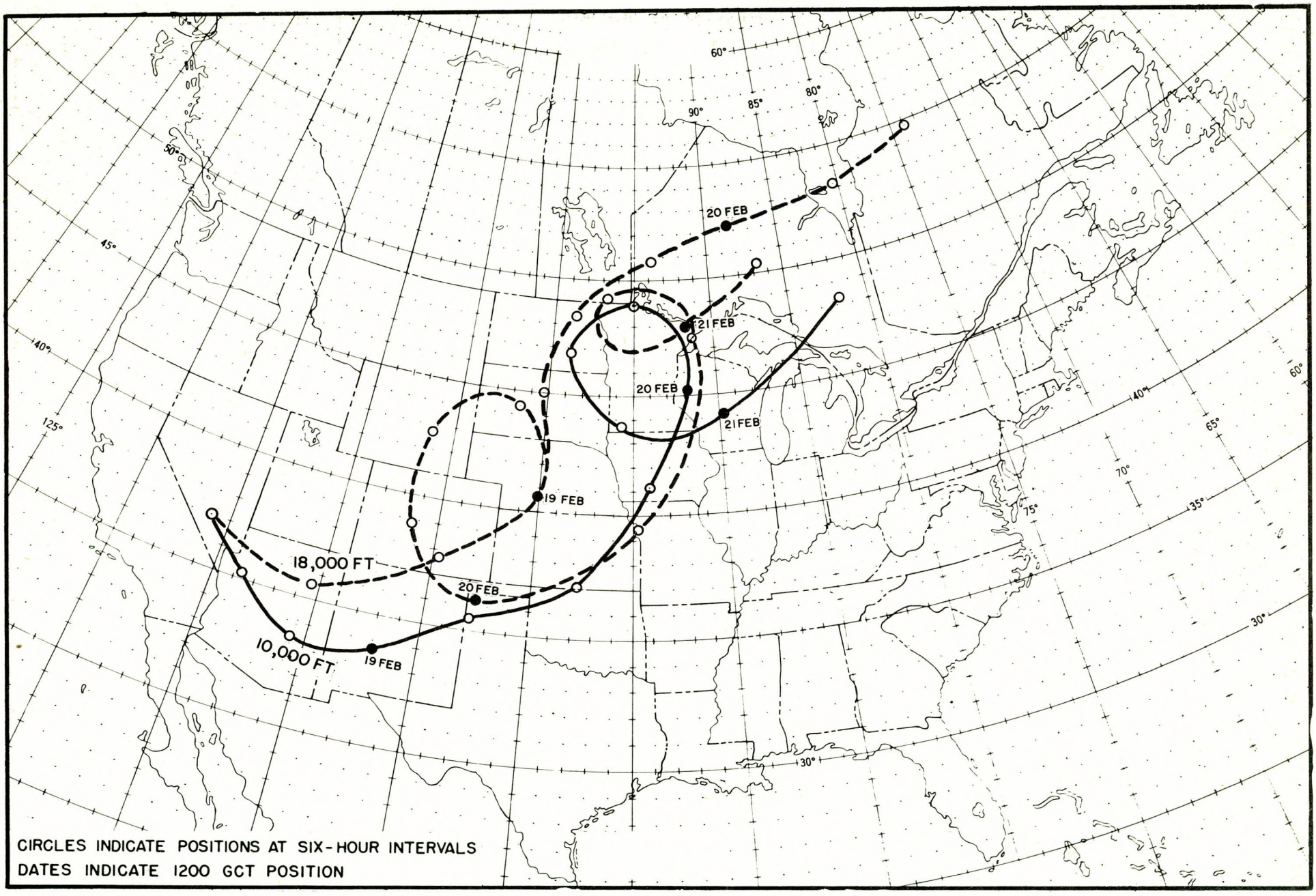

Figure 3.1 Meteorological trajectories for burst No. 1

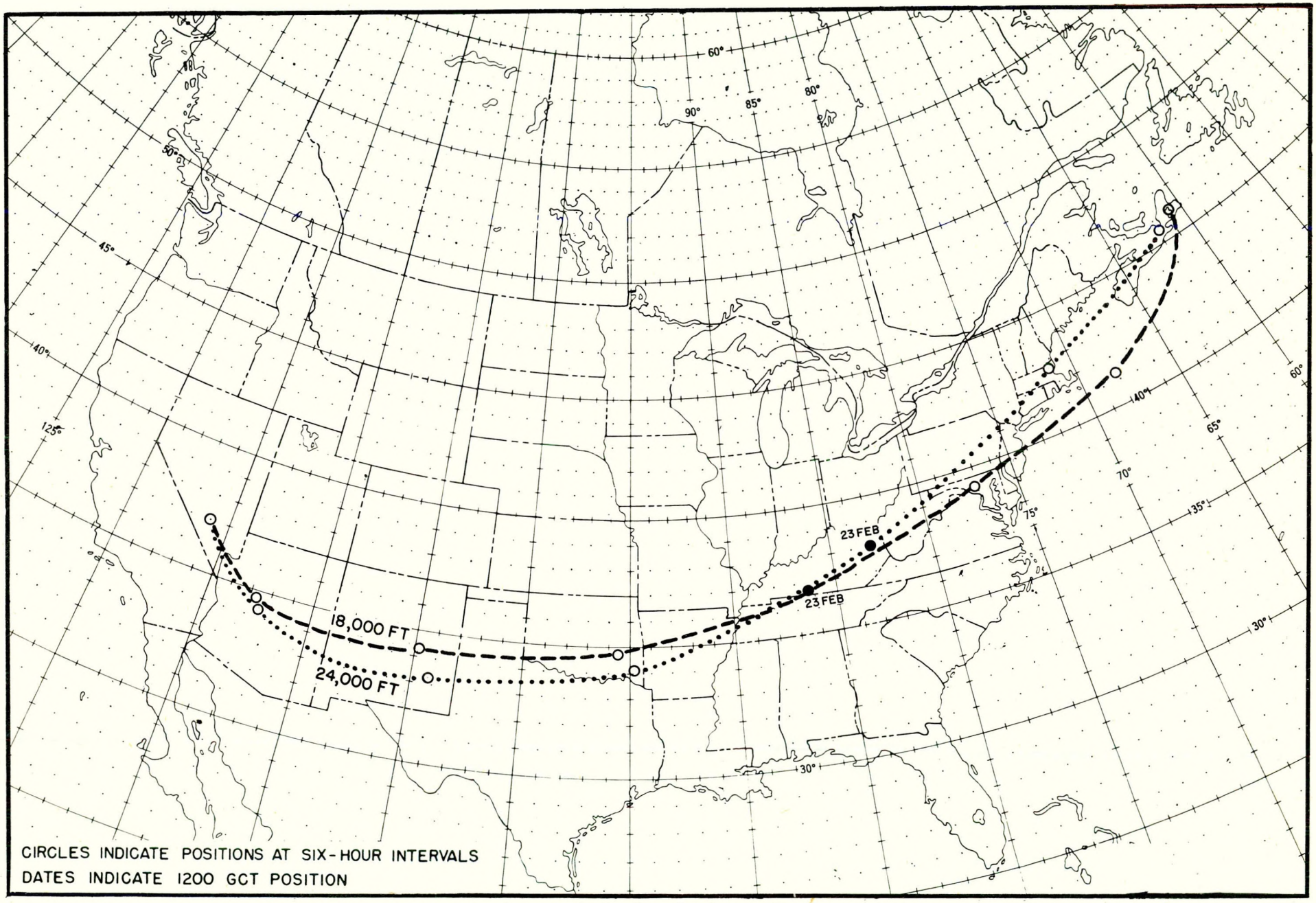

Figure 3.2 Meteorological trajectories for burst No. 2

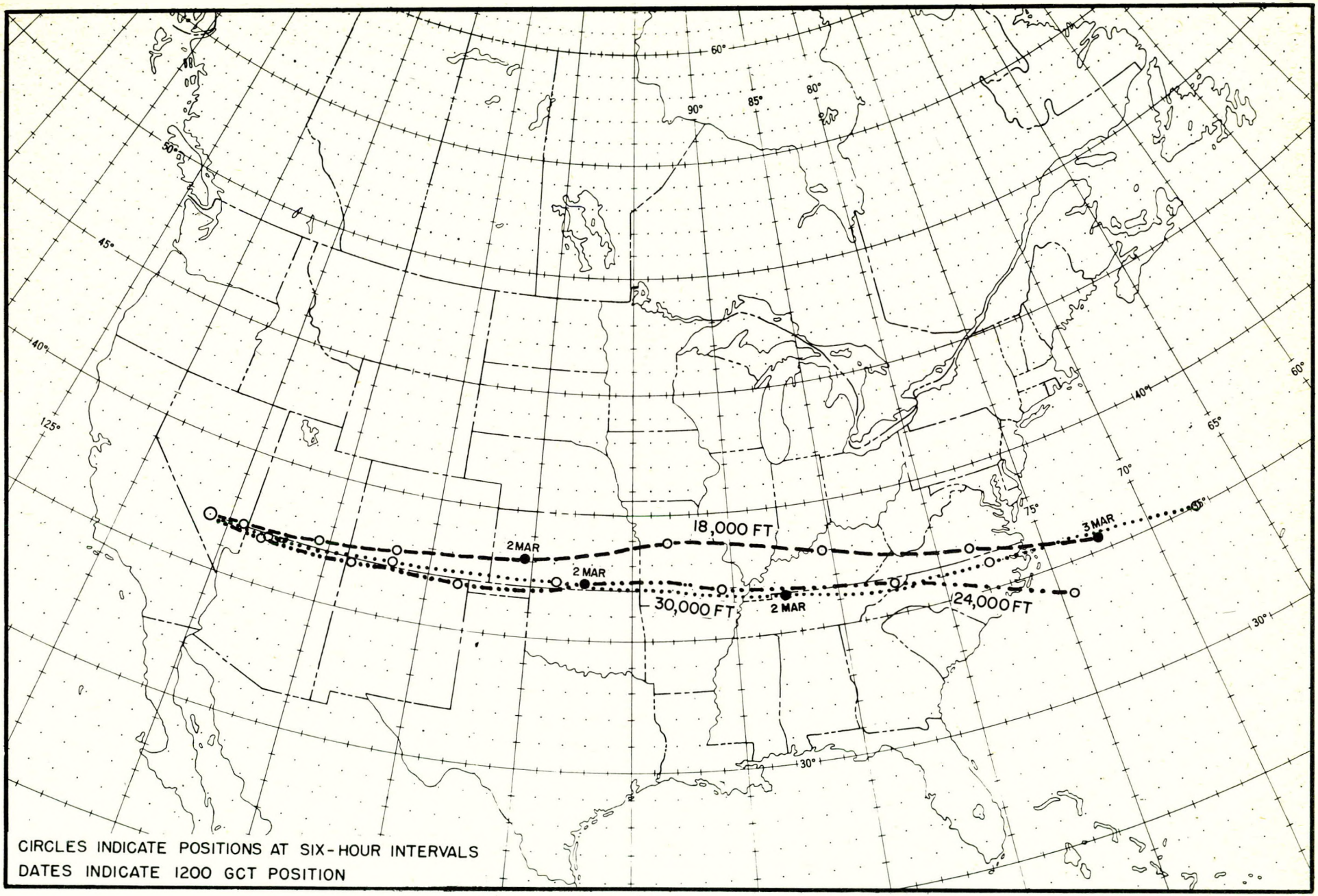

Figure 3.3 Meteorological trajectories for burst No.3

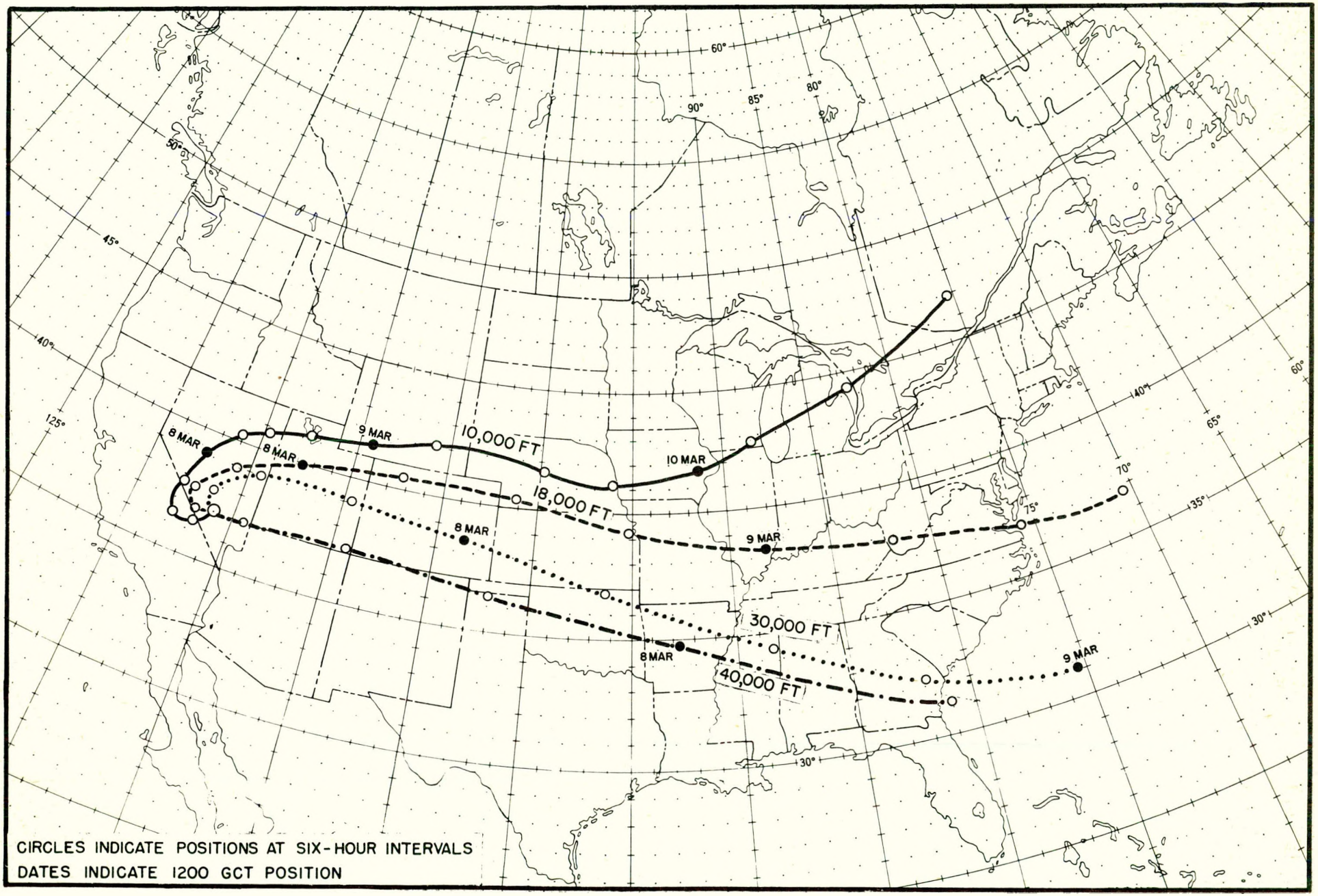

Figure 3.4 Meteorological trajectories for burst No.4

carried some debris to the west, very little deposition occurred in California.

3.2.5 Burst 5, March 12

The meteorological trajectories of the burst (Fig. 3.5) indicates that the debris was carried eastward and fanned out to cover most of the central and eastern United States. A large precipitation area in the central states on March 14 resulted in deposition of debris from the Gulf states northward to the Great Lakes, and radioactivity continued to be associated with the precipitation area as it moved eastward on the following day.

3.2.6 Burst 6, March 22

Debris from this burst moved eastward (Fig. 3.6) across the southern tier of states and resulted in dry fallout eastward to the Mississippi Valley on the 23rd, reaching the coast on the 24th. Very little precipitation occurred along the path of the debris.

3.2.7 Burst 7, March 23

Since this was an underground burst, most of the debris was at low levels. The upper part of the cloud moved southeastward (Fig. 3.7) and the lowest levels moved in a more southerly direction, presumably over Mexico. Since the # 7 test followed # 6 by only one day, it is not possible to differentiate the source of debris in the southern and southwestern states after March 24.

3.2.8 Bursts 8 and 9, March 29

These two devices were tested within six hours of each other and the same general cloud movement prevailed for both (Figs. 3.8 and 3.9). The upper position moved east-southeastward over the southern states, the lower portion passed northeastward over North Dakota and into Canada. However, there was some variation in the paths of the middle portions. At 18,000 feet the earlier debris moved in the same direction at the upper parts, but by the time of the # 9 burst the low pressure area to the west had moved eastward enough to make for a more northerly movement of the 18,000-foot debris. As a result of these movements, debris was widespread over the United States for several days following the bursts. By April 1, rainout from the trailing portion of the upper clouds was prevalent over the south-central states while dry fallout from the lower part of the cloud was occurring over the Great Lakes. Debris from these bursts continued

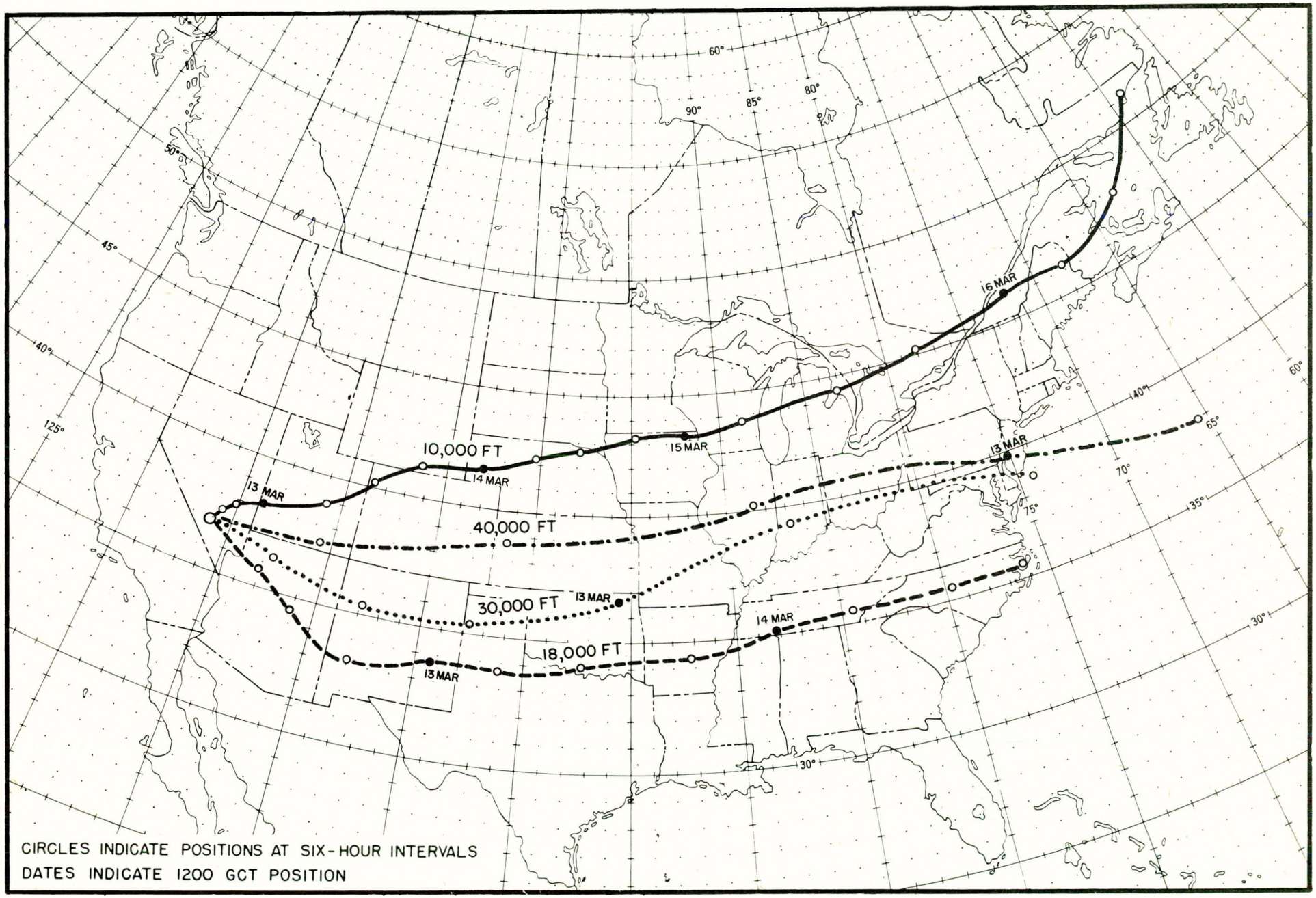

Figure 3.5 Meteorological trajectories for burst No.5

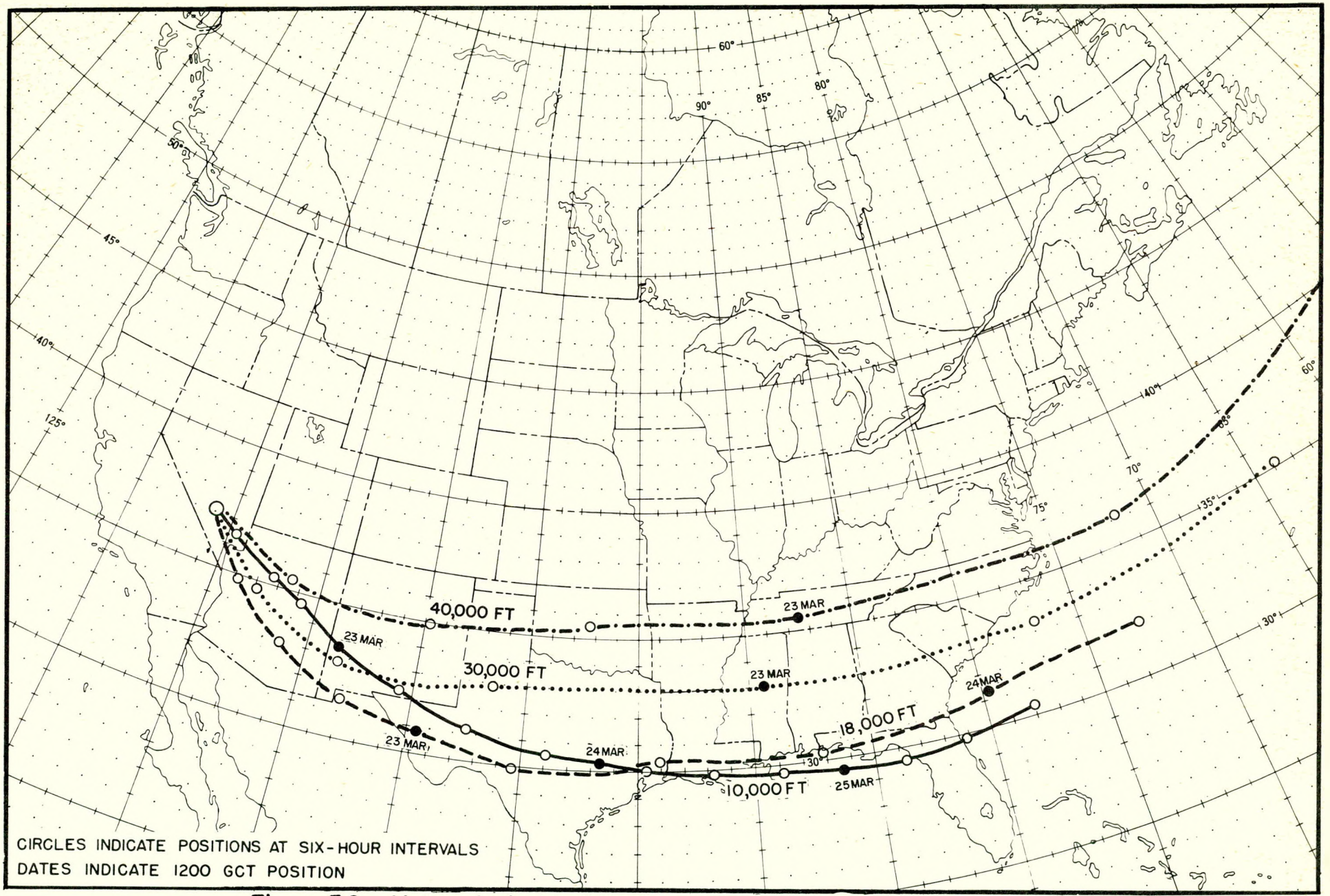

Figure 3.6 Meteorological trajectories for burst No. 6

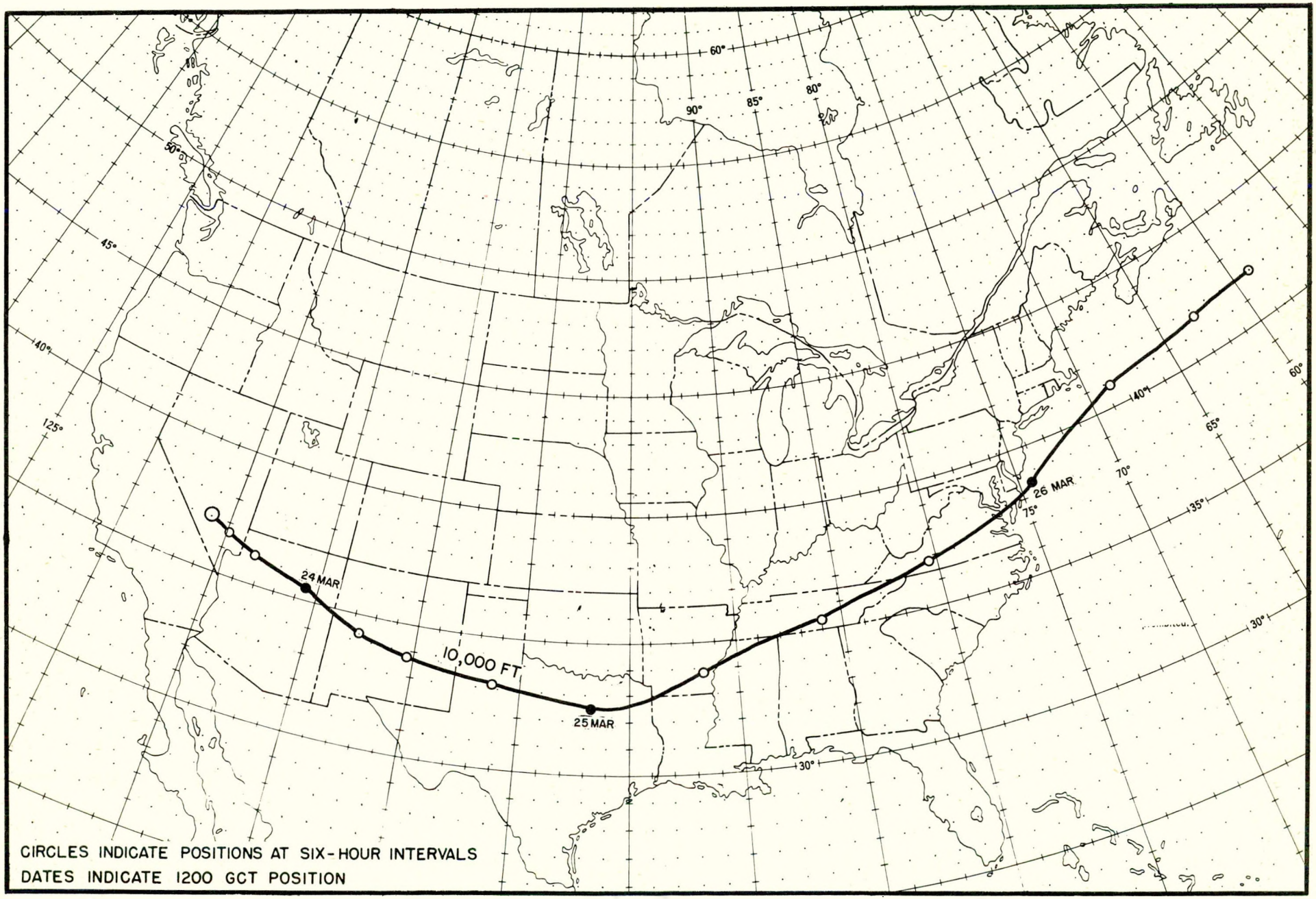

Figure 3.7 Meteorological trajectories for burst No.7

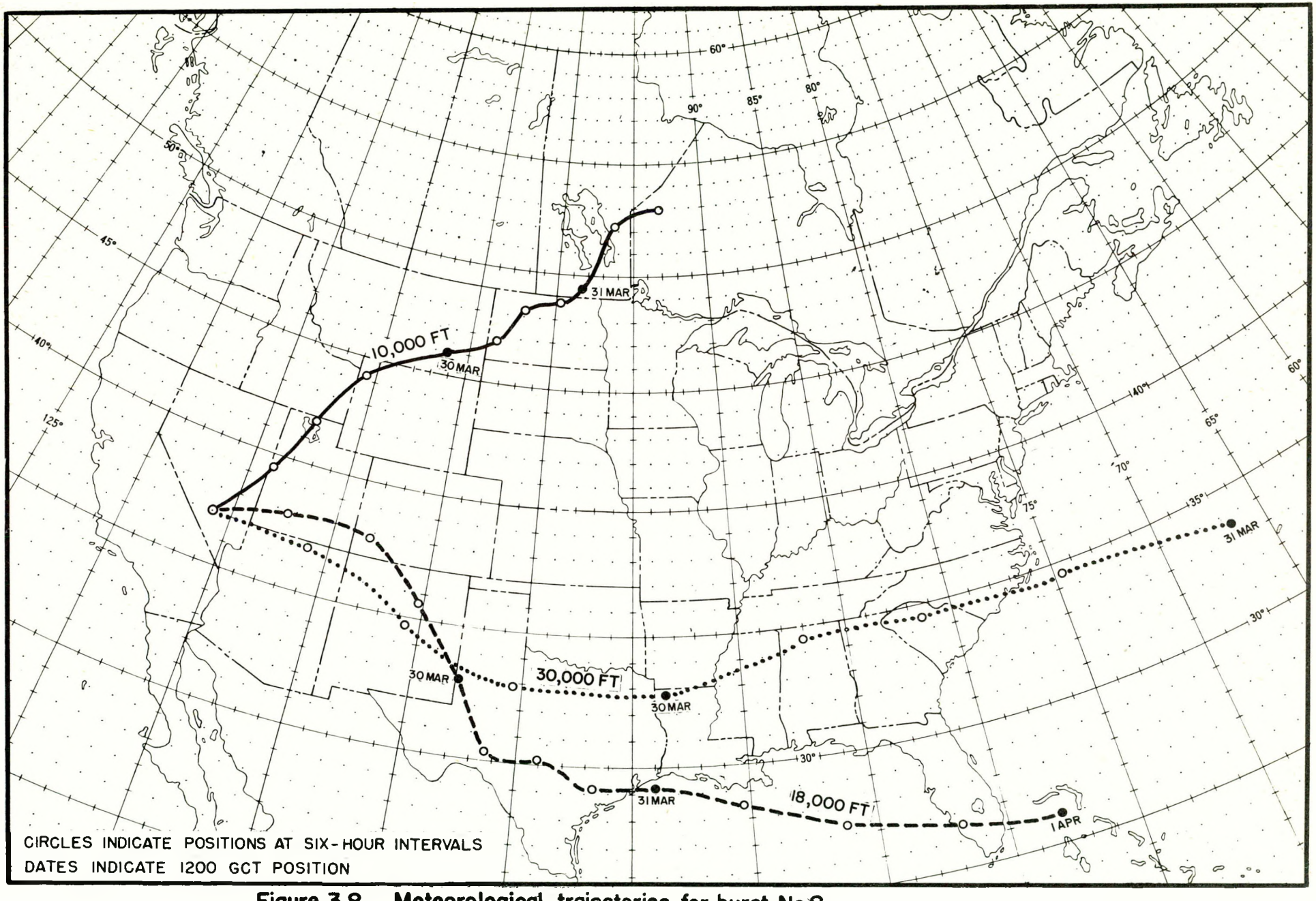

Figure 3.8 Meteorological trajectories for burst No.8

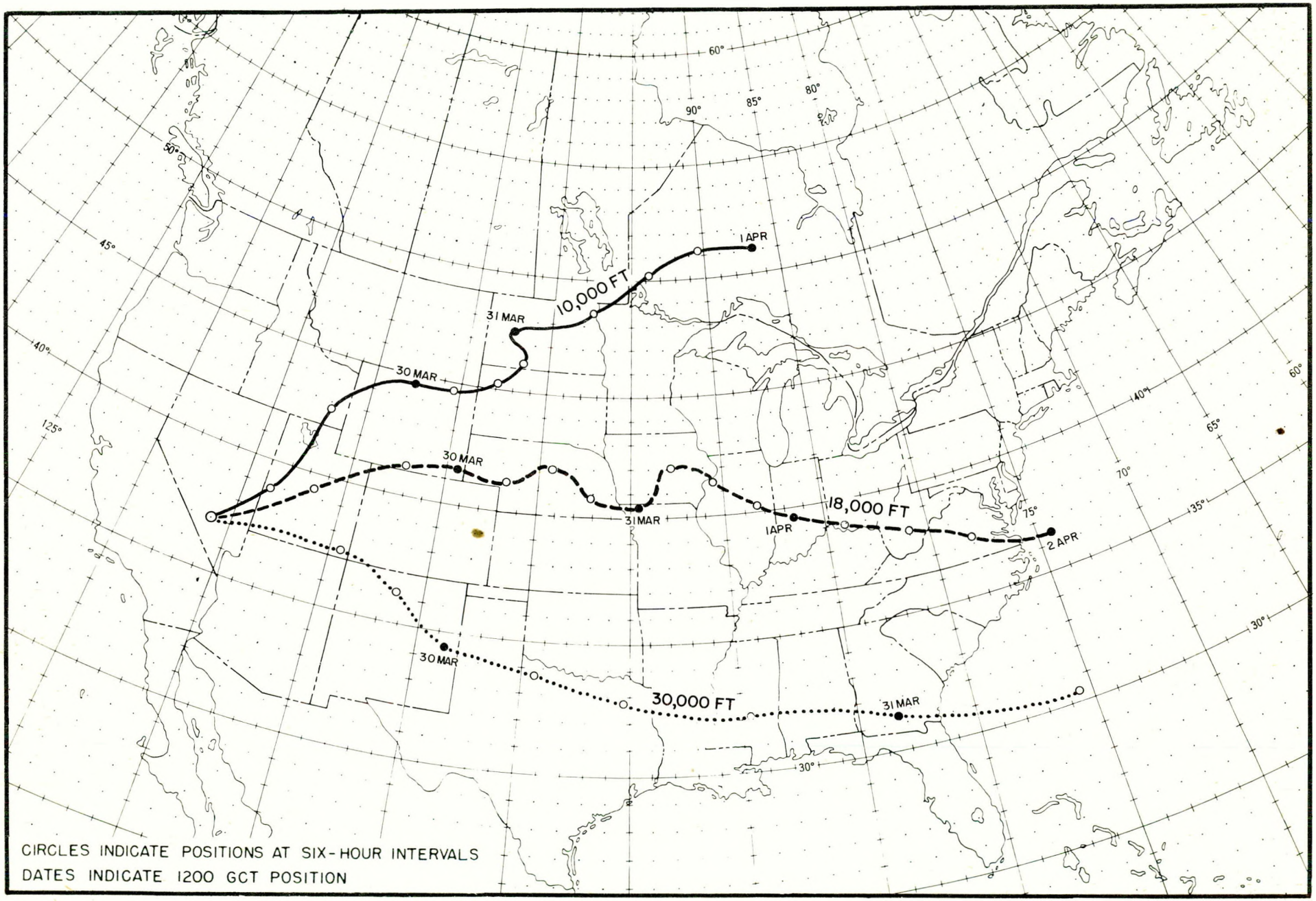

Figure 3.9 Meteorological trajectories for burst No.9

to fall out over the United States for quite a few days following the tests, primarily in rain areas.

3.2.9 Burst 10, April 6

Since this was a very high altitude burst and the cloud moved rapidly eastward (Fig. 3.10), no evidence of fallout attributable with certainty to this burst is to be found. The cloud consisted of a torus ring with the base estimated at 37,000 feet, the top at 55,000 feet.

3.2.10 Burst 11, April 9

Meteorological trajectories for the 10,000- and 14,000-foot levels indicate an initial southward movement of debris (Fig. 3.11). However, below 10,000 feet the winds carried the cloud northward and the principal fallout on April 10, the day following the burst, was apparently associated with the movement of the lower part of the cloud.

3.2.11 Burst 12, April 15

The upper portion of the # 12 cloud moved eastward in a fairly narrow path, while the stem spread out over the northeastern quarter of the United States (Fig. 3.12). Rain in the eastern Great Lakes on April 16 and in the northeast on the 17th resulted in the highest deposition from this test series in these areas. Although twenty days elapsed before another burst occurred, there was some fallout in the United States on each day of this twenty-day period.

3.2.12 Burst 13, May 5

Burst 13 was the so-called "open" or Civil Defense shot. As indicated by the meteorological trajectories (Fig. 3.13), the cloud initially moved northward from the test site and then curved to the east. Dry fallout at Ely, Nevada on the day of the burst resulted in the highest activity observed at any station during the test series. On the following day, Colorado experienced its highest activity for this series. Trajectories below 10,000 feet were in a more westerly direction and moved with slower speeds, resulting in deposition in Central California on May 7. The activity in the San Francisco area on the 6th is most probably globe-circling debris from an earlier test. Deposition continued to be heavy, both in and out of rain areas, for several days following burst 13 over most of the United States east of the test site and was still giving values of the order of hundreds of microcuries per 100 square miles at some stations more than a week later.

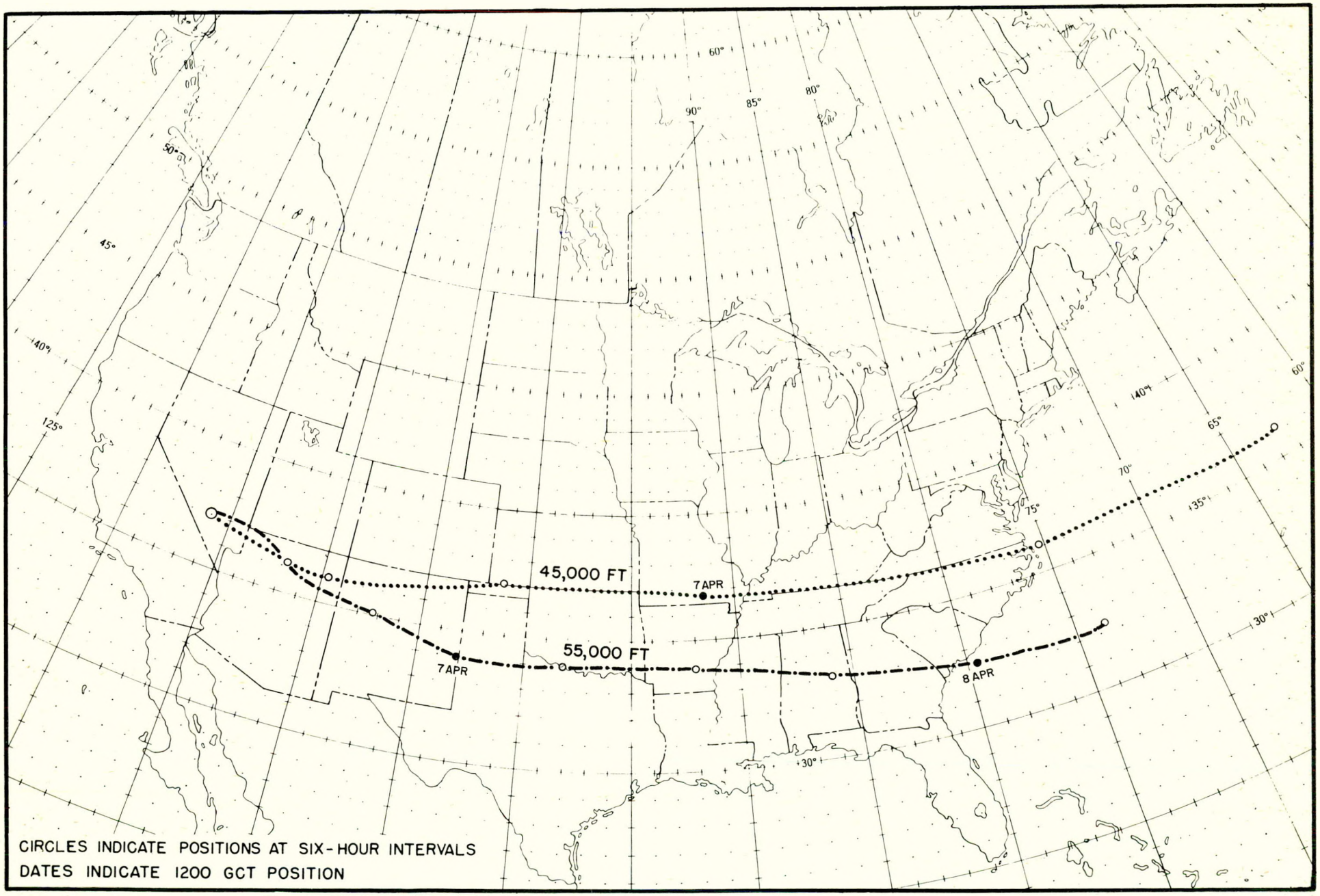

Figure 3.10 Meteorological trajectories for burst No. 10

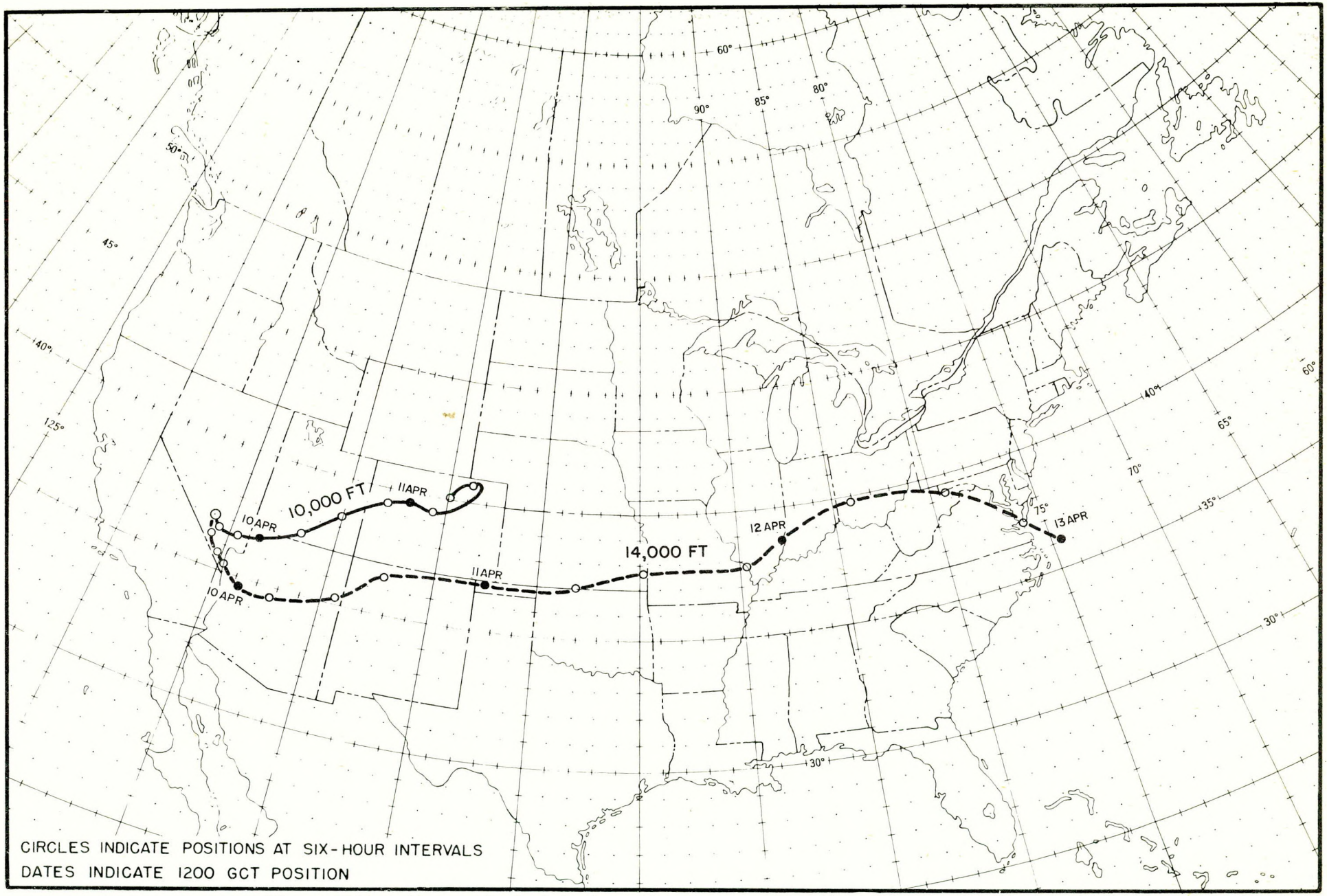

Figure 3.11 Meteorological trajectories for burst No. 11

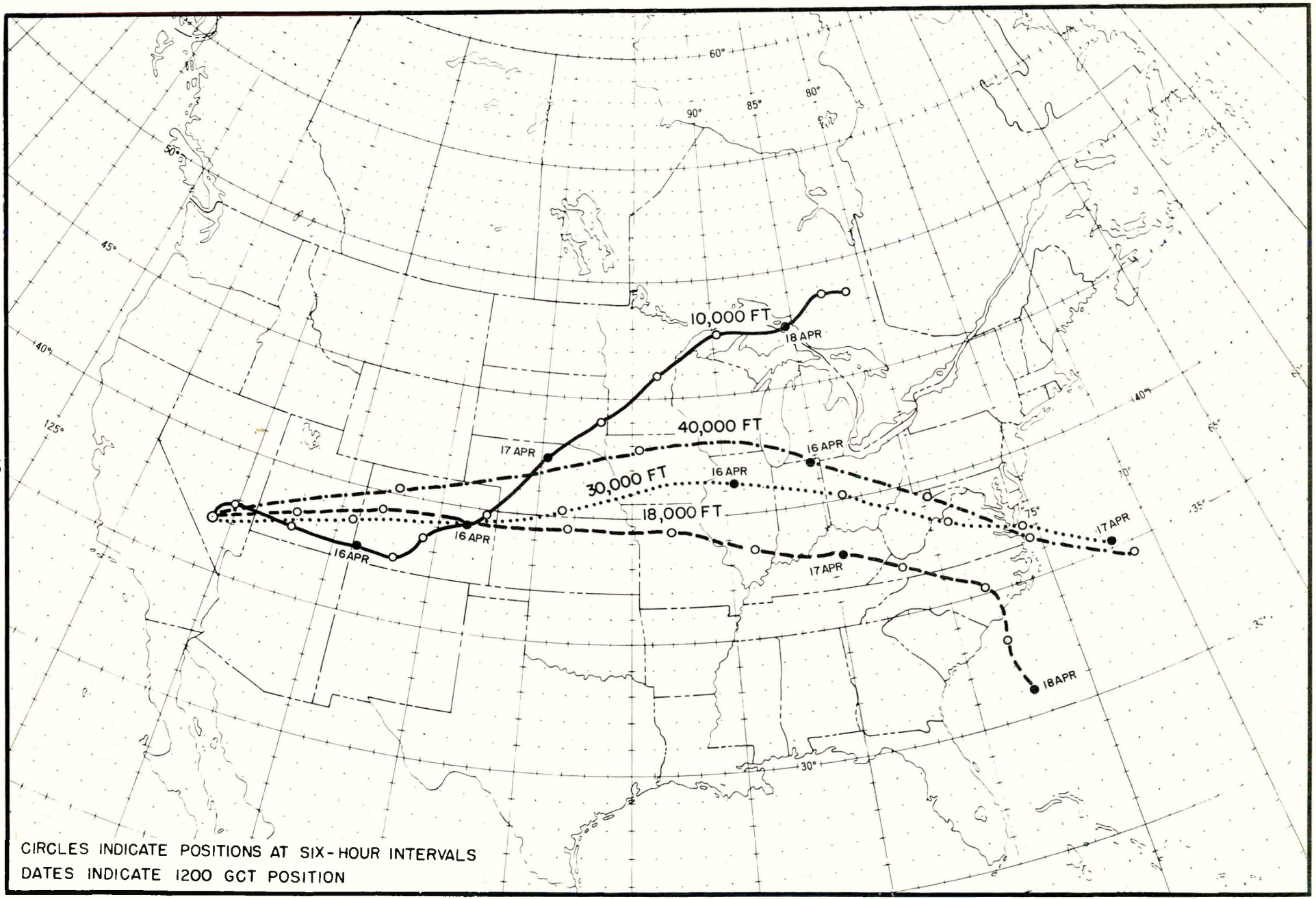

Figure 3.12 Meteorological trajectories for burst No. 12

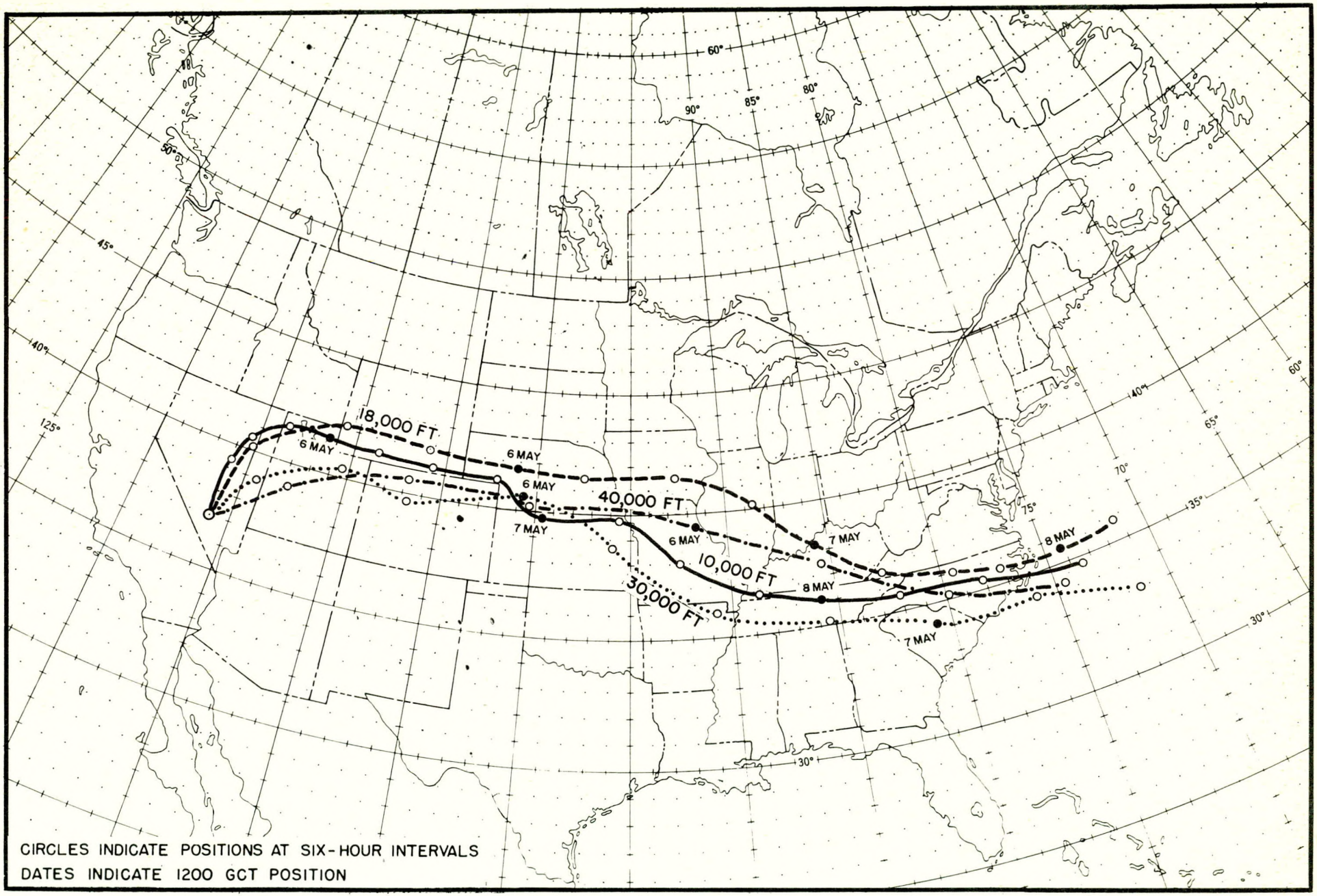

Figure 3.13 Meteorological trajectories for burst No. 13

3.2.13 Burst 14, May 15

The last burst of the Teapot Series was detonated when a major cyclonic circulation moving from the west was just north of the test site. The movement of the debris at all levels of the cloud was affected by this circulation and the trajectories moved initially counterclockwise about the center of the low. As is inherent in such situations, the meteorological trajectories (Fig. 3.14) are uncertain because of the rapidly changing wind fields and these uncertainties are indicated by the branching of the trajectories. The absence of normal west-east flow in the troposphere is reflected in the fact that on May 18, three days after the burst, almost all fallout was occurring west of the 95th meridian and had barely reached the Atlantic coast by the 20th. Unfortunately, individual processing of daily samples ended on this date (subsequent samples were combined for longer period averages).

3.3 FALLOUT AFTER MAY 20, 1955

It is evident that fallout of the order of several hundred millicuries per hundred square miles must have continued to occur for quite a few days following May 20. To investigate this point, the daily samples at six northeastern stations were counted for the period May 21 - June 30, 1955. A summary of the data is given in Table 3.2.

TABLE 3.2 - Fallout, May 21 - June 30, 1955 (Millicuries per 100 Square Miles on January 1, 1956)

Station	Cumulative Total	Average Daily Fallout
Philadelphia, Pennsylvania	1,500	38
Pittsburgh, Pennsylvania	2,000	50
New York, New York	1,300	32
Rochester, New York	1,400*	160*
Washington, D. C.	670	17
Boston, Massachusetts	420	10

* May 21 - May 30, 1955

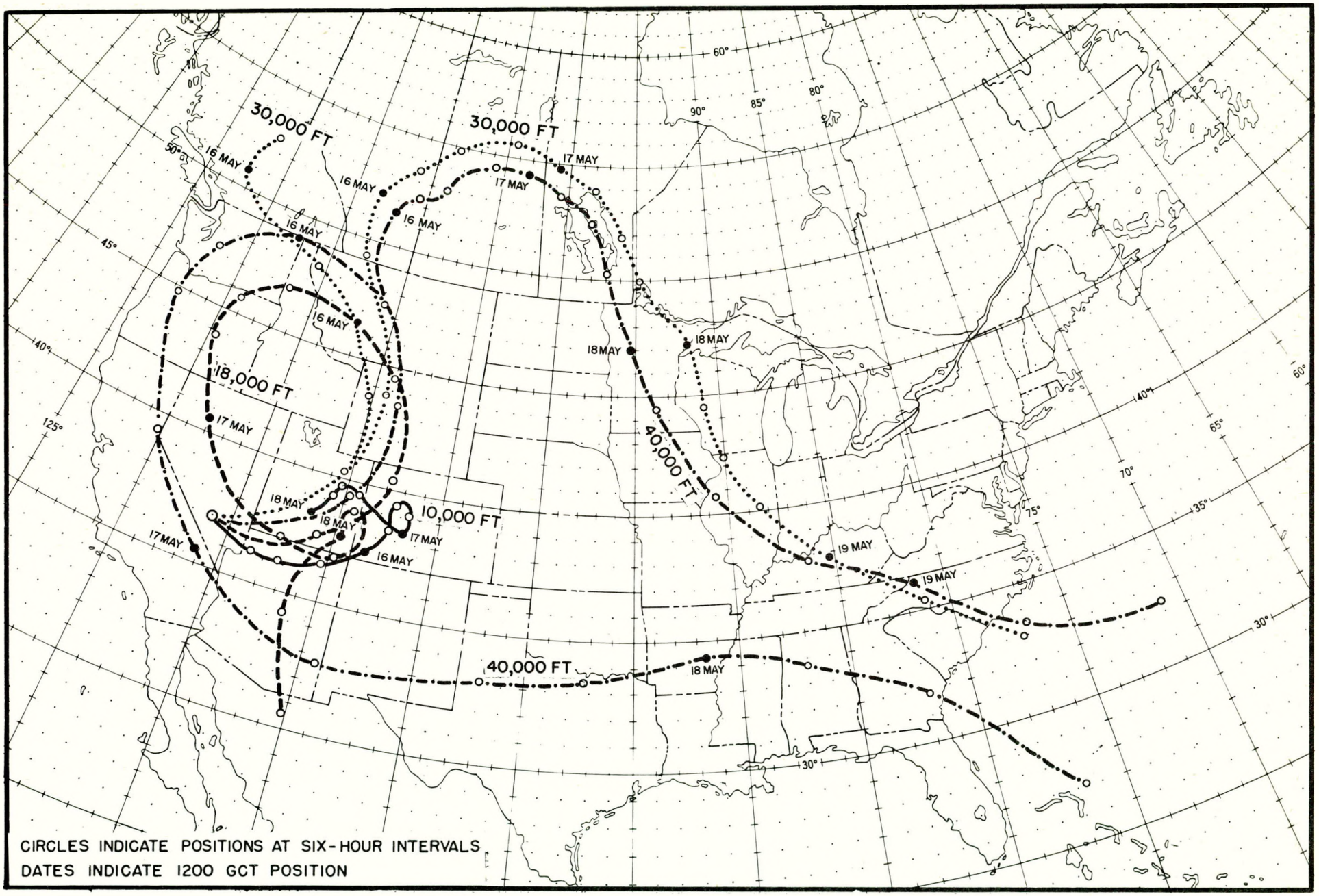

Figure 3.14 Meteorological trajectories for burst No. 14

3.4 TOTAL FALLOUT

The total fallout from February 18 through May 20, 1955 at stations making daily observations in North America is shown in Fig. 3.15[1]. The values are in millicuries per square mile as of January 1, 1956. The totals have been corrected for missing data.

It is evident from Fig. 3.15 that most of the debris is carried eastward by the prevailing westerlies and that fallout decreases with increasing distance from the test site. However, the effect of distance is overshadowed by the prevailing winds, resulting in the lowest fallout occurring in the Pacific coastal states.

Numerical integration of the total fallout indicates that less than 5 percent of the total beta activity released during the Teapot Series was deposited in the United States, exclusive of the "close-in" fallout, from February 18 through May 20. This result is similar to that found in the two previous Nevada test series.

---

1. Lynch, Daniel E., Radicactive Debris in North America from Operation Teapot, U. S. Atomic Energy Commission, New York Operations Office, NYO-4659, August 1955.

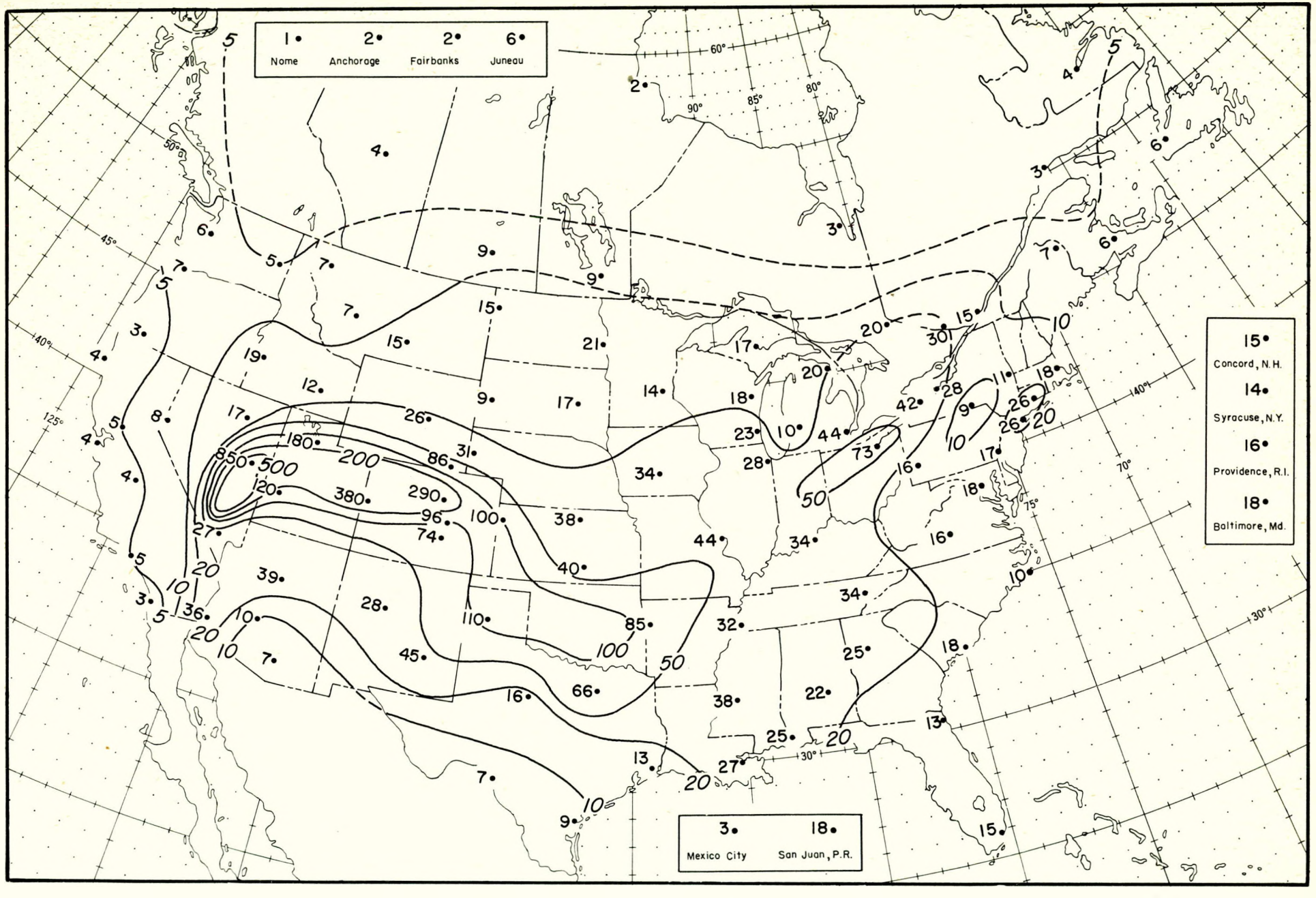

Figure 3.15 Total Fallout, February 18—May 20, 1955
(Millicuries per square mile on January 1, 1956)

CHAPTER 4

SPECIAL OBSERVATIONS AT ARGONNE NATIONAL LABORATORY

4.1 GUMMED FILM

A series of special gummed film observations were made at Argonne National Laboratory, about 20 miles southwest of Chicago, through the cooperation of Mr. Harry Moses of the Radiological Physics Division, with personnel of the Industrial Hygiene and Safety Division assisting in the routine work.

The experiments were conducted at the Meteorology Building, which is located in an isolated section on a level grass area with no nearby obstructions. Seven gummed film exposures were made simultaneously for each 12-hour period, beginning at 7:00 a.m. and 7:00 p.m., CST. Five films were mounted vertically, four on the outside walls of the Meteorology Building facing West, East, North, and South and the fifth on the west wall of a small storage shack 35 feet west of the Meteorology Building. The latter film is designated as WW. In addition, two films were exposed horizontally three feet above the grass about 100 feet from the nearest obstruction. One of these faced up in the normal manner, the other faced downward.

Observations were made from March 9 through April 12 and from April 22 through May 25, 1955. The results of the observations during periods when significant fallout occurred are given in Table 4.1. (For this purpose, significant fallout is considered to have occurred when more than 50 millicuries per 100 square miles extrapolated to January 1, 1956 was observed on one or more films.) No noteworthy differences were found between day and night exposures; however, the number of cases of significant fallout with no precipitation was too small (only three cases) for any conclusions on this point.

It is interesting to note the striking difference between days with and without precipitation. In the former, about one percent of the activity on the upward-facing film was found on the downward film, and about 4 percent, on the average, on the vertical films. However, on the three dry days forty percent of the activity on the upward-facing papers was found on the downward

TABLE 4.1 - Gummed Film Observations at Argonne National Laboratory

Date	Precipitation	Activity (Millicuries per 100 Square Miles on January 1, 1956) on Gummed Film Facing: Up	Down	W	WW	N	E	S
			0100 - 1300 GCT (Night)					
March 10	None	110	23	4	3	4	41	1
March 15	Moderate	388	4	31	37	16	11	11
March 24	None	18	6	36	12	4	3	54
April 5	Light	65	0	2	1	1	21	6
May 10	Moderate	120	0	1	1	0	18	12
May 22	Trace	295	2	3	6	2	25	2
May 23	Moderate	361	1	12	6	5	3	4
			1300 - 0100 GCT (Day)					
March 23	None	52	47	79	28	31	30	29
May 7	Trace	544	5	25	139	18	8	17
May 9	Light	150	2	2	2	4	32	4
May 22	Moderate	403	2	1	13	17	5	74
May 24	Heavy	160	9	12	13	1	12	14
		Totals						
No precipitation (3 cases)		180	76	119	43	39	74	84
Precipitation (9 cases)		2486	25	89	79	64	135	144

film and on the average of the vertical films.

Some confusion in numbering of samples by the counting laboratory occurred in the data for May 22 and 23; however, it is felt that the results are now correctly reported.

4.2 RAINDROP RADIOAUTOGRAPHS

Another experiment performed at Argonne consisted of exposing a sheet of Ozalid paper horizontally for a few seconds during a rain, which results in clear, permanent outlines of the individual raindrops on the Ozalid paper. The papers were then dried and sent to New York where radioautographs were made by an approximately 10-day exposure with DuPont X-ray film.

Of the eight papers which were successfully radioautographed, five, of rain collected on March 20, 21, 22, 26, and April 11, showed negative results. These were all exposed on days when essentially no fallout was collected on the gummed film exposed during the same period. Three papers, one exposed at 0800 GCT, March 11 and two at 0500 GCT, March 15, 1955, showed positive activity. One of the latter papers showed the most radioactivity.

A portion of the 8- by 10-inch Ozalid paper and the corresponding radioautograph are shown full size in Figs. 4.1 and 4.2. The corresponding droplets and film spots are indicated. Of the more than 200 rain droplets which fell on the Ozalid paper, only 7 exhibited radioactivity. In all cases, most of the activity seemed to be concentrated in an active particle contained in the droplet, no active particles not associated with droplets were found. In at least two of the droplets, A and B, in addition to the activity from the particle, a fogging of the film coincides exactly with the outline of the droplet, indicating the presence of dissolved radioactivity in the droplets. The rain collection was made near the beginning of a brief rainfall of slightly over 0.1 inch which lasted less than two hours. This period had the third highest value of radioactivity on the gummed film observed at Argonne, 388 millicuries per 100 square miles as of January 1, 1956, a result of burst # 5.

The other two Ozalid papers showing positive activity had one and three radioactive particles respectively.

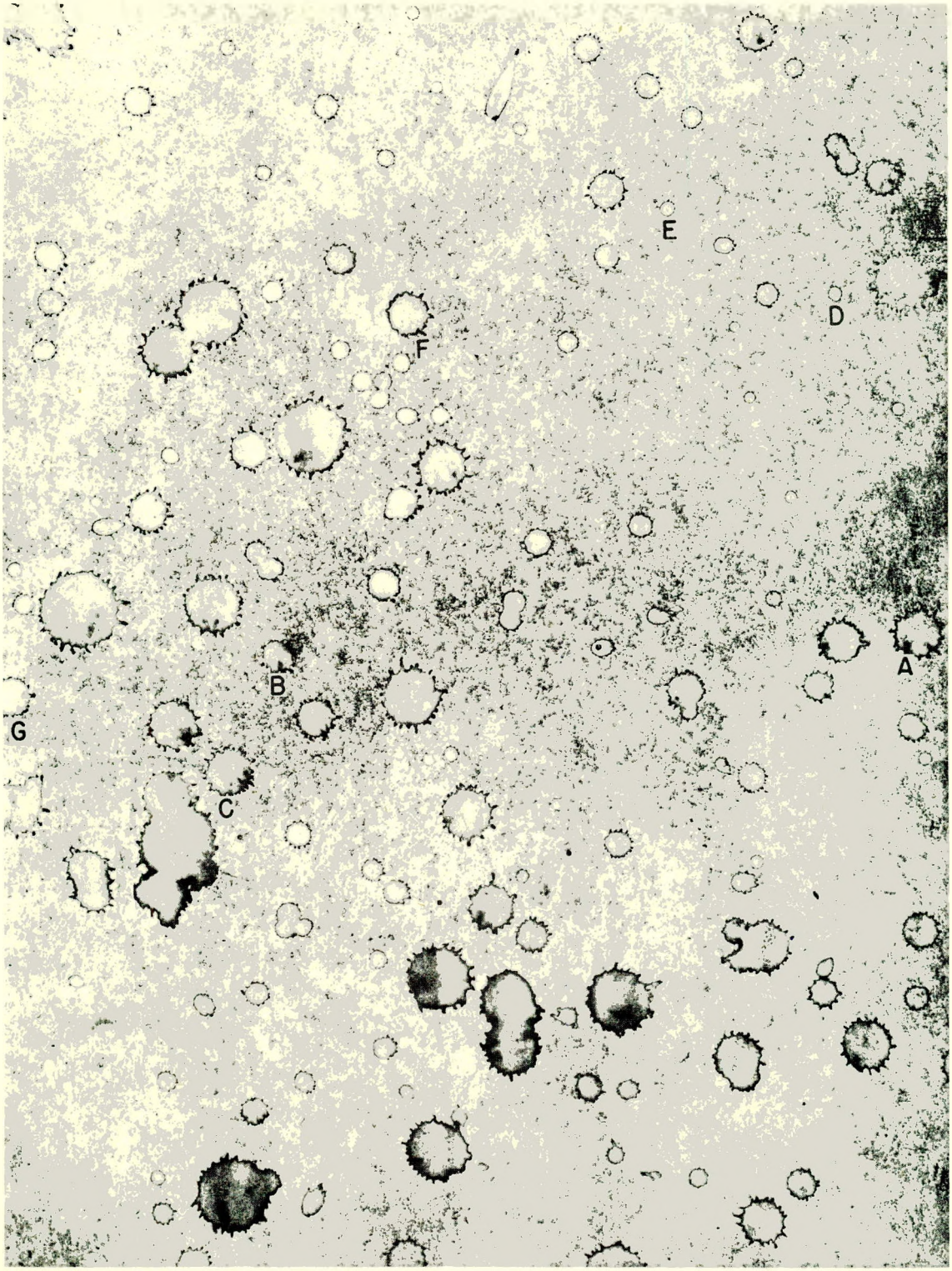

Fig. 4.1 Rain Collection on Ozalid Paper

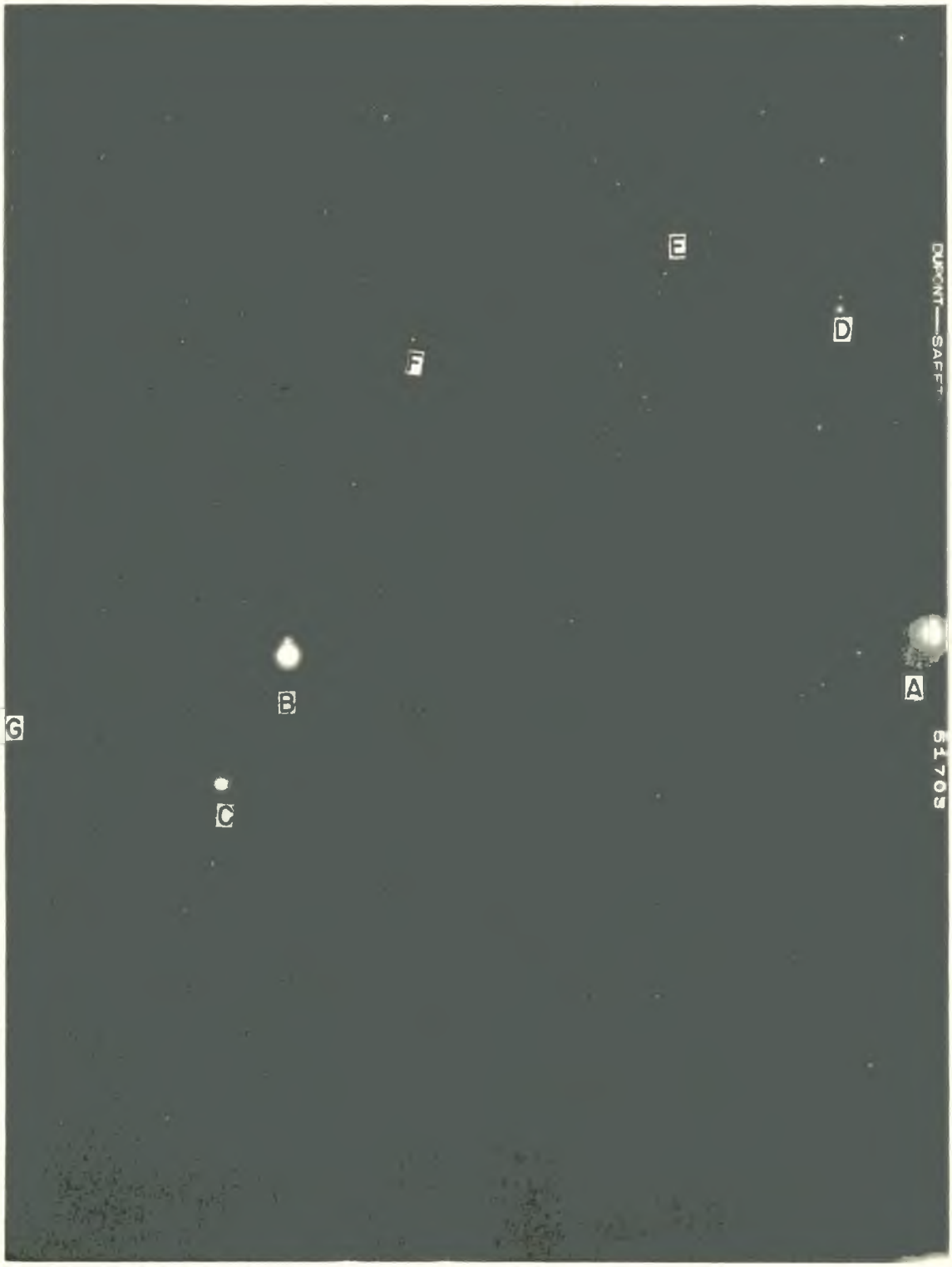

Fig. 4.2 Radioautograph of Rain Collection

APPENDIX A

MAPS OF DAILY FALLOUT IN NORTH AMERICA

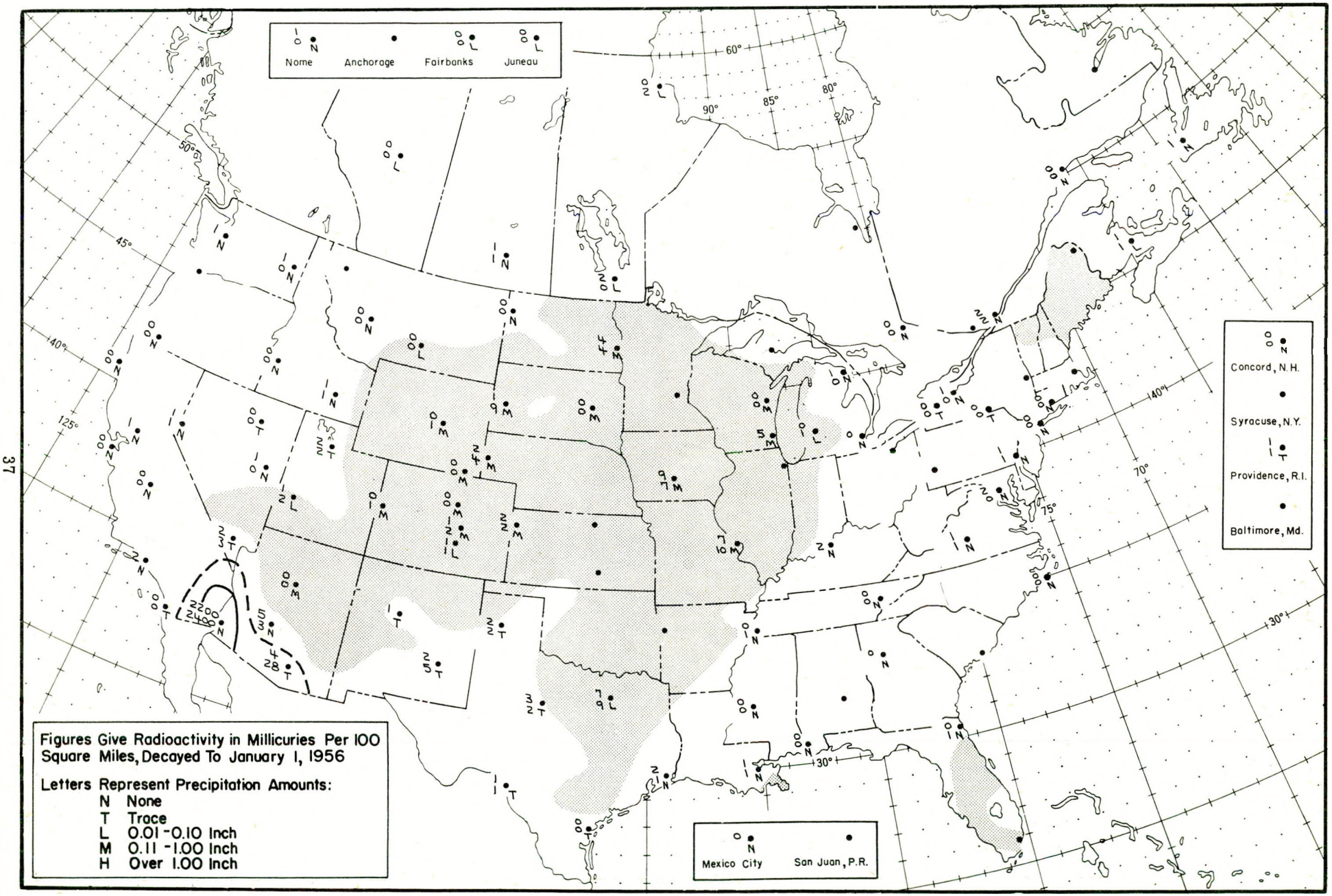

Figure A.1 Radioactive fallout in the 24-hour period beginning 1230 G.C.T., February 18, 1955

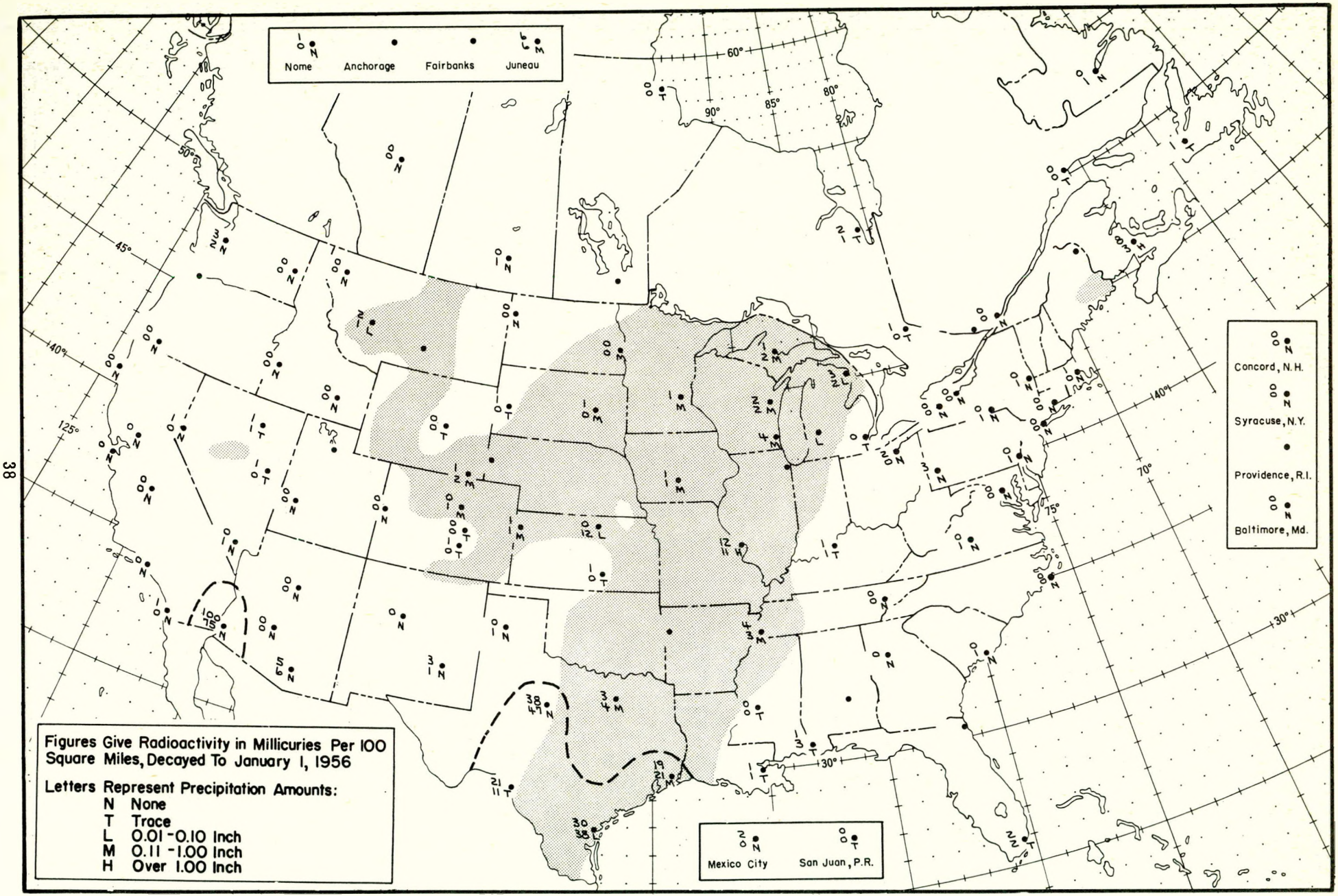

Figure A.2 Radioactive fallout in the 24-hour period beginning 1230 G.C.T., February 19, 1955

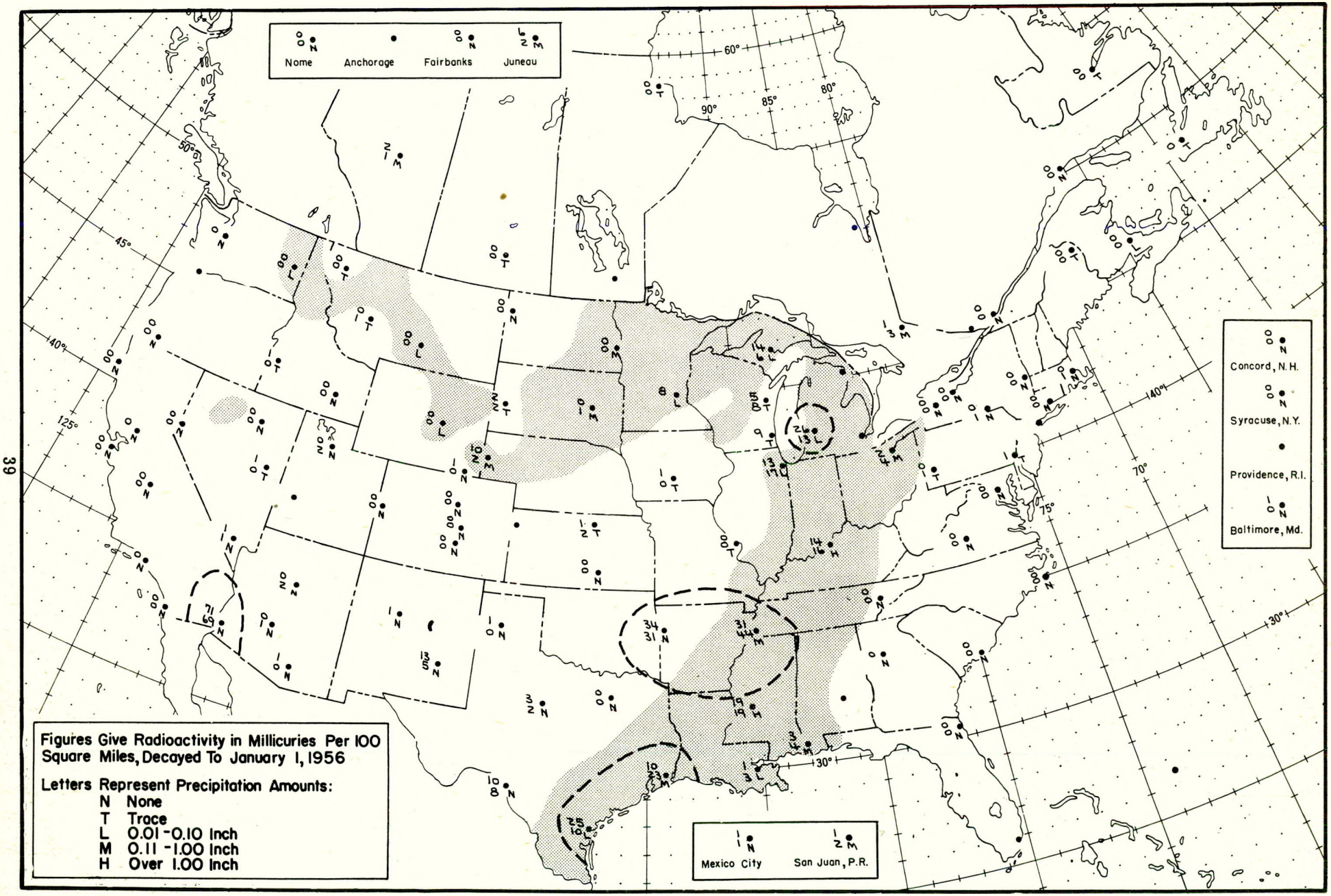

Figure A.3 Radioactive fallout in the 24-hour period beginning 1230 G.C.T., February 20, 1955

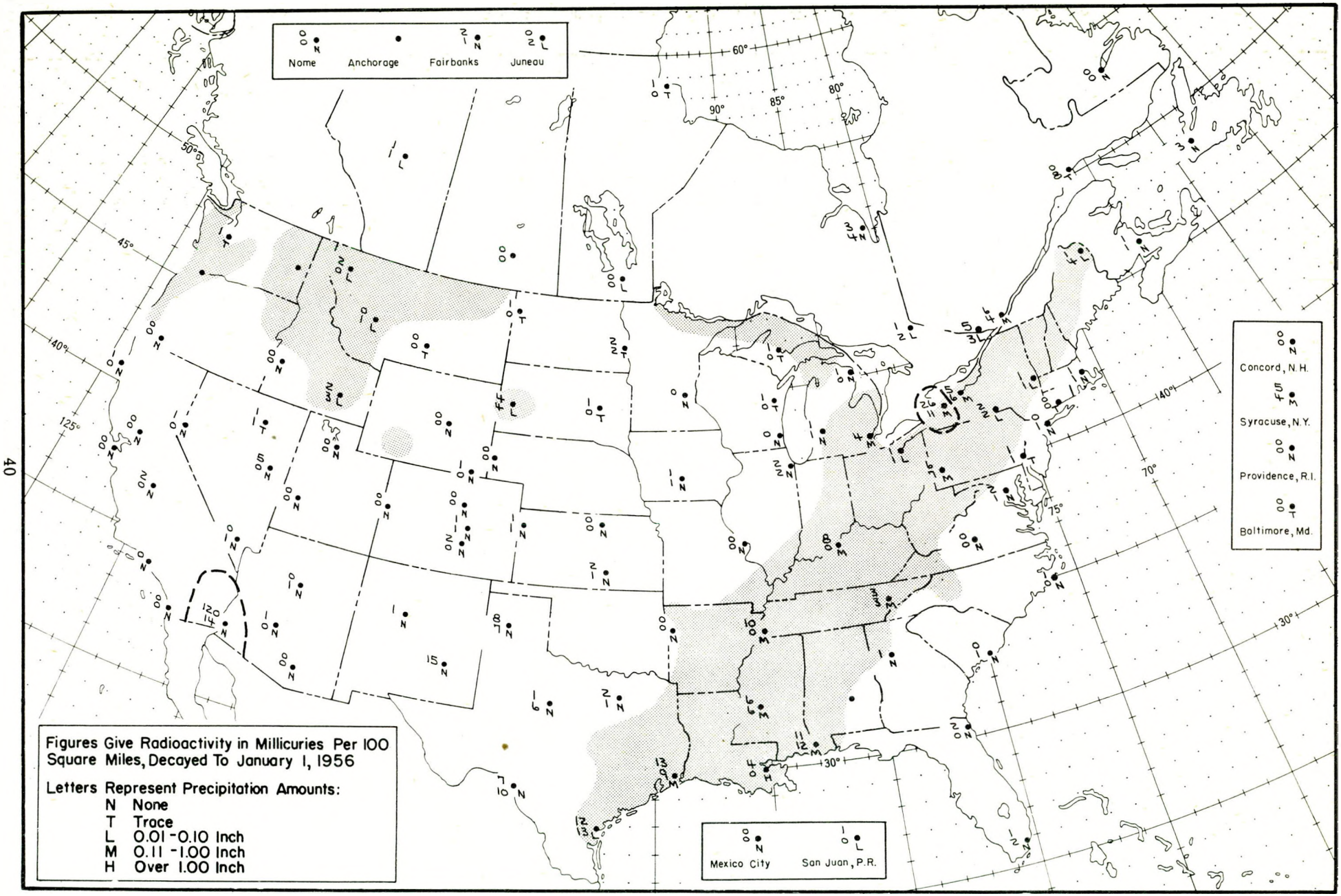

Figure A. 4 Radioactive fallout in the 24-hour period beginning 1230 G.C.T., February 21, 1955

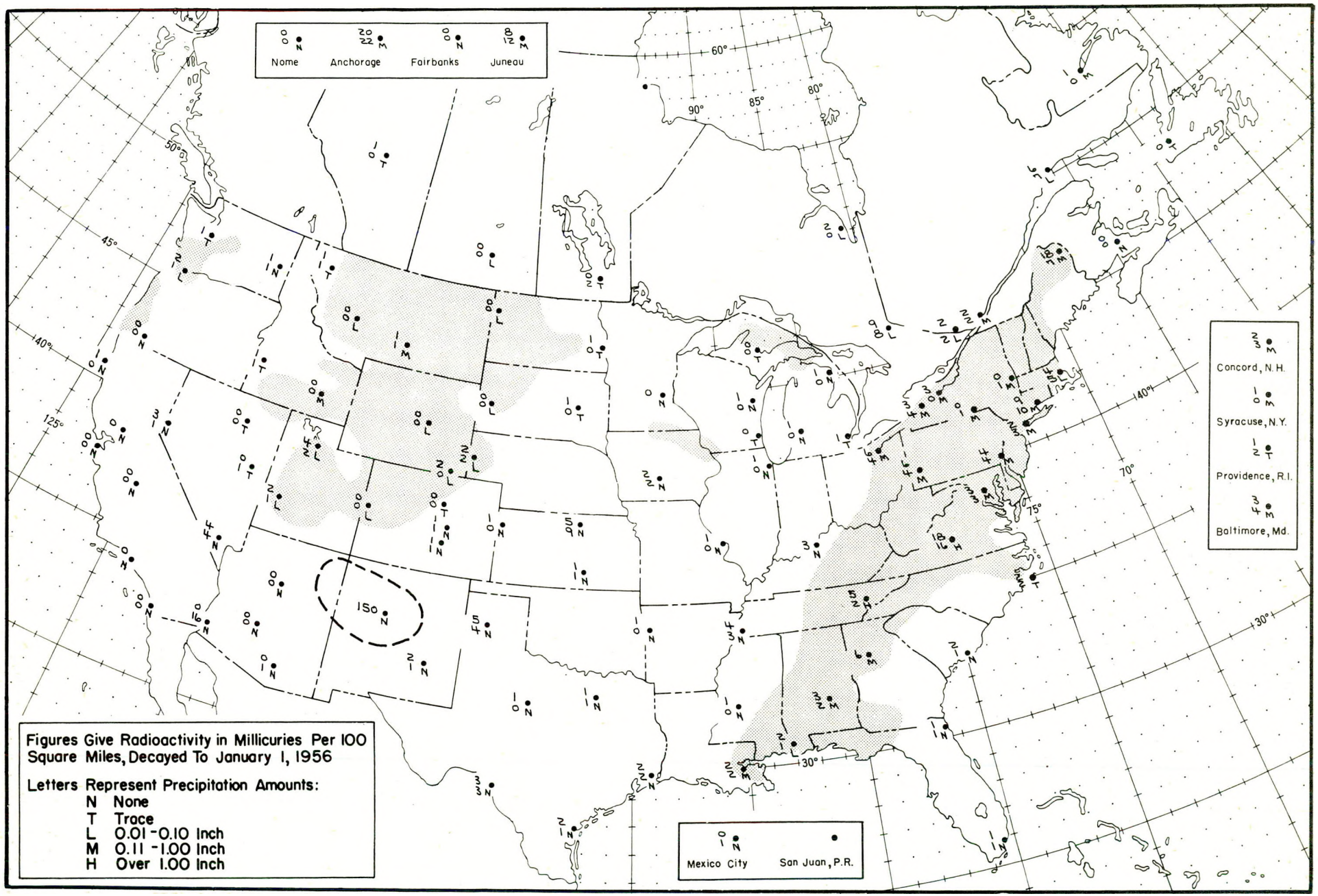

Figure A.5 Radioactive fallout in the 24-hour period beginning 1230 G.C.T., February 22, 1955

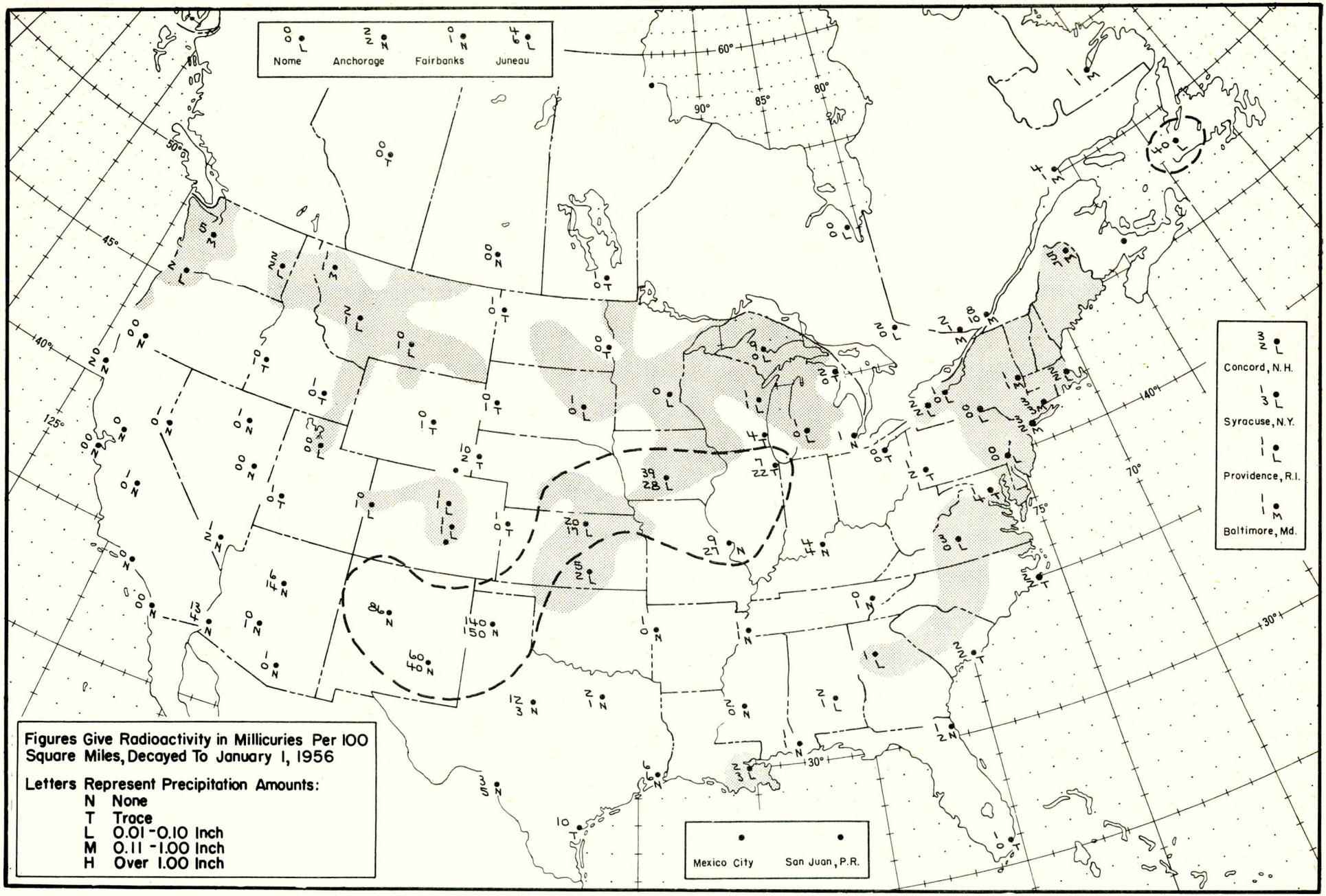

Figure A.6 Radioactive fallout in the 24-hour period beginning 1230 G.C.T., February 23, 1955

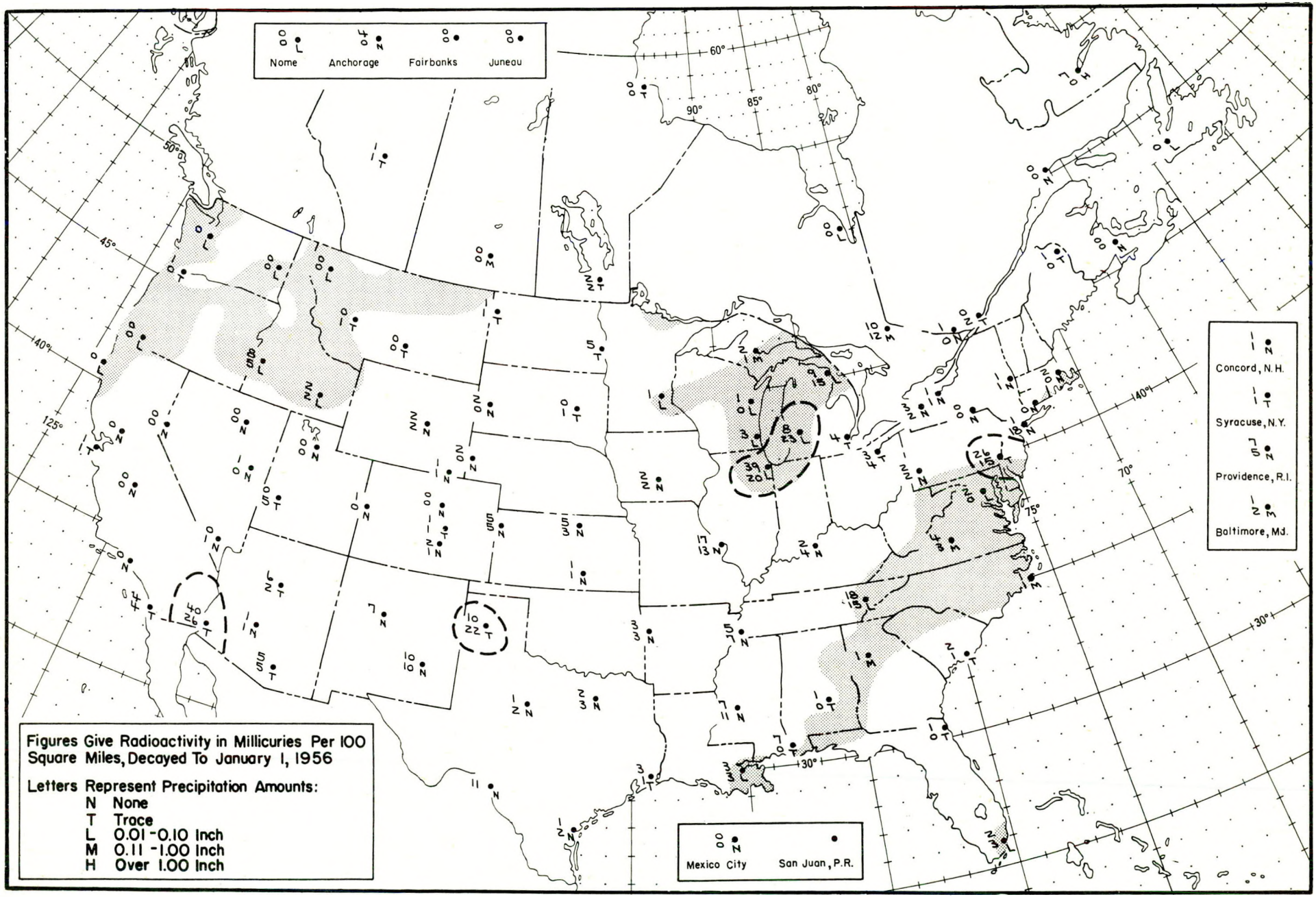

Figure A. 7 Radioactive fallout in the 24-hour period beginning 1230 G.C.T., February 24, 1955

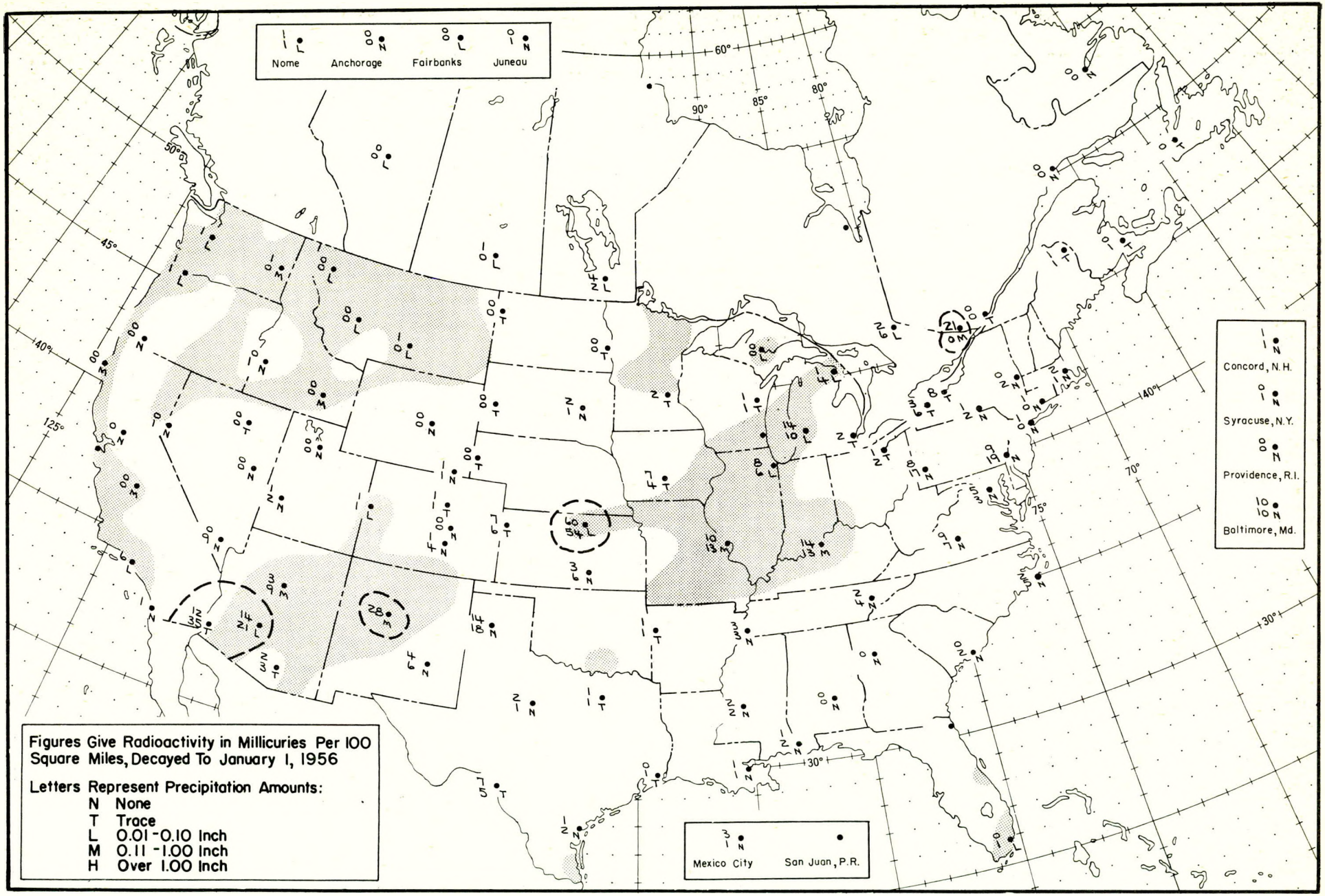

Figure A.8 Radioactive fallout in the 24-hour period beginning 1230 G.C.T., February 25, 1955

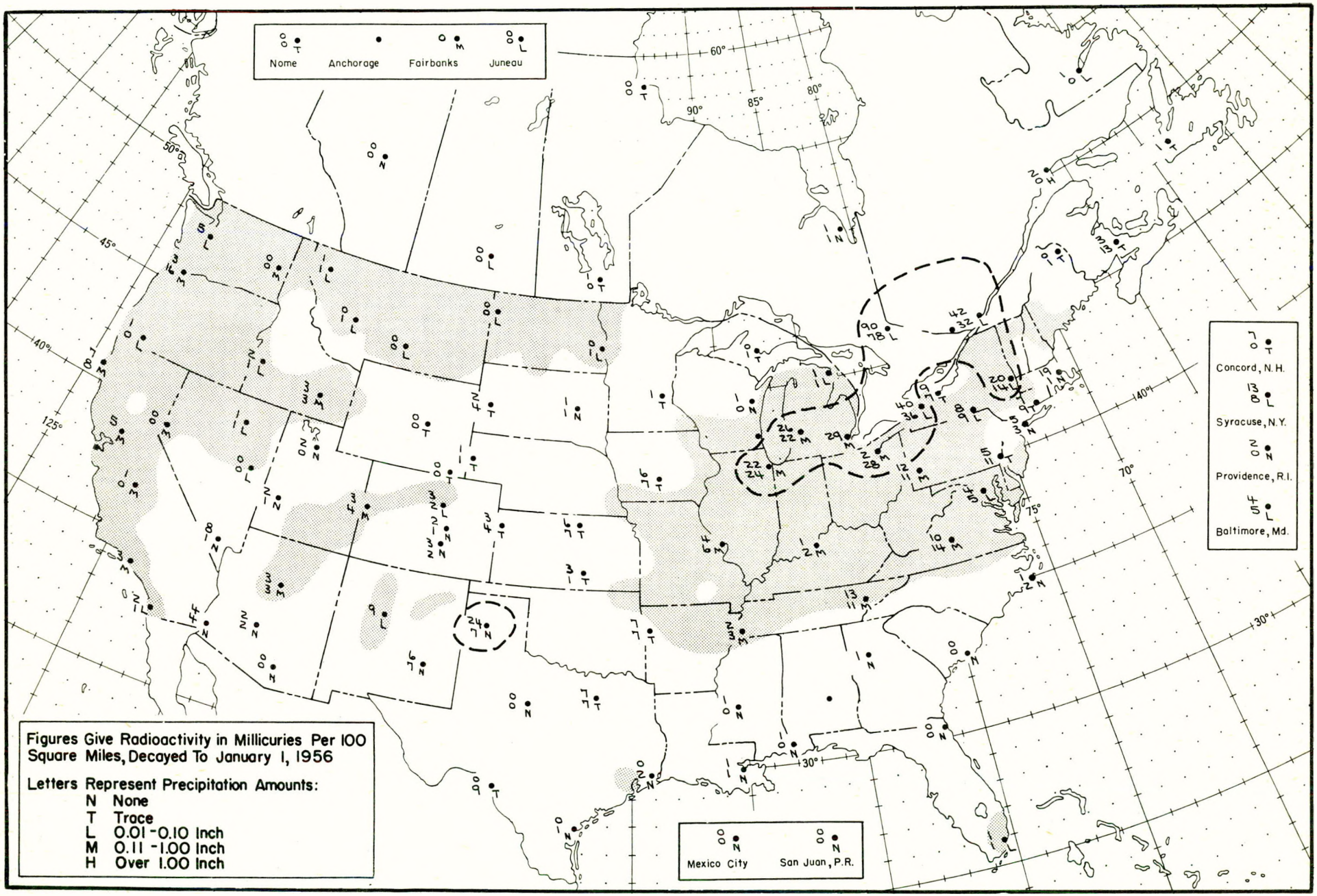

Figure A.9 Radioactive fallout in the 24-hour period beginning 1230 G.C.T., February 26, 1955

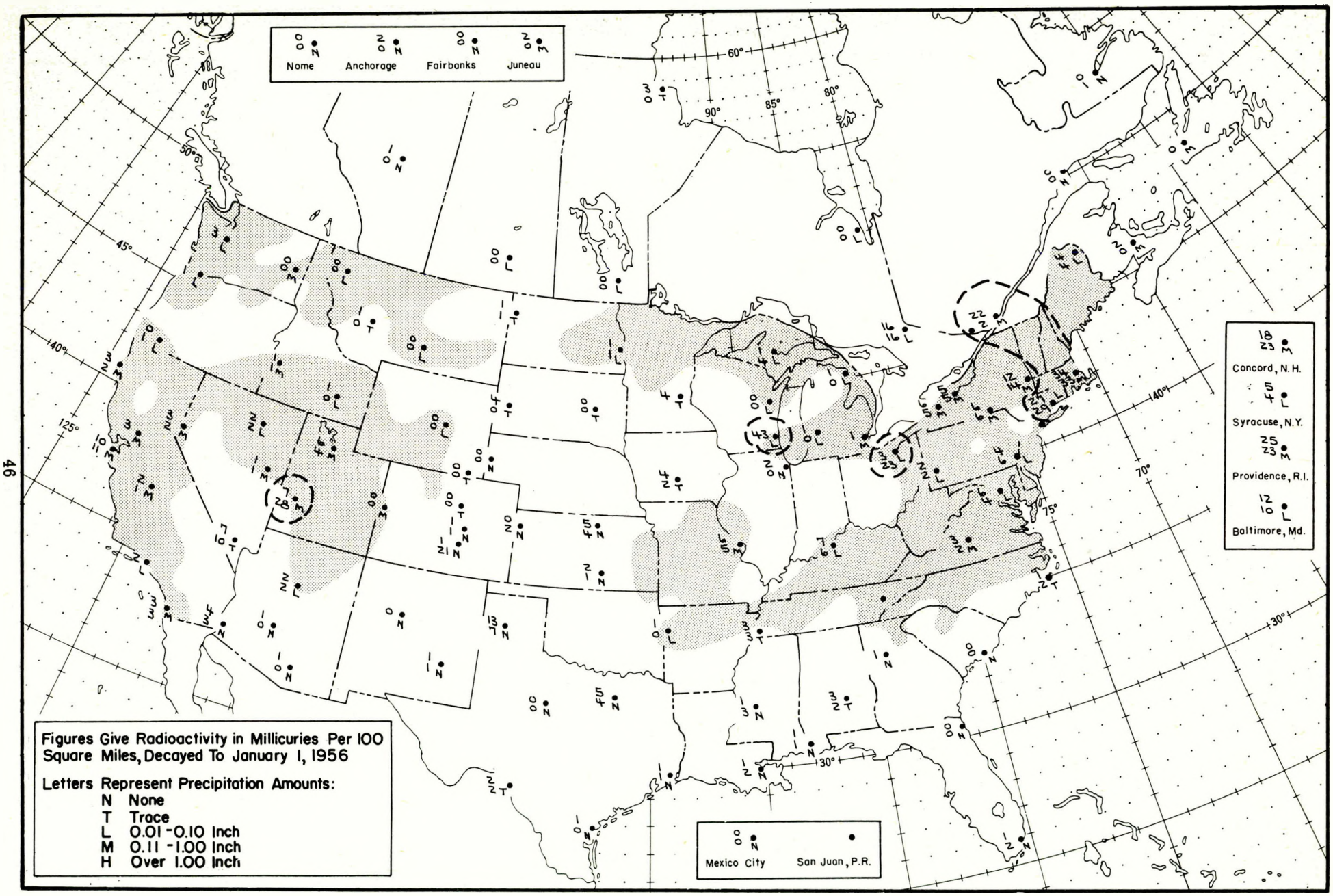

Figure A.10 Radioactive fallout in the 24-hour period beginning 1230 G.C.T., February 27, 1955

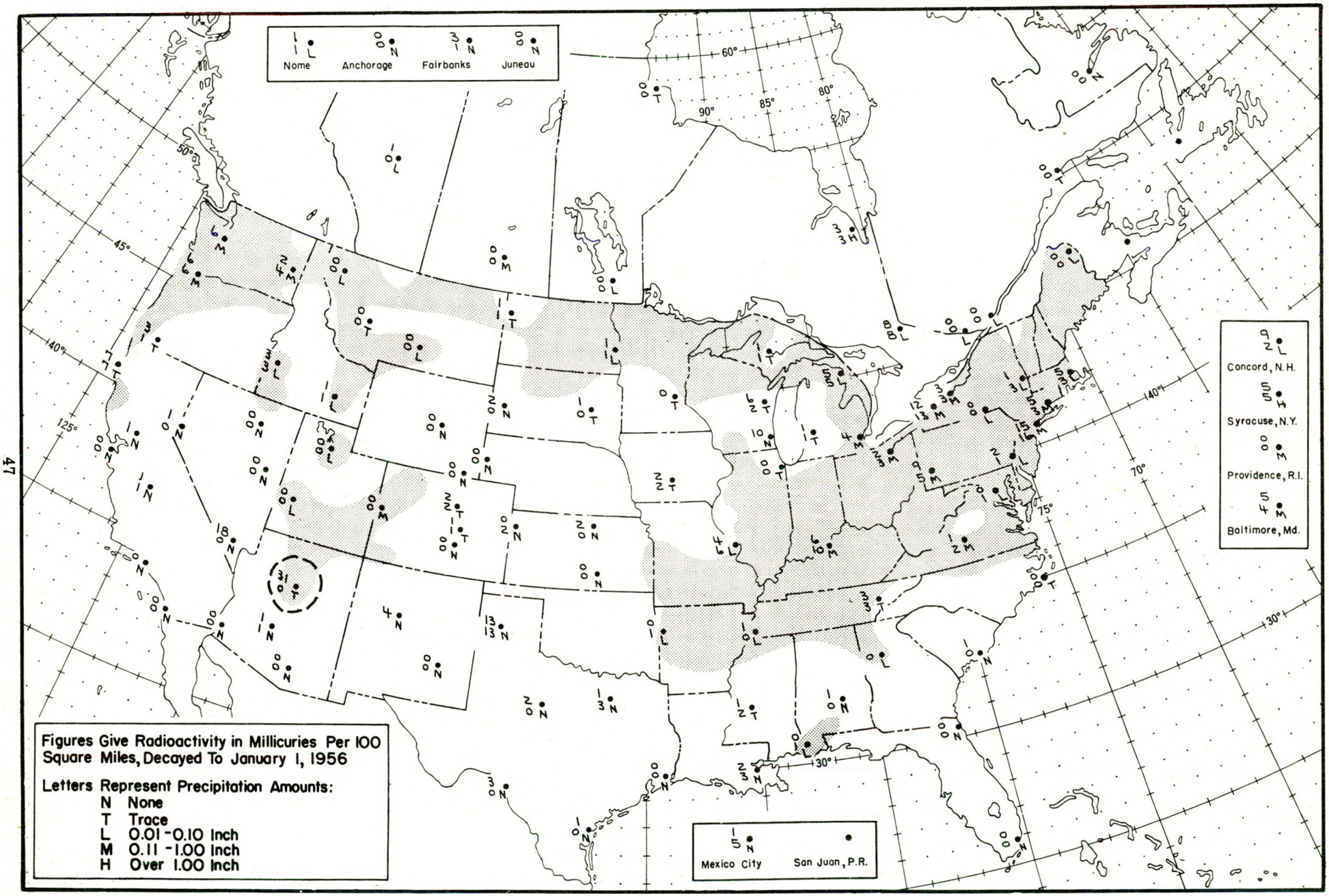

Figure A.11 Radioactive fallout in the 24-hour period beginning 1230 G.C.T., February 28, 1955

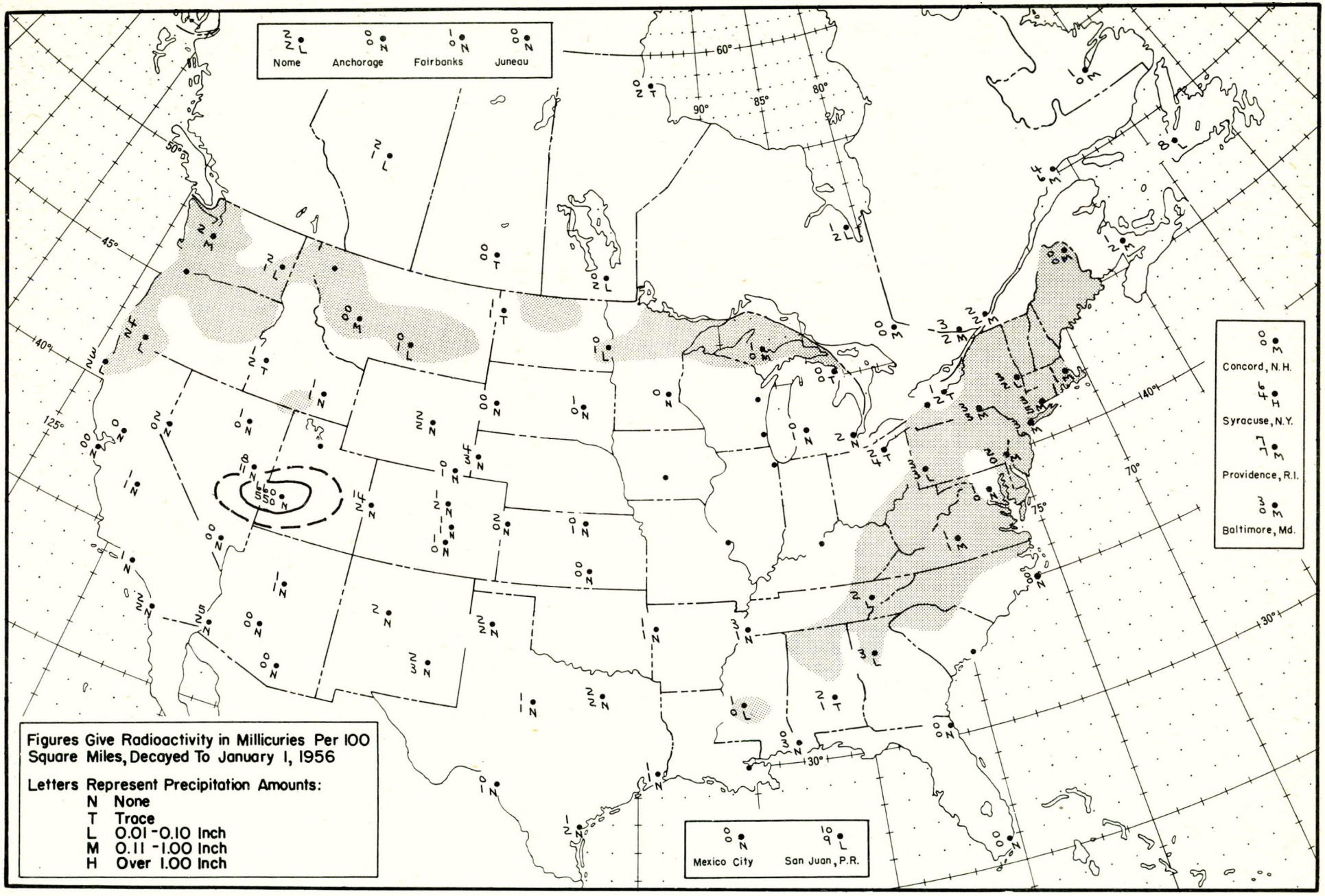

Figure A. 12 Radioactive fallout in the 24-hour period beginning 1230 G.C.T., March 1, 1955

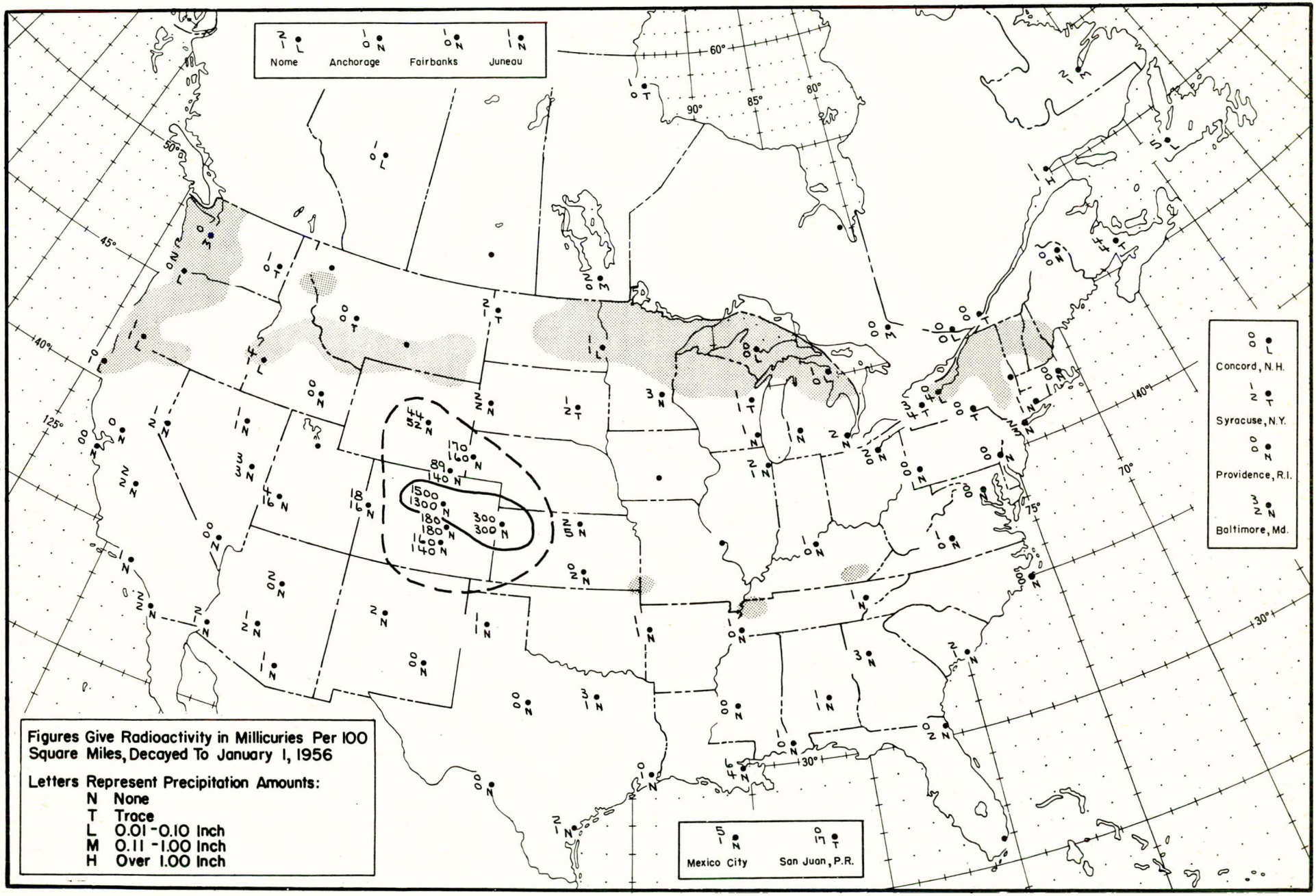

Figure A.13 Radioactive fallout in the 24-hour period beginning 1230 G.C.T., March 2, 1955

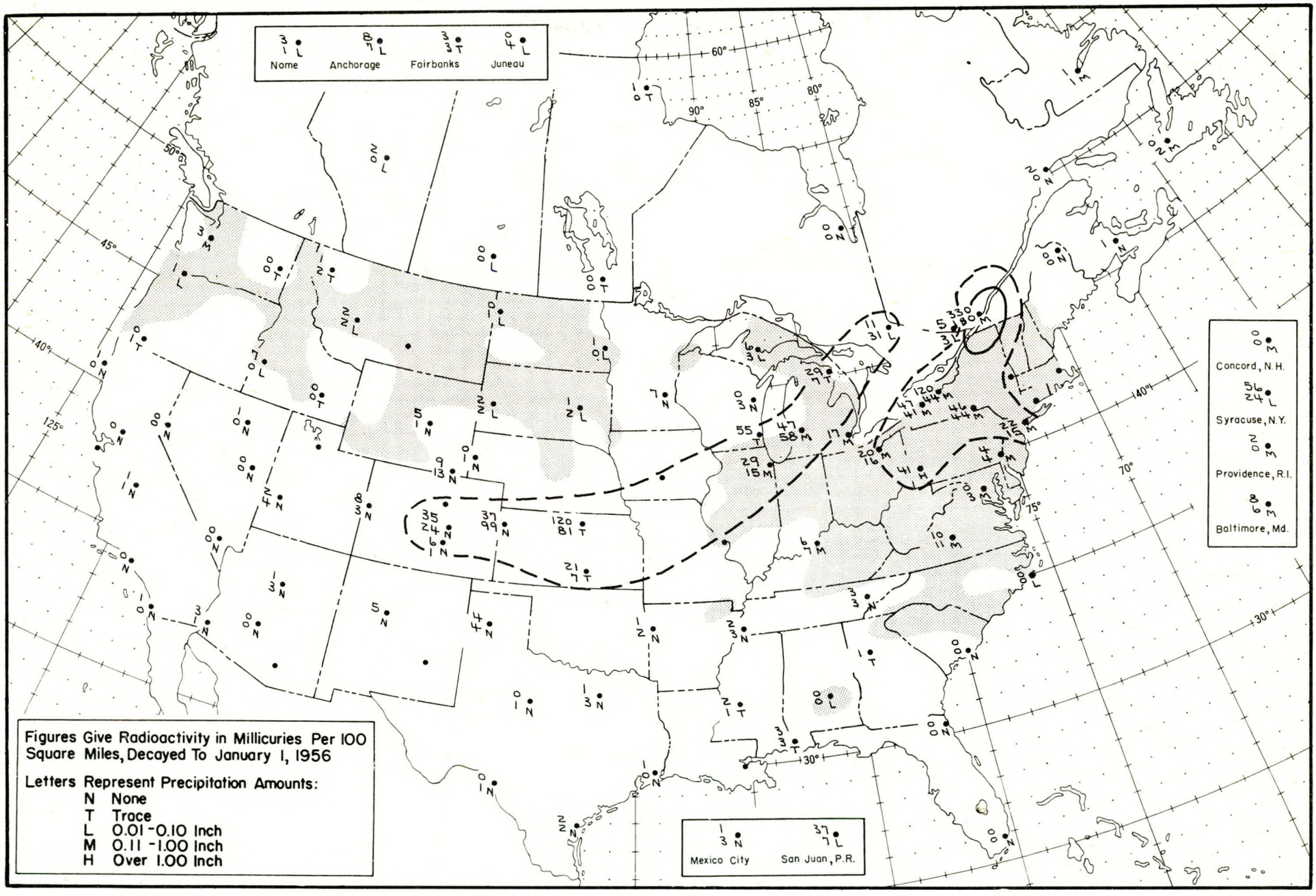

Figure A.14 Radioactive fallout in the 24-hour period beginning 1230 G.C.T., March 3, 1955

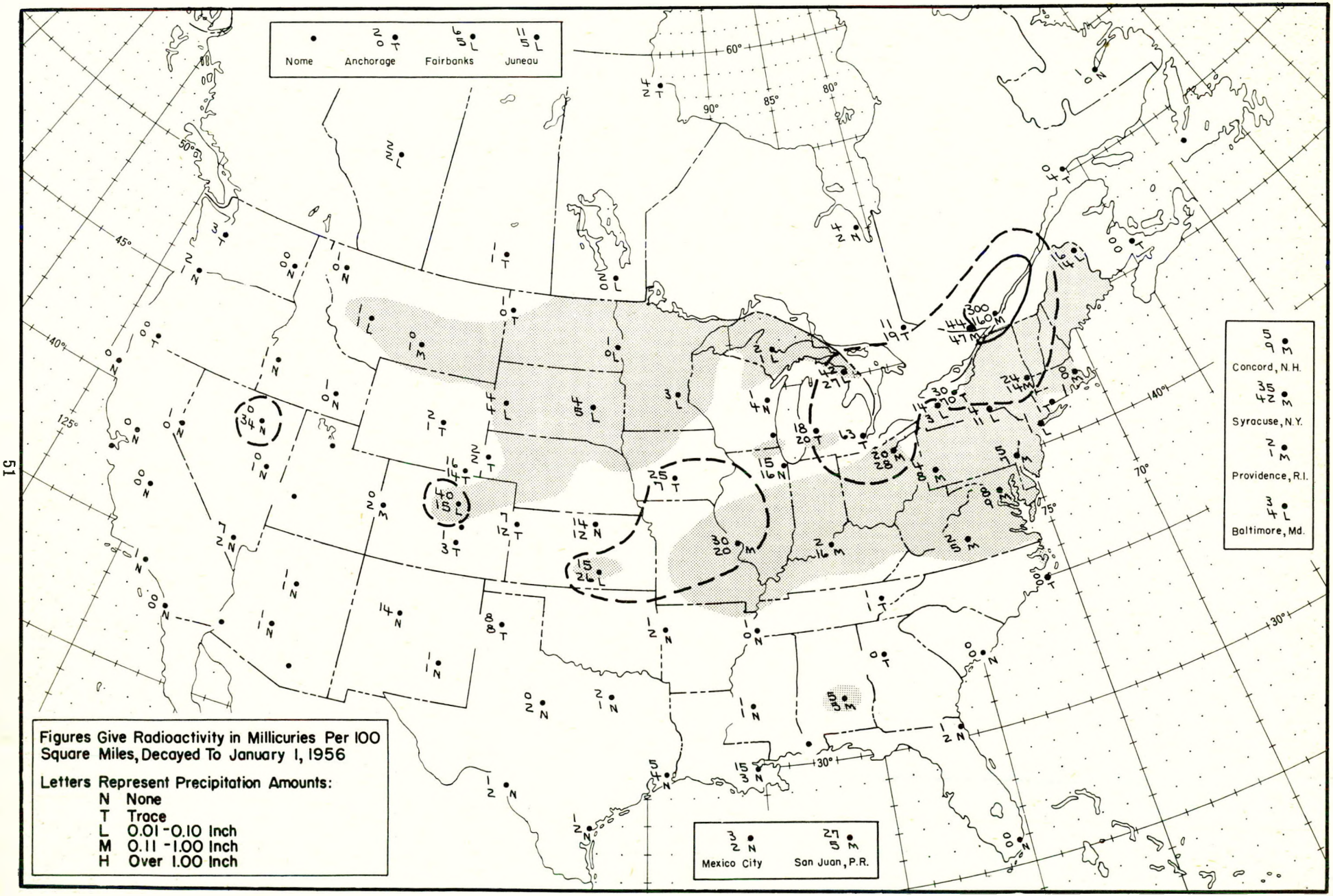

Figure A.15 Radioactive fallout in the 24-hour period beginning 1230 G.C.T., March 4, 1955

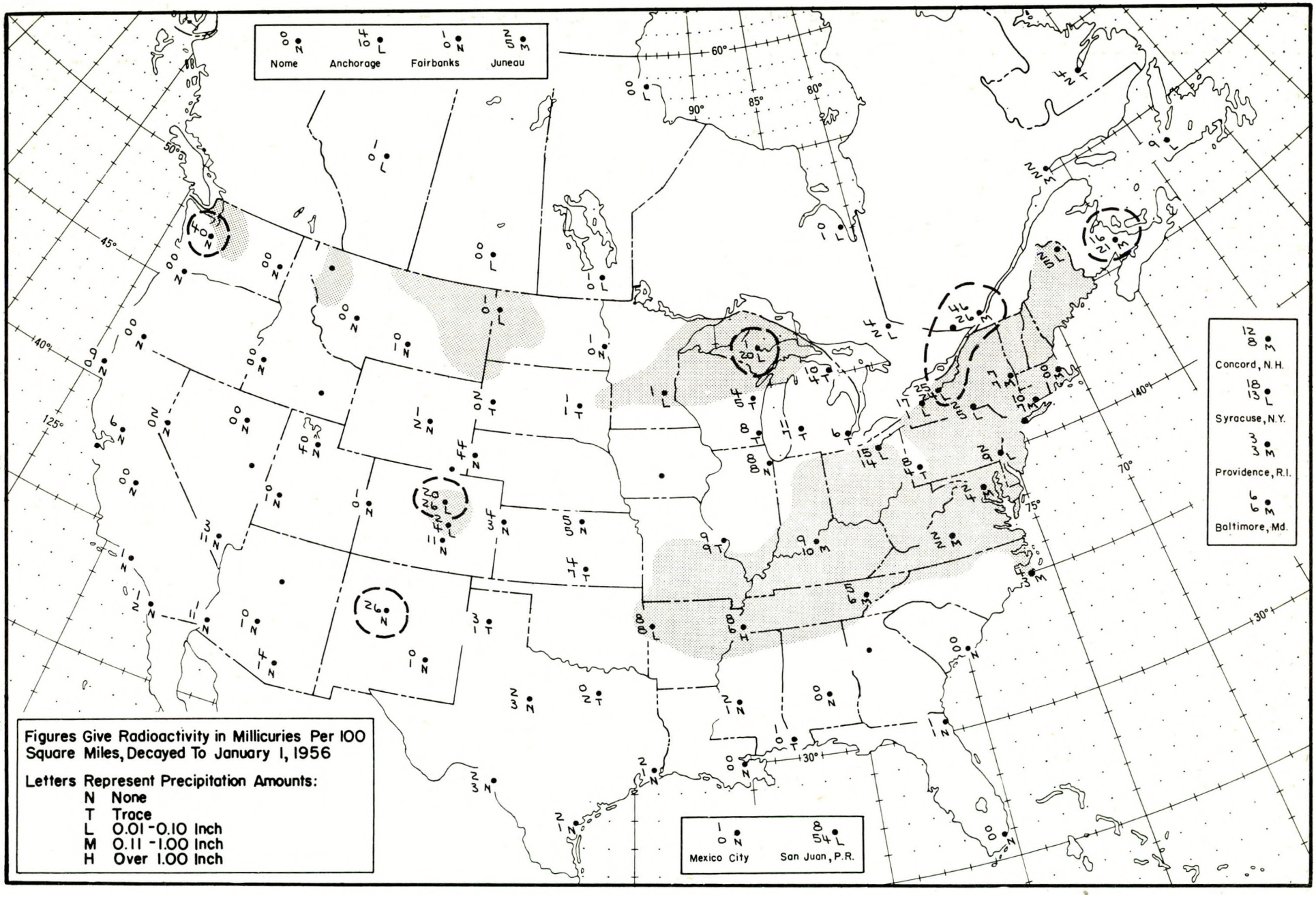

Figure A.16 Radioactive fallout in the 24-hour period beginning 1230 G.C.T., March 5, 1955

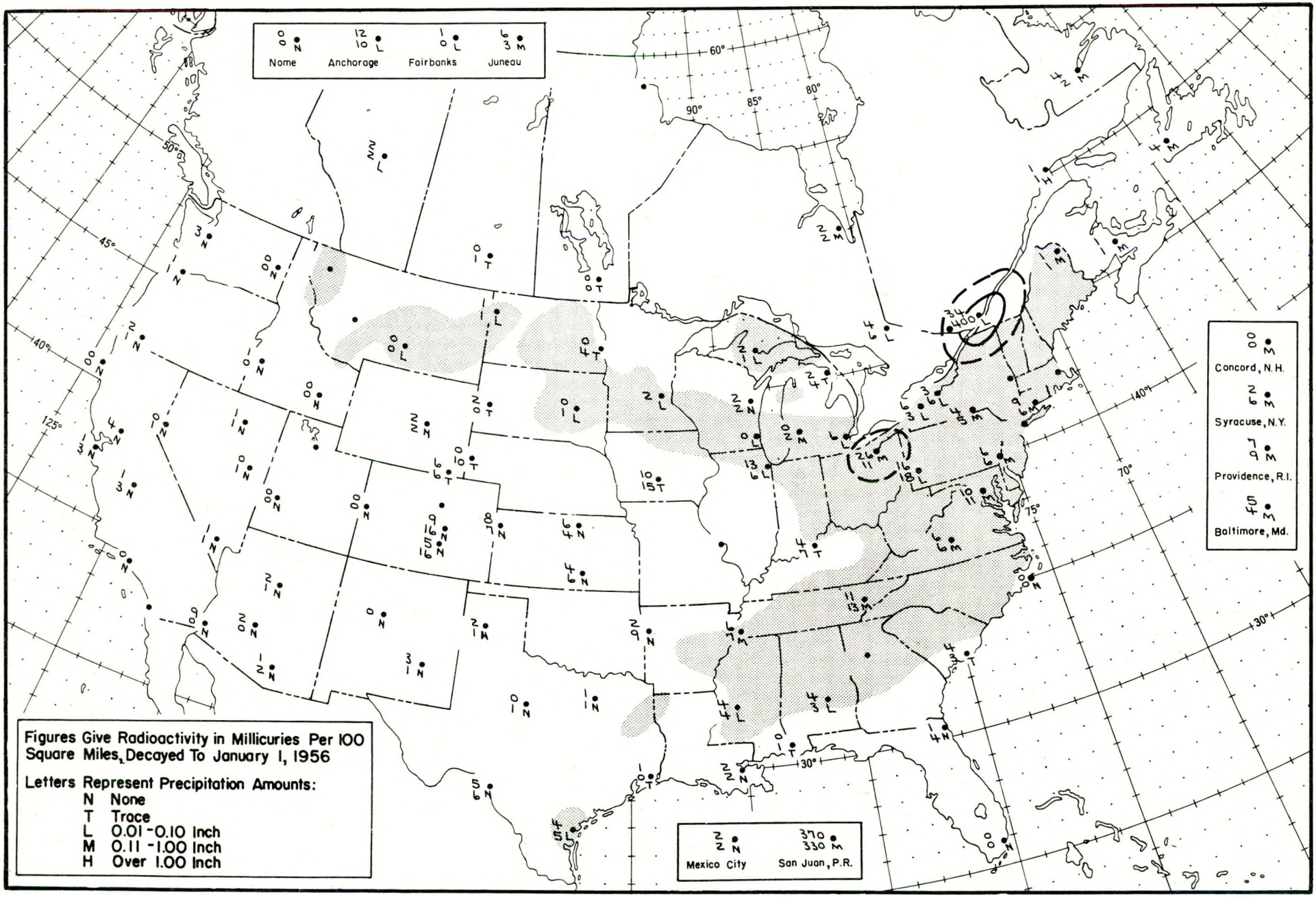

Figure A.17 Radioactive fallout in the 24-hour period beginning 1230 G.C.T., March 6, 1955

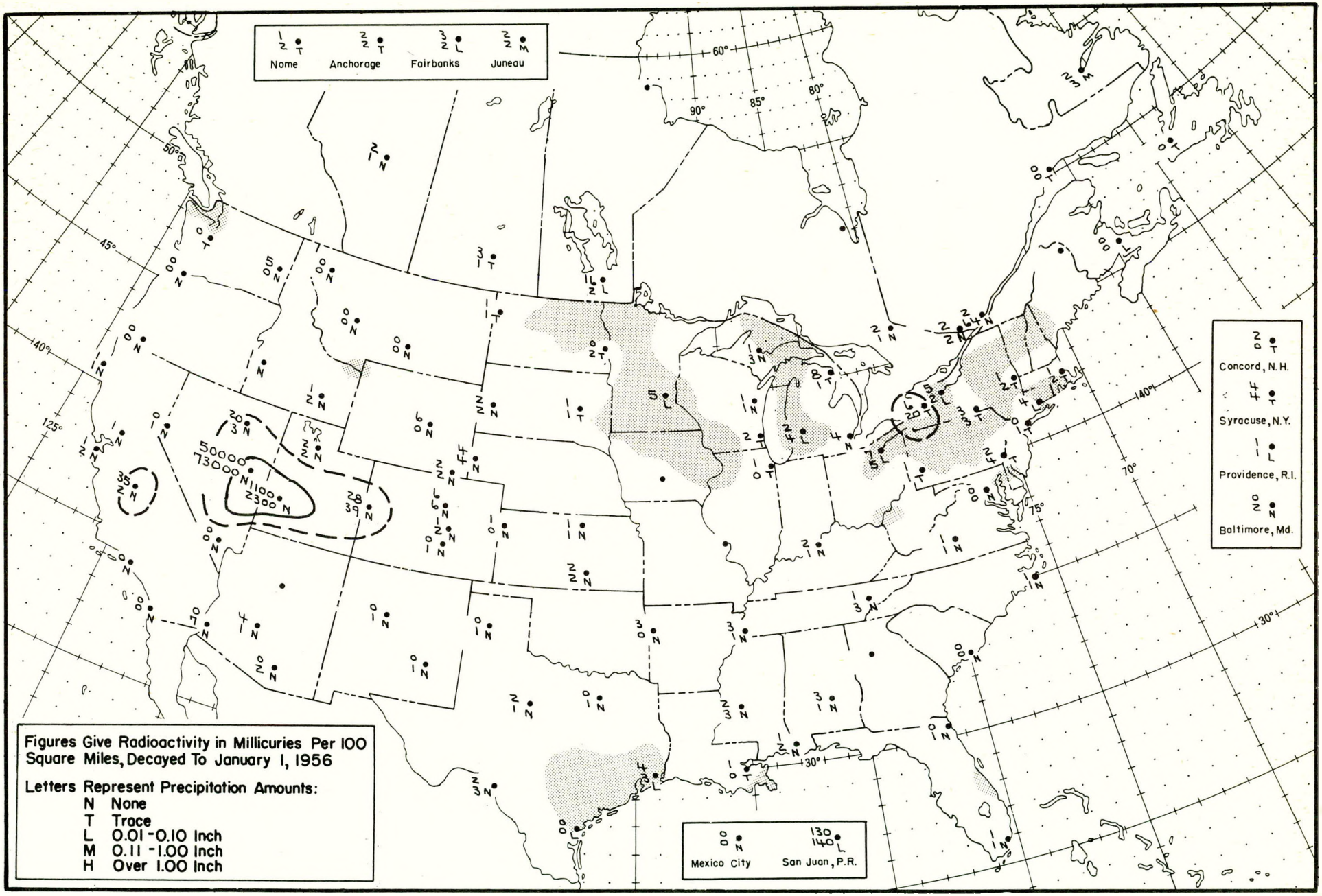

Figure A.18 Radioactive fallout in the 24-hour period beginning 1230 G.C.T., March 7, 1955

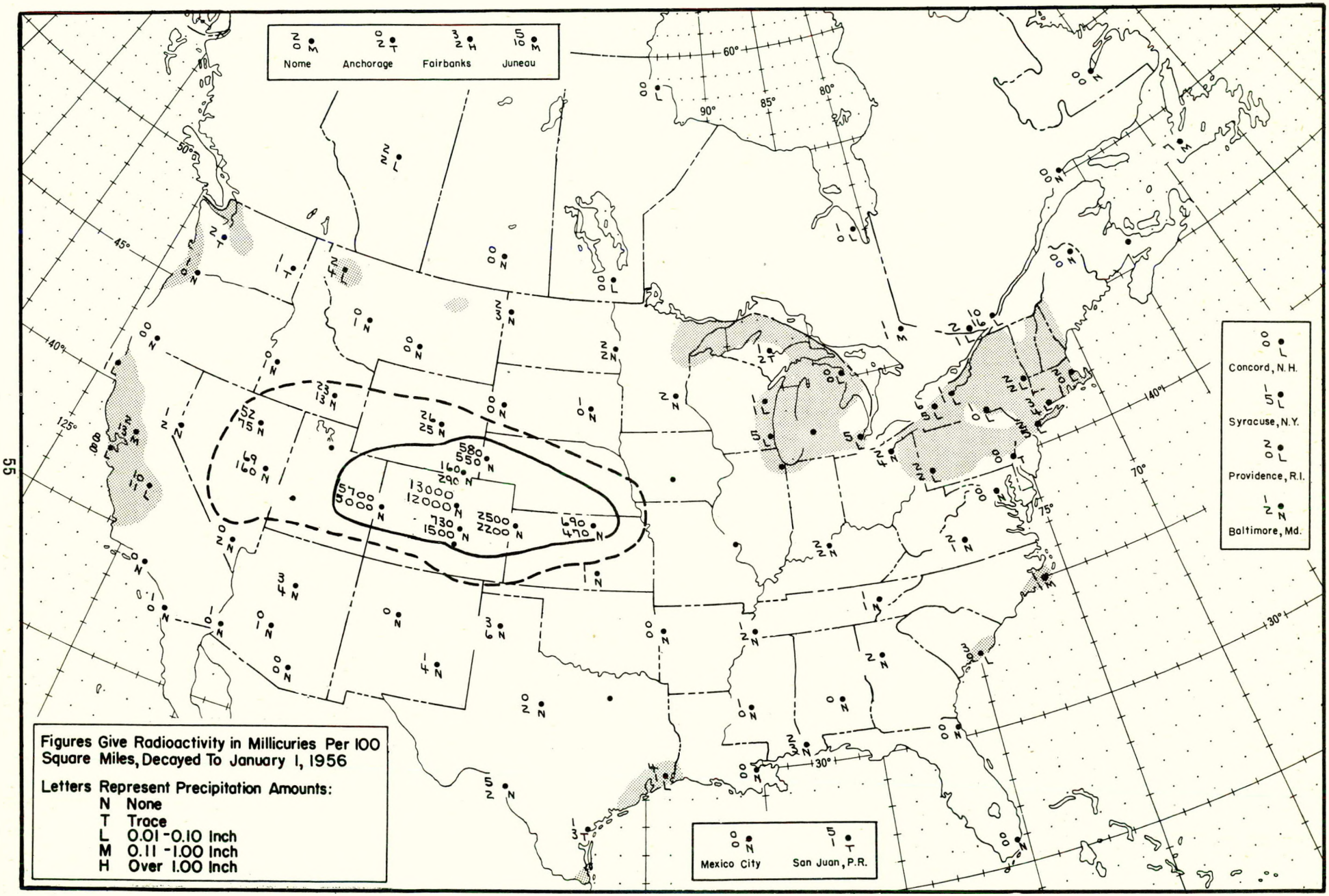

Figure A. 19 Radioactive fallout in the 24-hour period beginning 1230 G.C.T., March 8, 1955

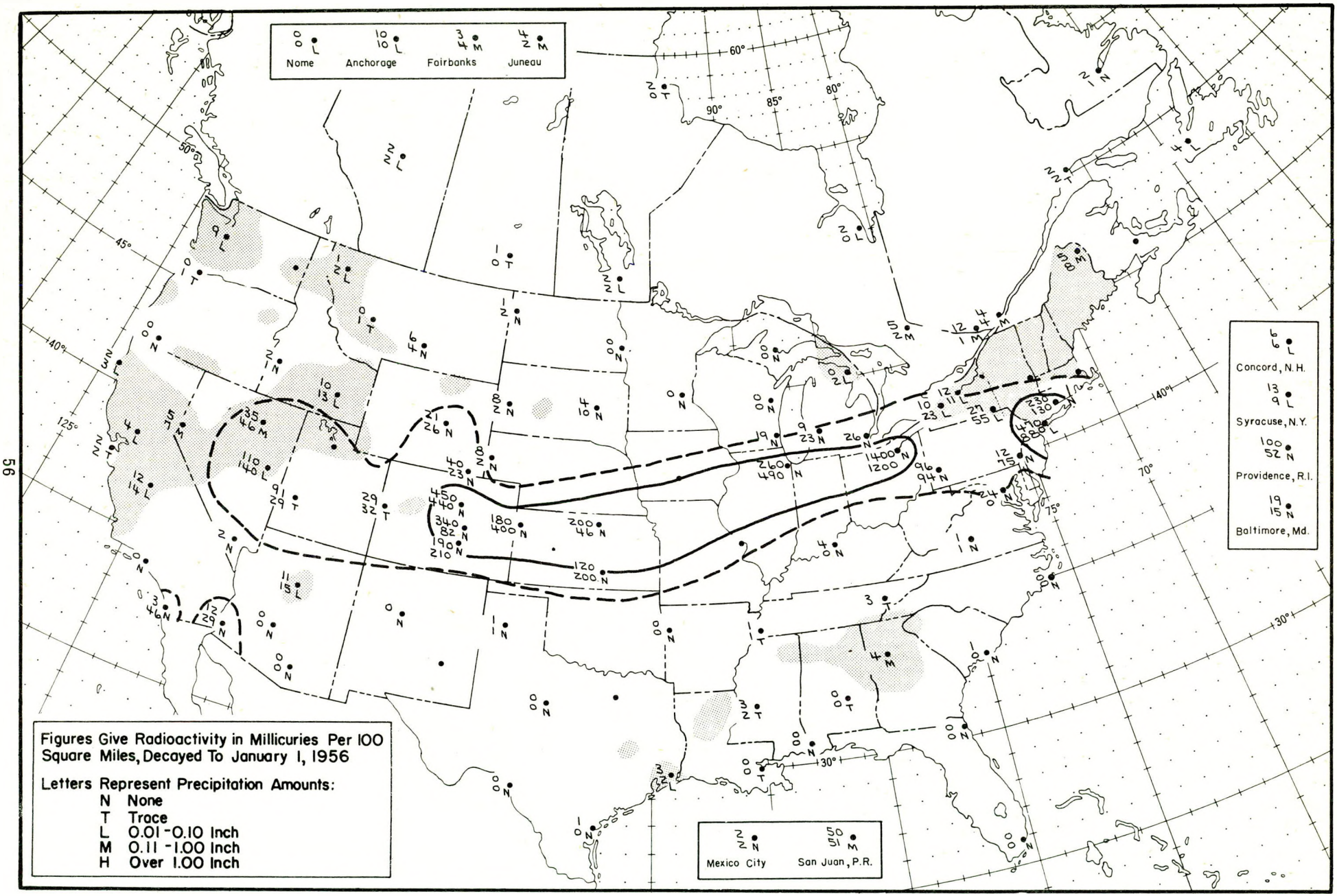

Figure A. 20 Radioactive fallout in the 24-hour period beginning 1230 G.C.T., March 9, 1955

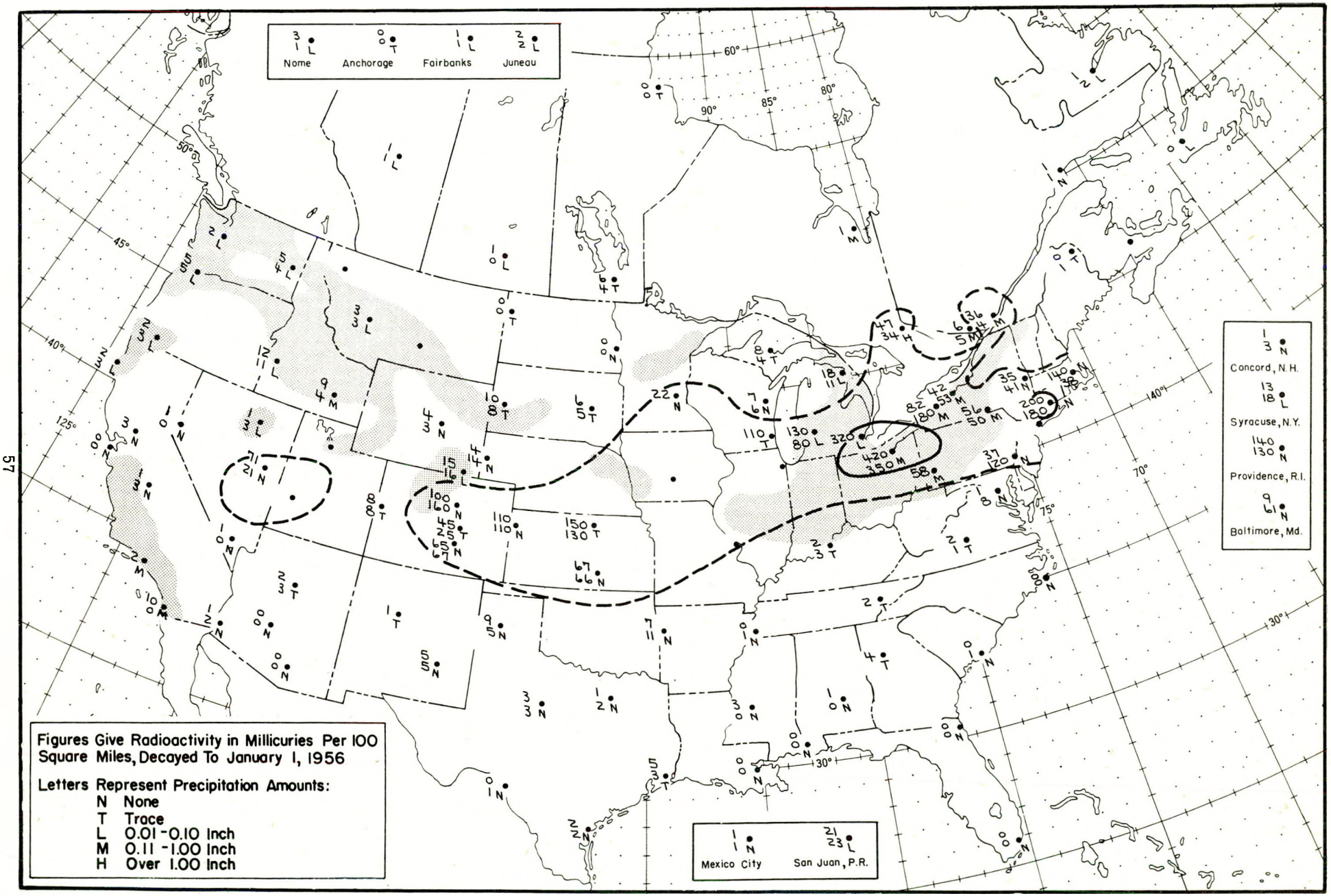

Figure A. 21 Radioactive fallout in the 24-hour period beginning 1230 G.C.T., March 10, 1955

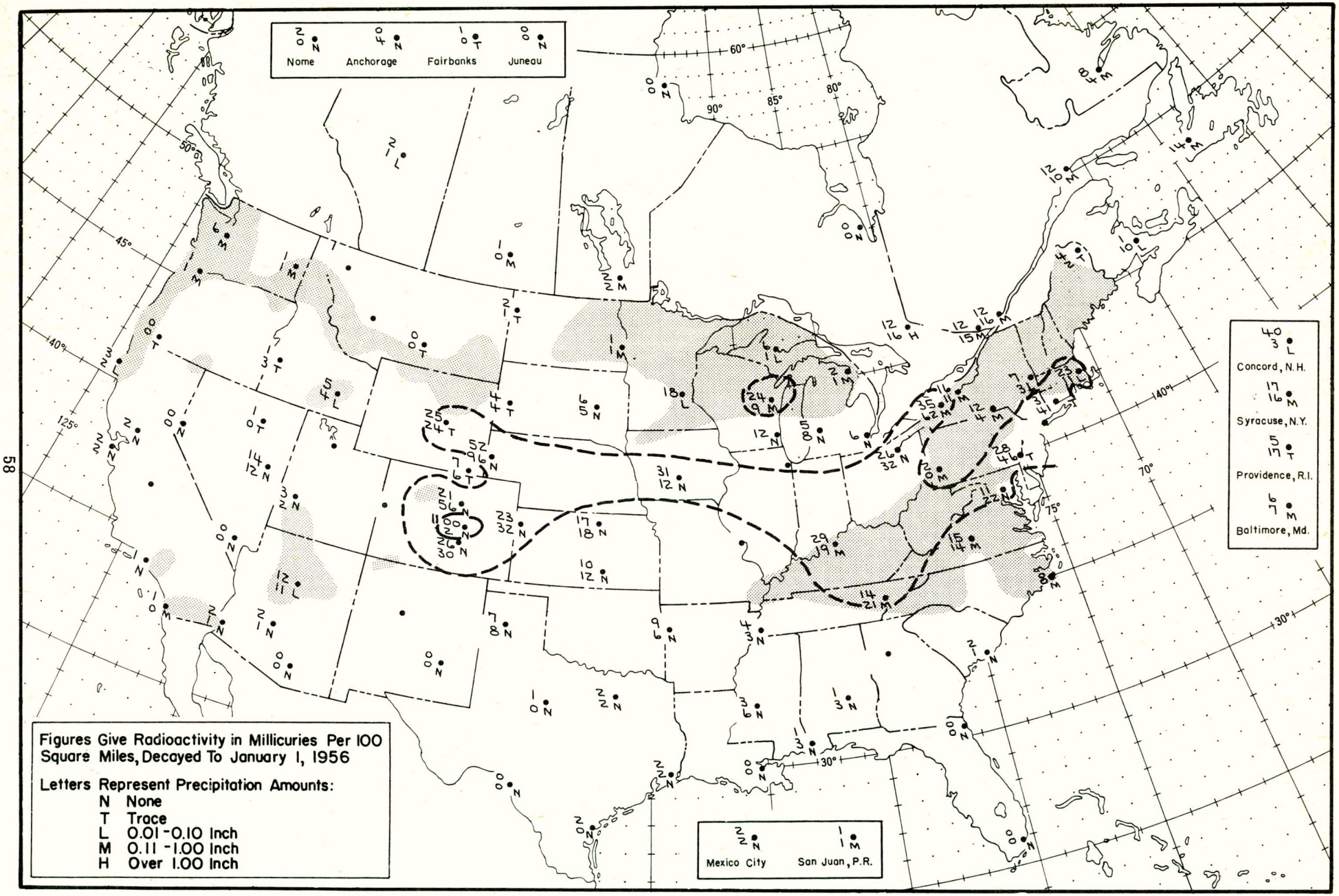

Figure A.22 Radioactive fallout in the 24-hour period beginning 1230 G.C.T., March 11, 1955

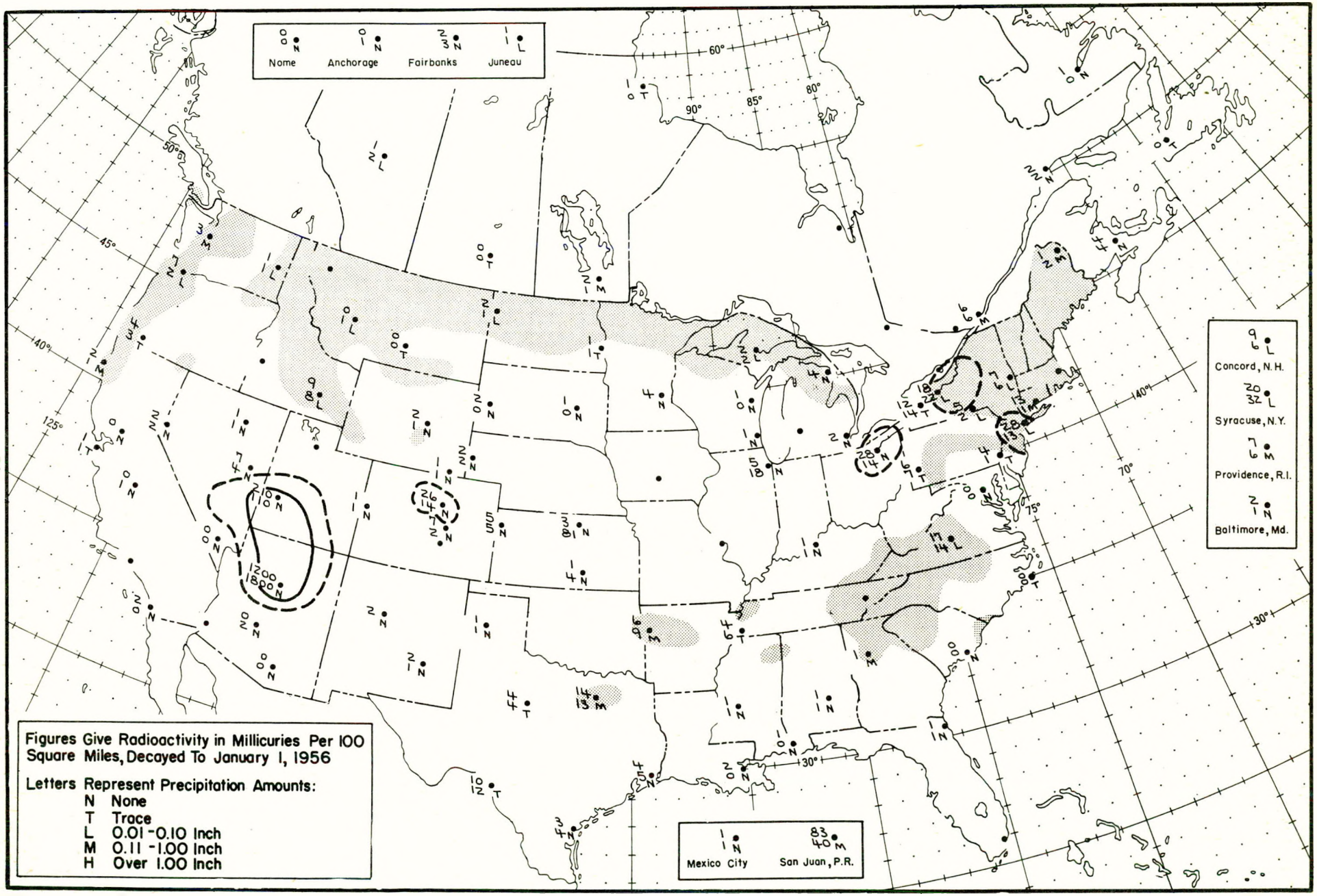

Figure A.23 Radioactive fallout in the 24-hour period beginning 1230 G.C.T., March 12, 1955

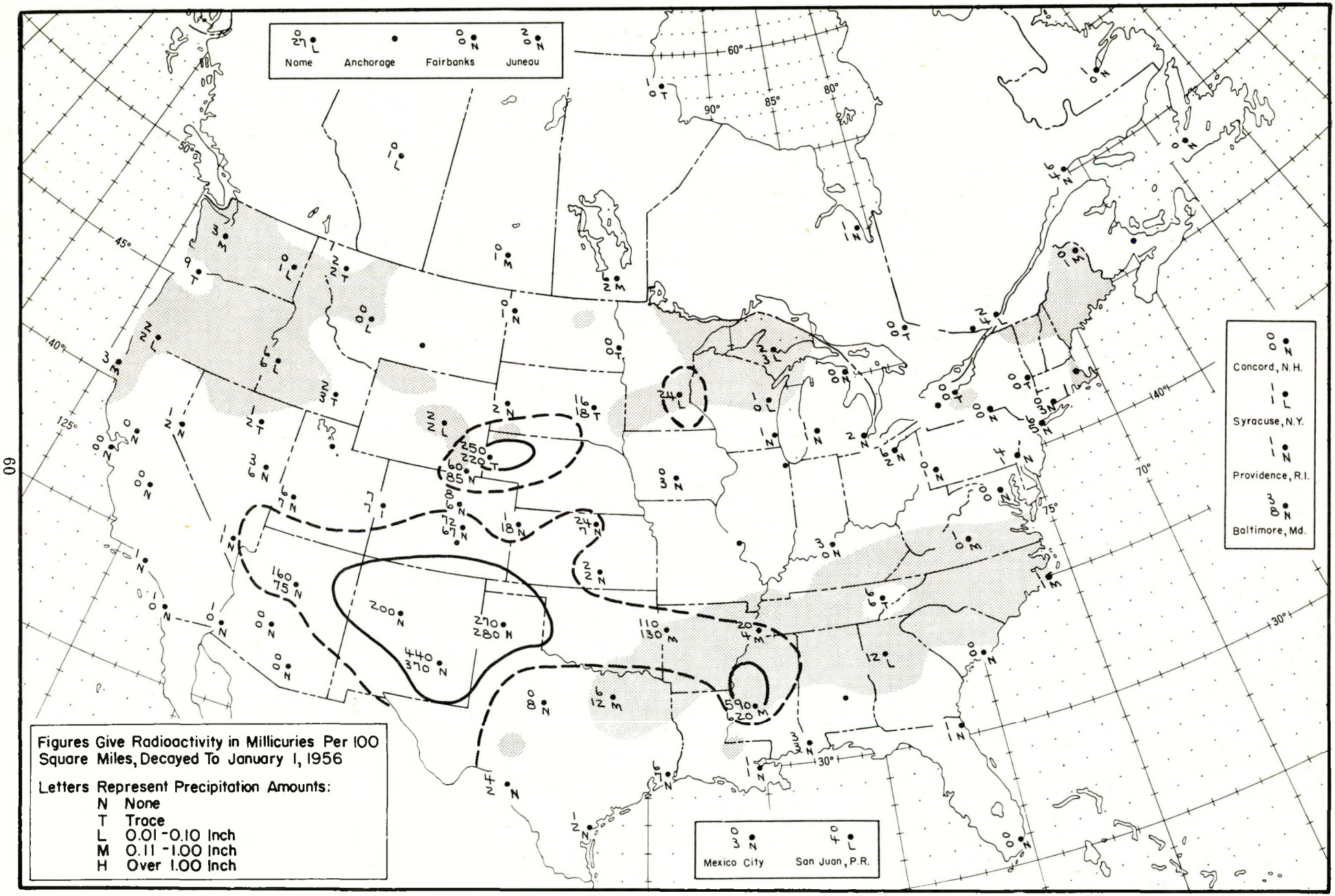

Figure A. 24 Radioactive fallout in the 24-hour period beginning 1230 G.C.T., March 13, 1955

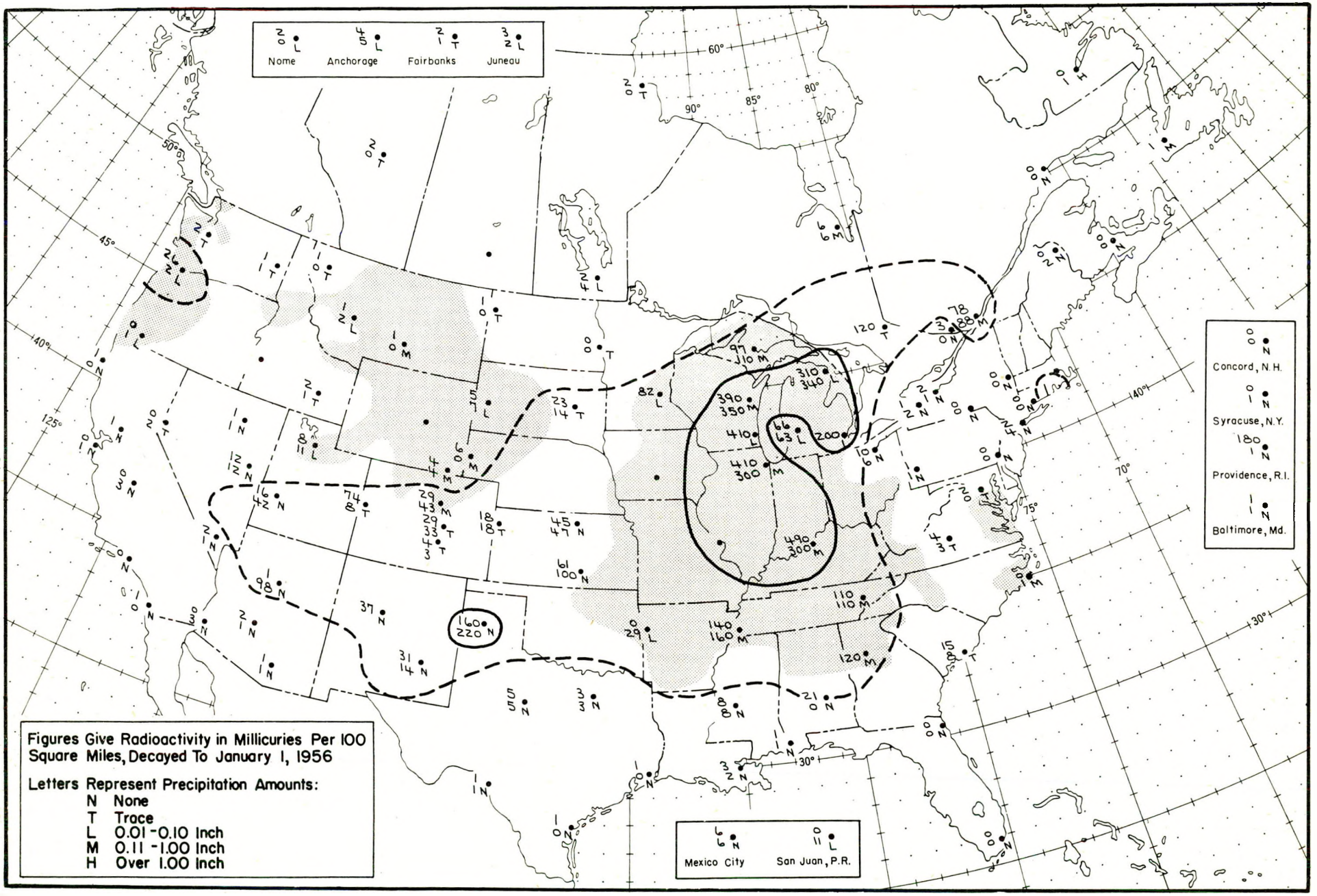

Figure A.25 Radioactive fallout in the 24-hour period beginning 1230 G.C.T., March 14, 1955

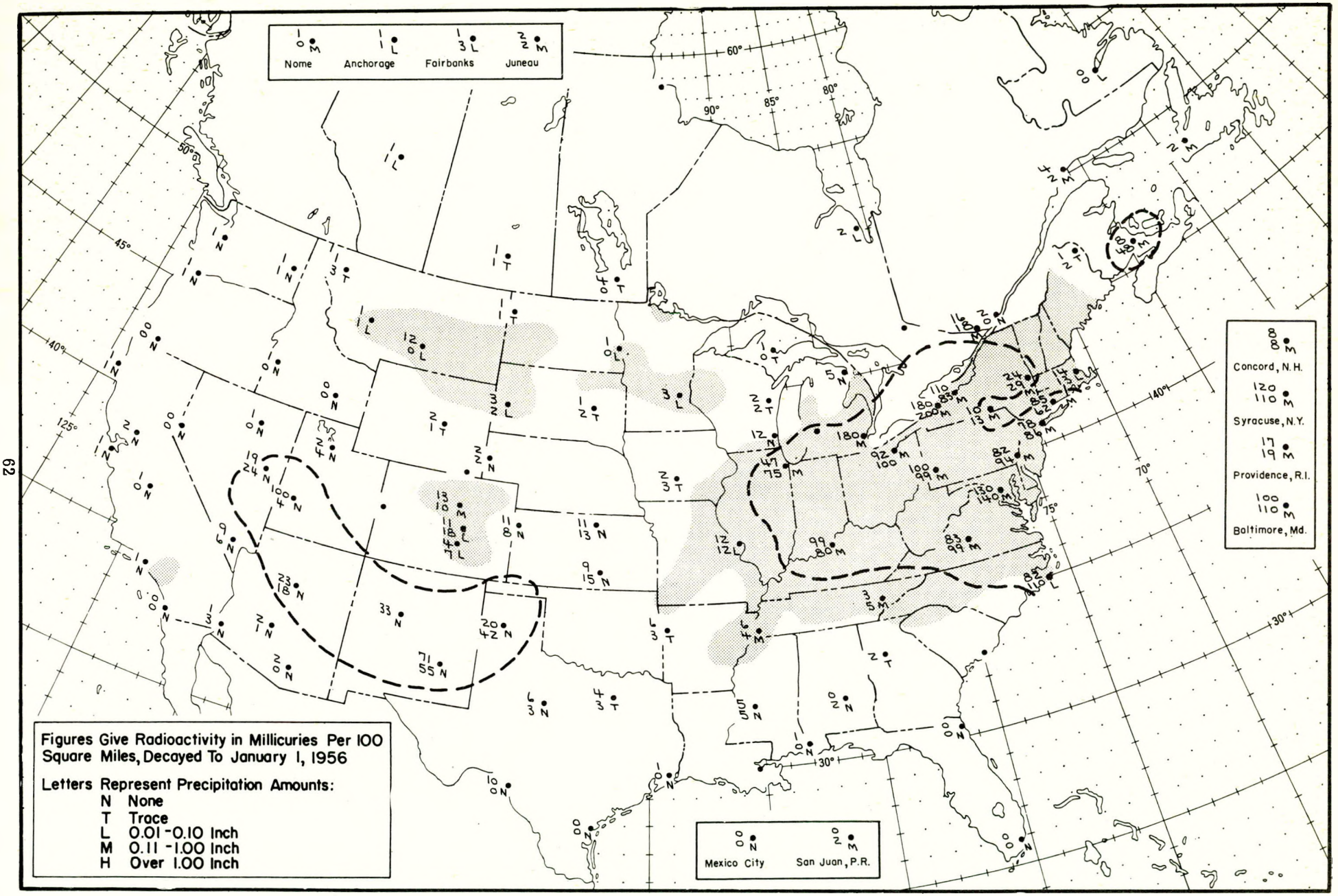

Figure A.26 Radioactive fallout in the 24-hour period beginning 1230 G.C.T., March 15, 1955

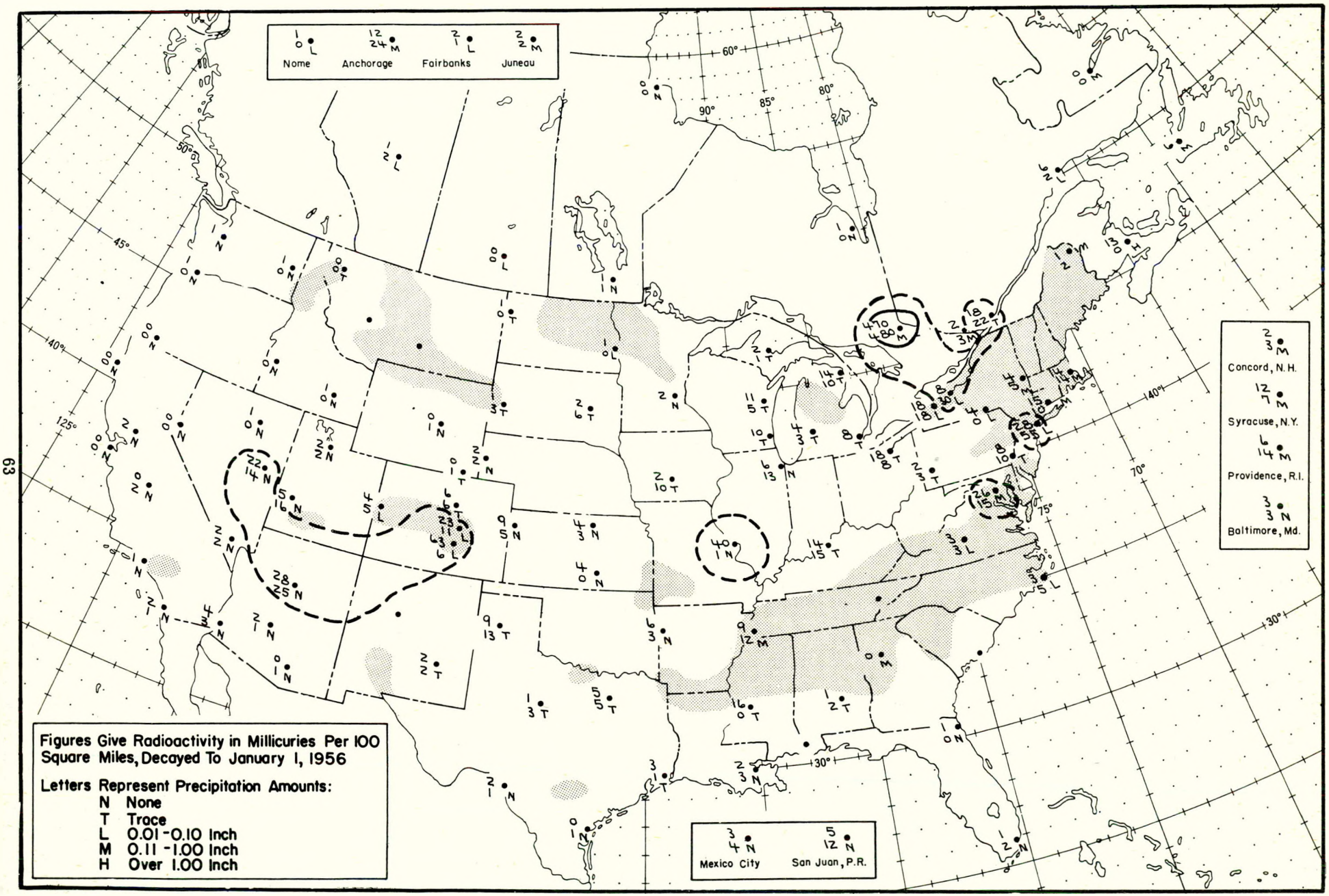

Figure A. 27 Radioactive fallout in the 24-hour period beginning 1230 G.C.T., March 16, 1955

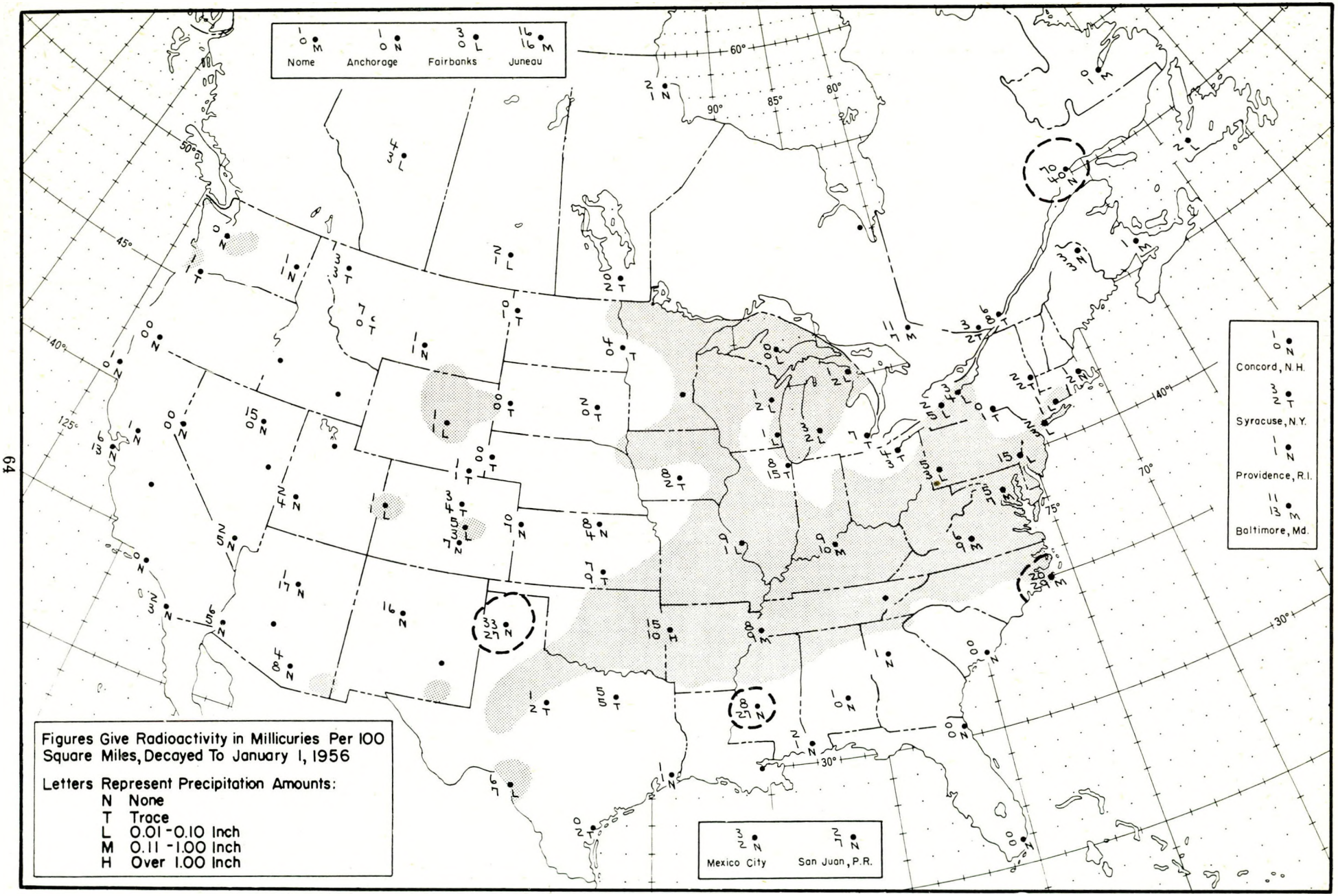

Figure A. 28 Radioactive fallout in the 24-hour period beginning 1230 G.C.T., March 17, 1955

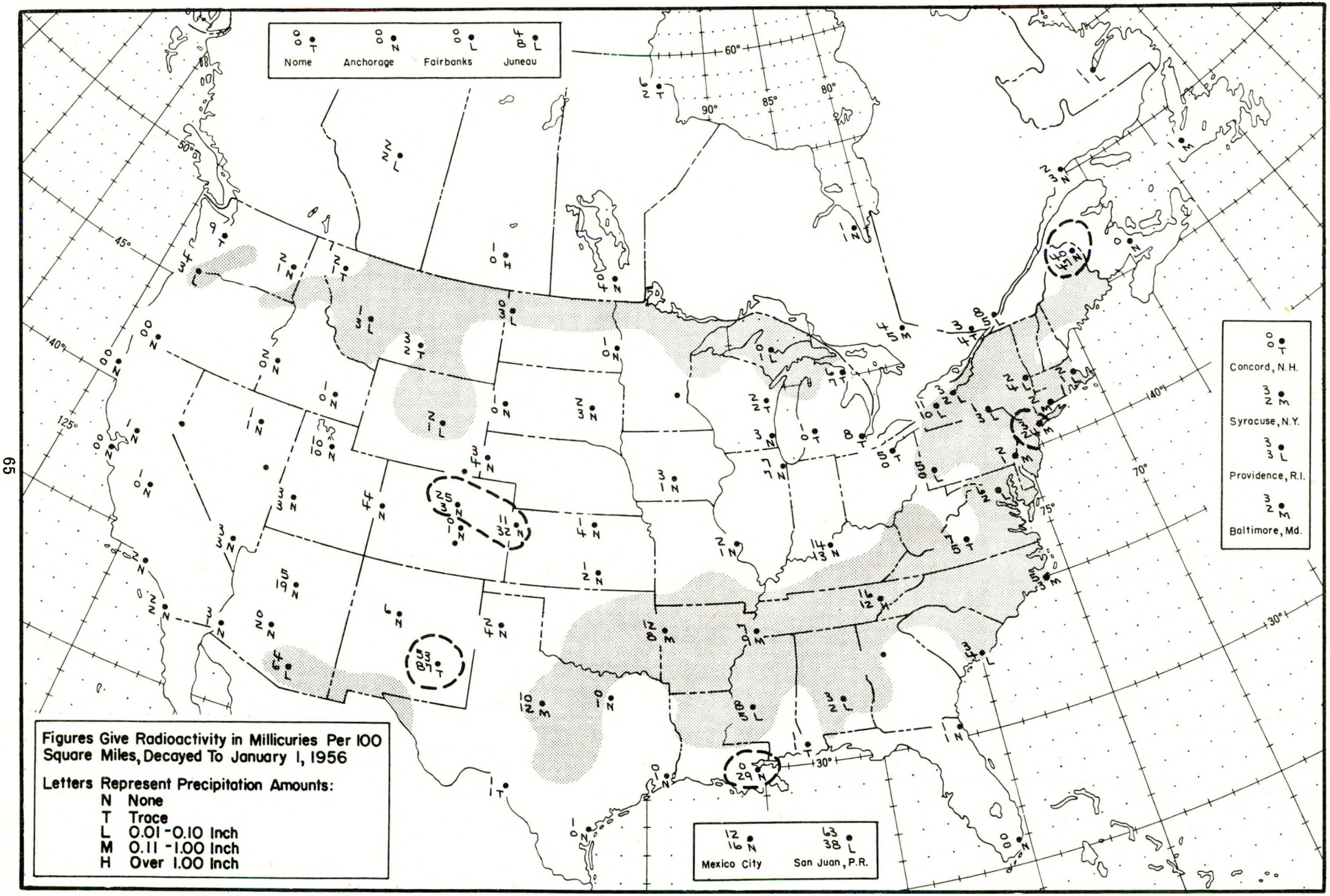

Figure A.29 Radioactive fallout in the 24-hour period beginning 1230 G.C.T., March 18, 1955

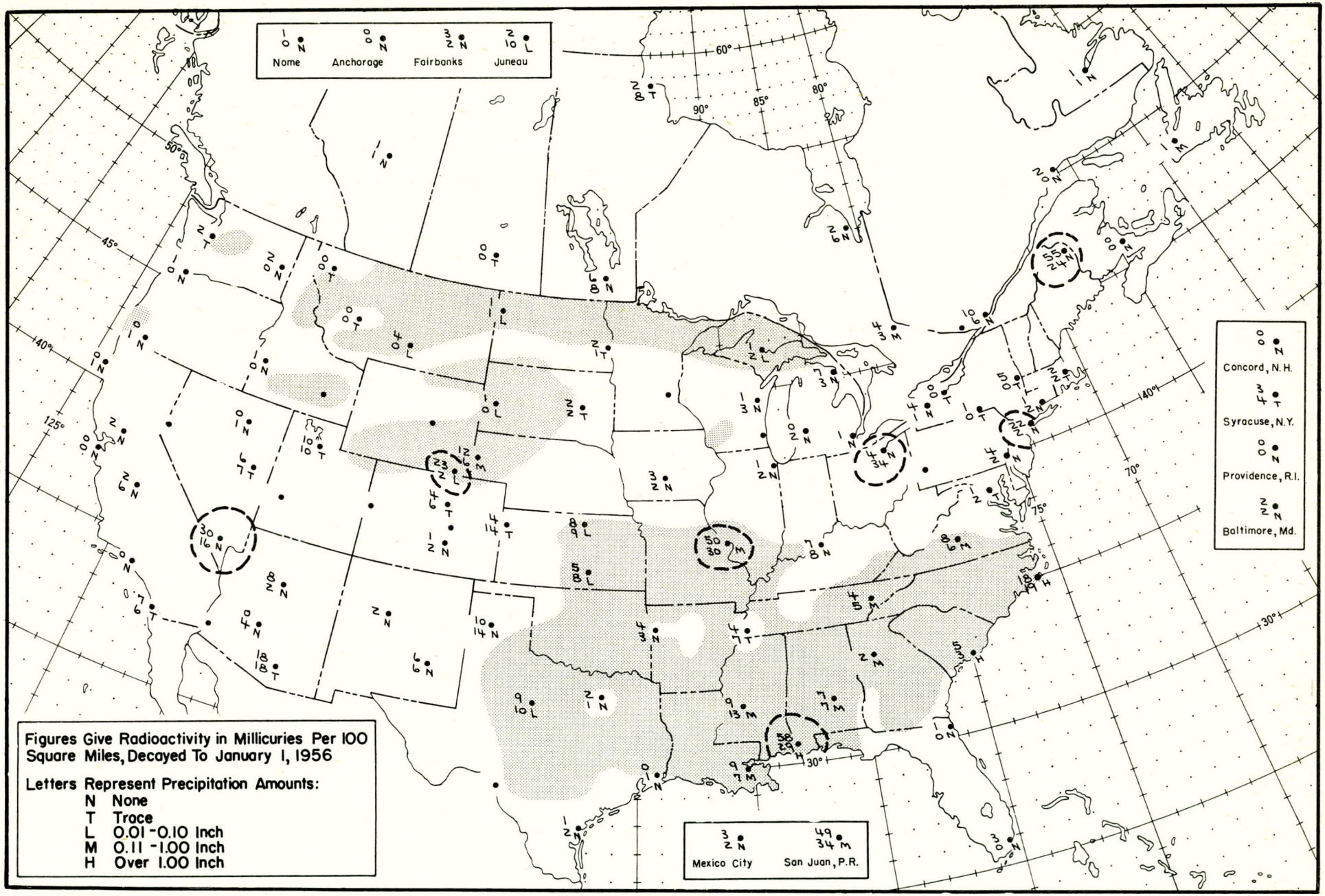

Figure A. 30 Radioactive fallout in the 24-hour period beginning 1230 G.C.T., March 19, 1955

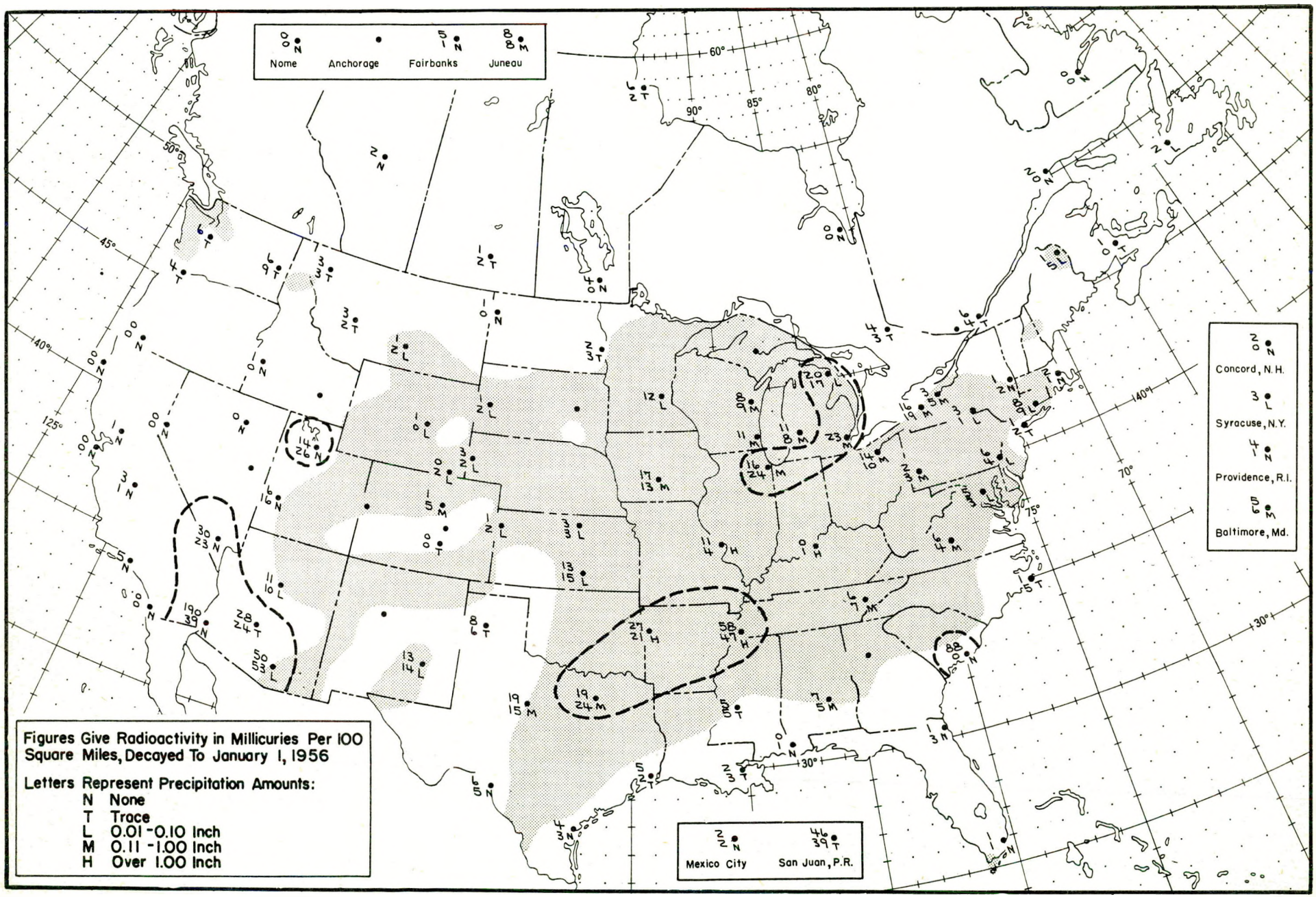

Figure A.31 Radioactive fallout in the 24-hour period beginning 1230 G.C.T., March 20, 1955

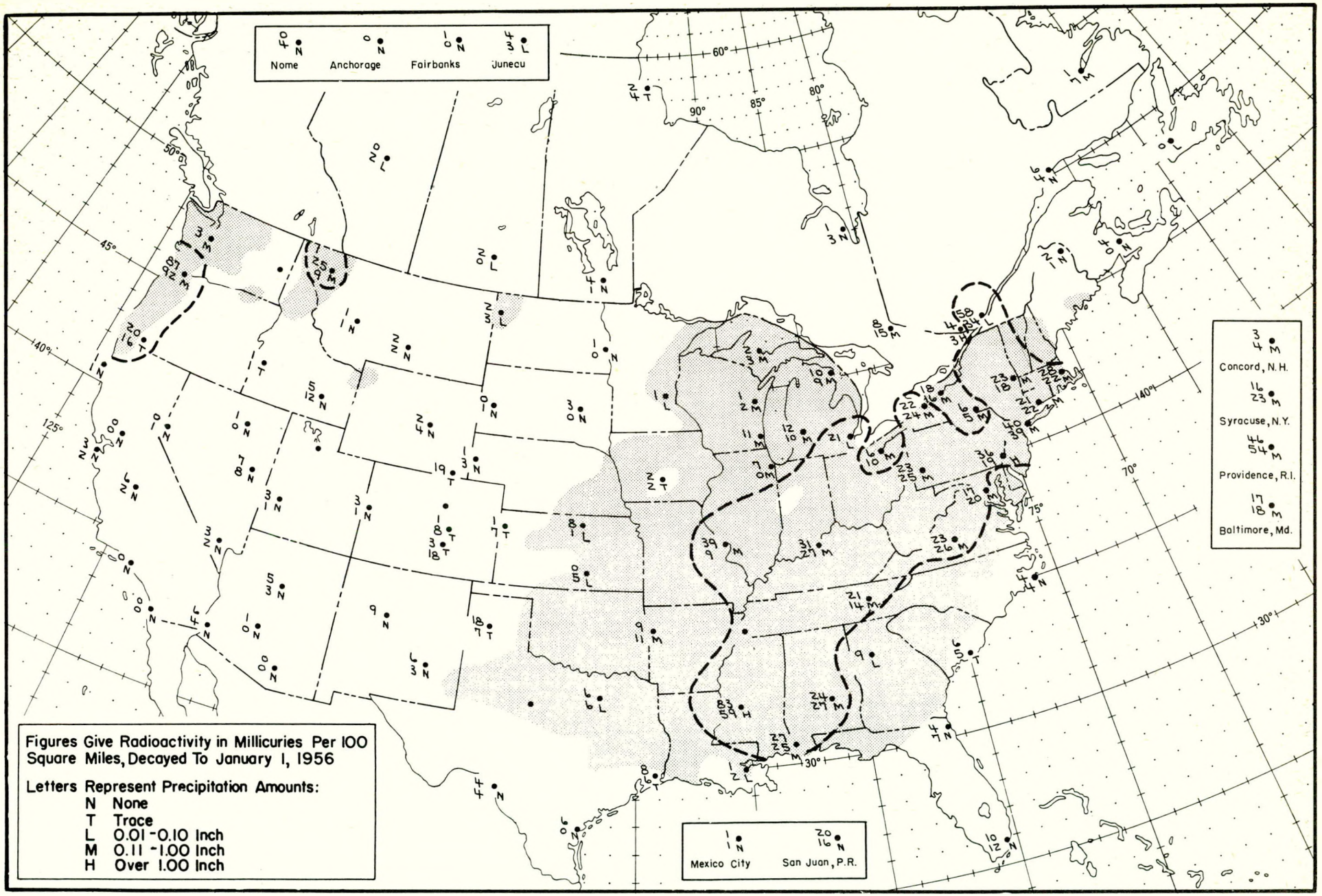

Figure A.32 Radioactive fallout in the 24-hour period beginning 1230 G.C.T., March 21, 1955

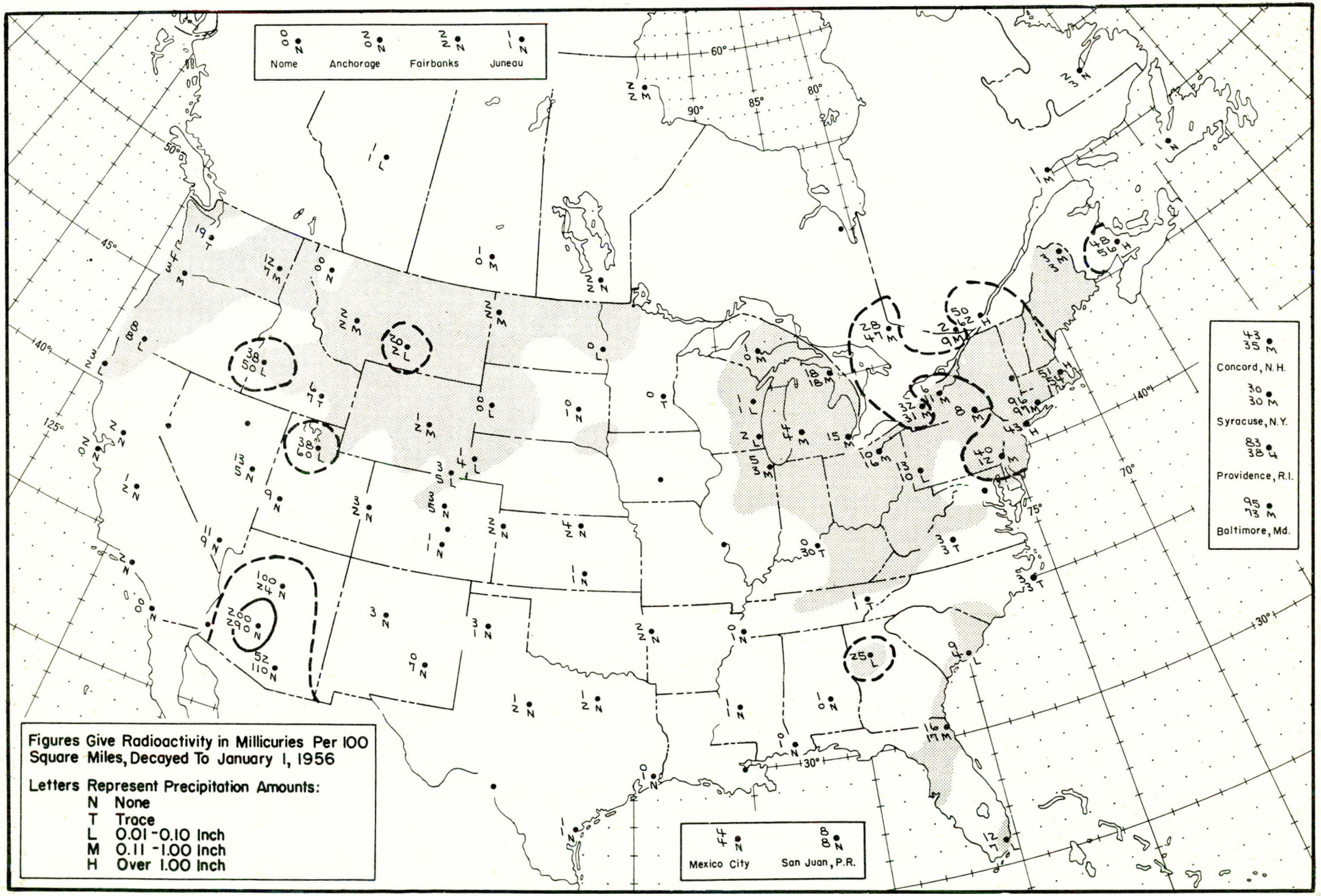

Figure A. 33 Radioactive fallout in the 24-hour period beginning 1230 G.C.T., March 22, 1955

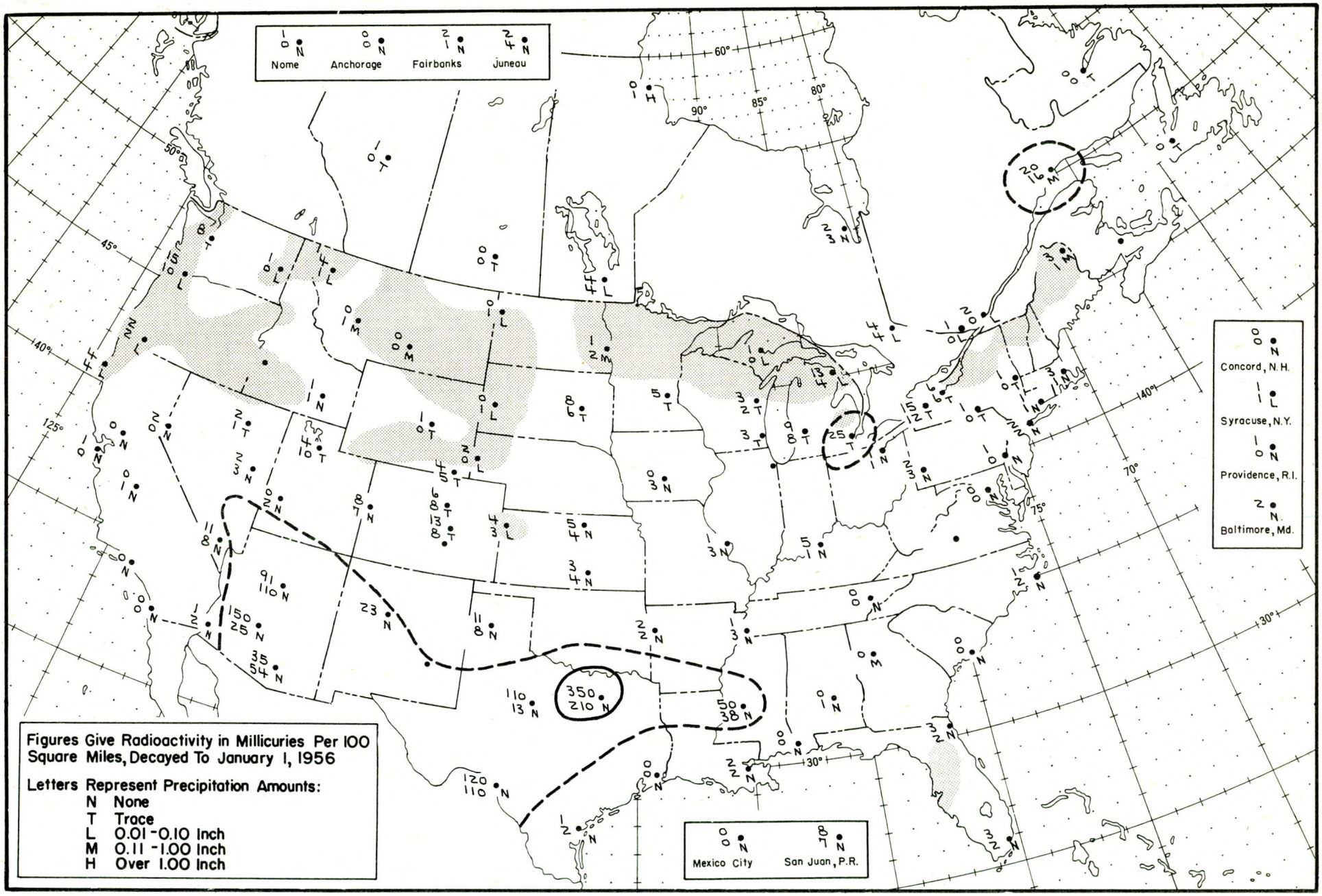

Figure A.34 Radioactive fallout in the 24-hour period beginning 1230 G.C.T., March 23, 1955

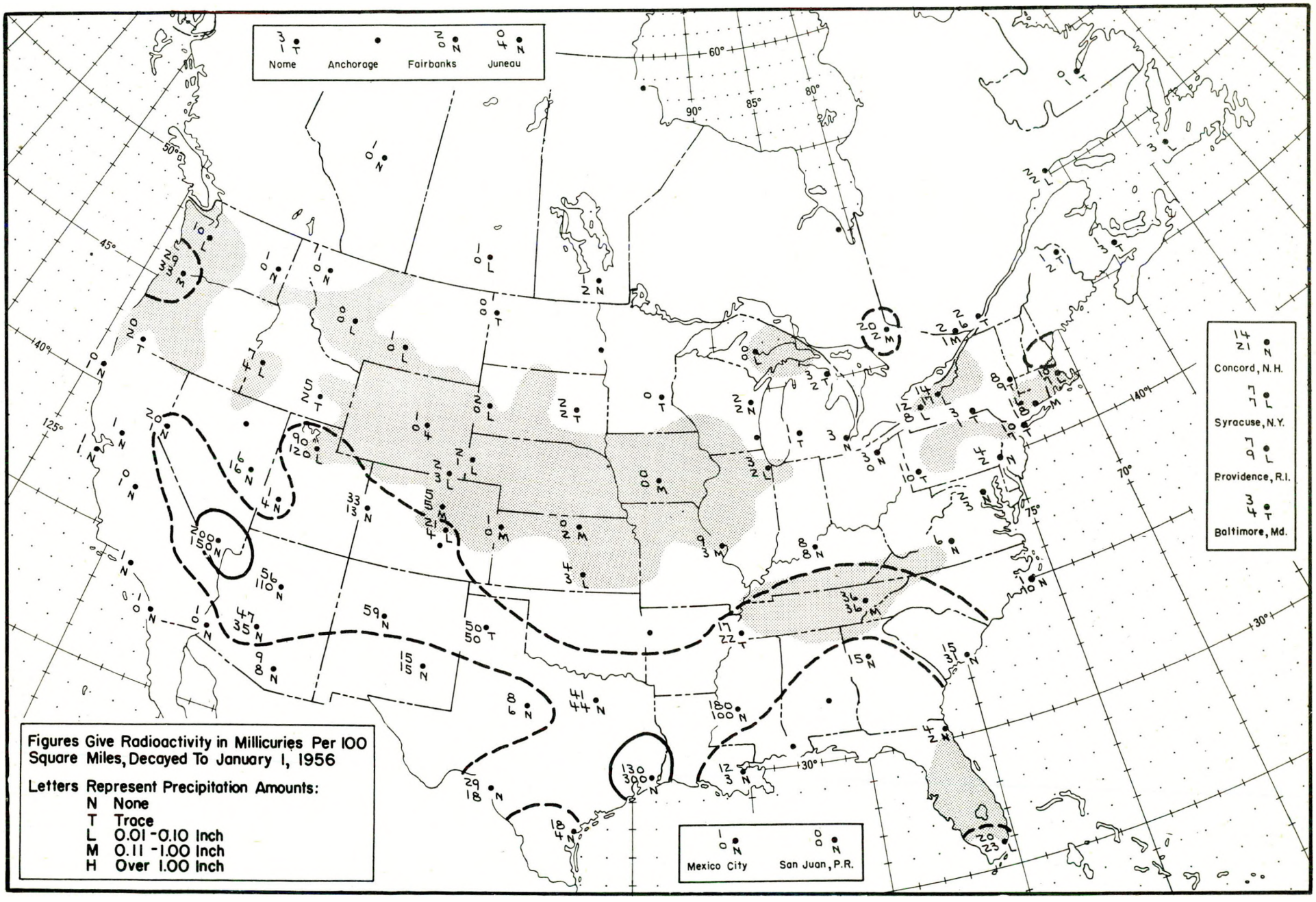

Figure A.35 Radioactive fallout in the 24-hour period beginning 1230 G.C.T., March 24, 1955

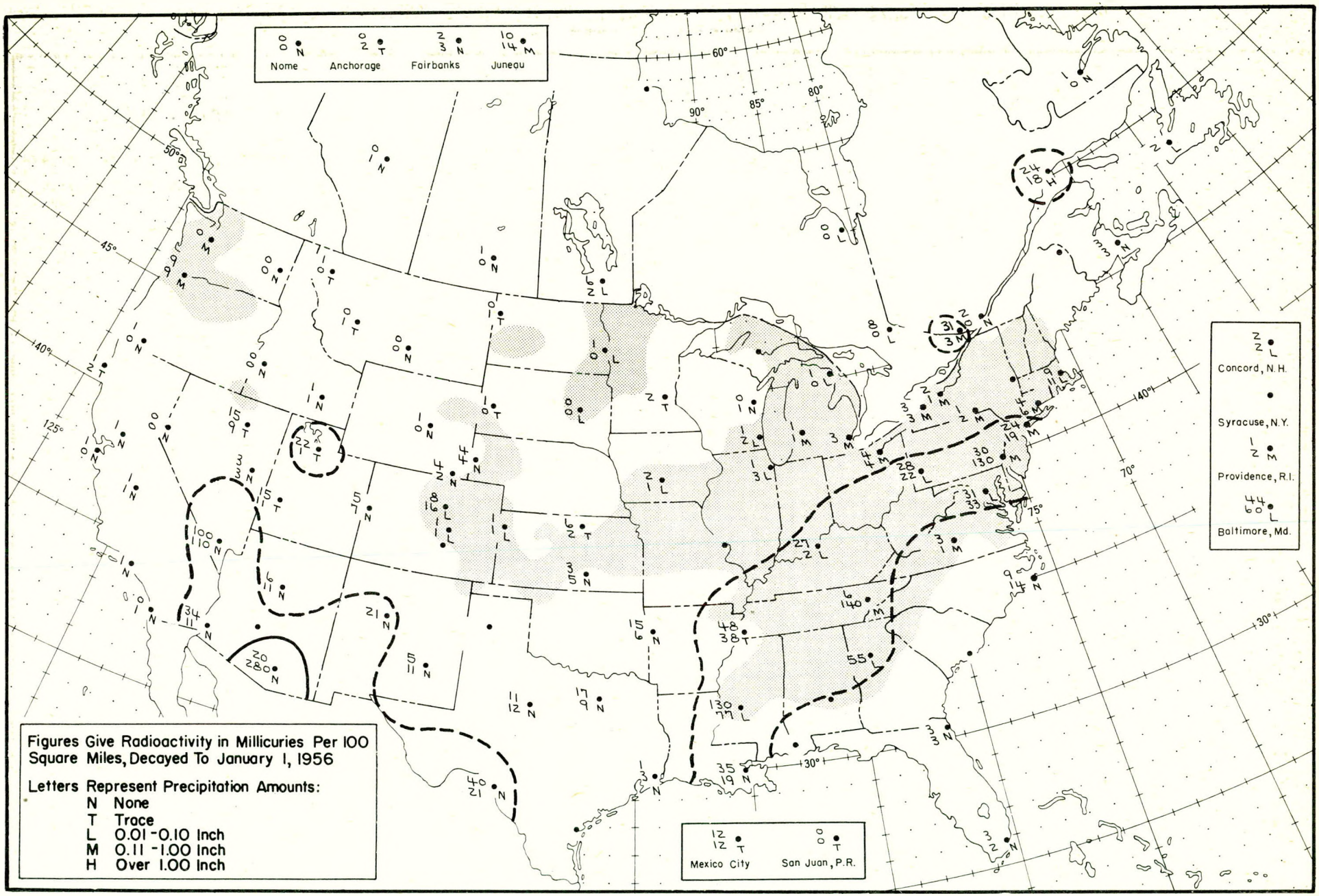

Figure A.36 Radioactive fallout in the 24-hour period beginning 1230 G.C.T., March 25, 1955

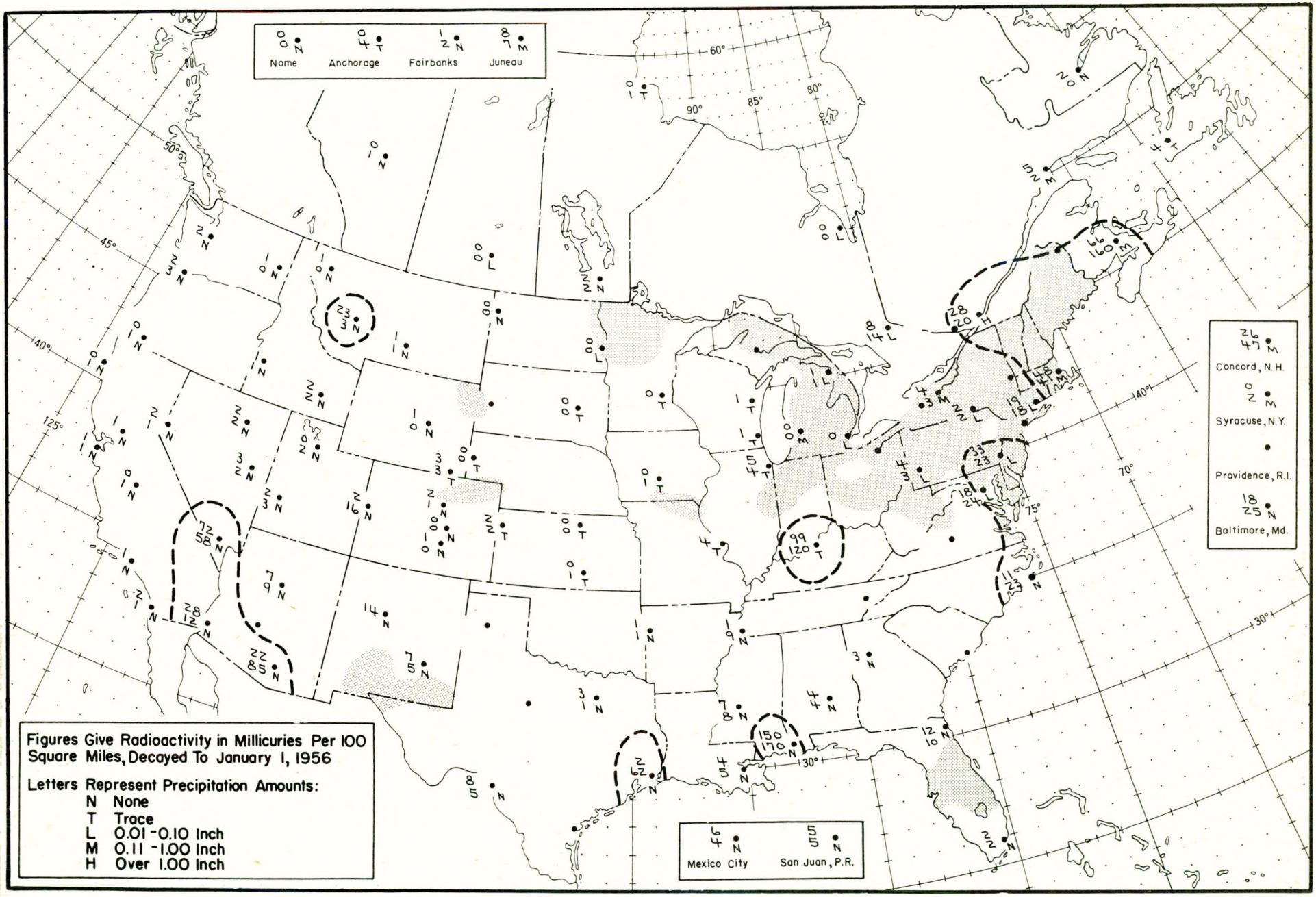

Figure A. 37 Radioactive fallout in the 24-hour period beginning 1230 G.C.T., March 26, 1955

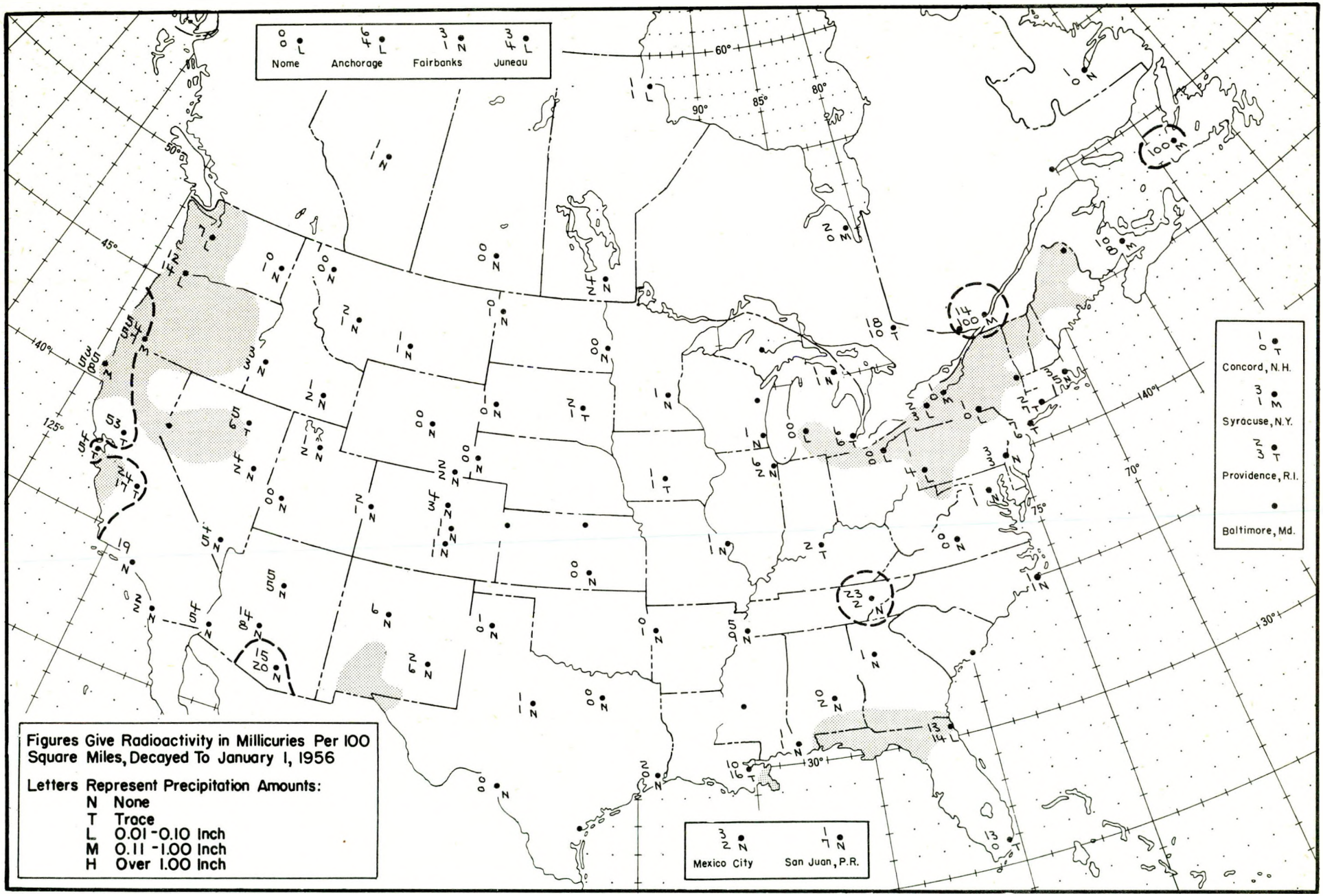

Figure A.38 Radioactive fallout in the 24-hour period beginning 1230 G.C.T., March 27, 1955

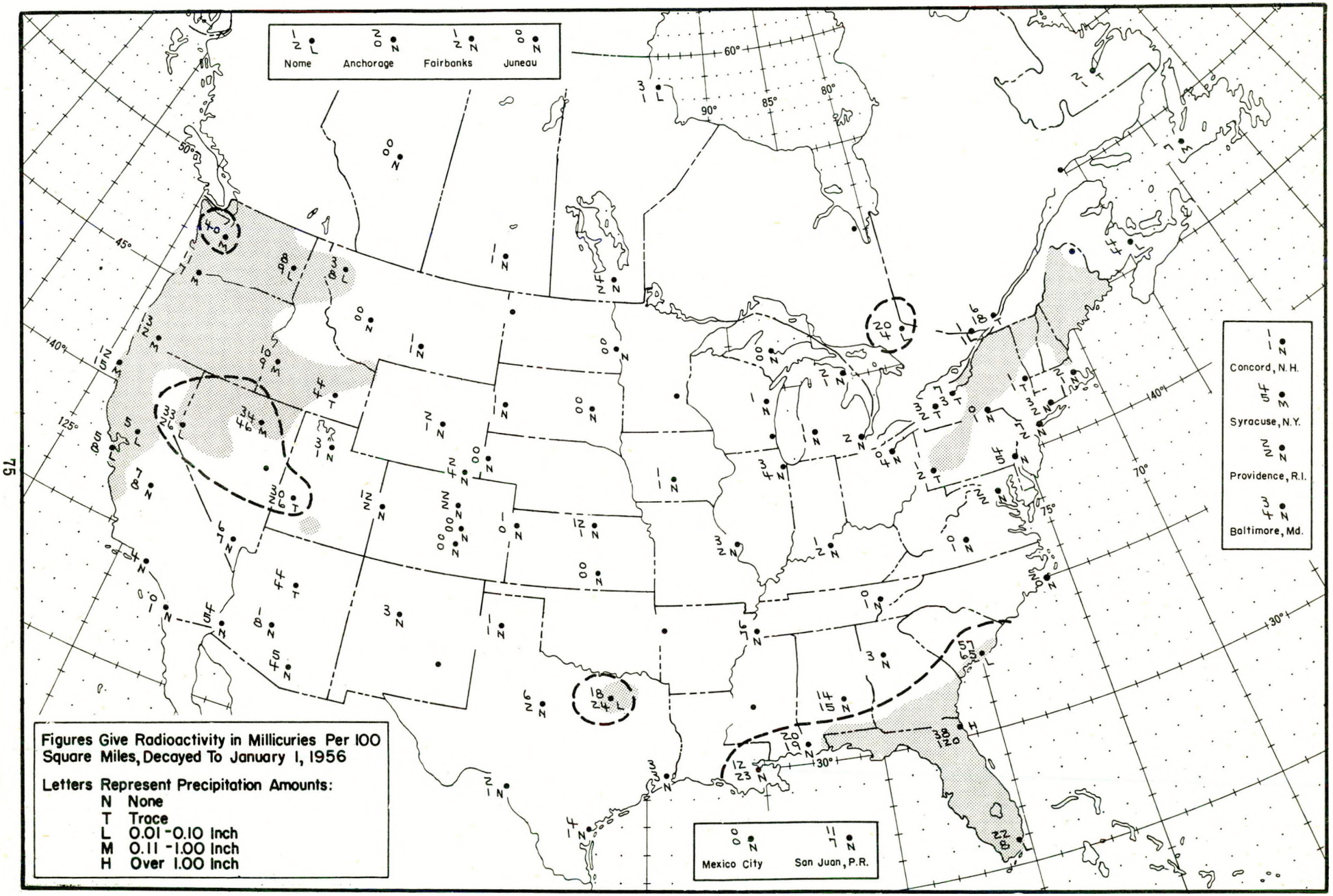

Figure A.39 Radioactive fallout in the 24-hour period beginning 1230 G.C.T., March 28, 1955

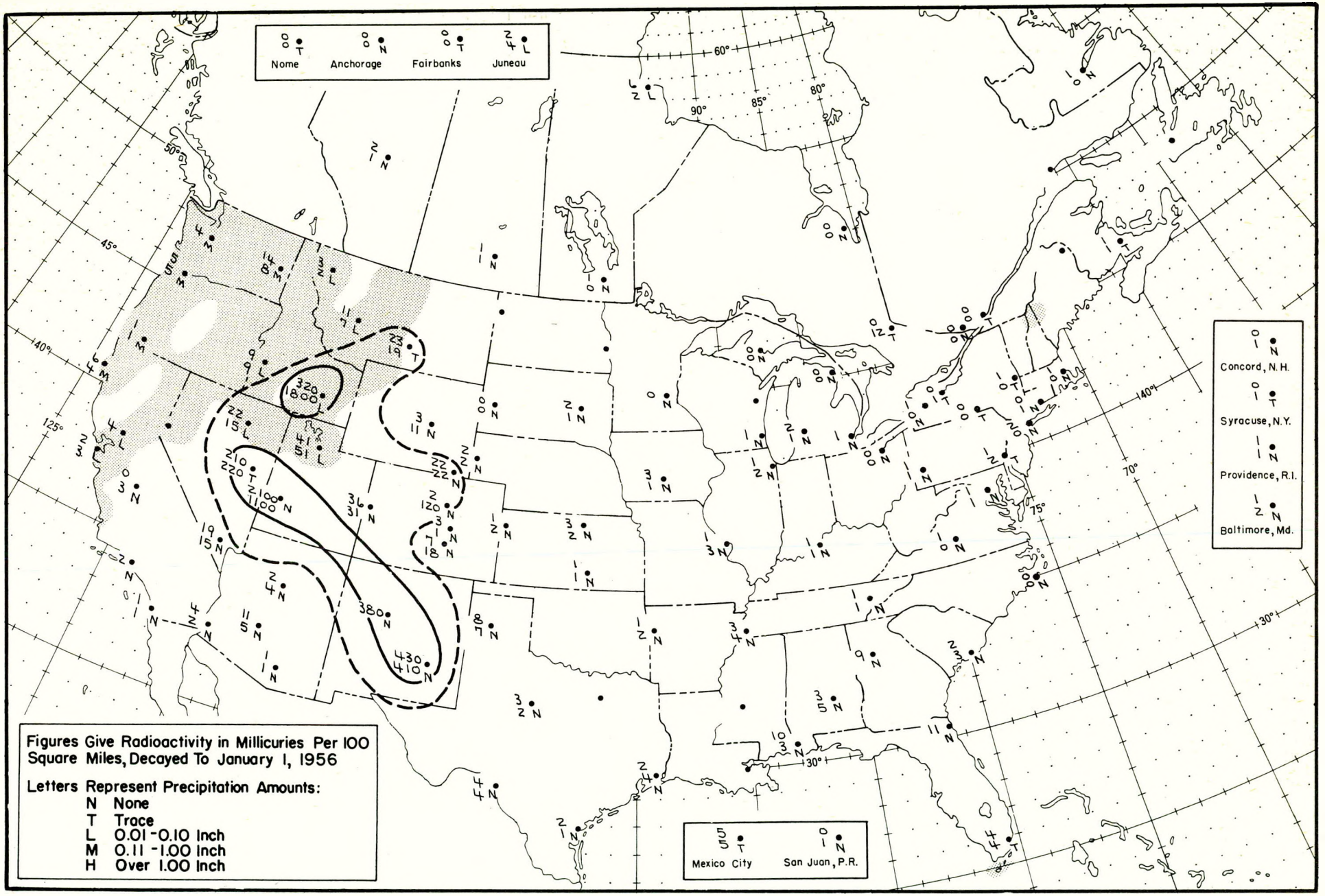

Figure A.40 Radioactive fallout in the 24-hour period beginning 1230 G.C.T., March 29, 1955

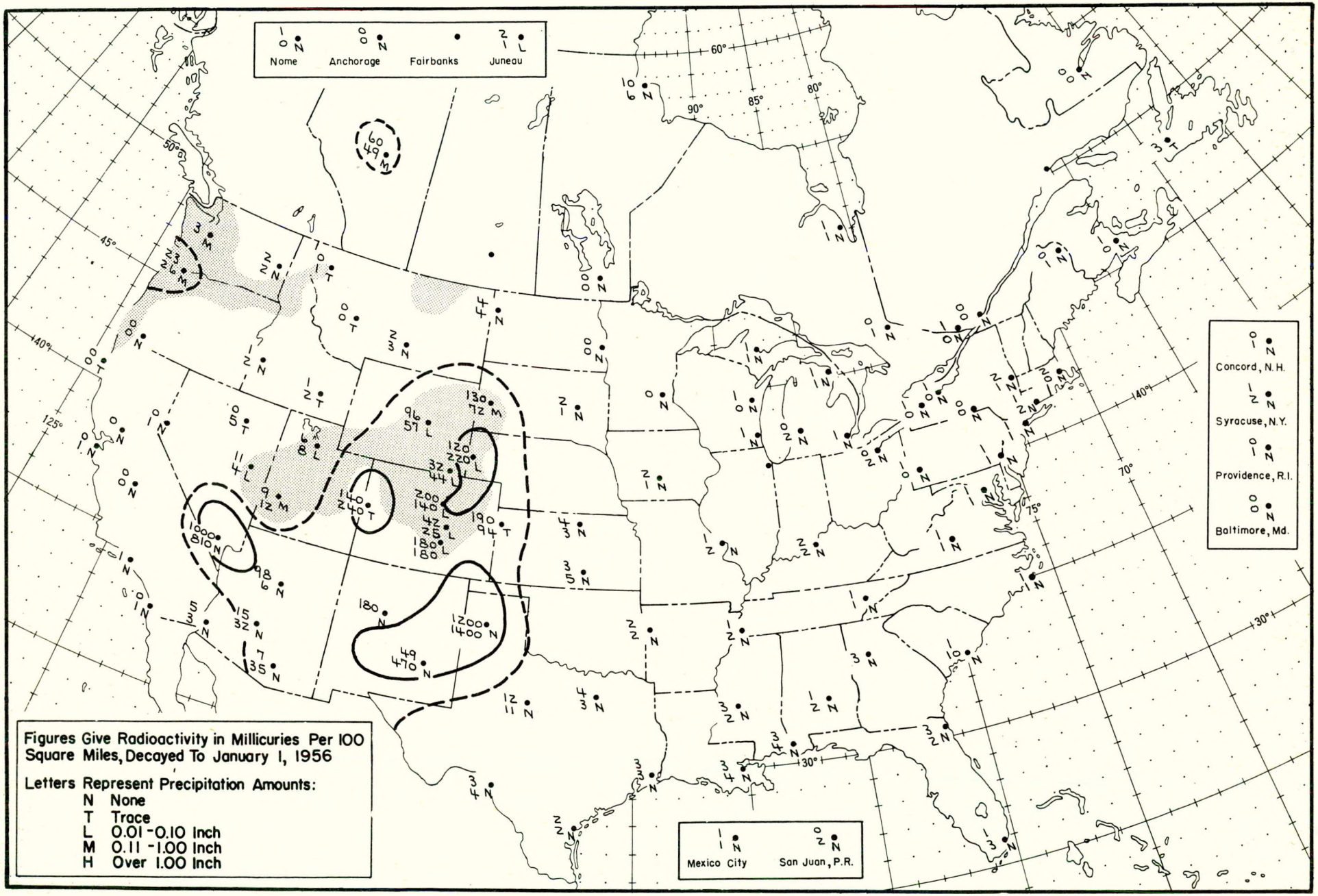

Figure A. 41 Radioactive fallout in the 24-hour period beginning 1230 G.C.T., March 30, 1955

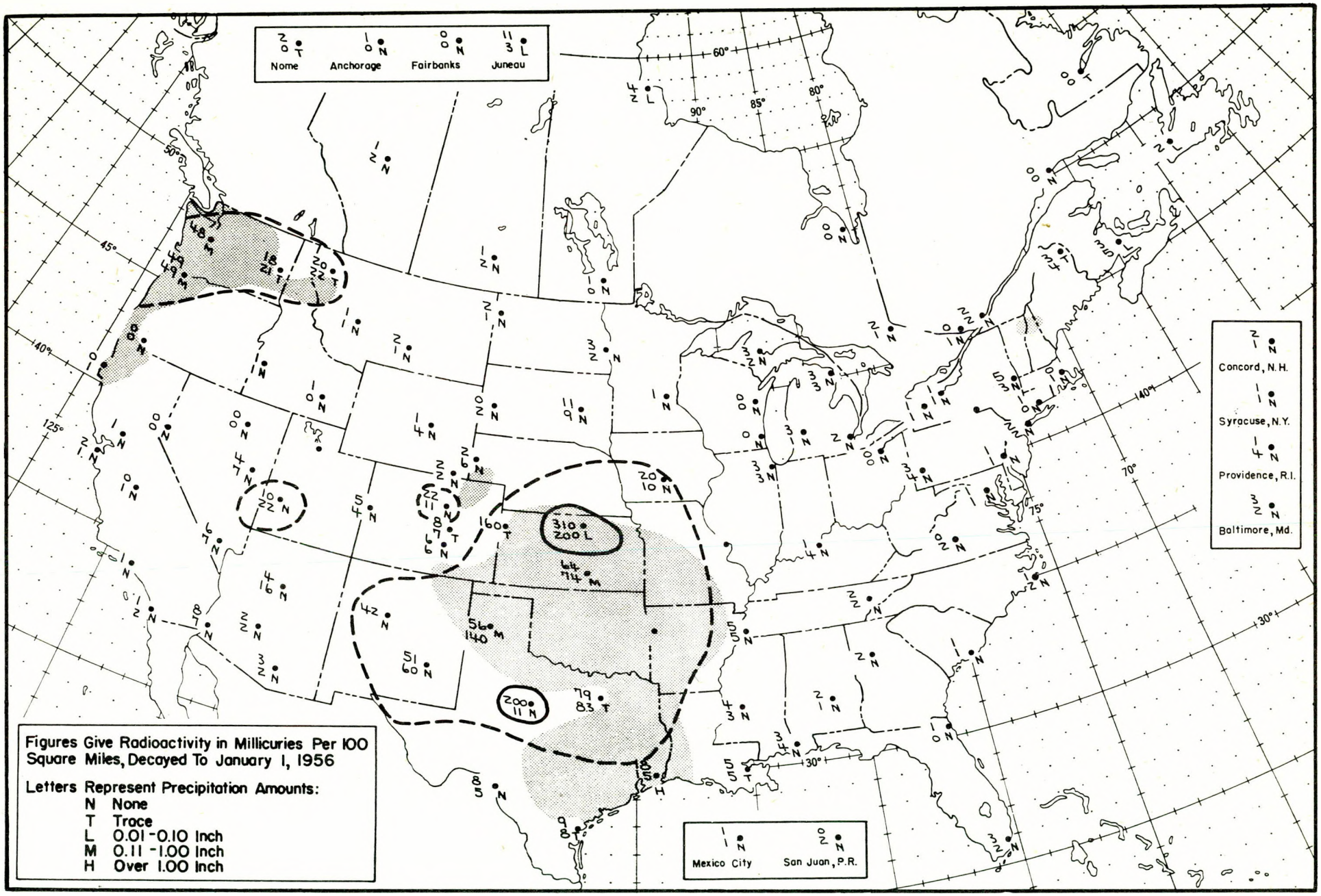

Figure A.42 Radioactive fallout in the 24-hour period beginning 1230 G.C.T., March 31, 1955

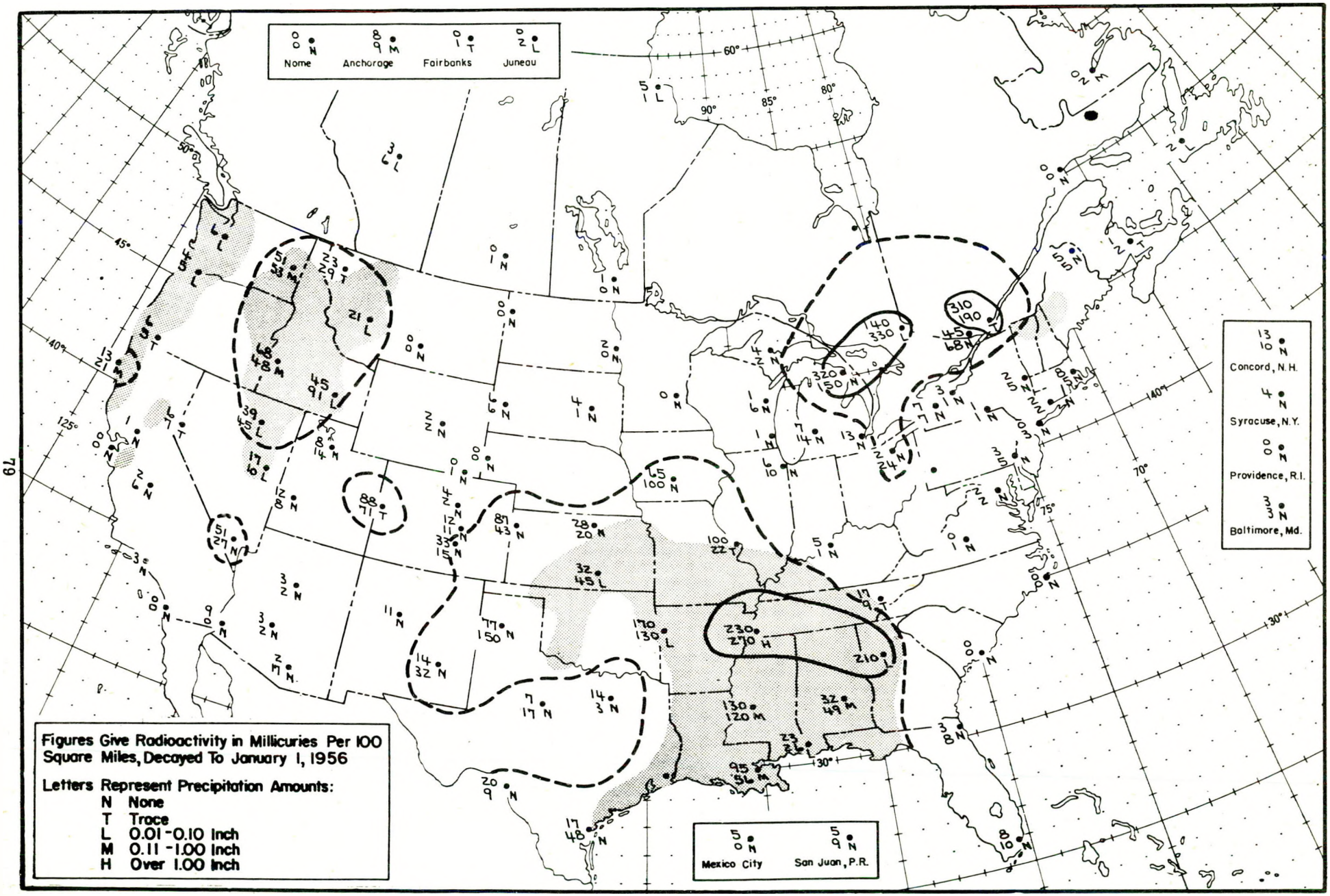

Figure A. 43 Radioactive fallout in the 24-hour period beginning 1230 G.C.T., April 1, 1955

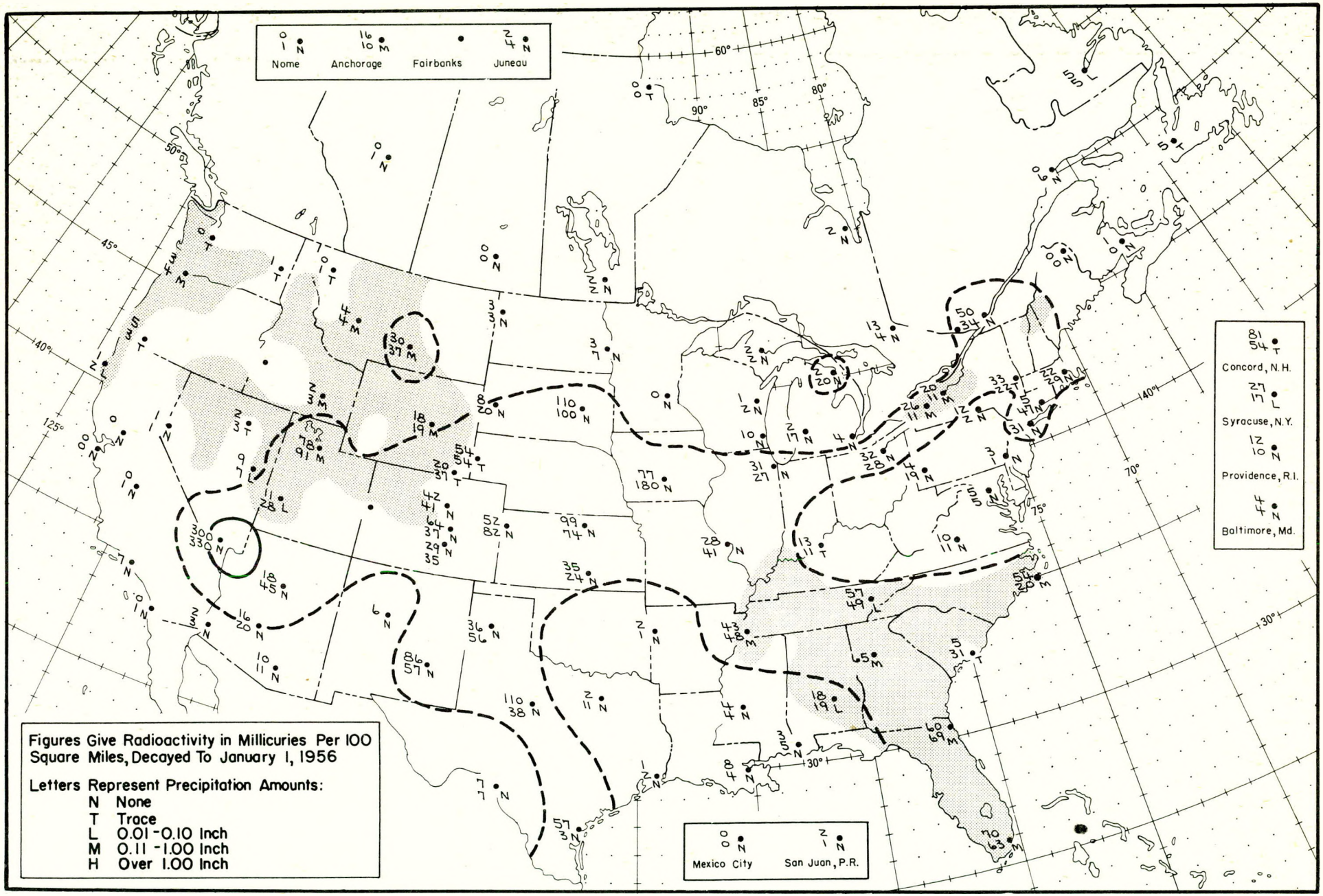

Figure A.44 Radioactive fallout in the 24-hour period beginning 1230 G.C.T., April 2, 1955

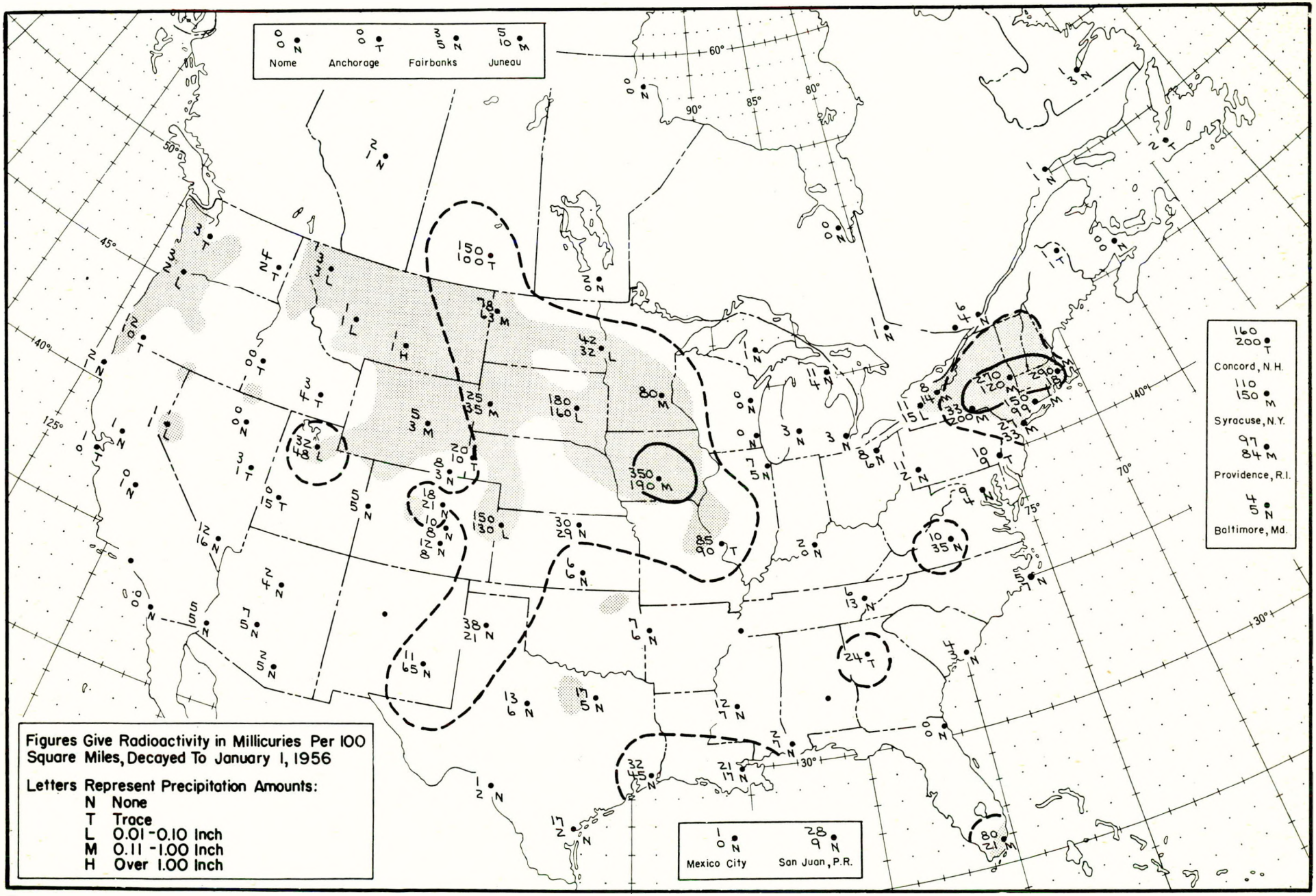

Figure A. 45 Radioactive fallout in the 24-hour period beginning 1230 G.C.T., April 3, 1955

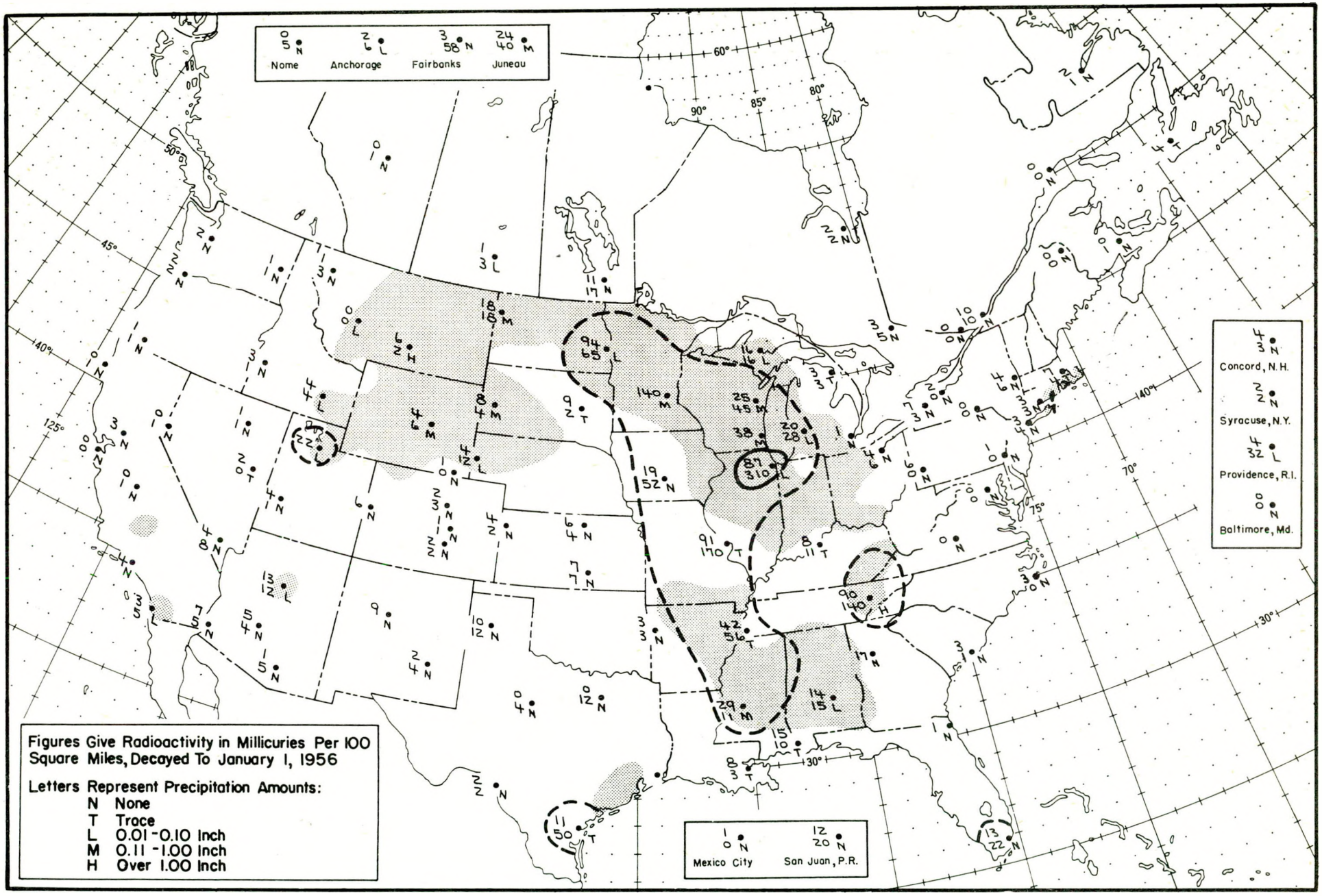

Figure A.46 Radioactive fallout in the 24-hour period beginning 1230 G.C.T., April 4, 1955

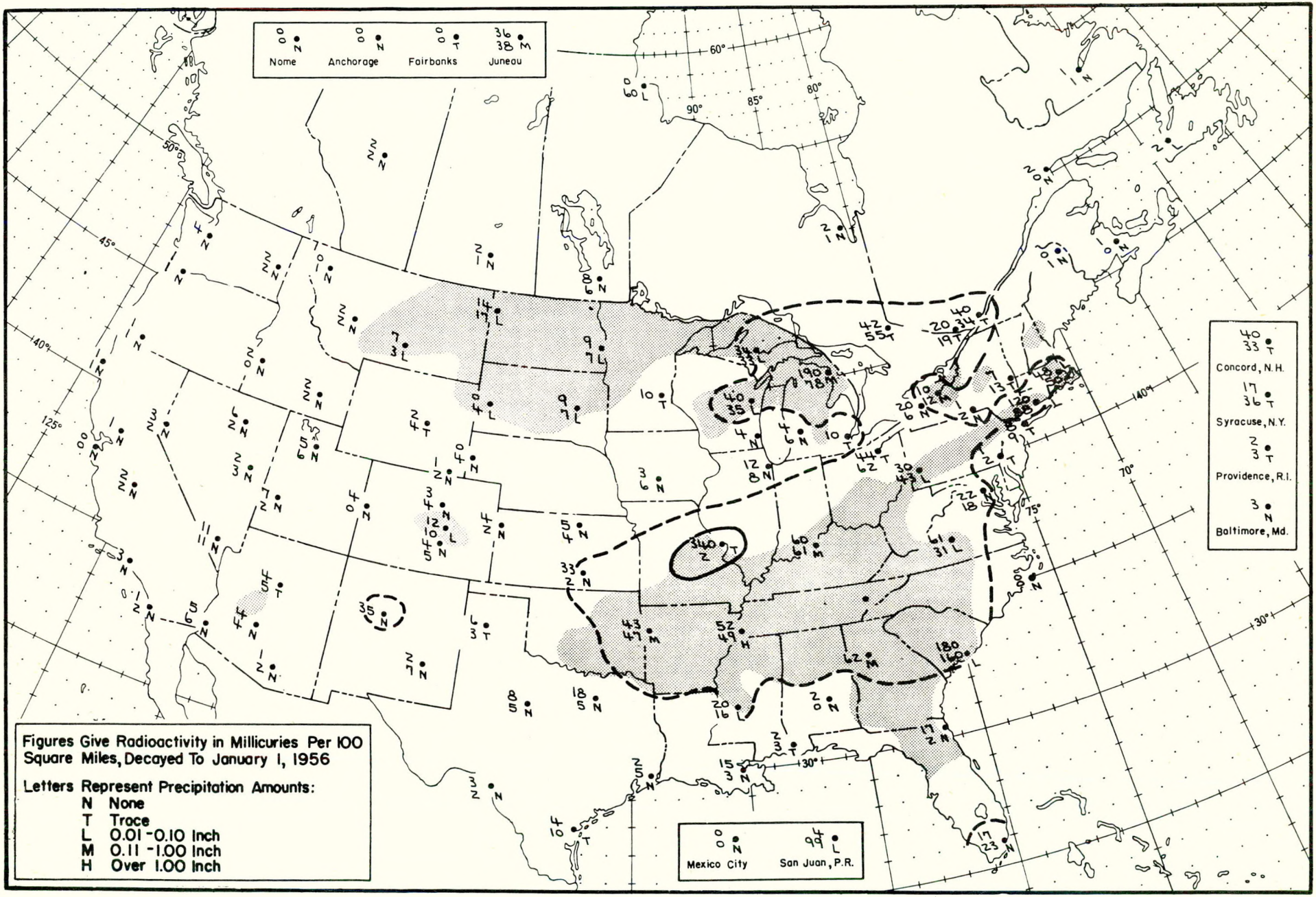

Figure A. 47 Radioactive fallout in the 24-hour period beginning 1230 G.C.T., April 5, 1955

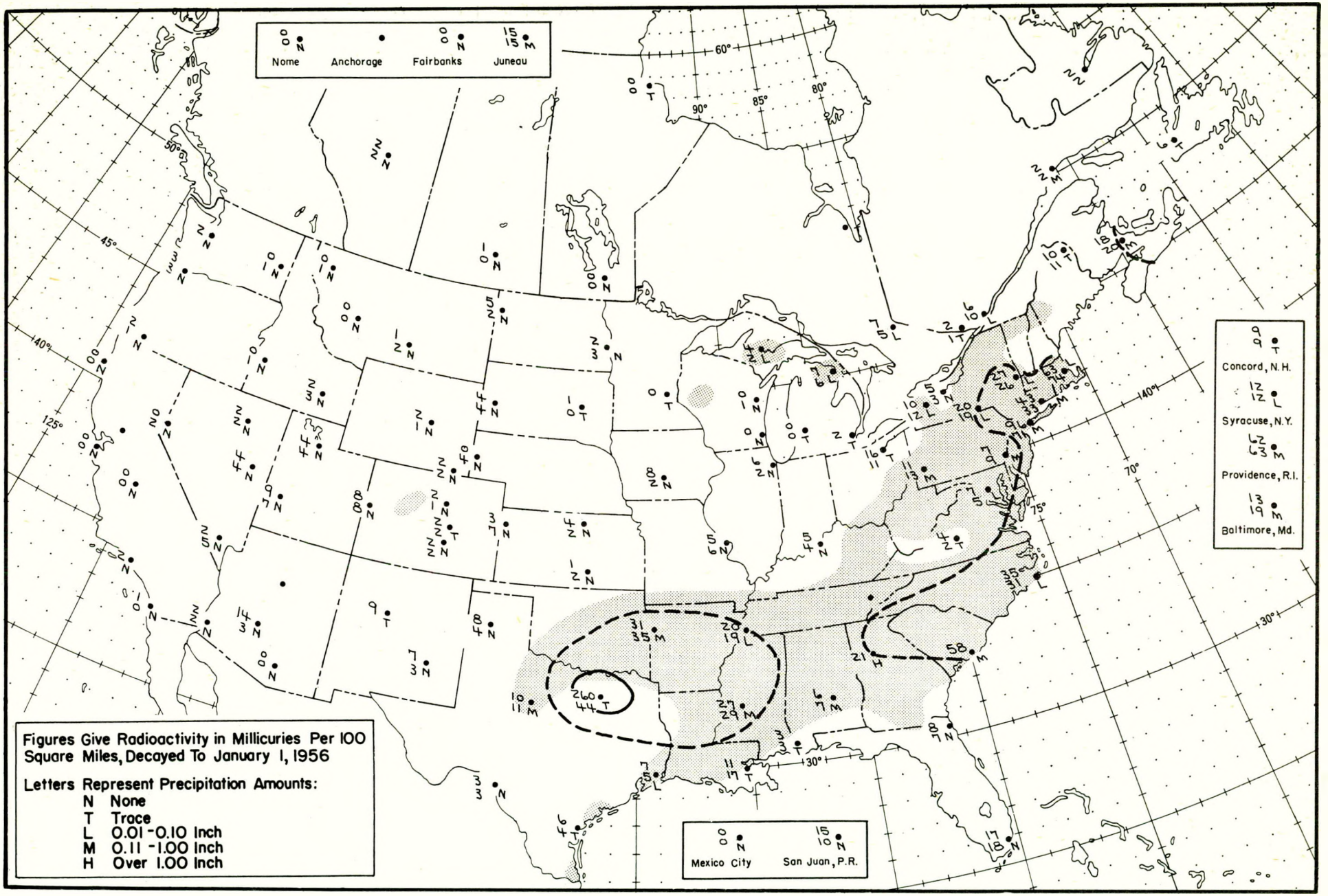

Figure A. 48 Radioactive fallout in the 24-hour period beginning 1230 G.C.T., April 6, 1955

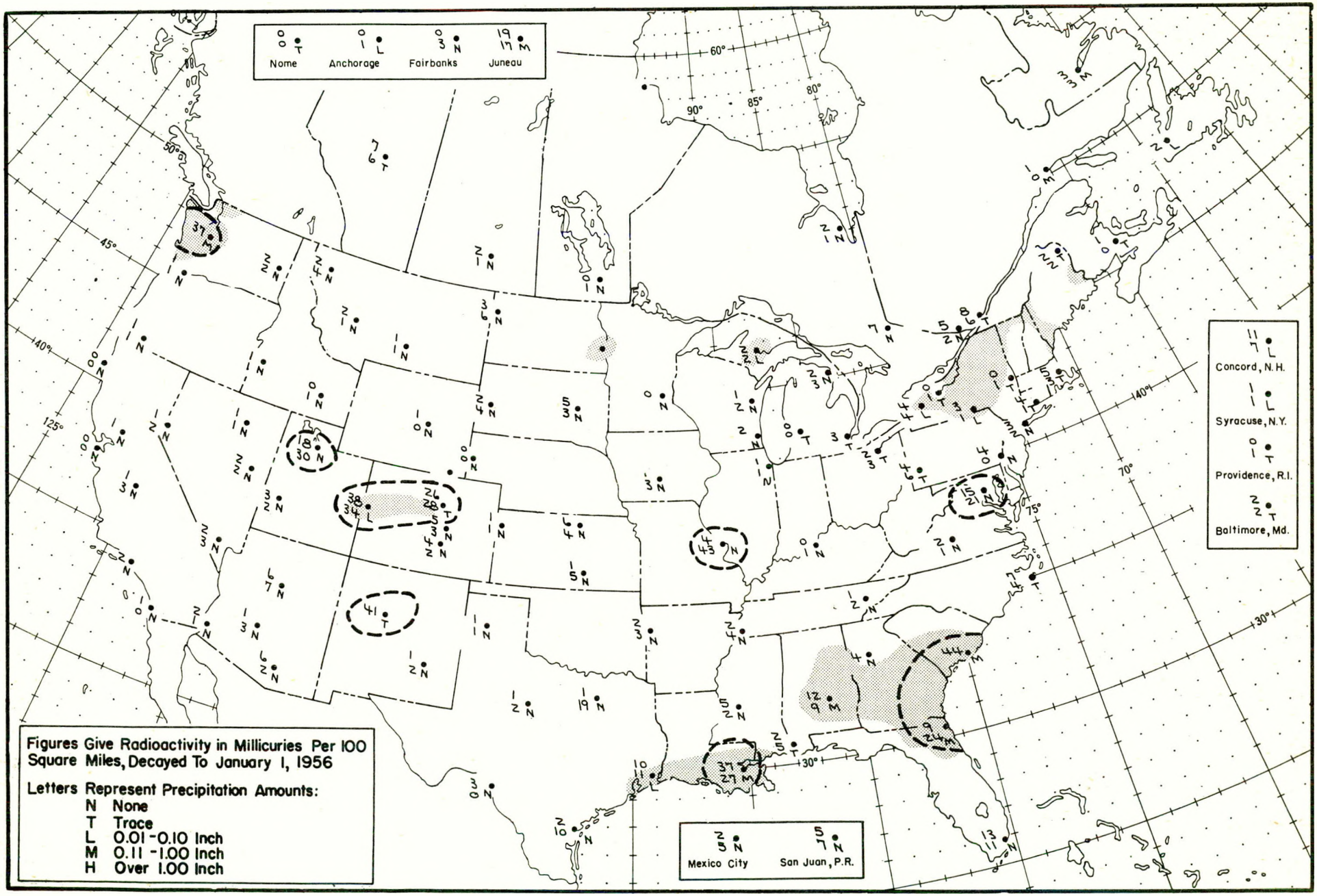

Figure A.49 Radioactive fallout in the 24-hour period beginning 1230 G.C.T., April 7, 1955

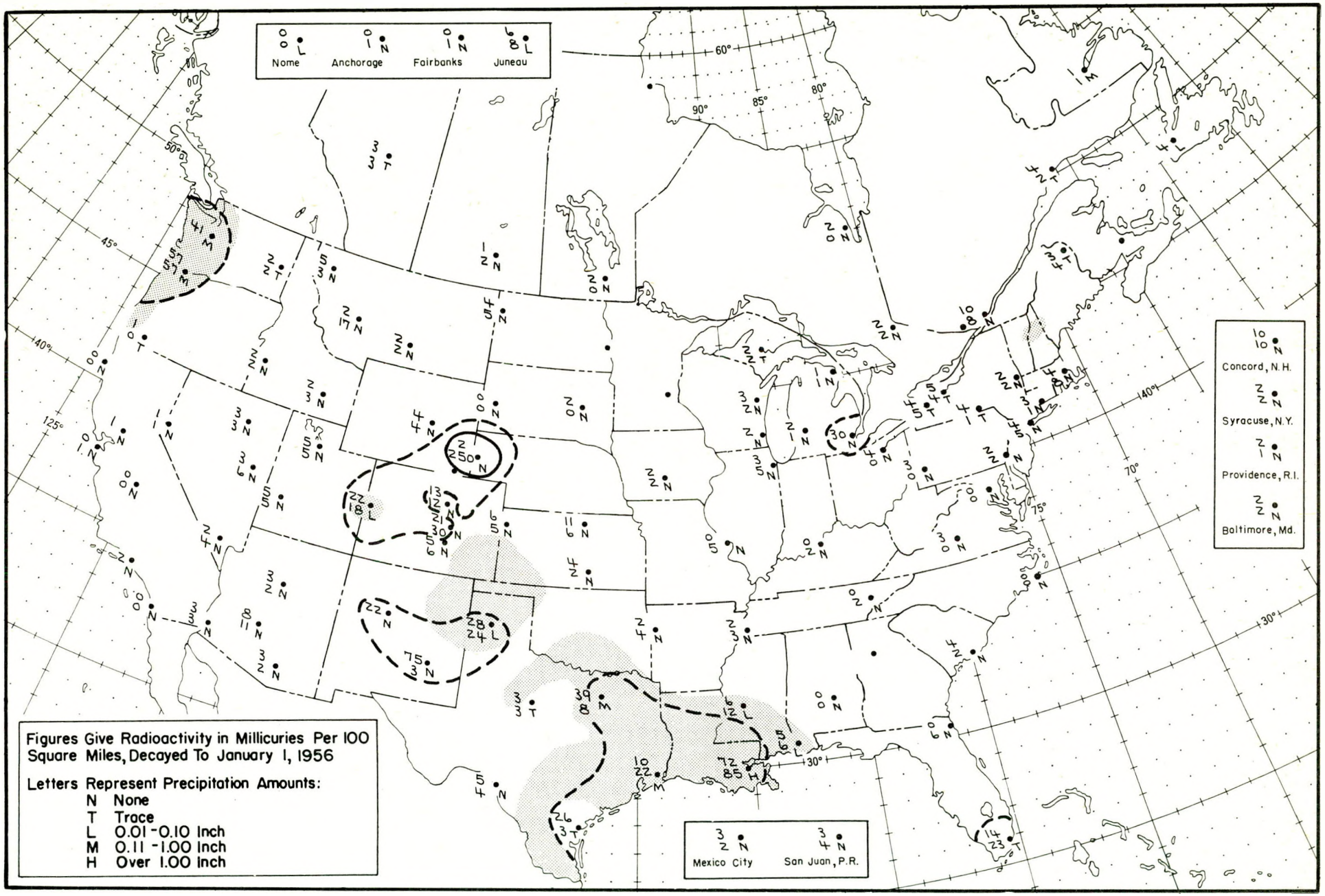

Figure A.50 Radioactive fallout in the 24-hour period beginning 1230 G.C.T., April 8, 1955

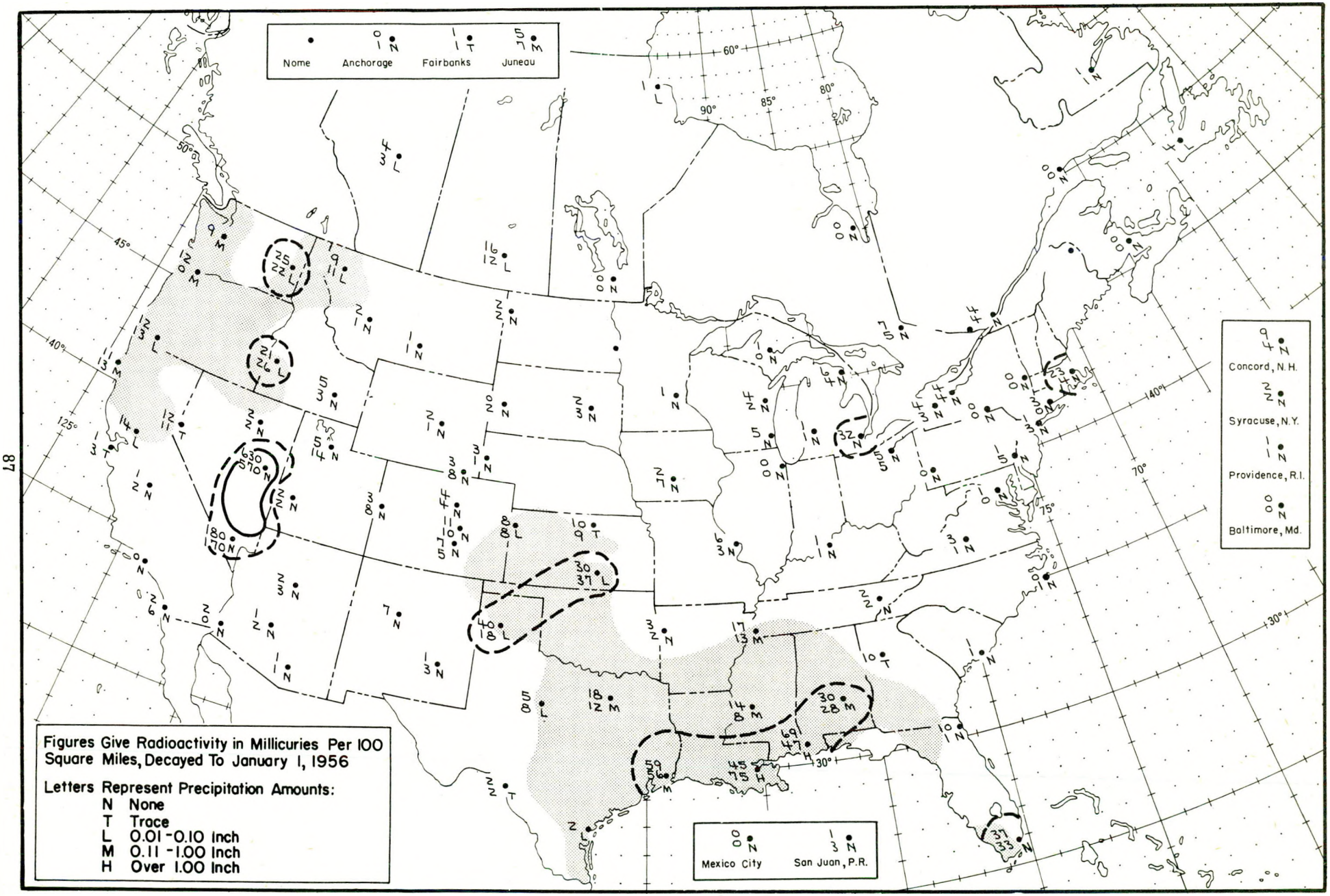

Figure A.51 Radioactive fallout in the 24-hour period beginning 1230 G.C.T., April 9, 1955

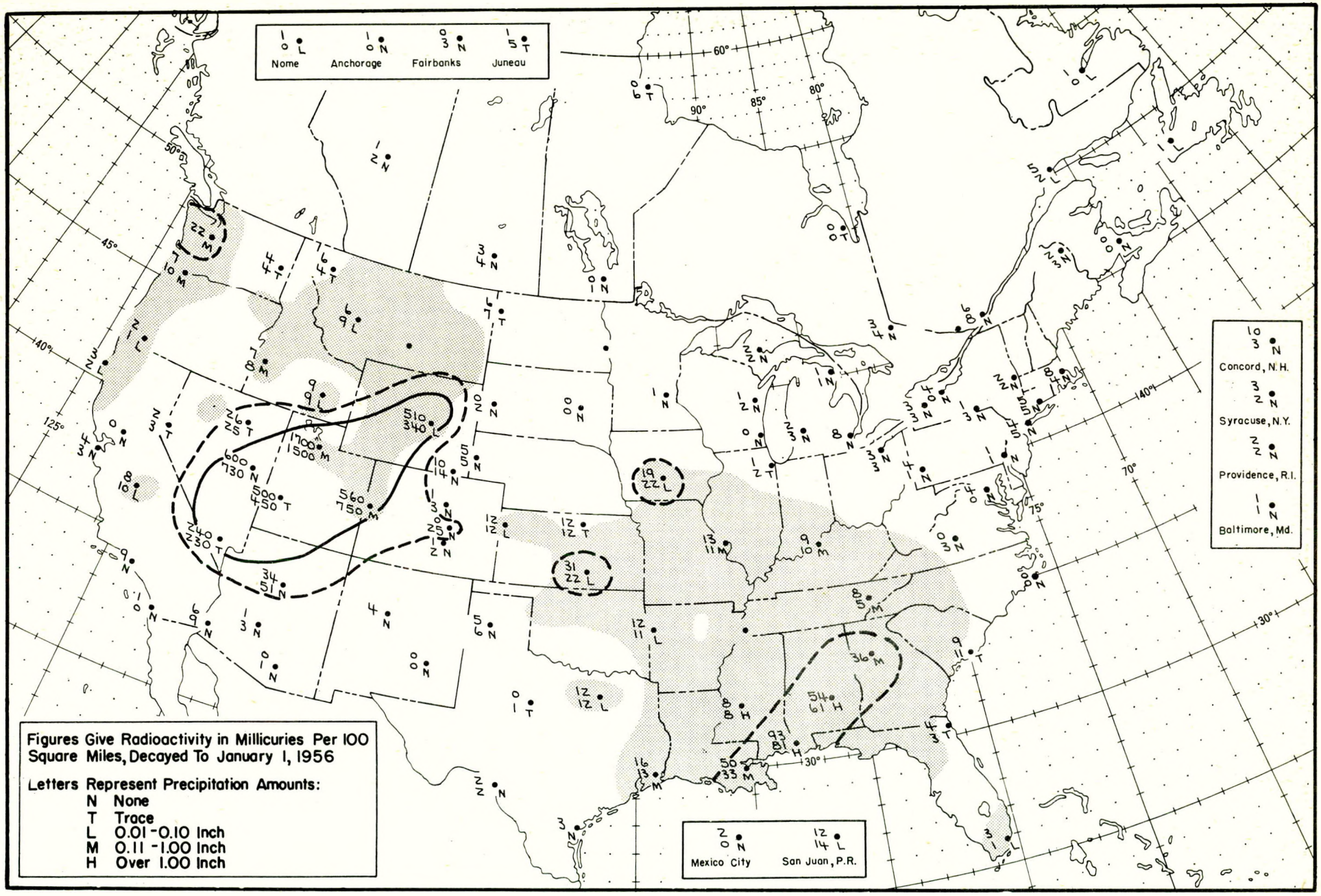

Figure A. 52 Radioactive fallout in the 24-hour period beginning 1230 G.C.T., April 10, 1955

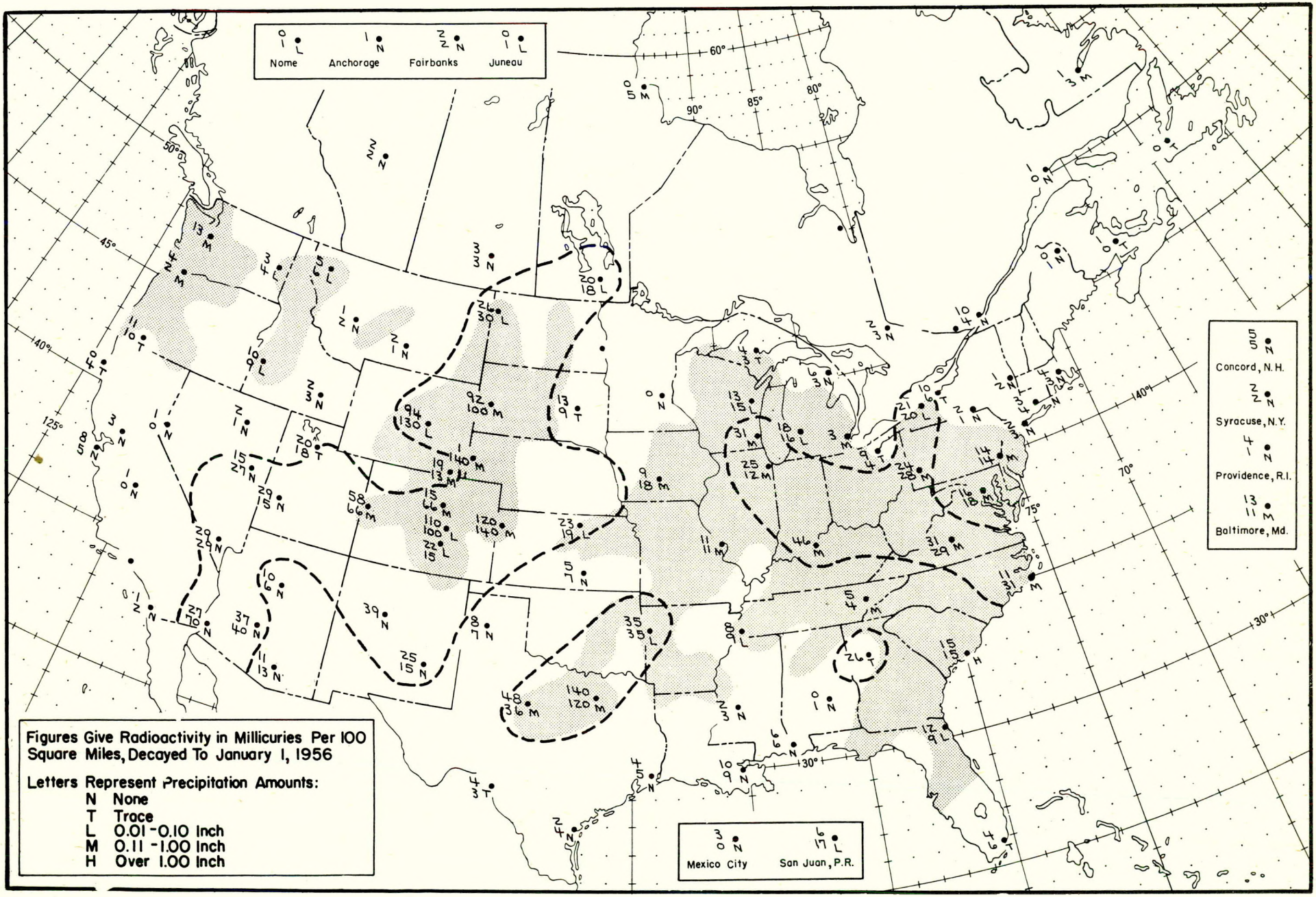

Figure A.53 Radioactive fallout in the 24-hour period beginning 1230 G.C.T., April 11, 1955

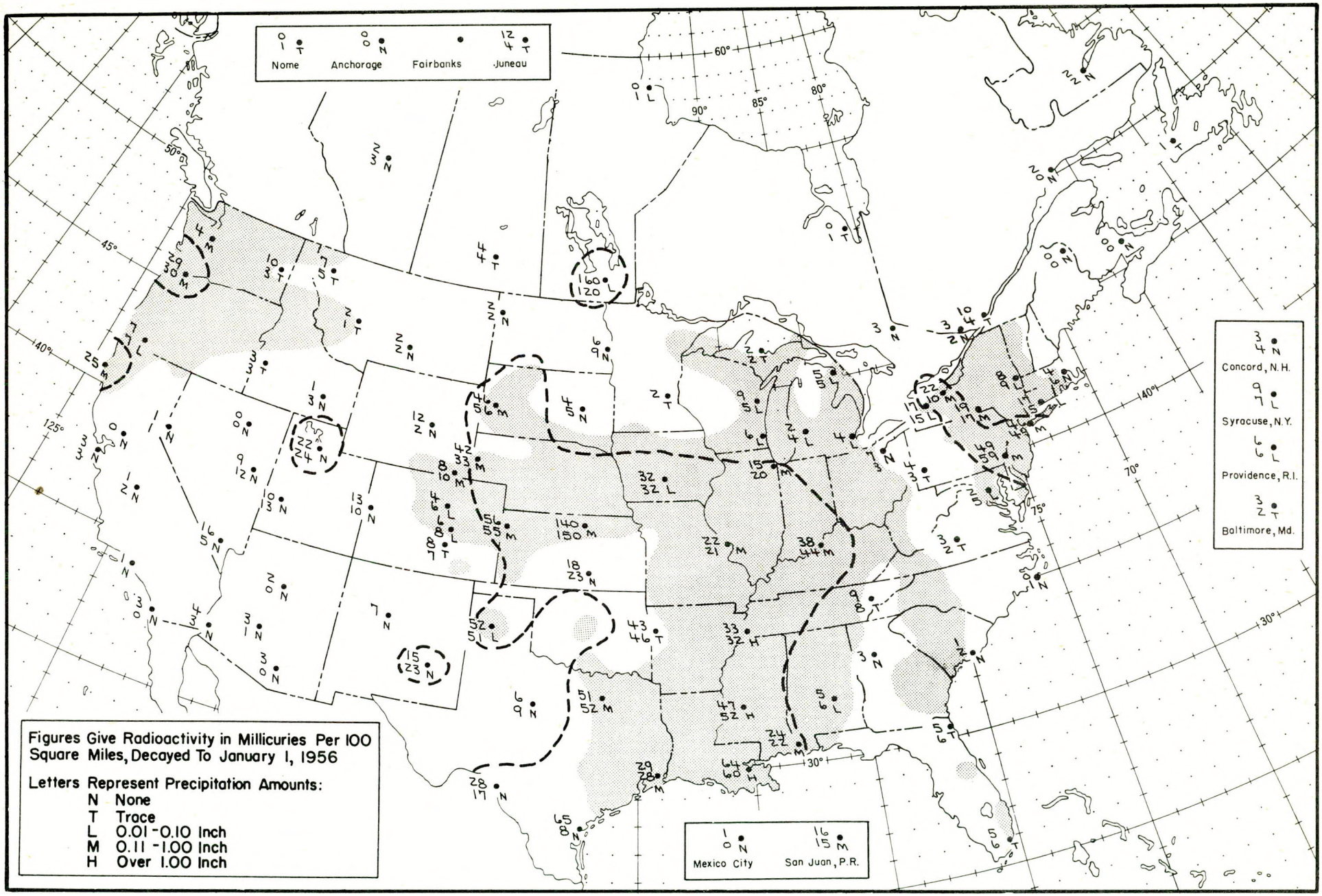

Figure A.54 Radioactive fallout in the 24-hour period beginning 1230 G.C.T., April 12, 1955

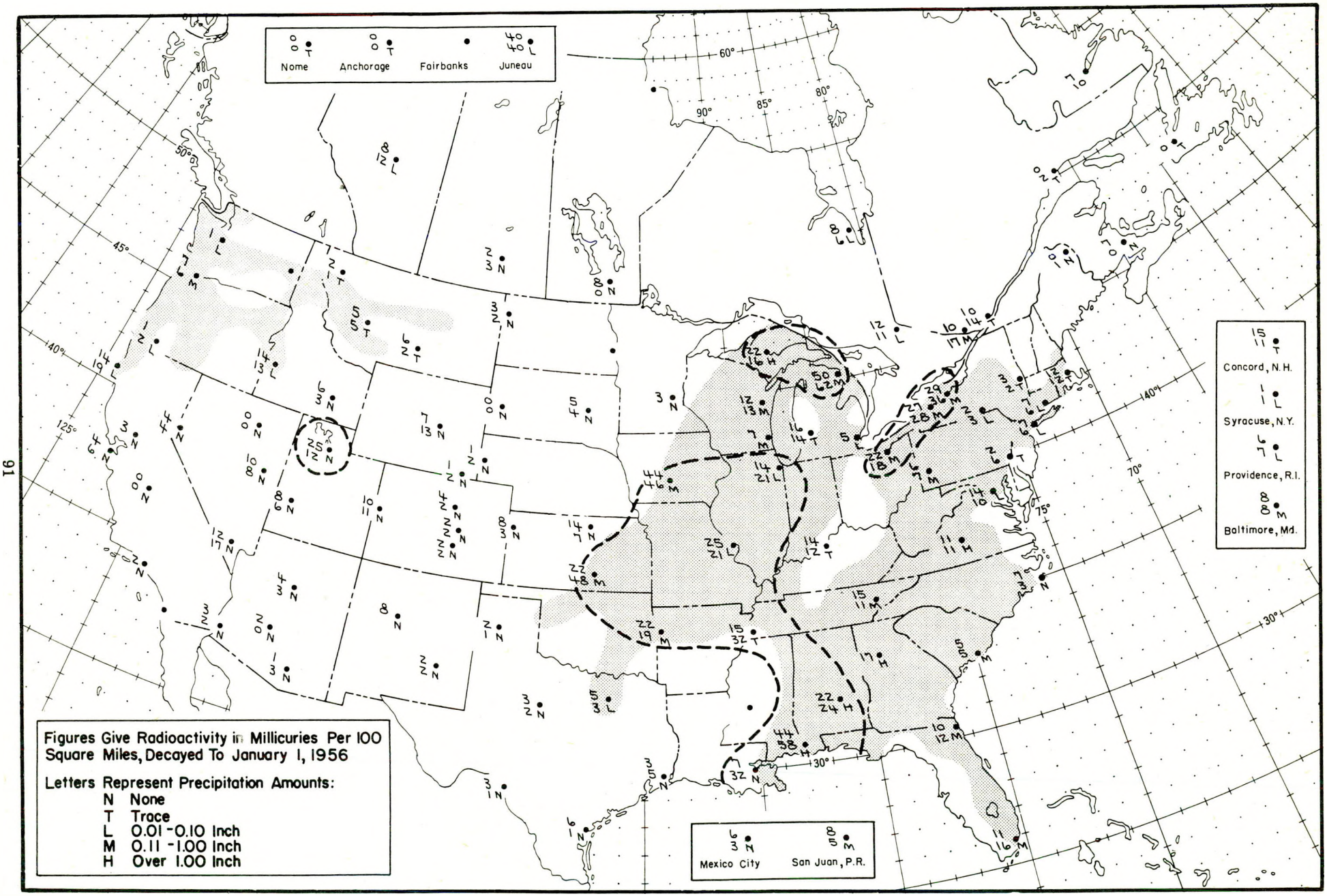

Figure A. 55 Radioactive fallout in the 24-hour period beginning 1230 G.C.T., April 13, 1955

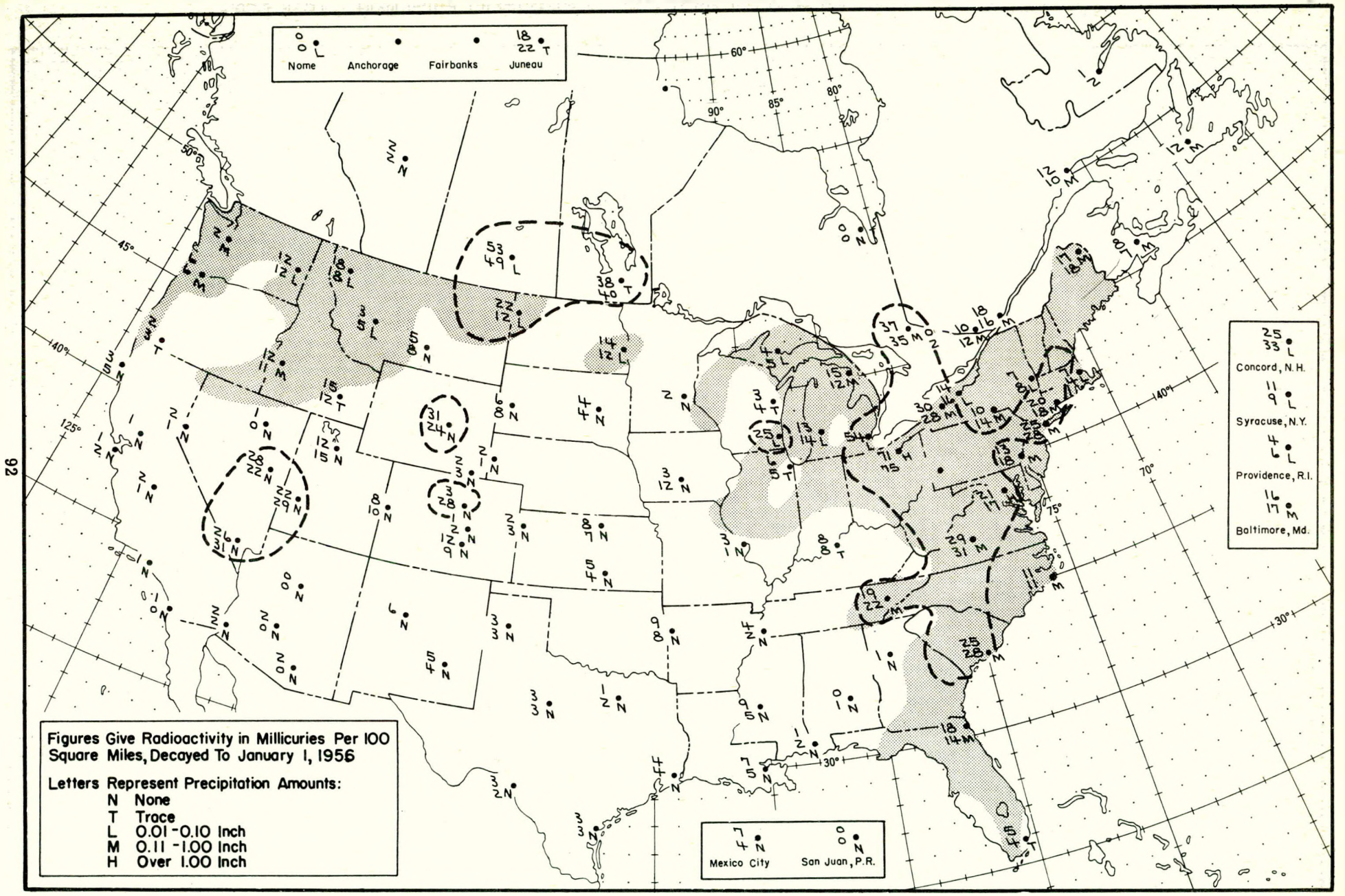

Figure A.56 Radioactive fallout in the 24-hour period beginning 1230 G.C.T., April 14, 1955

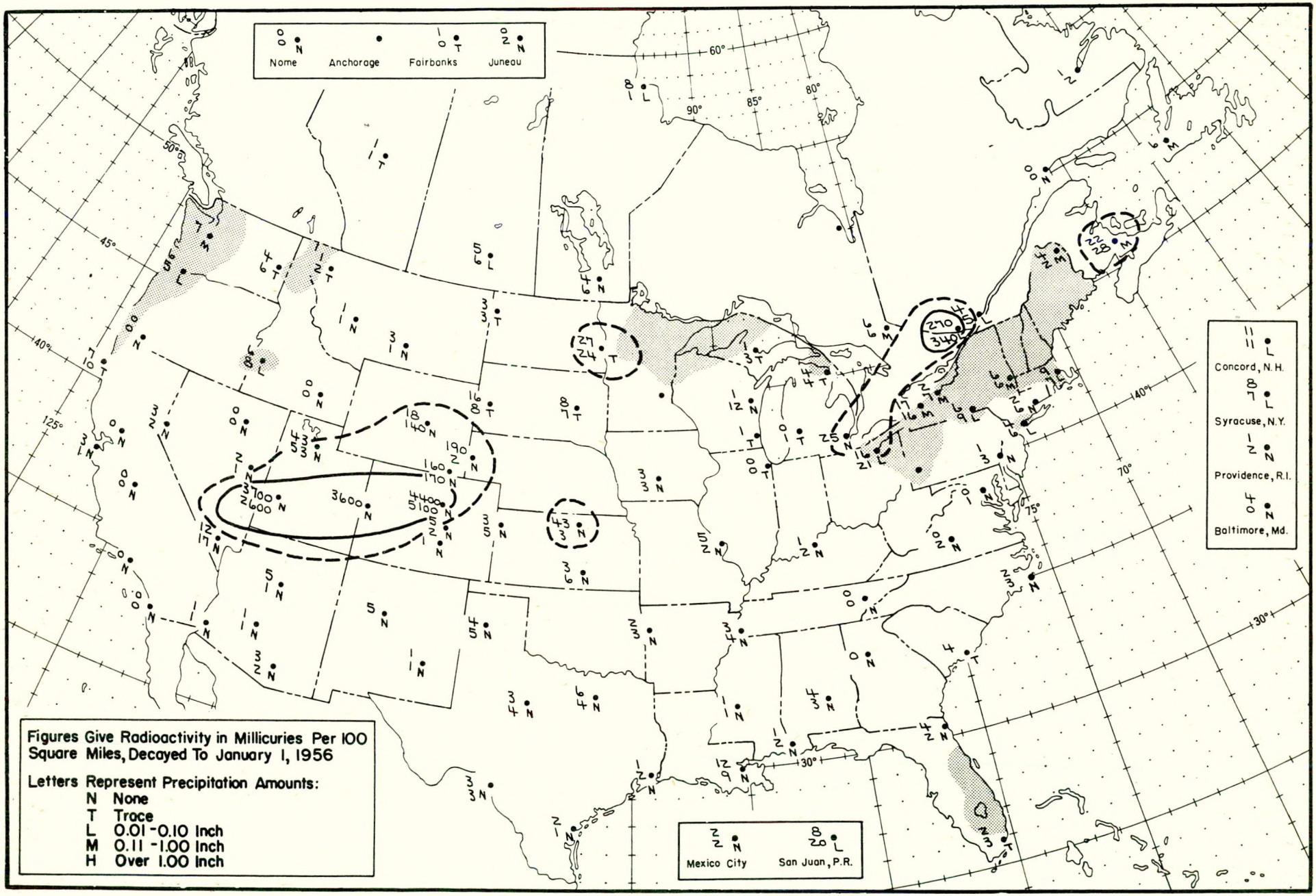

Figure A. 57 Radioactive fallout in the 24-hour period beginning 1230 G.C.T., April 15, 1955

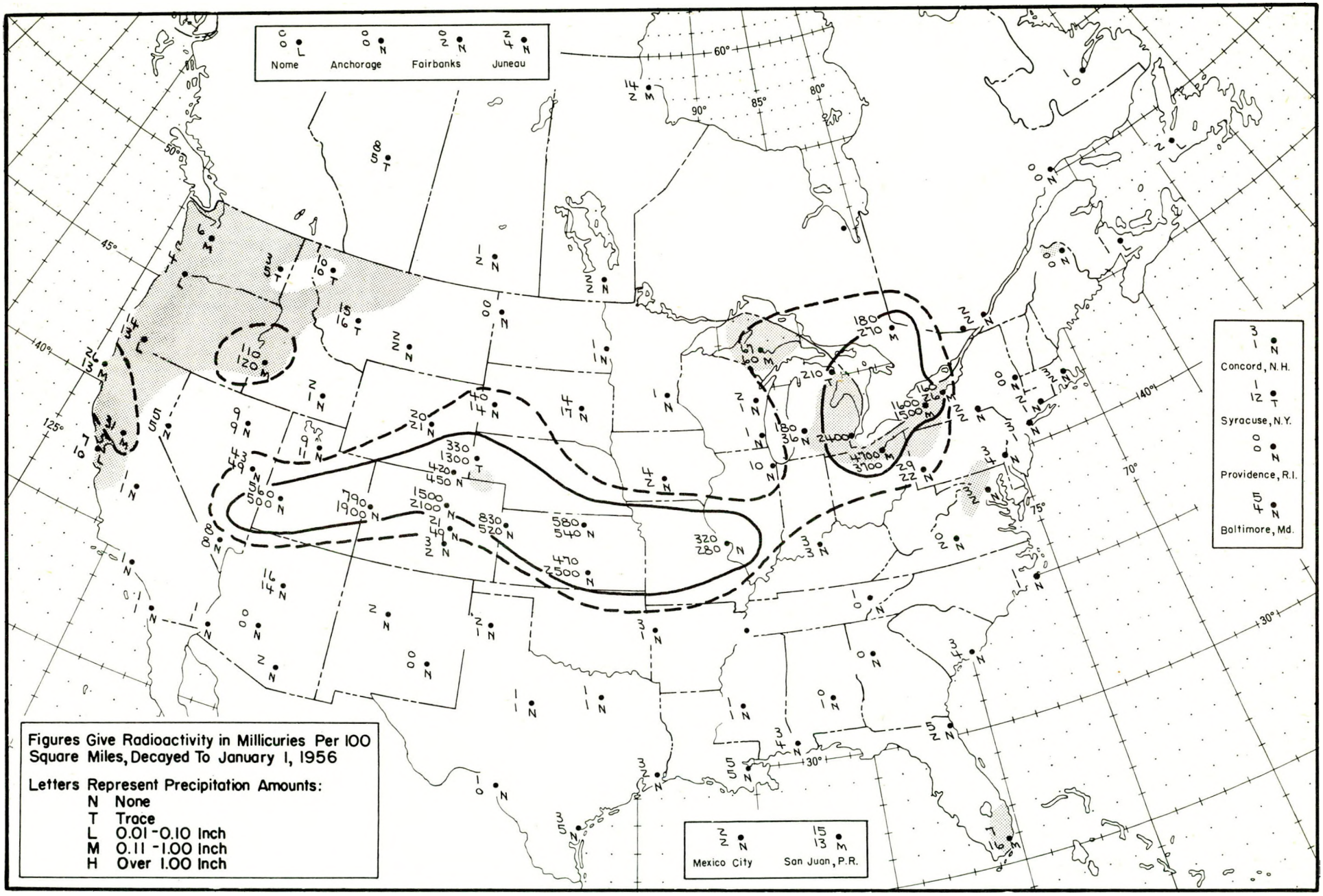

Figure A. 58 Radioactive fallout in the 24-hour period beginning 1230 G.C.T., April 16, 1955

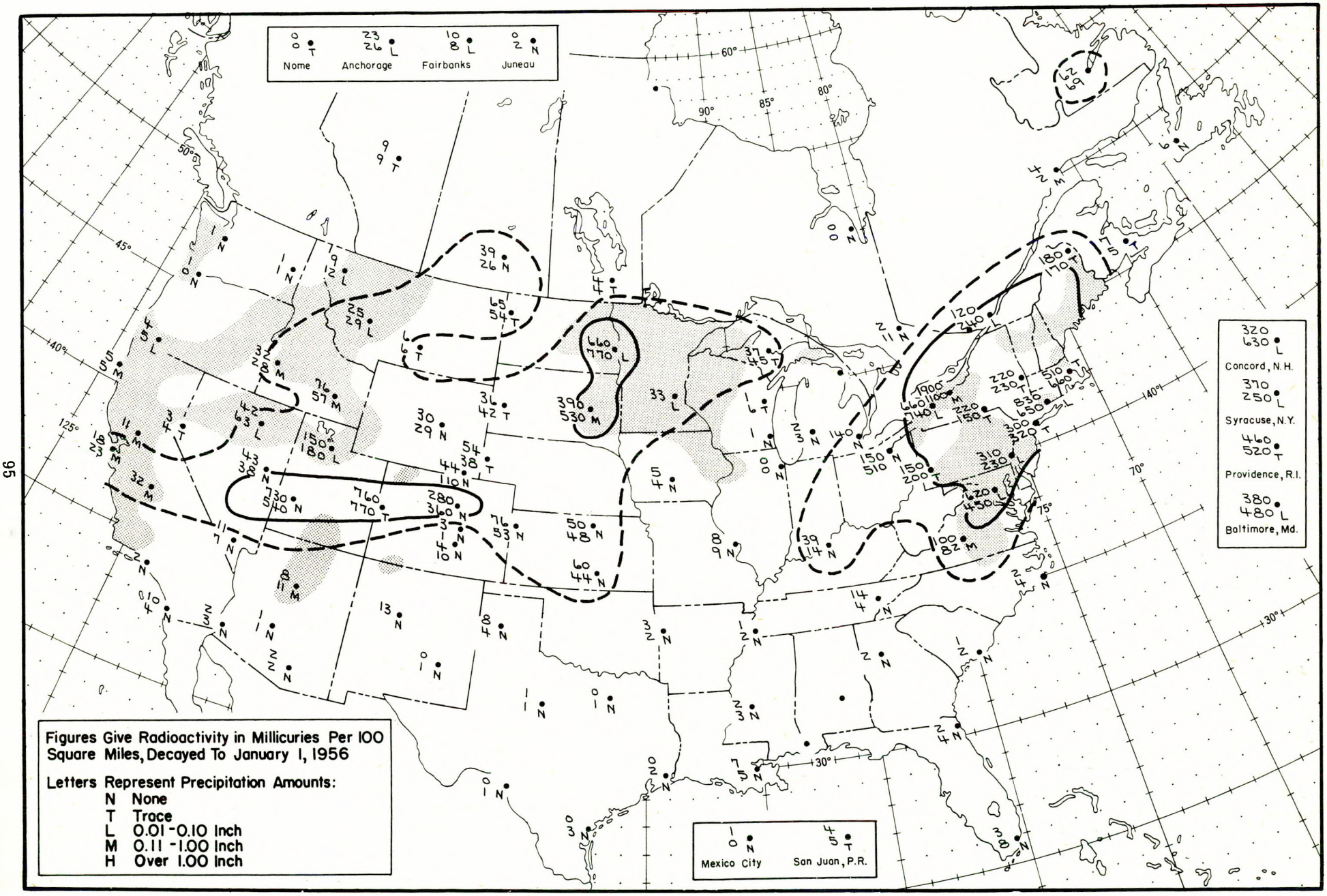

Figure A.59 Radioactive fallout in the 24-hour period beginning 1230 G.C.T., April 17, 1955

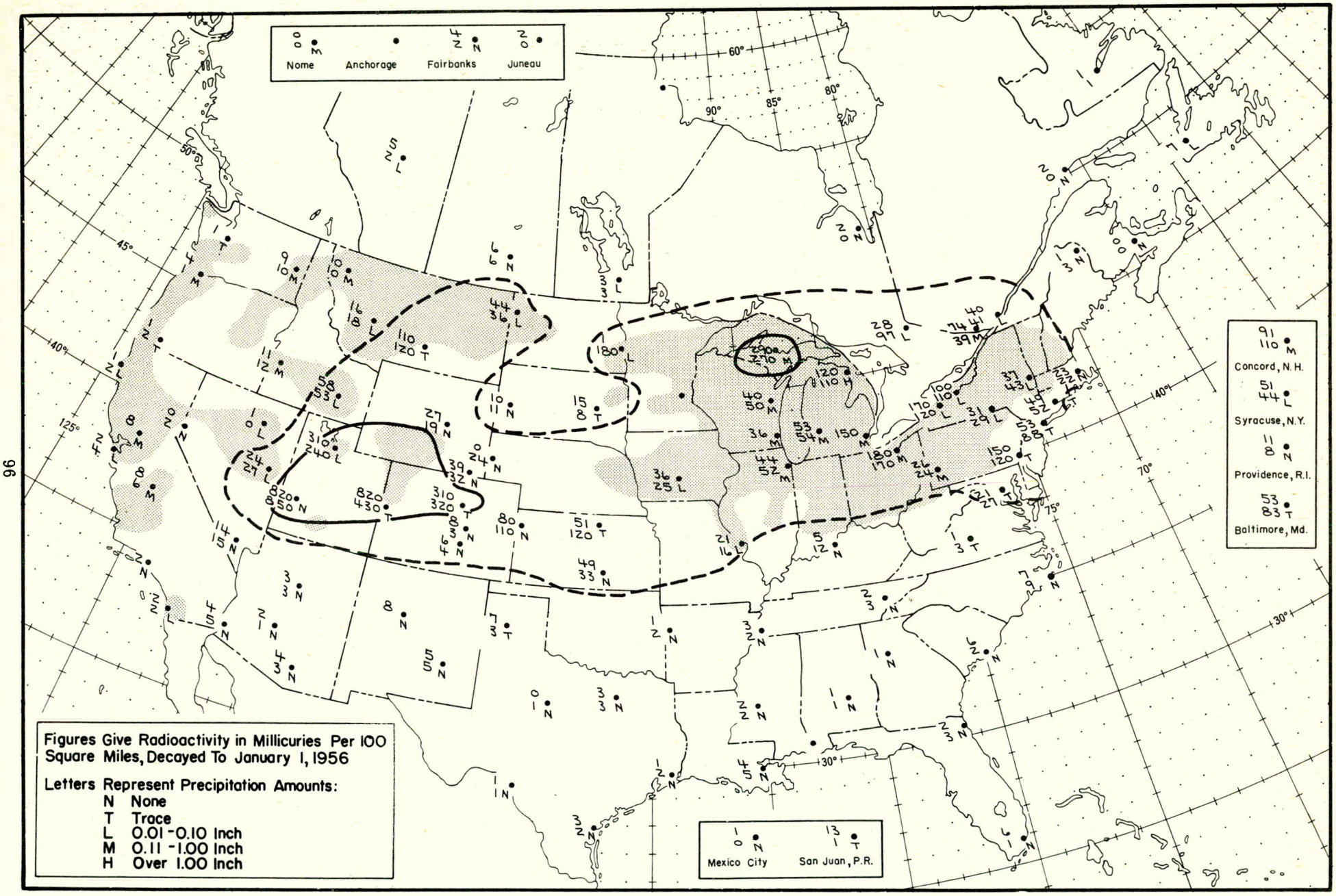

Figure A.60 Radioactive fallout in the 24-hour period beginning 1230 G.C.T., April 18, 1955

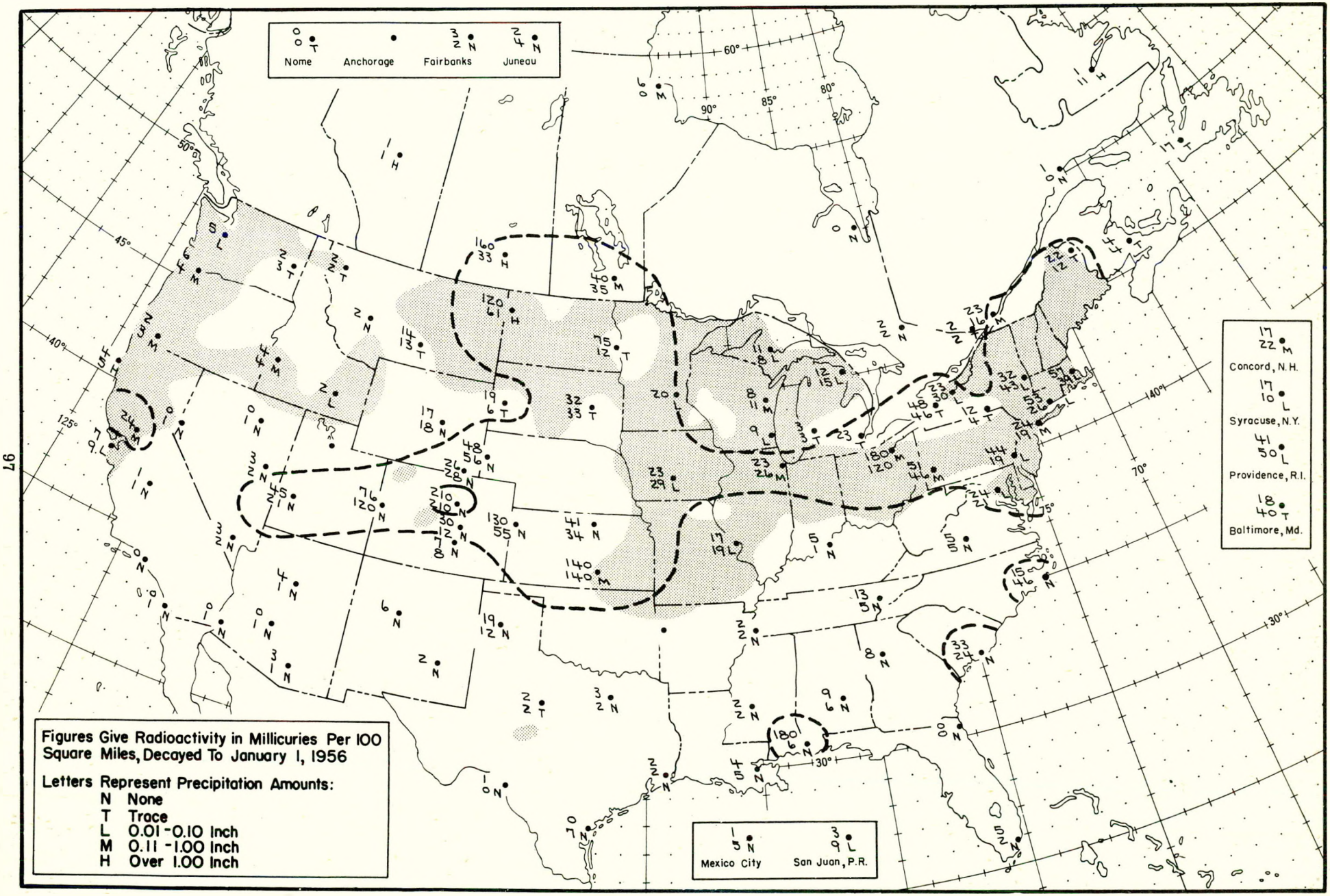

Figure A.61 Radioactive fallout in the 24-hour period beginning 1230 G.C.T., April 19, 1955

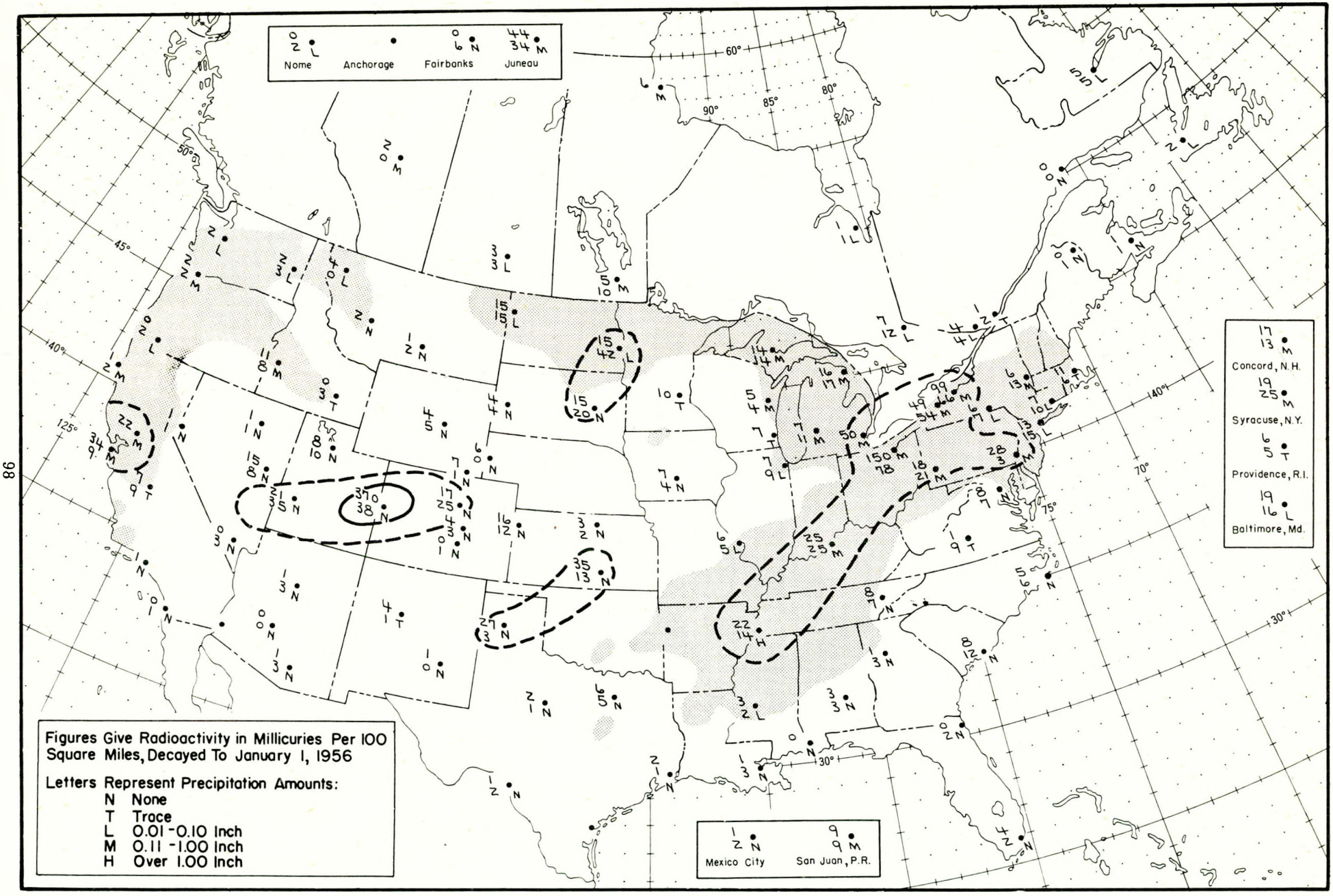

Figure A.62 Radioactive fallout in the 24-hour period beginning 1230 G.C.T., April 20, 1955

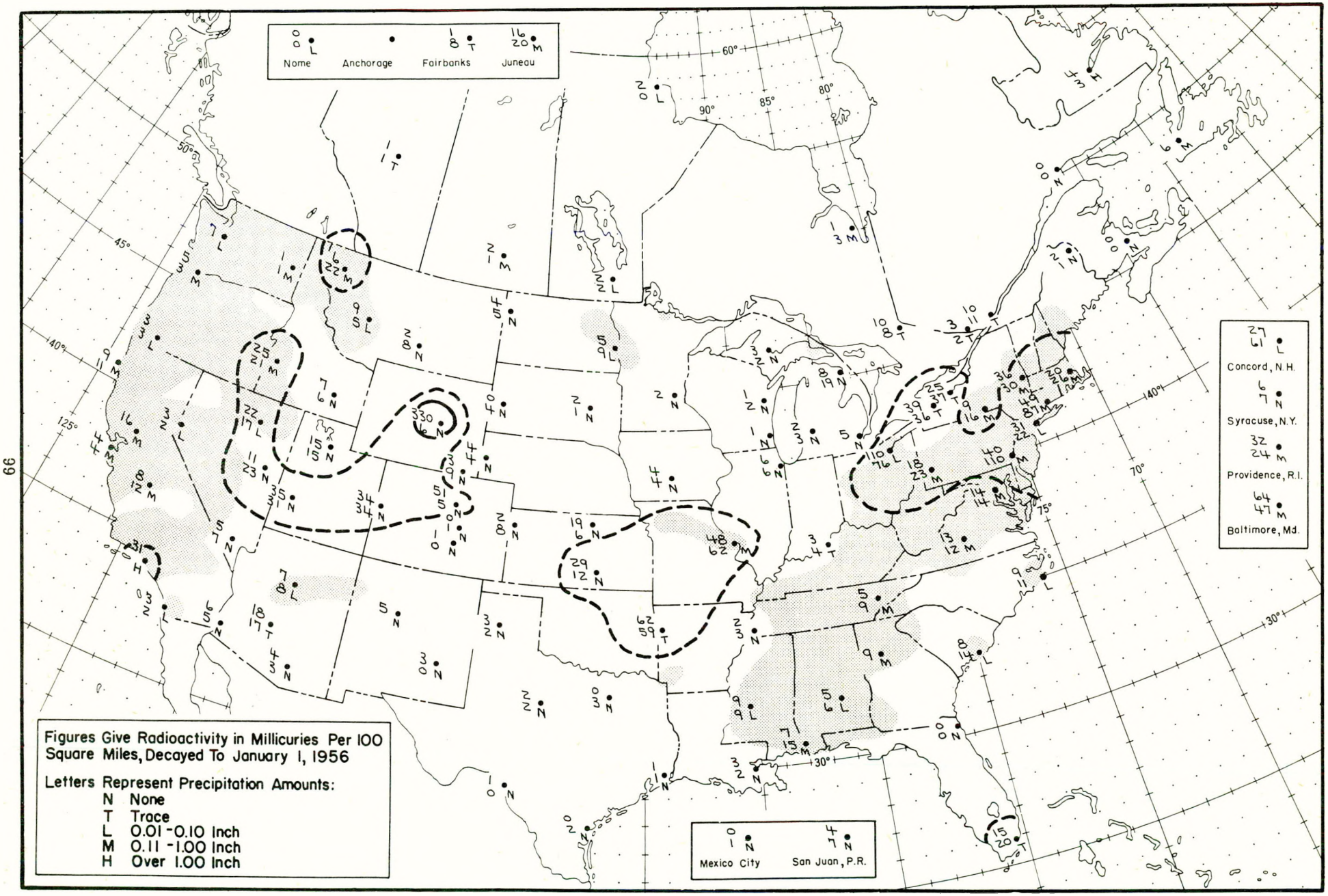

Figure A.63 Radioactive fallout in the 24-hour period beginning 1230 G.C.T., April 21, 1955

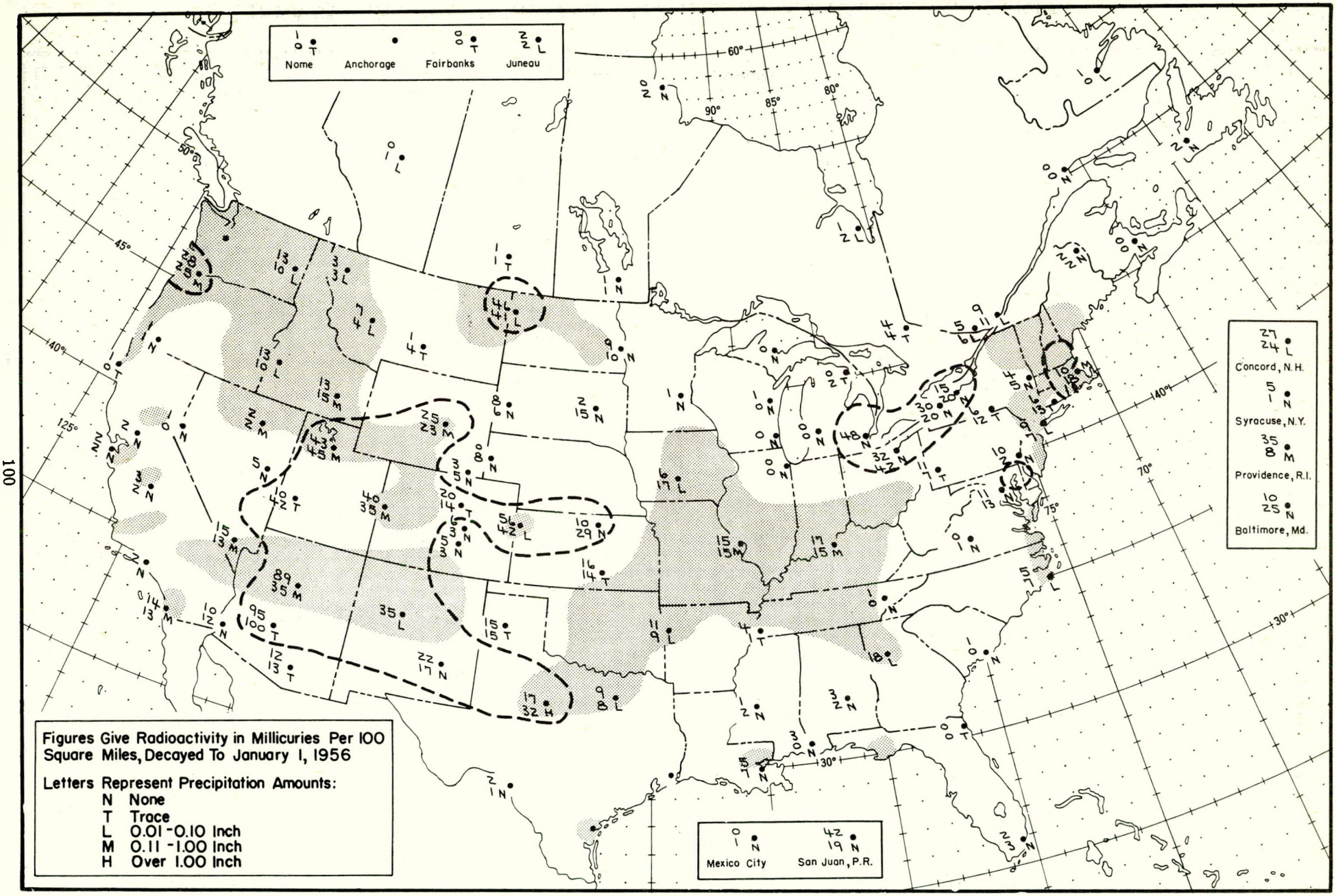

Figure A.64 Radioactive fallout in the 24-hour period beginning 1230 G.C.T., April 22, 1955

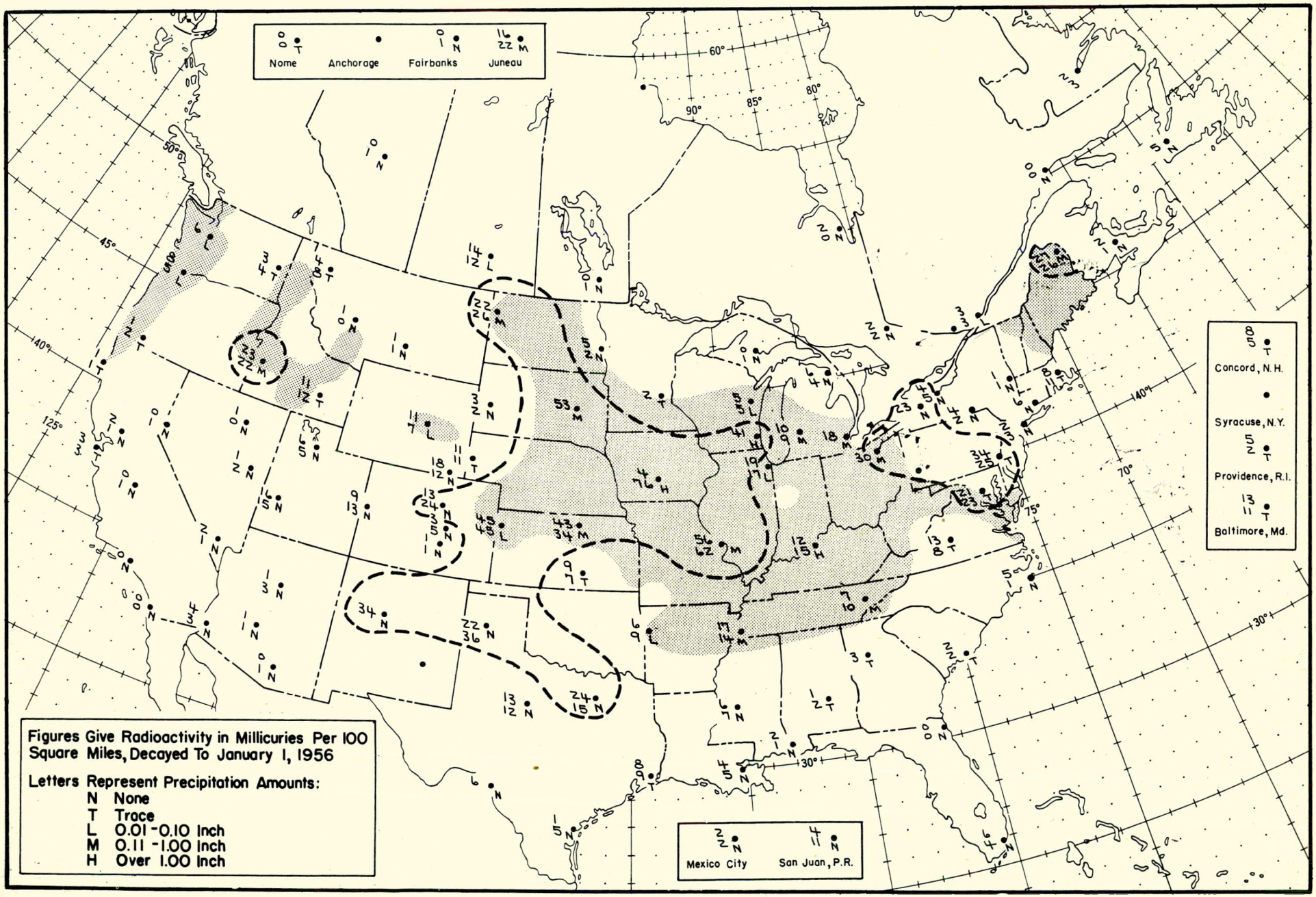

Figure A.65 Radioactive fallout in the 24-hour period beginning 1230 G.C.T., April 23, 1955

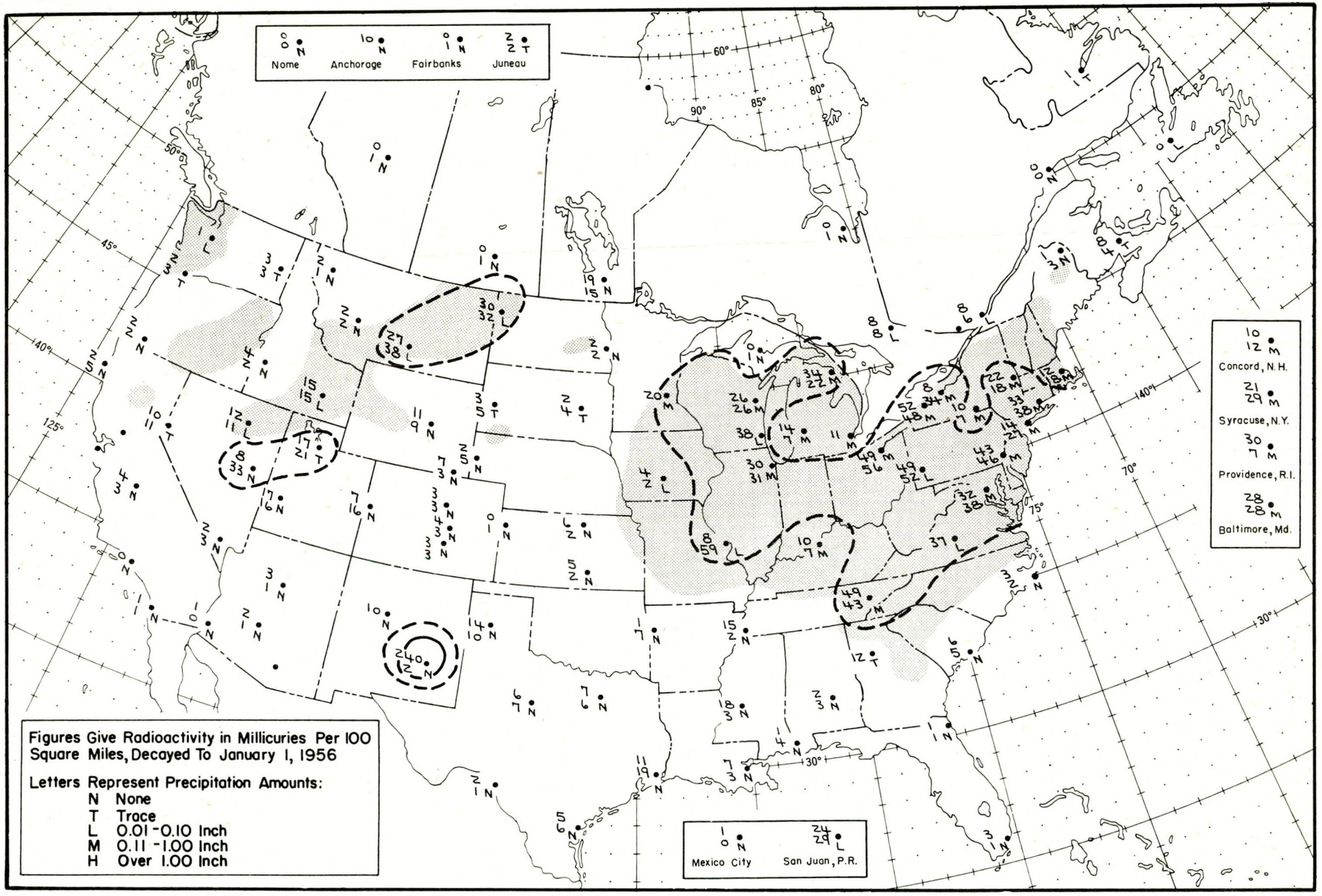

Figure A. 66 Radioactive fallout in the 24-hour period beginning 1230 G.C.T., April 24, 1955

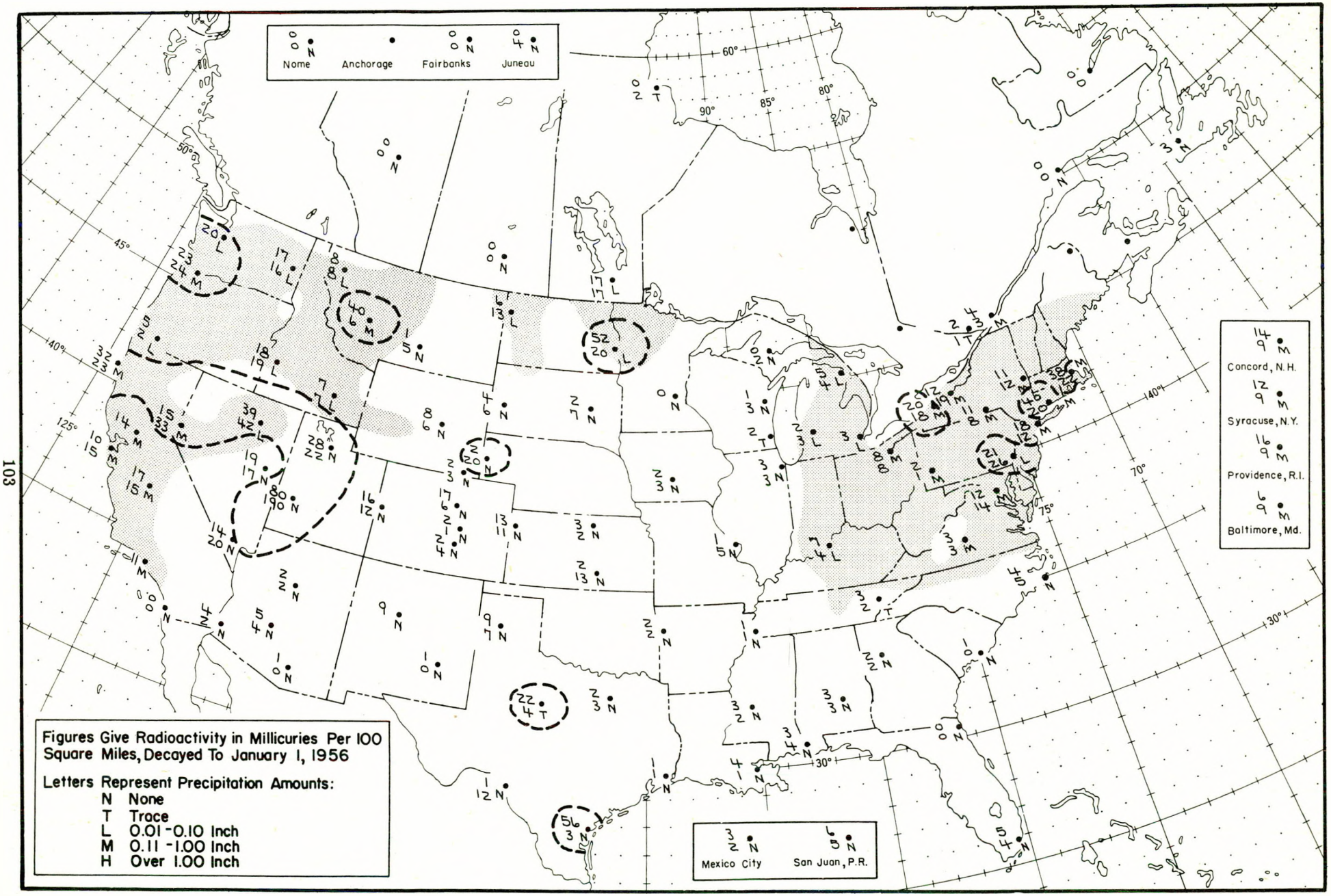

Figure A. 67 Radioactive fallout in the 24-hour period beginning 1230 G.C.T., April 25, 1955

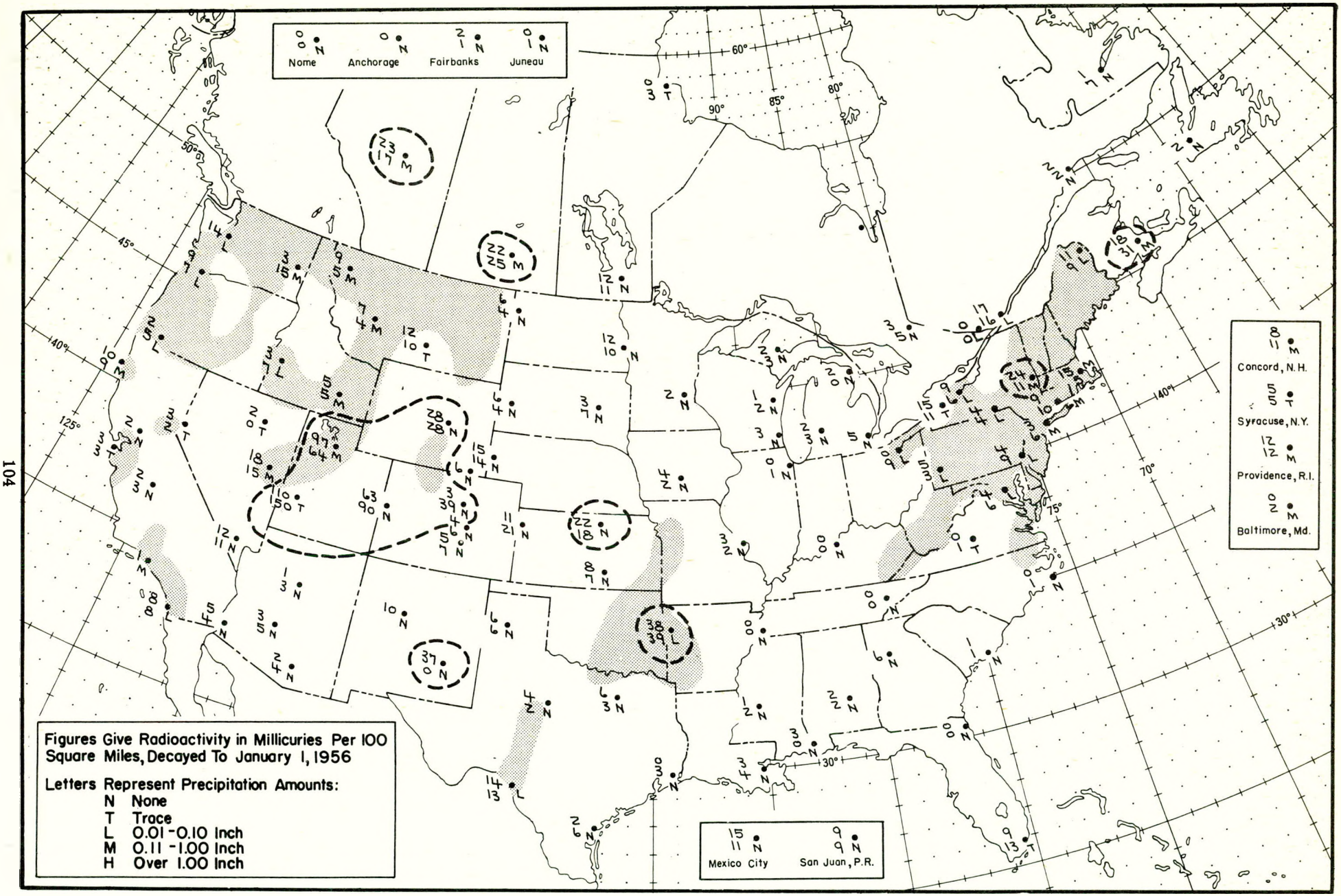

Figure A. 68 Radioactive fallout in the 24-hour period beginning 1230 G.C.T., April 26, 1955

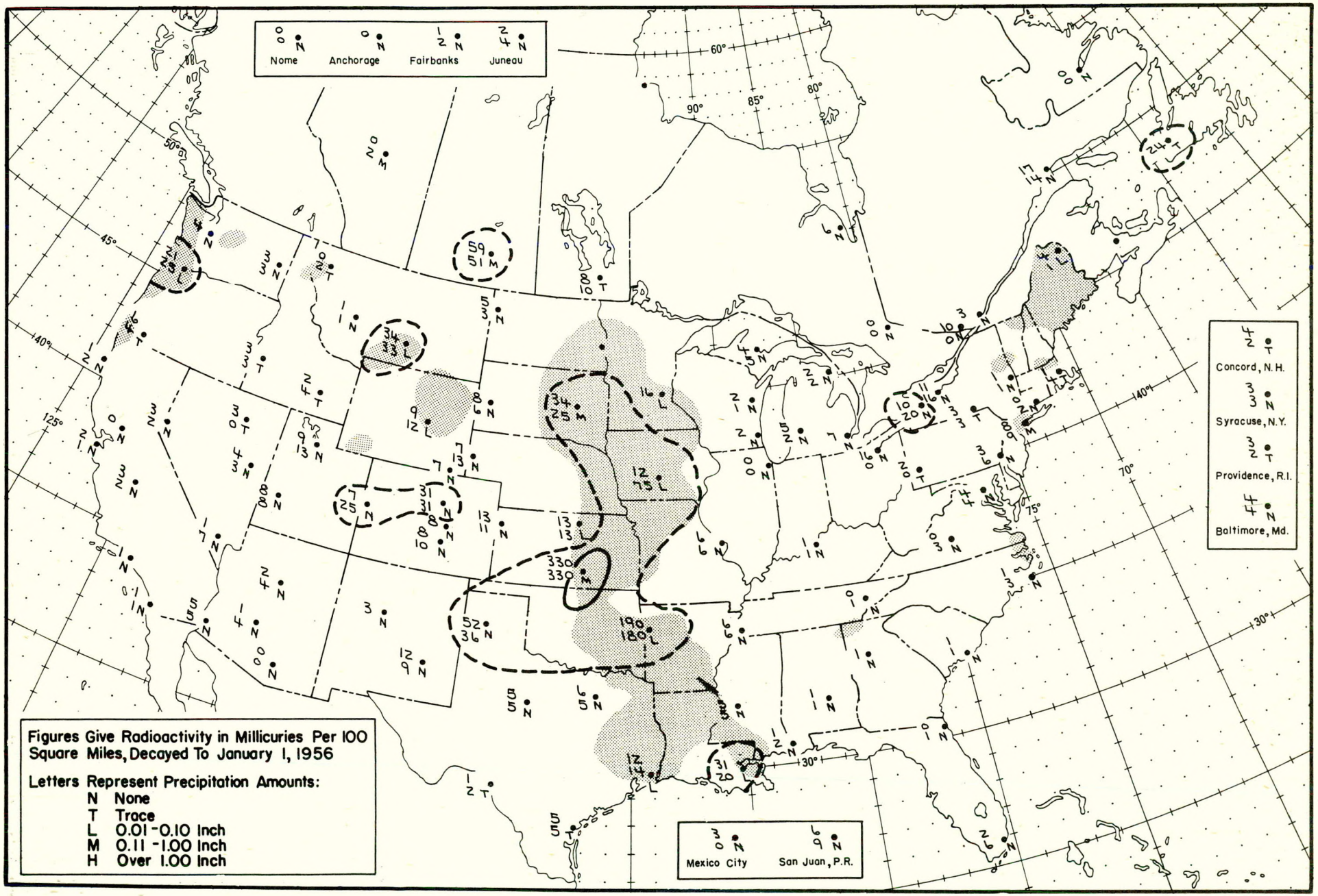

Figure A.69 Radioactive fallout in the 24-hour period beginning 1230 G.C.T., April 27, 1955

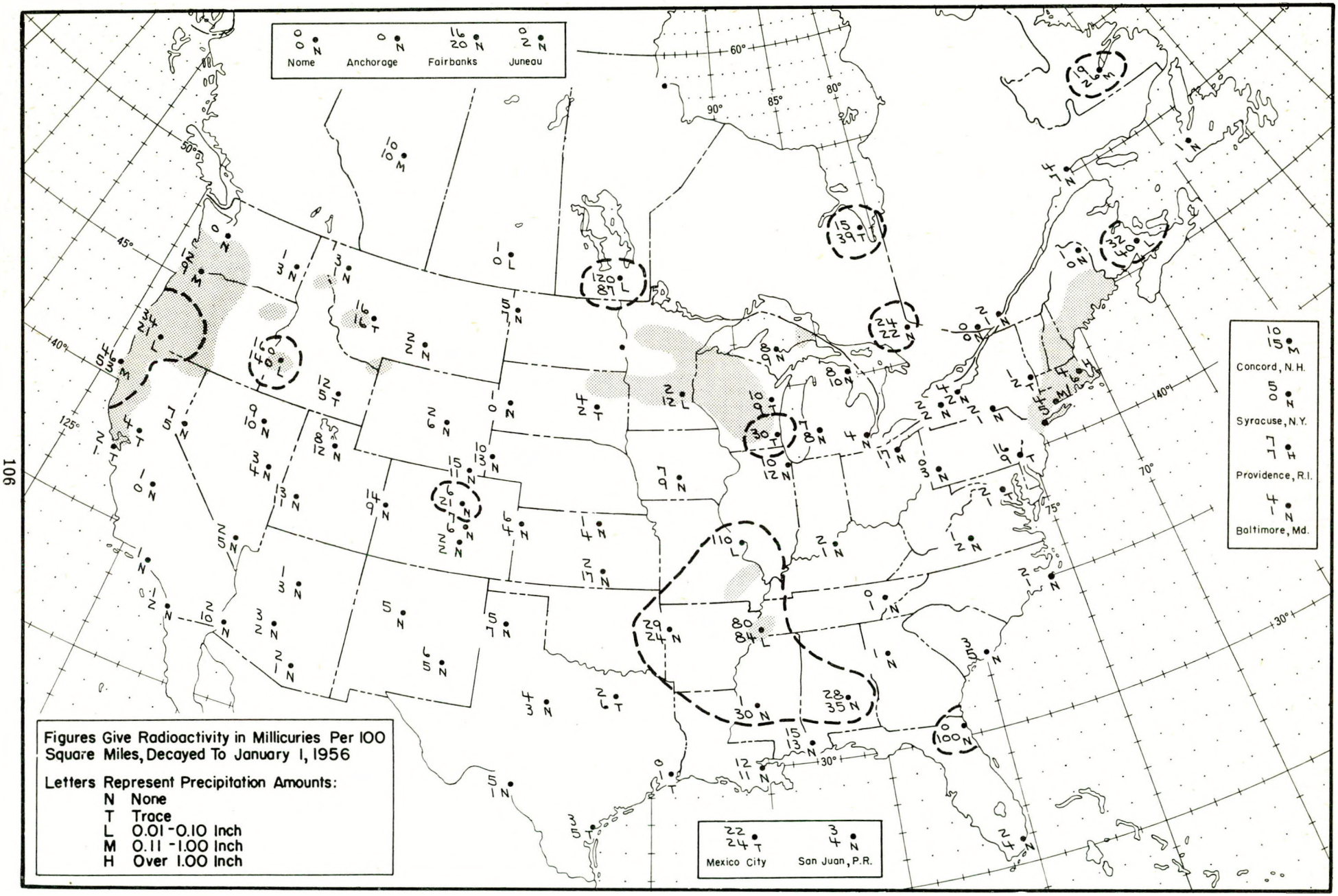

Figure A. 70 Radioactive fallout in the 24-hour period beginning 1230 G.C.T., April 28, 1955

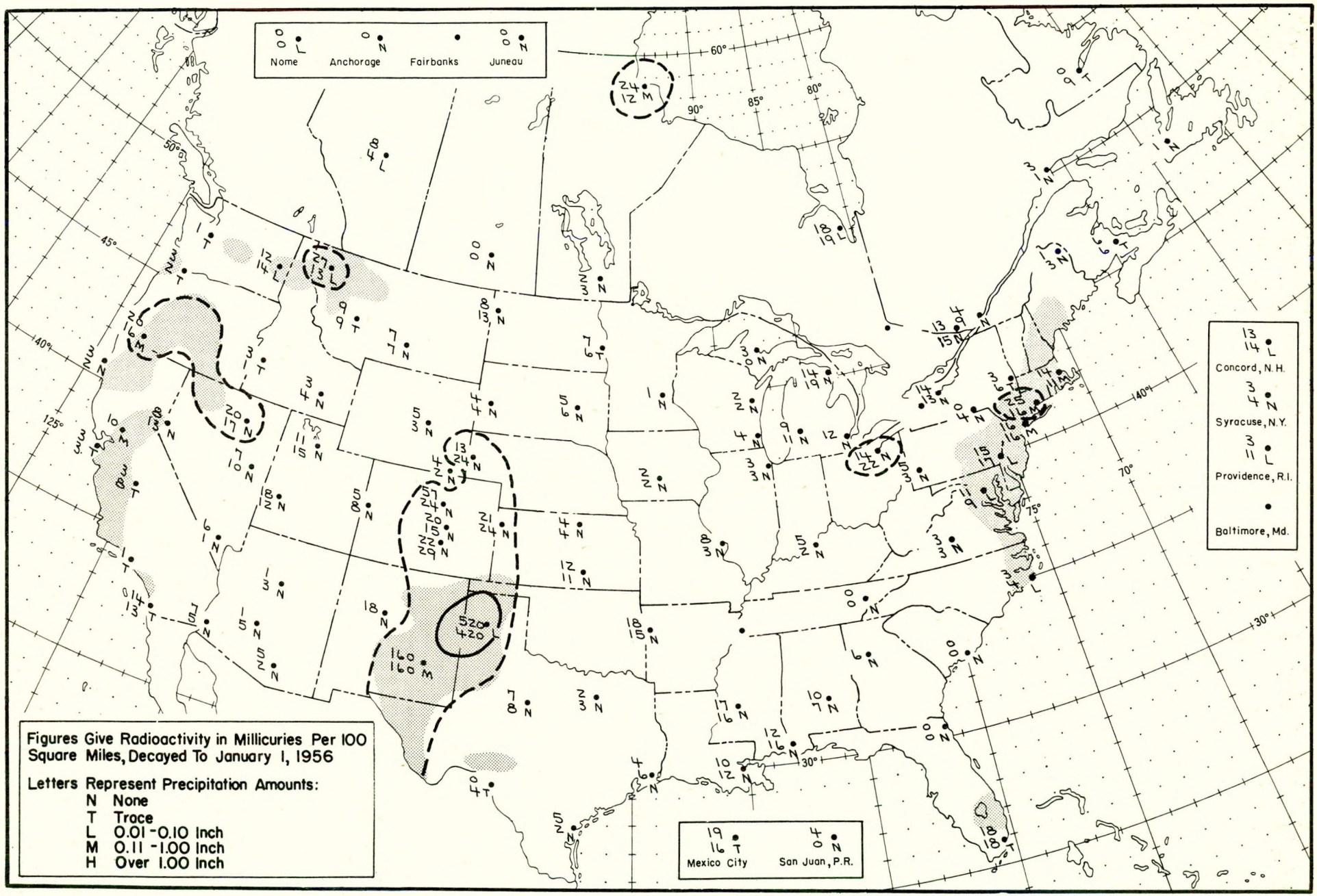

Figure A. 71 Radioactive fallout in the 24-hour period beginning 1230 G.C.T., April 29, 1955

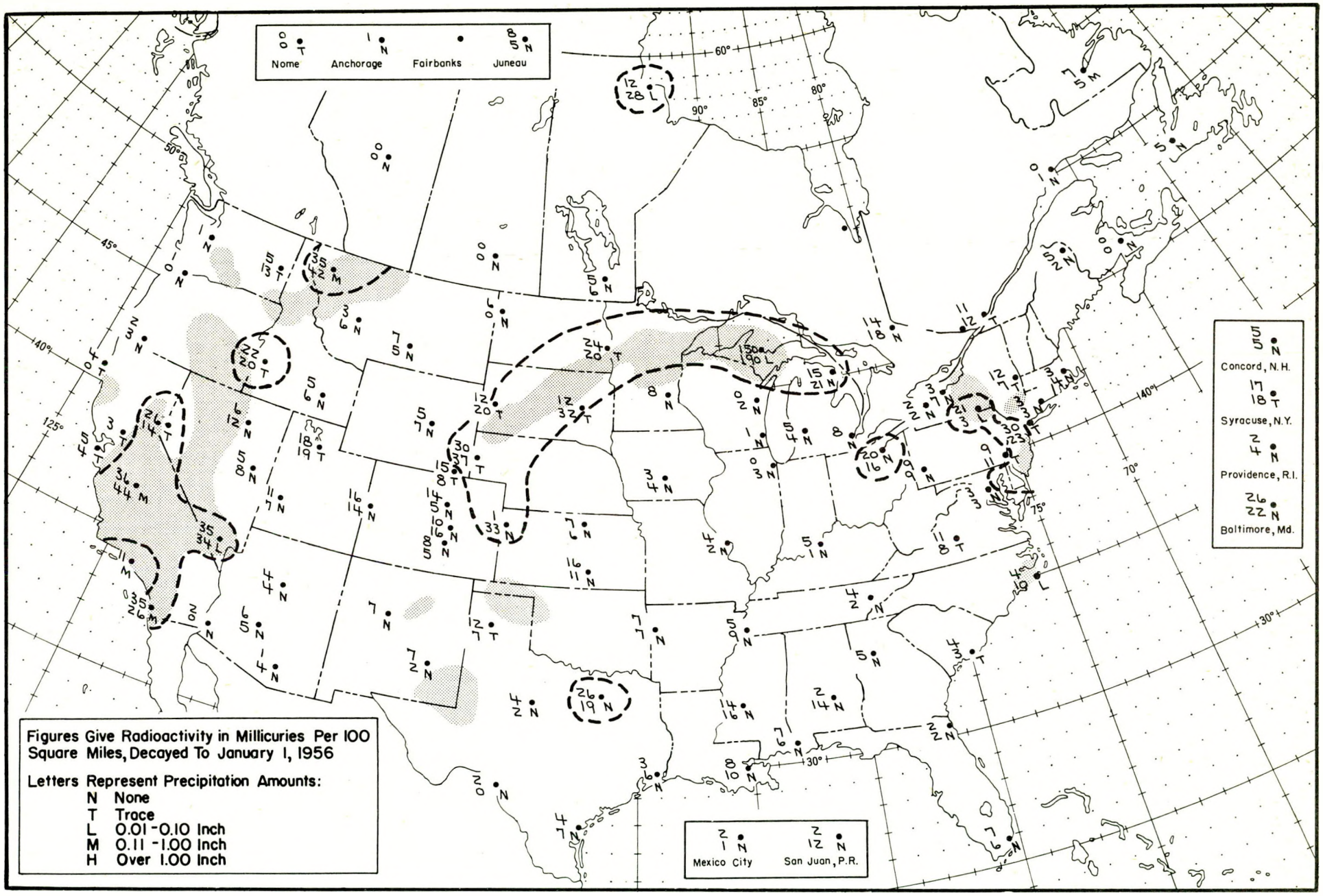

Figure A. 72 Radioactive fallout in the 24-hour period beginning 1230 G.C.T., April 30, 1955

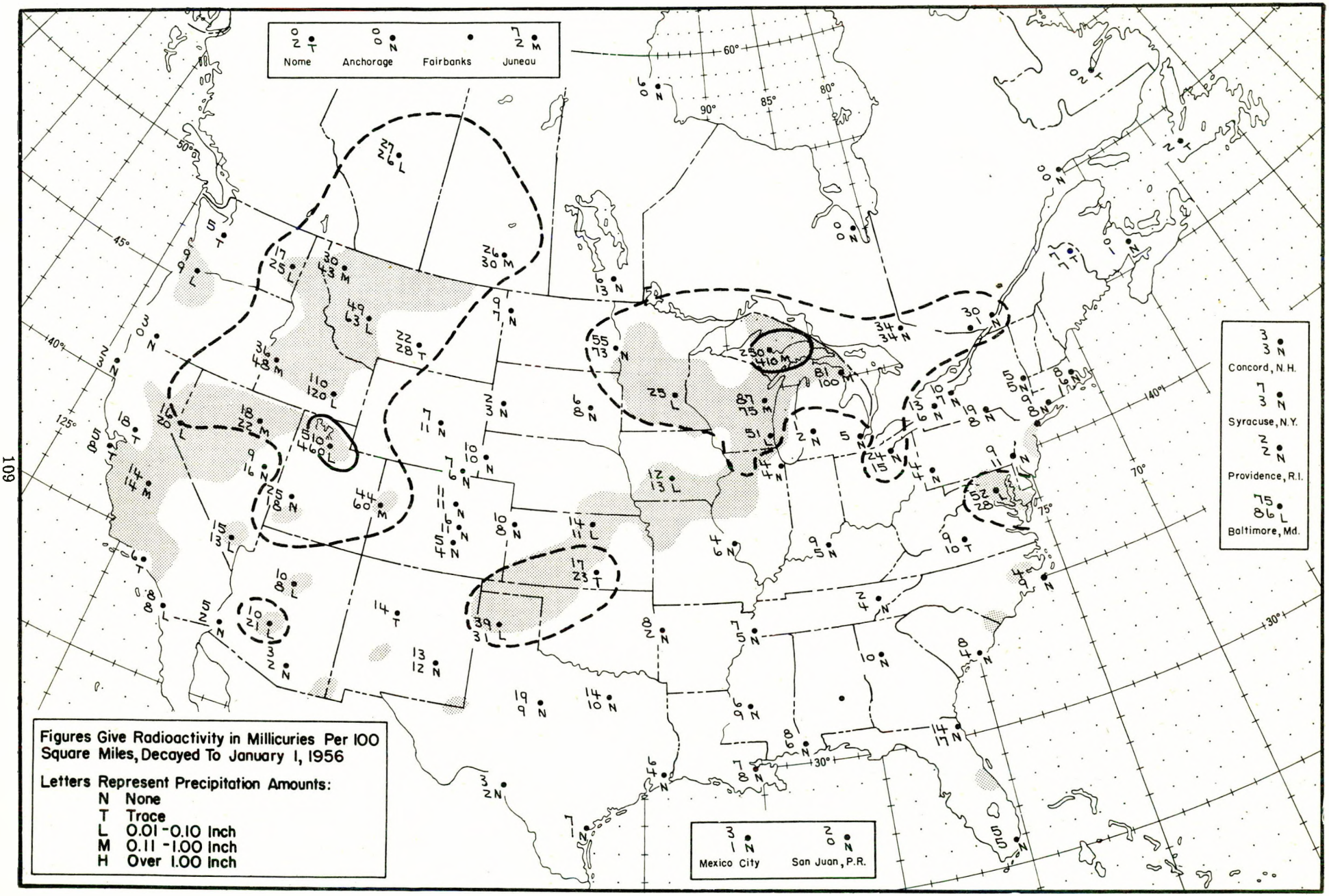

Figure A.73 Radioactive fallout in the 24-hour period beginning 1230 G.C.T., May 1, 1955

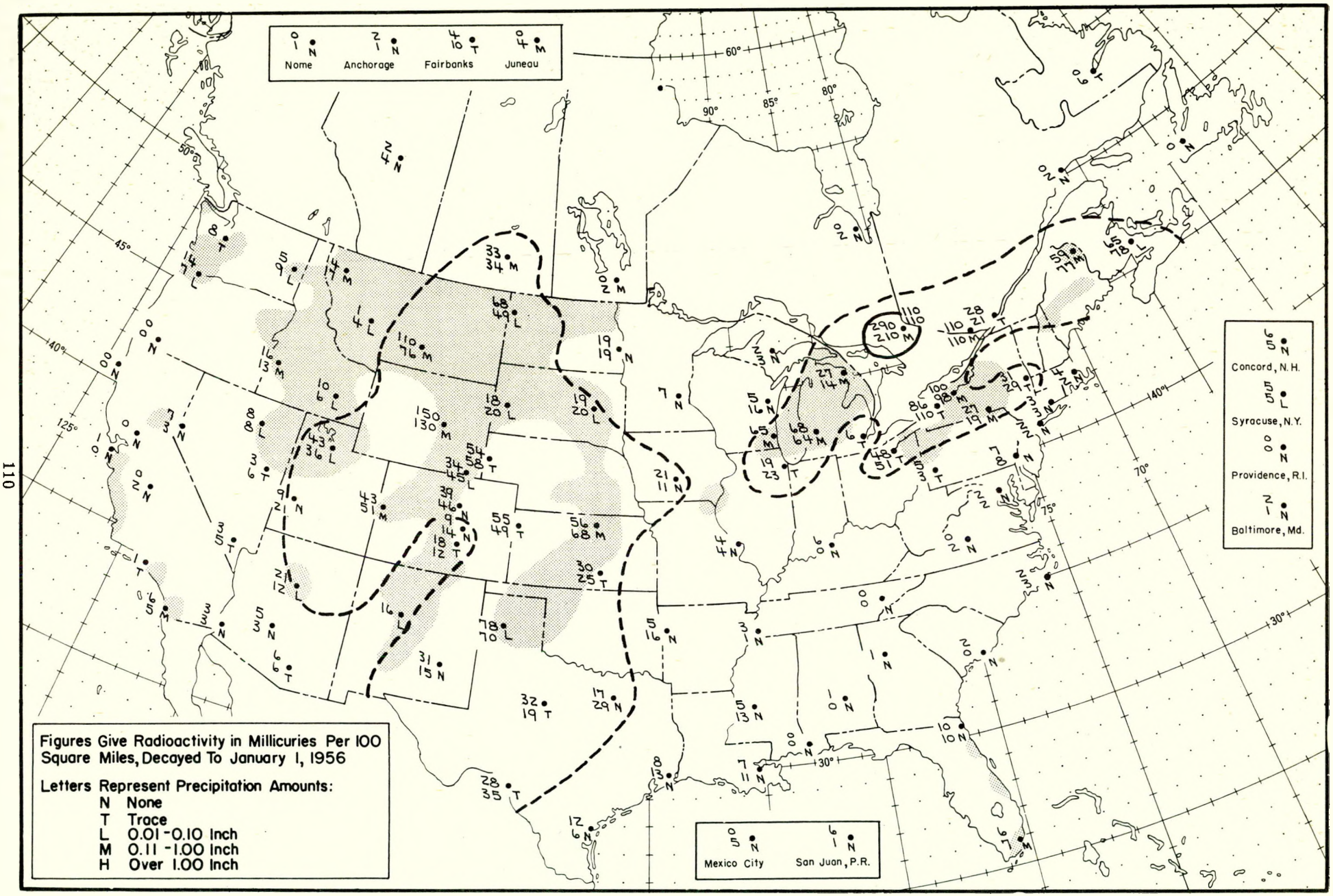

Figure A. 74 Radioactive fallout in the 24-hour period beginning 1230 G.C.T., May 2, 1955

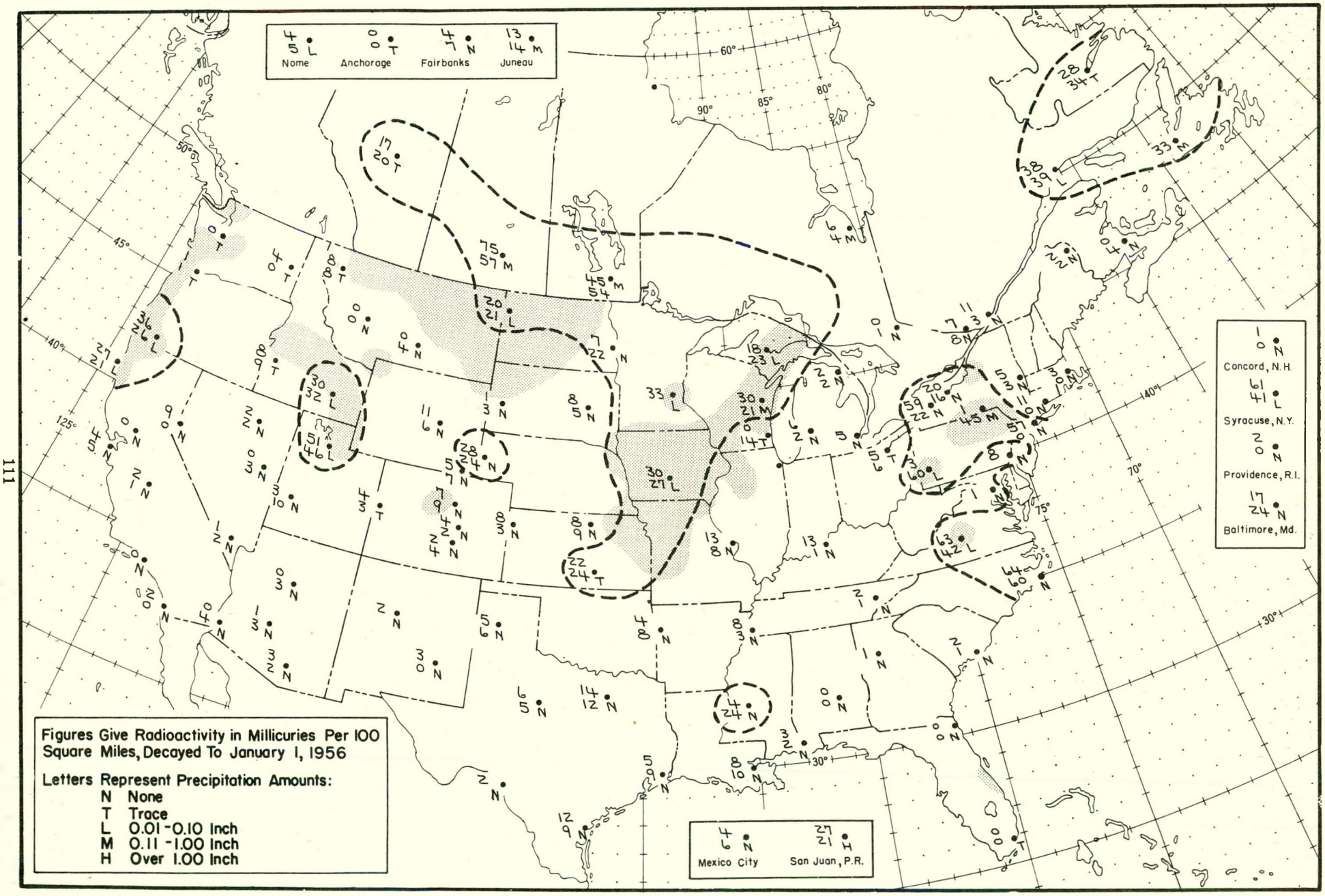

Figure A.75 Radioactive fallout in the 24-hour period beginning 1230 G.C.T., May 3, 1955

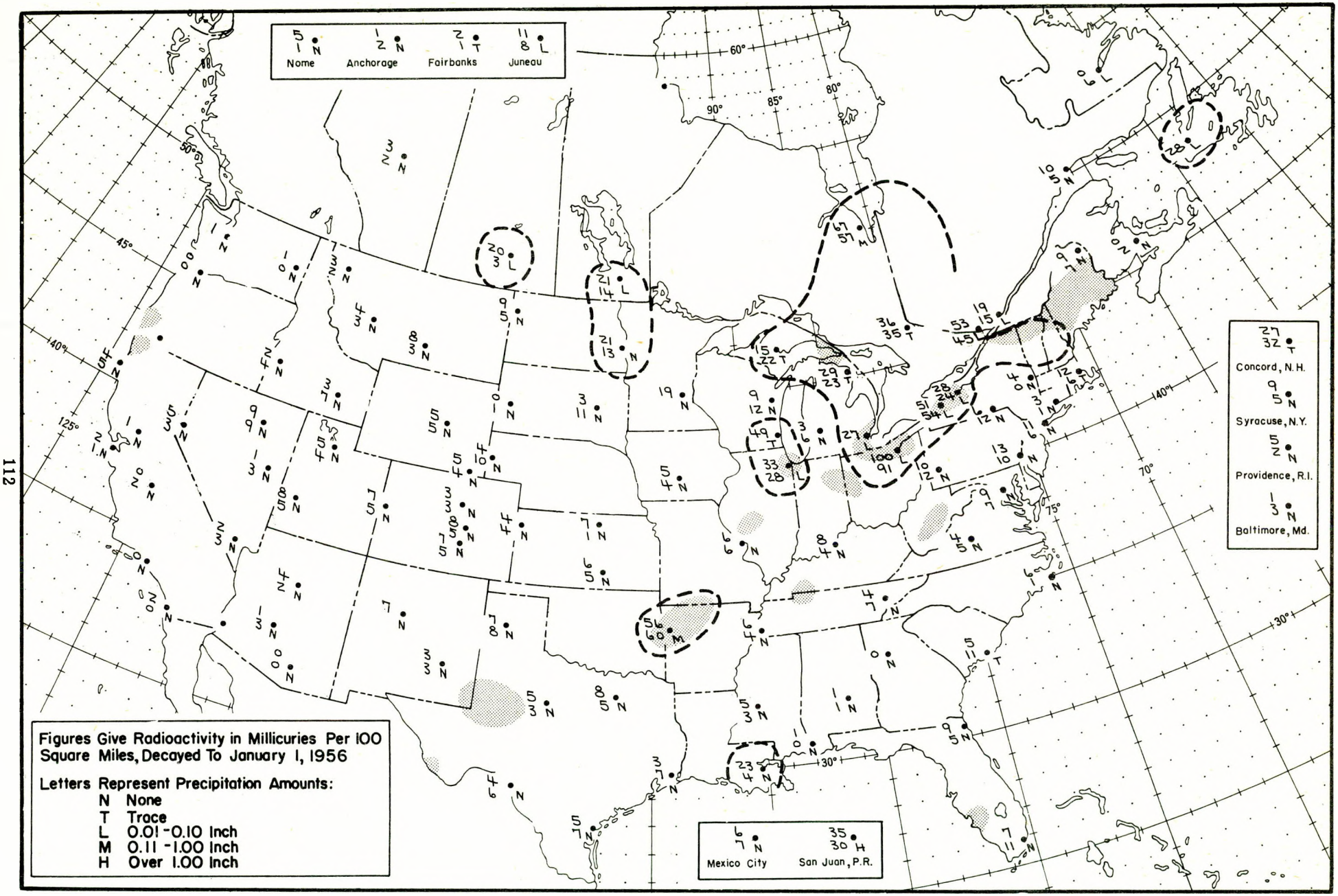

Figure A.76 Radioactive fallout in the 24-hour period beginning 1230 G.C.T., May 4, 1955

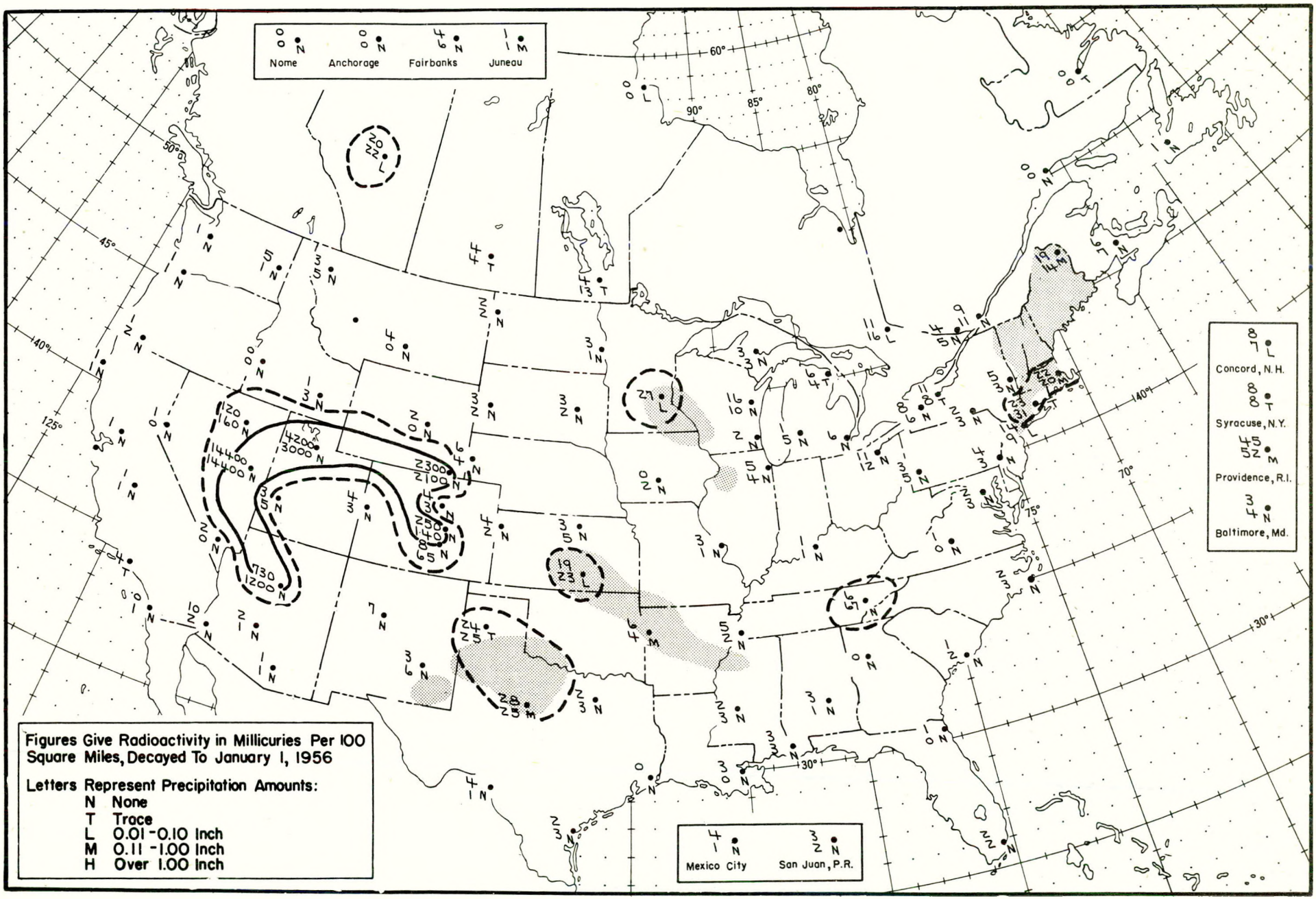

Figure A.77 Radioactive fallout in the 24-hour period beginning 1230 G.C.T., May 5, 1955

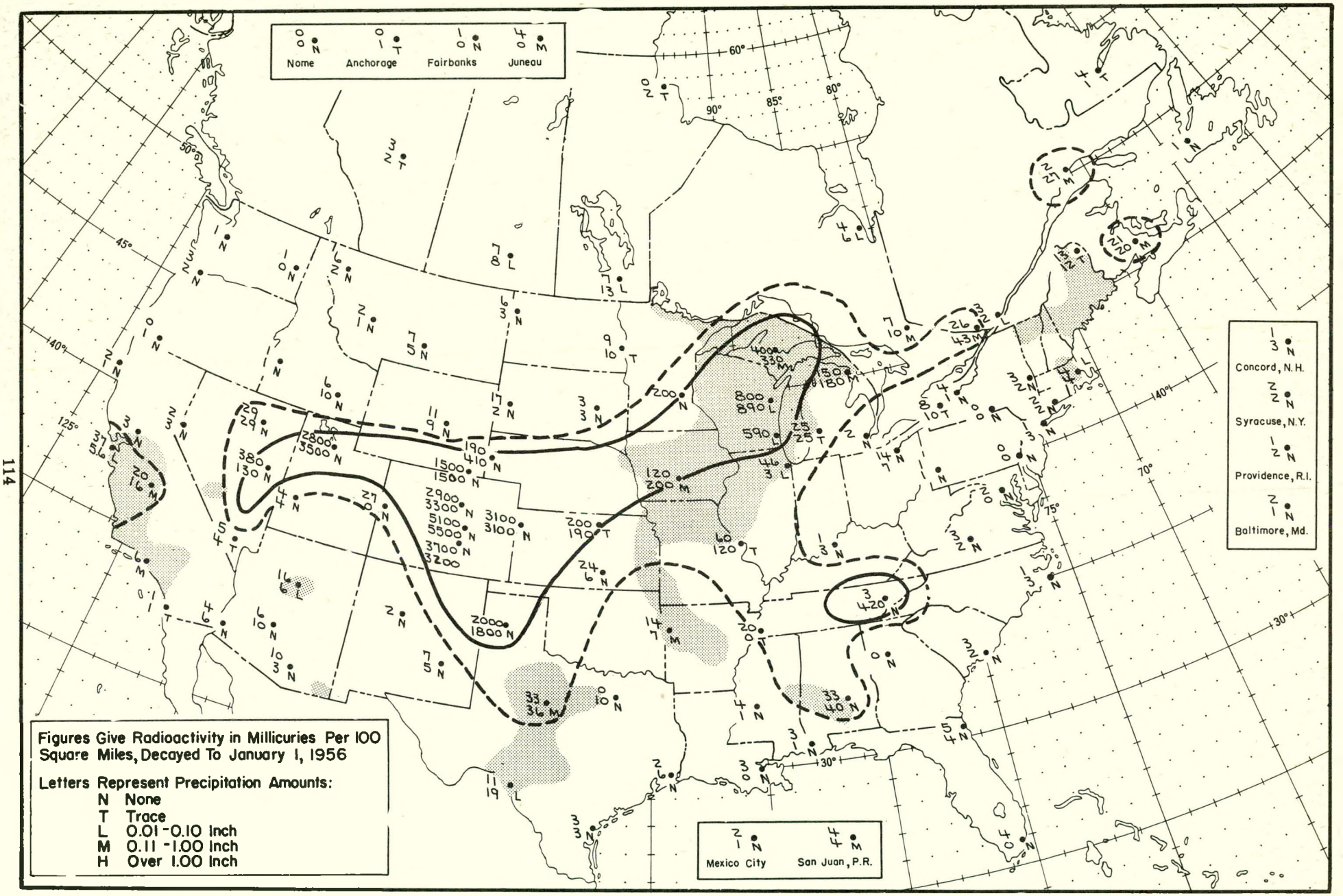

Figure A.78 Radioactive fallout in the 24-hour period beginning 1230 G.C.T., May 6, 1955

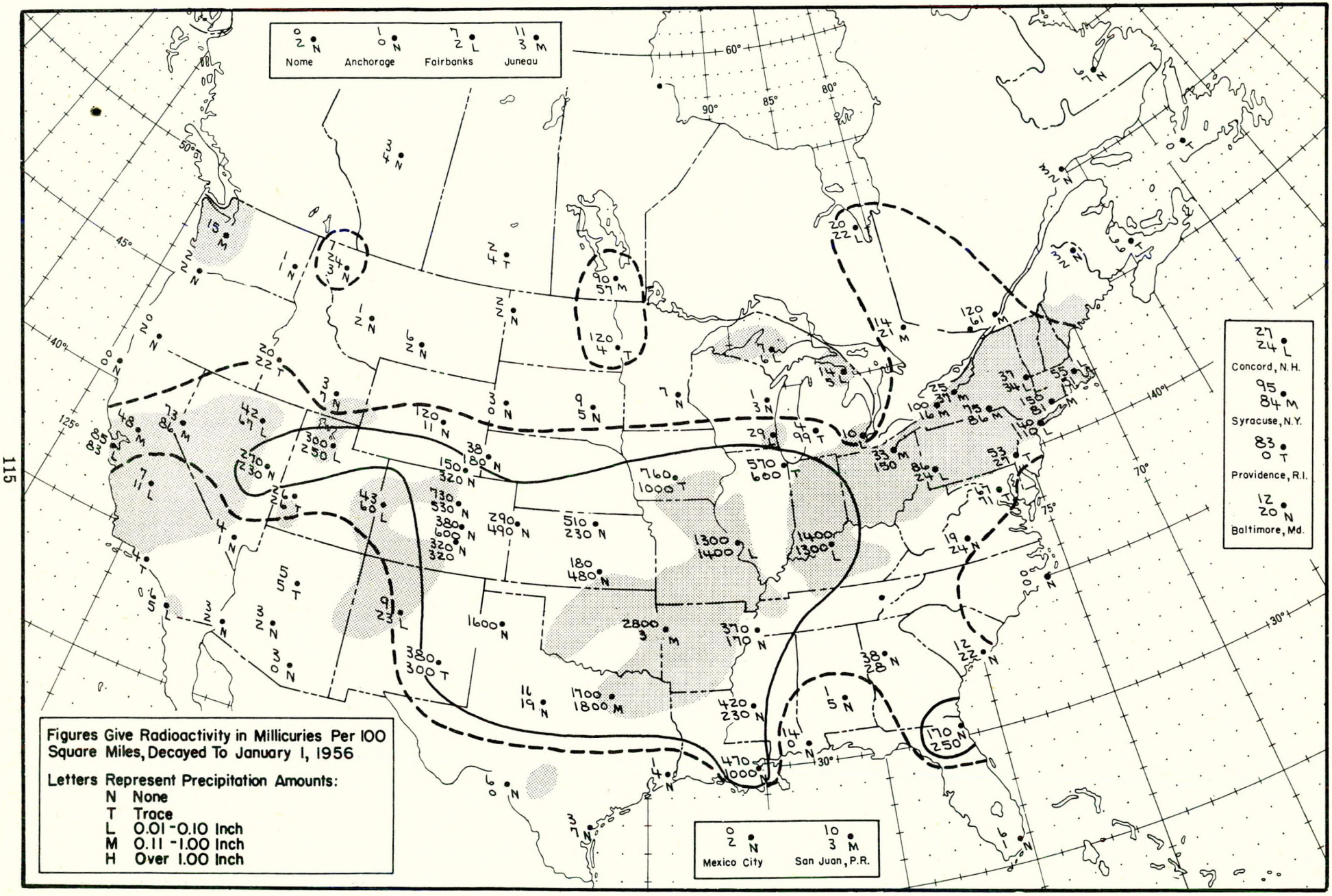

Figure A.79 Radioactive fallout in the 24-hour period beginning 1230 G.C.T., May 7, 1955

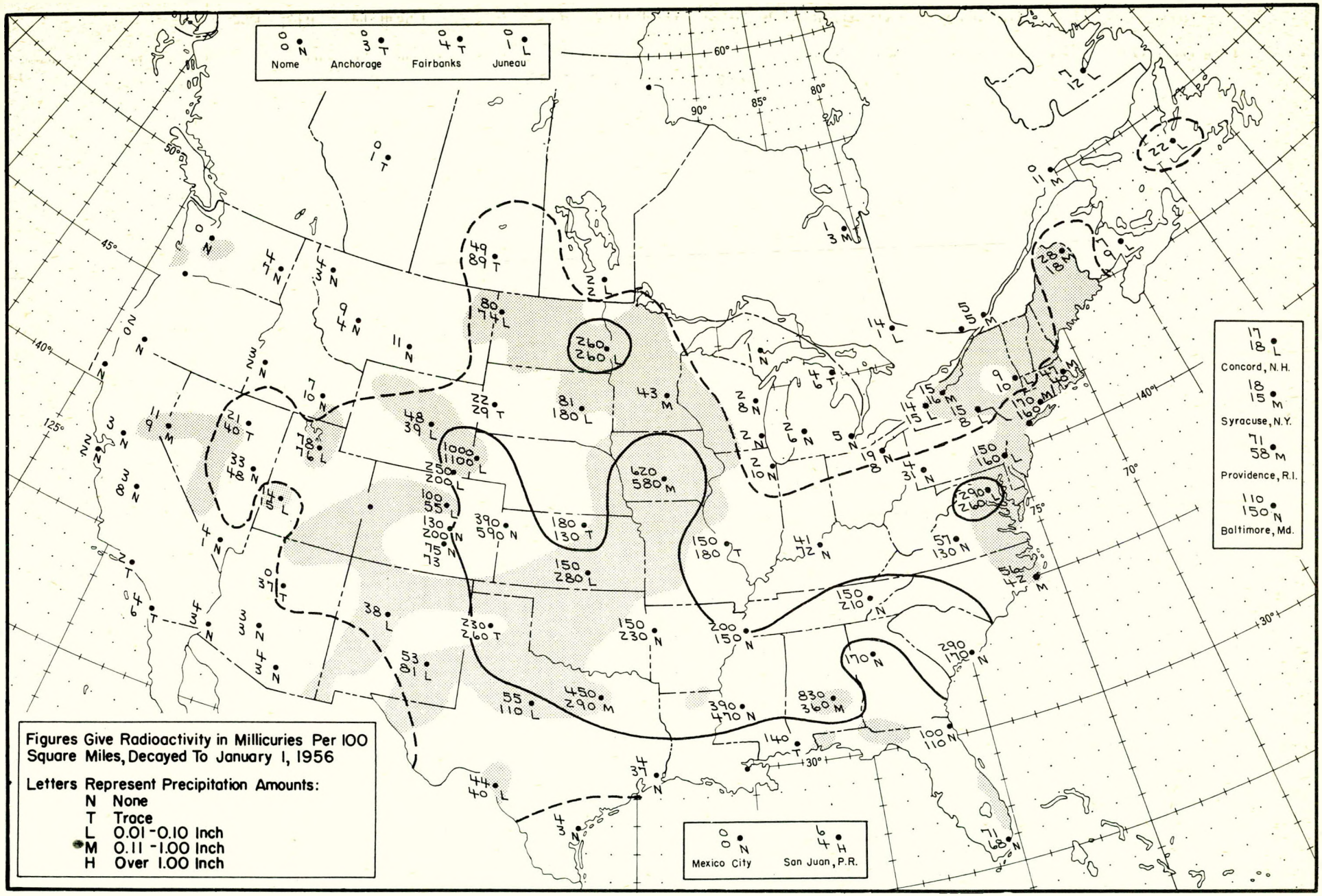

Figure A. 80 Radioactive fallout in the 24-hour period beginning 1230 G.C.T., May 8, 1955

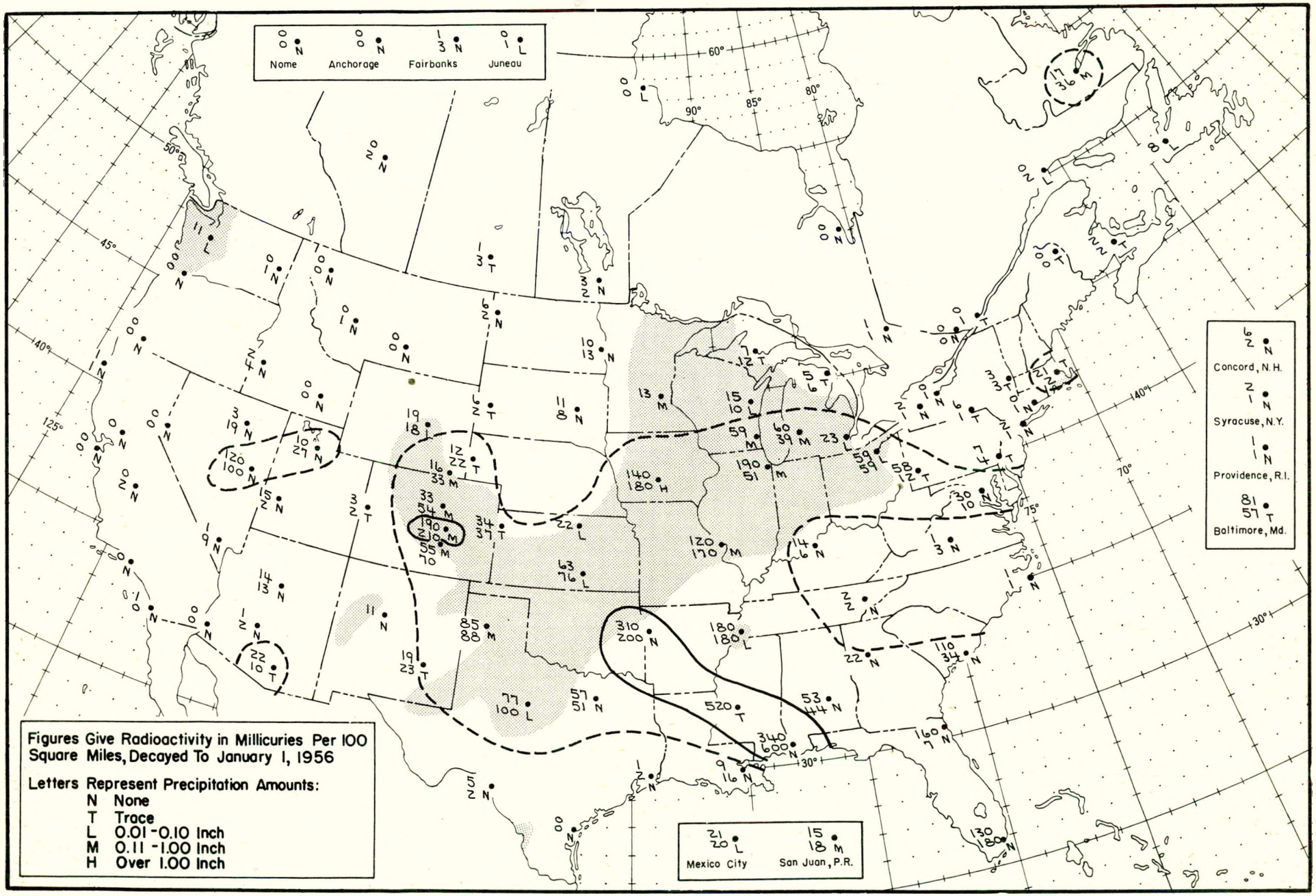

Figure A.81 Radioactive fallout in the 24-hour period beginning 1230 G.C.T., May 9, 1955

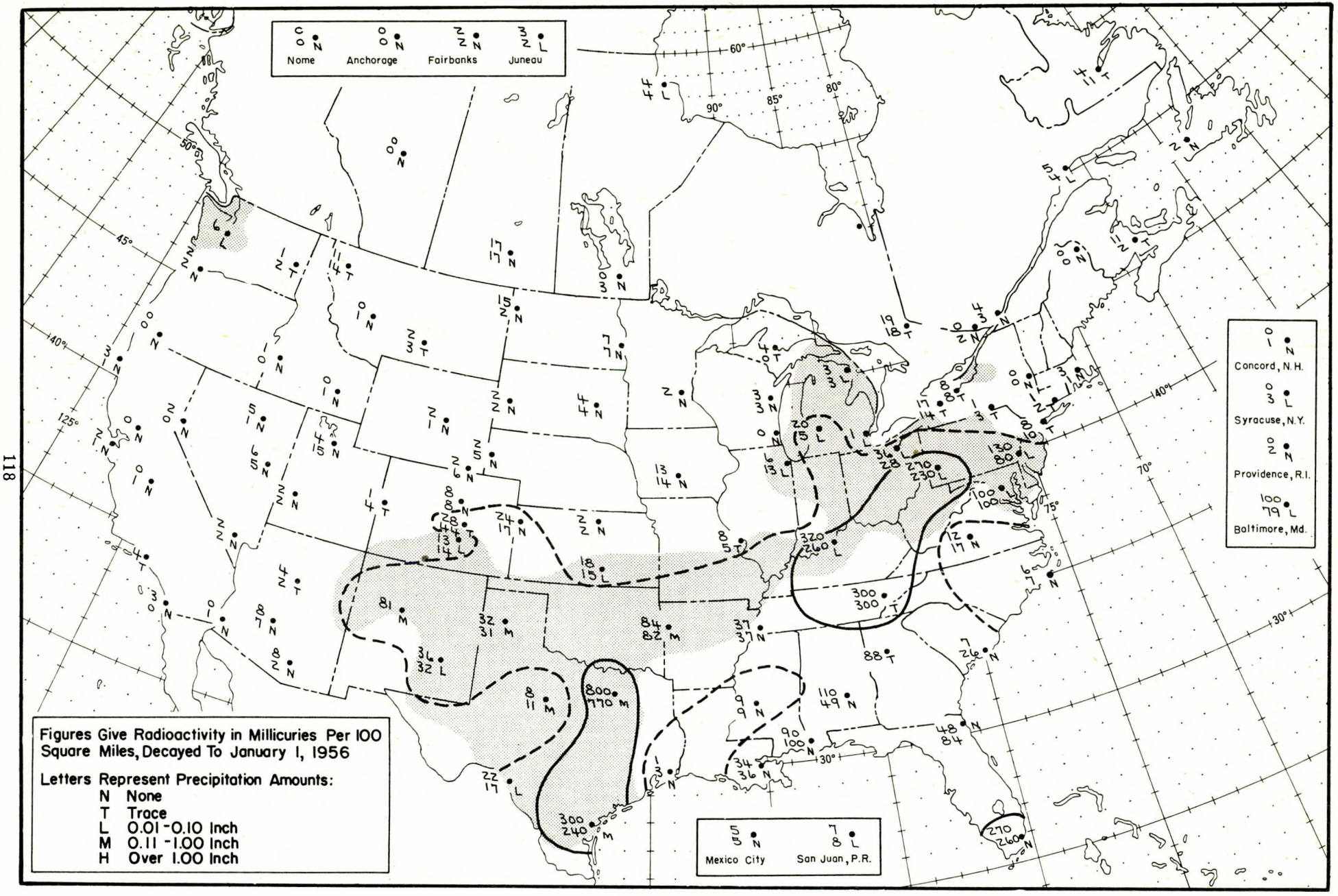

Figure A. 82 Radioactive fallout in the 24-hour period beginning 1230 G.C.T., May 10, 1955

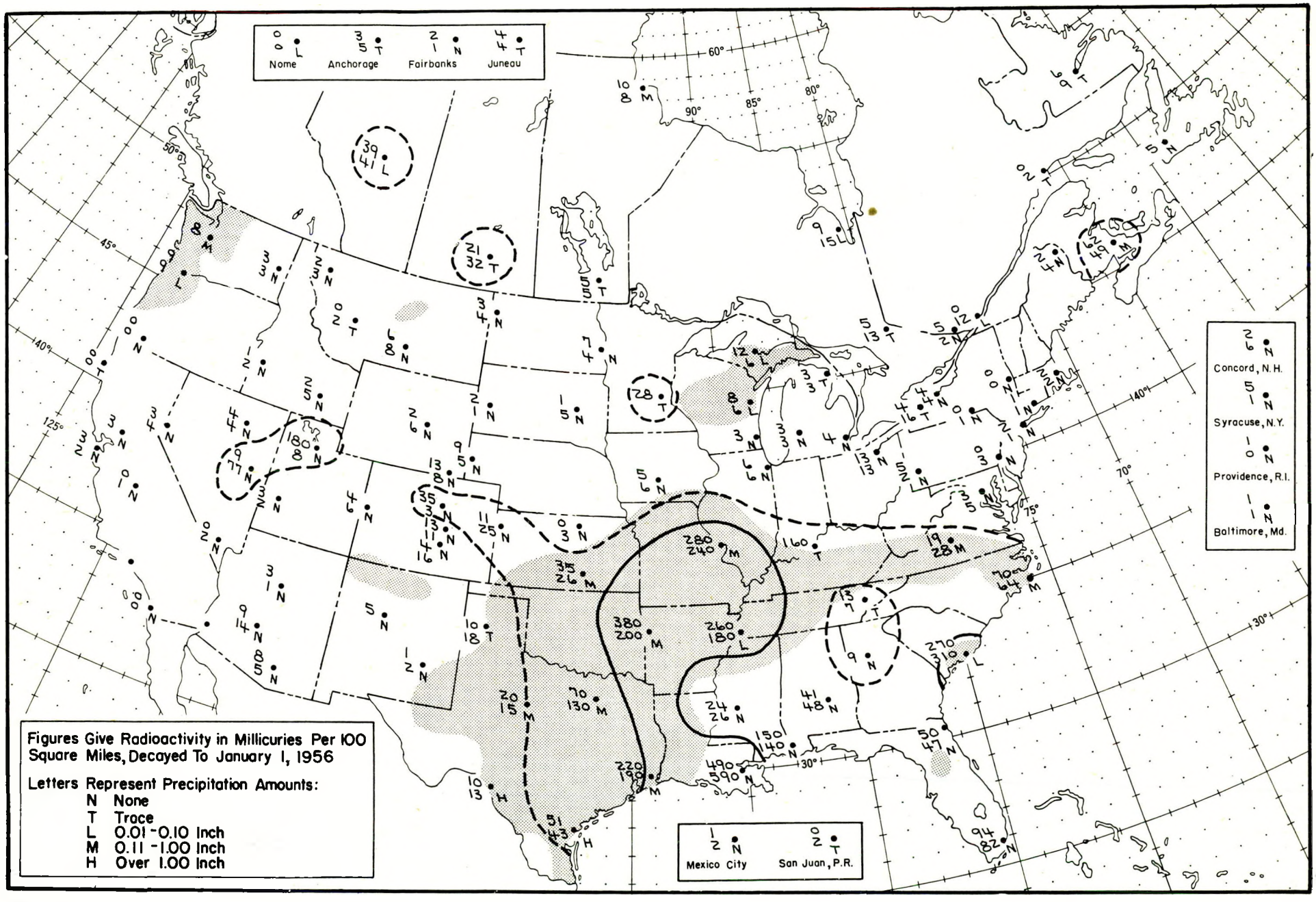

Figure A. 83 Radioactive fallout in the 24-hour period beginning 1230 G.C.T., May 11, 1955

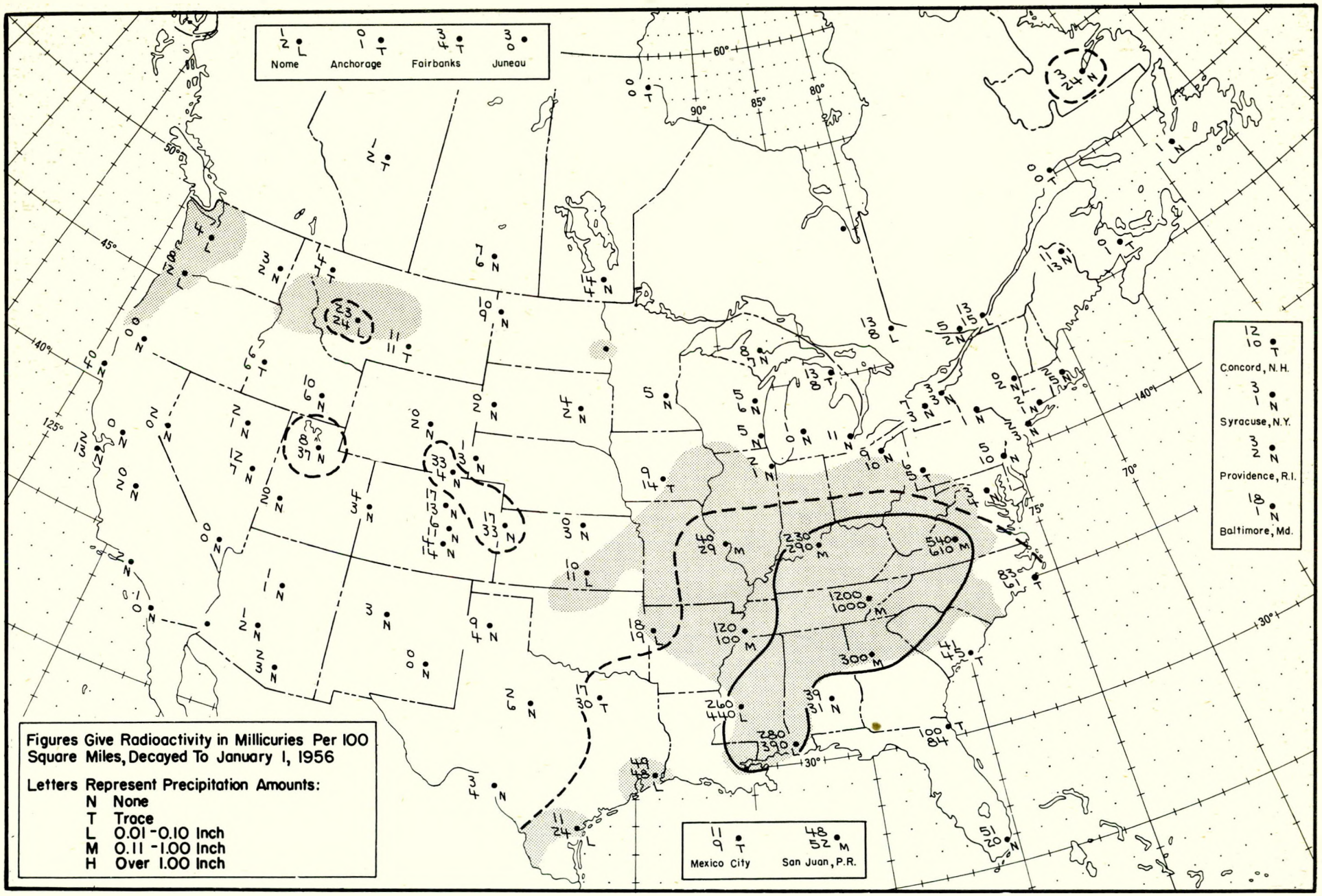

Figure A. 84 Radioactive fallout in the 24-hour period beginning 1230 G.C.T., May 12, 1955

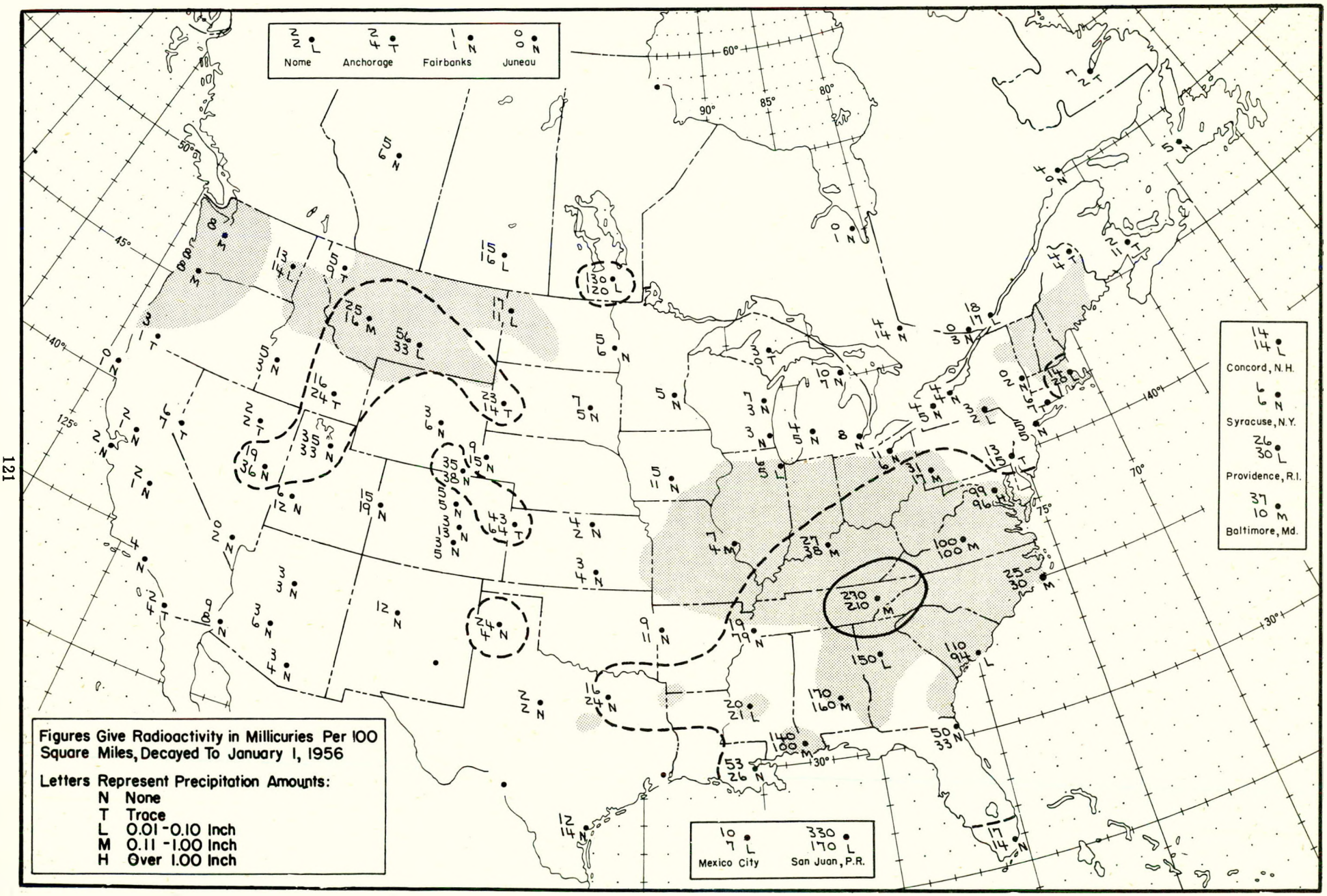

Figure A.85 Radioactive fallout in the 24-hour period beginning 1230 G.C.T., May 13, 1955

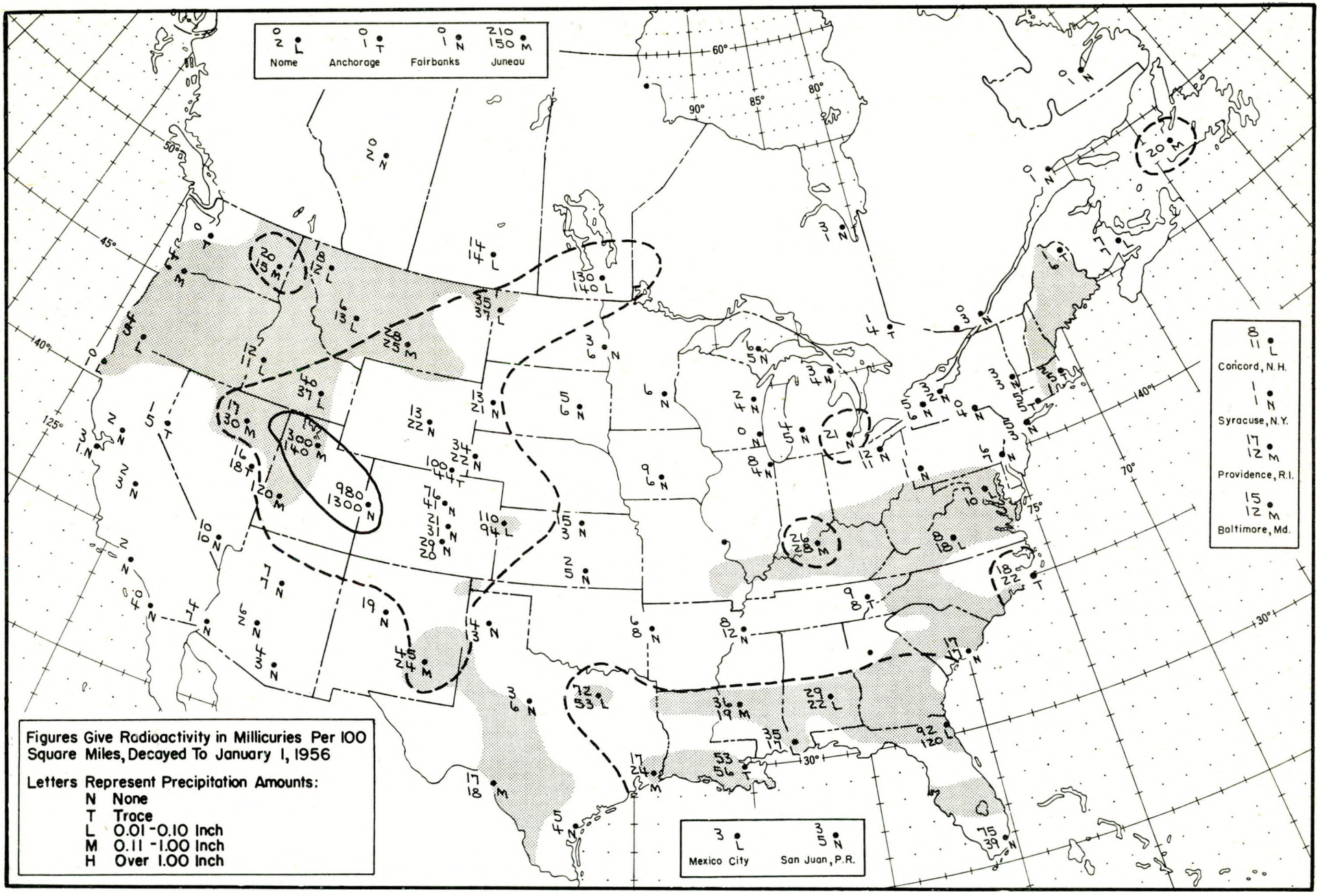

Figure A. 86 Radioactive fallout in the 24-hour period beginning 1230 G.C.T., May 14, 1955

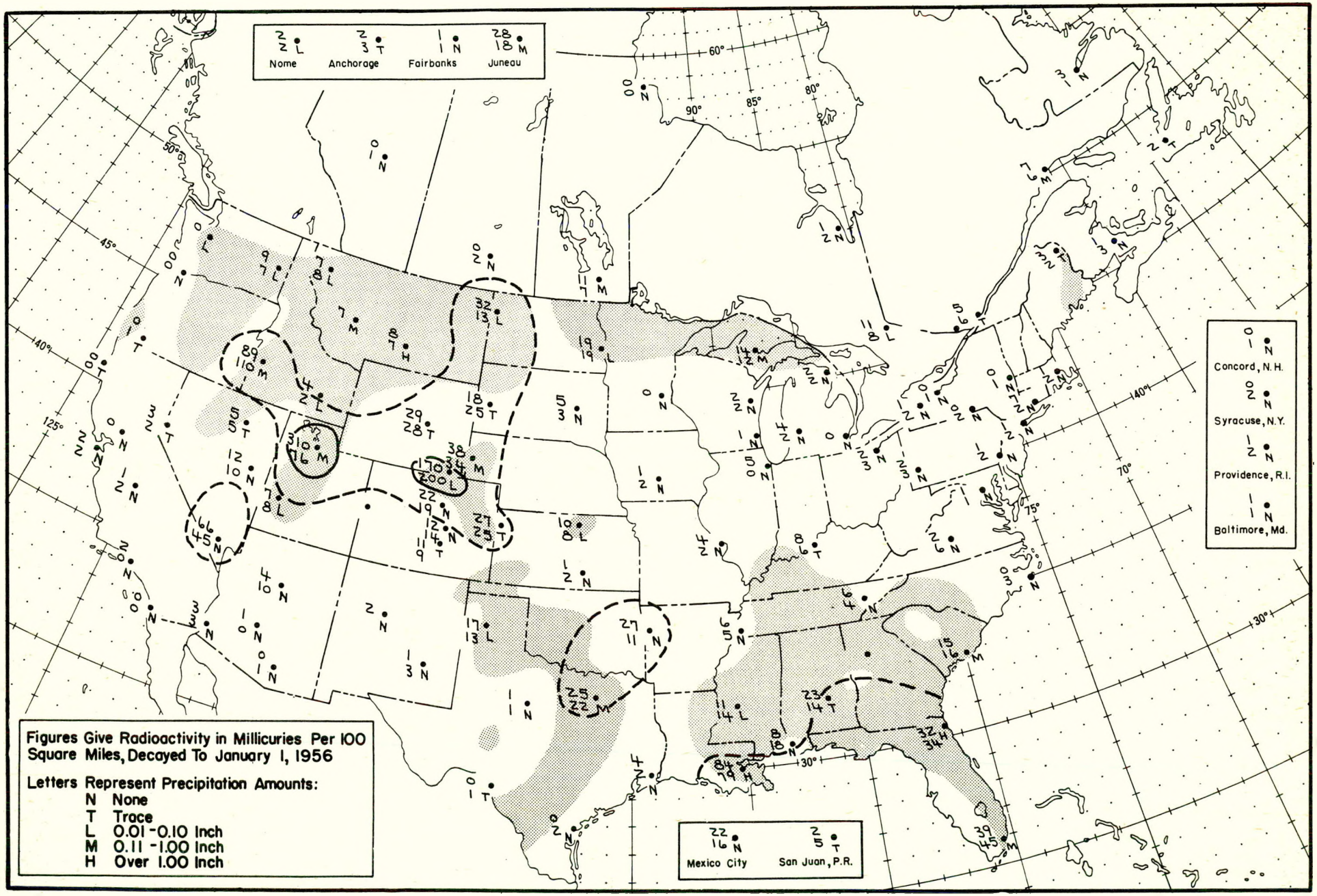

Figure A. 87 Radioactive fallout in the 24-hour period beginning 1230 G.C.T., May 15, 1955

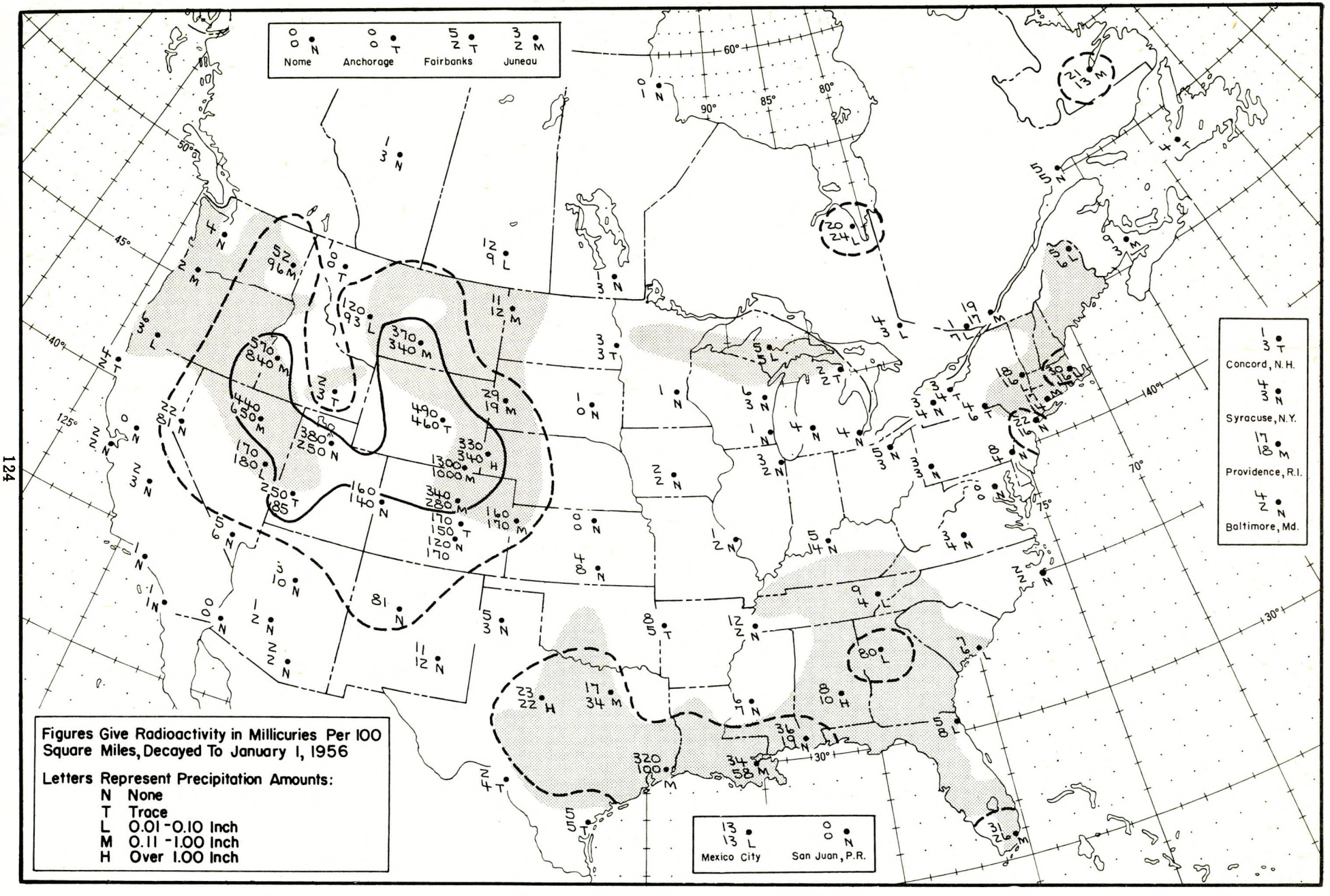

Figure A. 88 Radioactive fallout in the 24-hour period beginning 1230 G.C.T., May 16, 1955

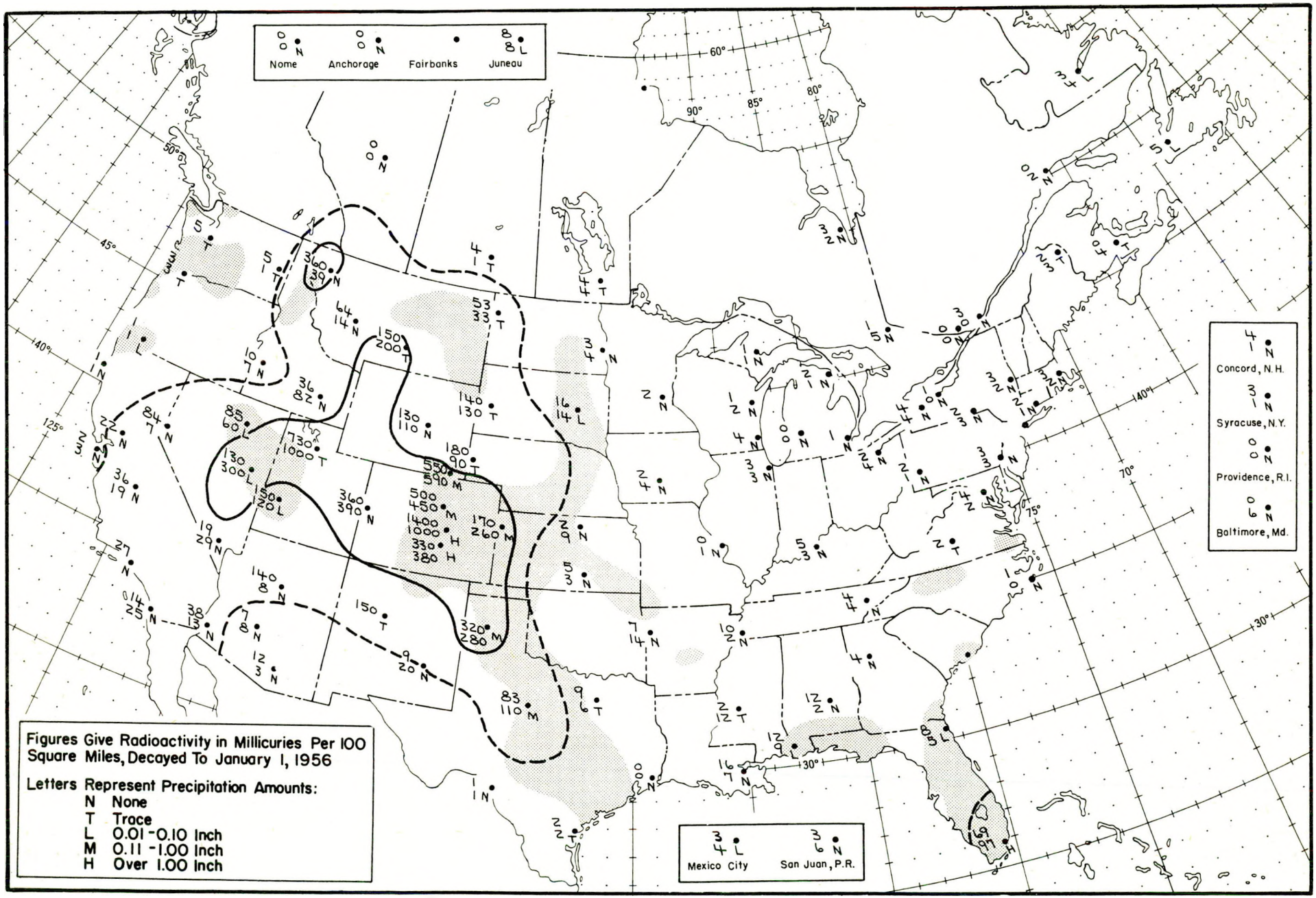

Figure A.89 Radioactive fallout in the 24-hour period beginning 1230 G.C.T., May 17, 1955

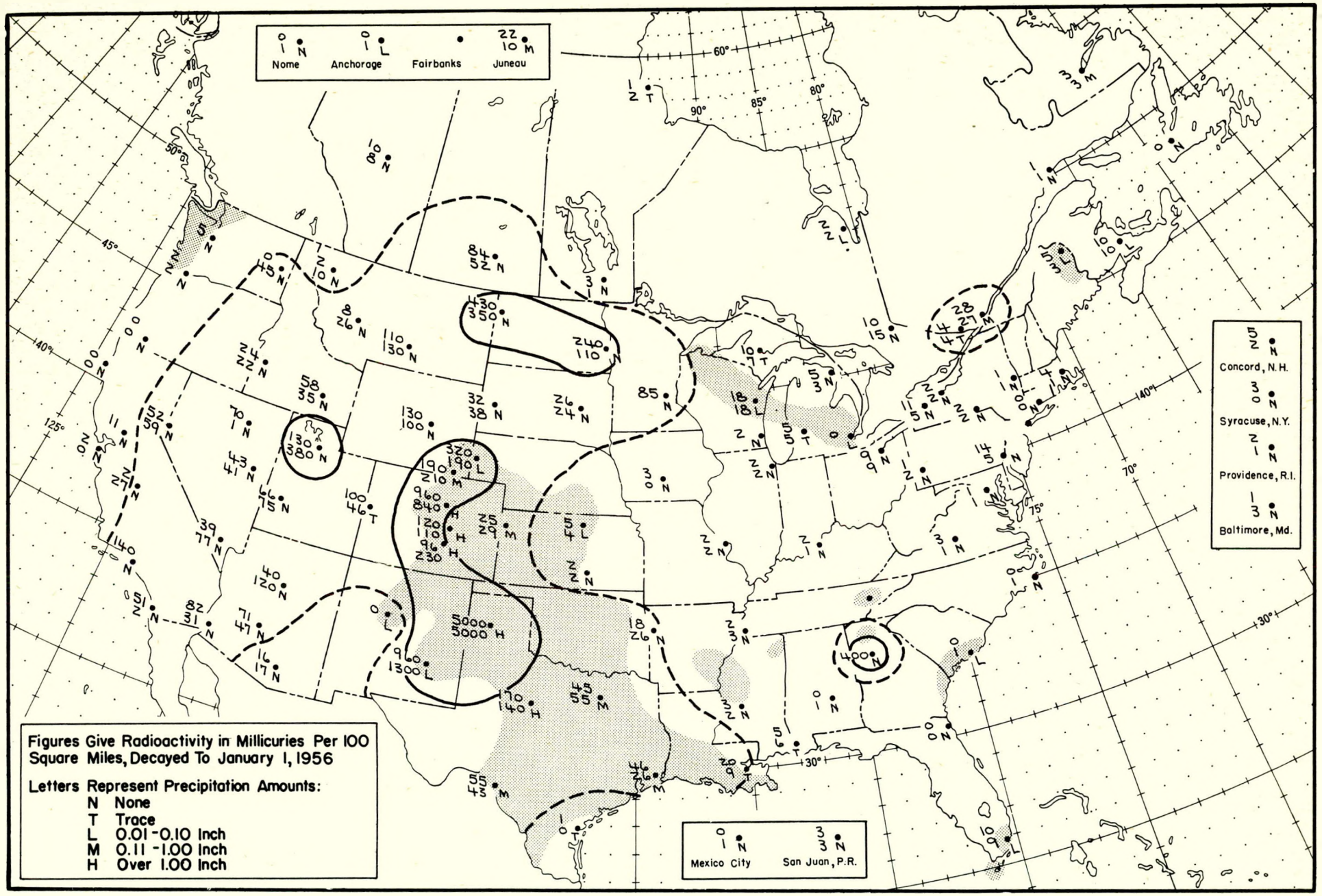

Figure A. 90 Radioactive fallout in the 24-hour period beginning 1230 G.C.T., May 18, 1955

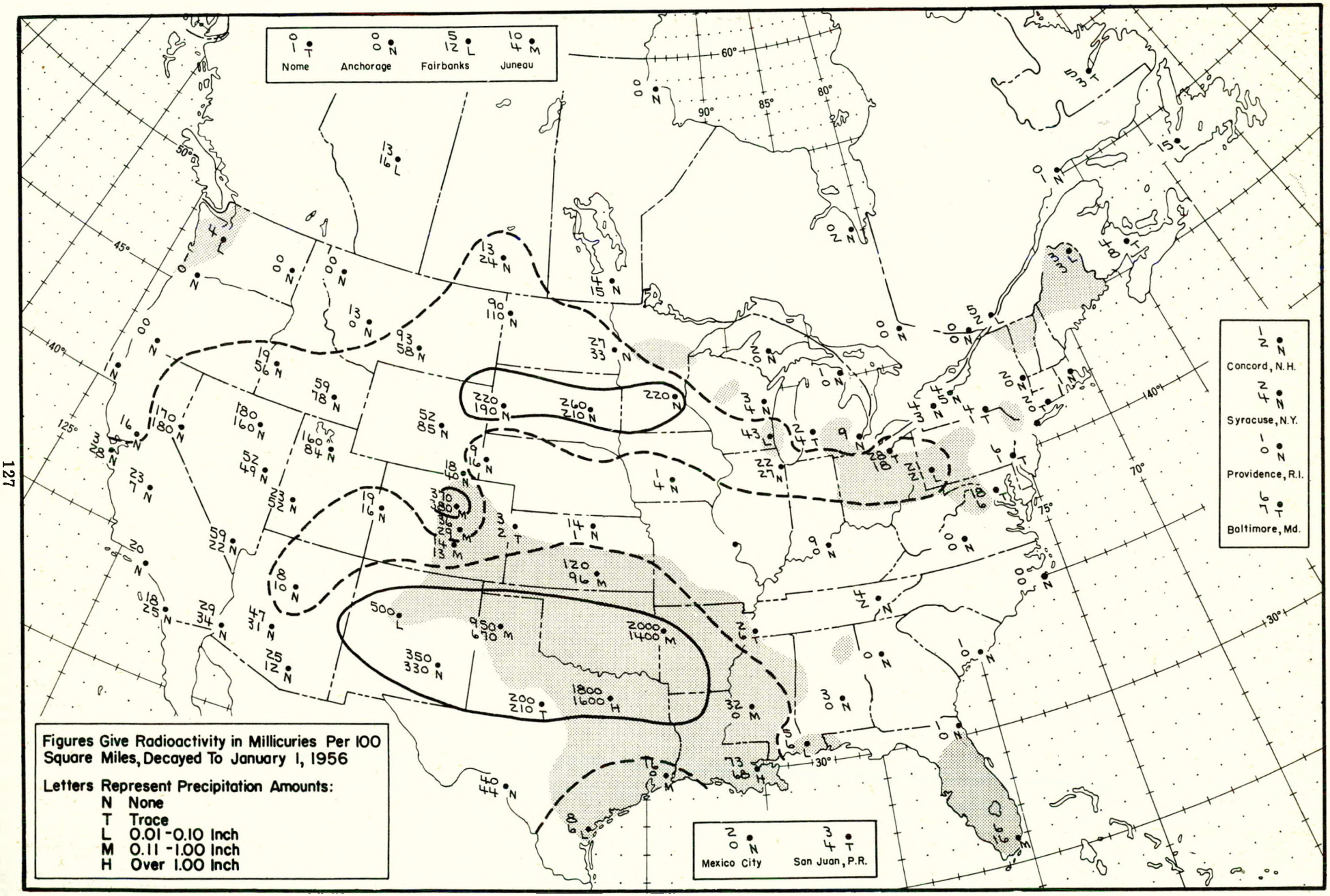

Figure A. 91 Radioactive fallout in the 24-hour period beginning 1230 G.C.T., May 19, 1955

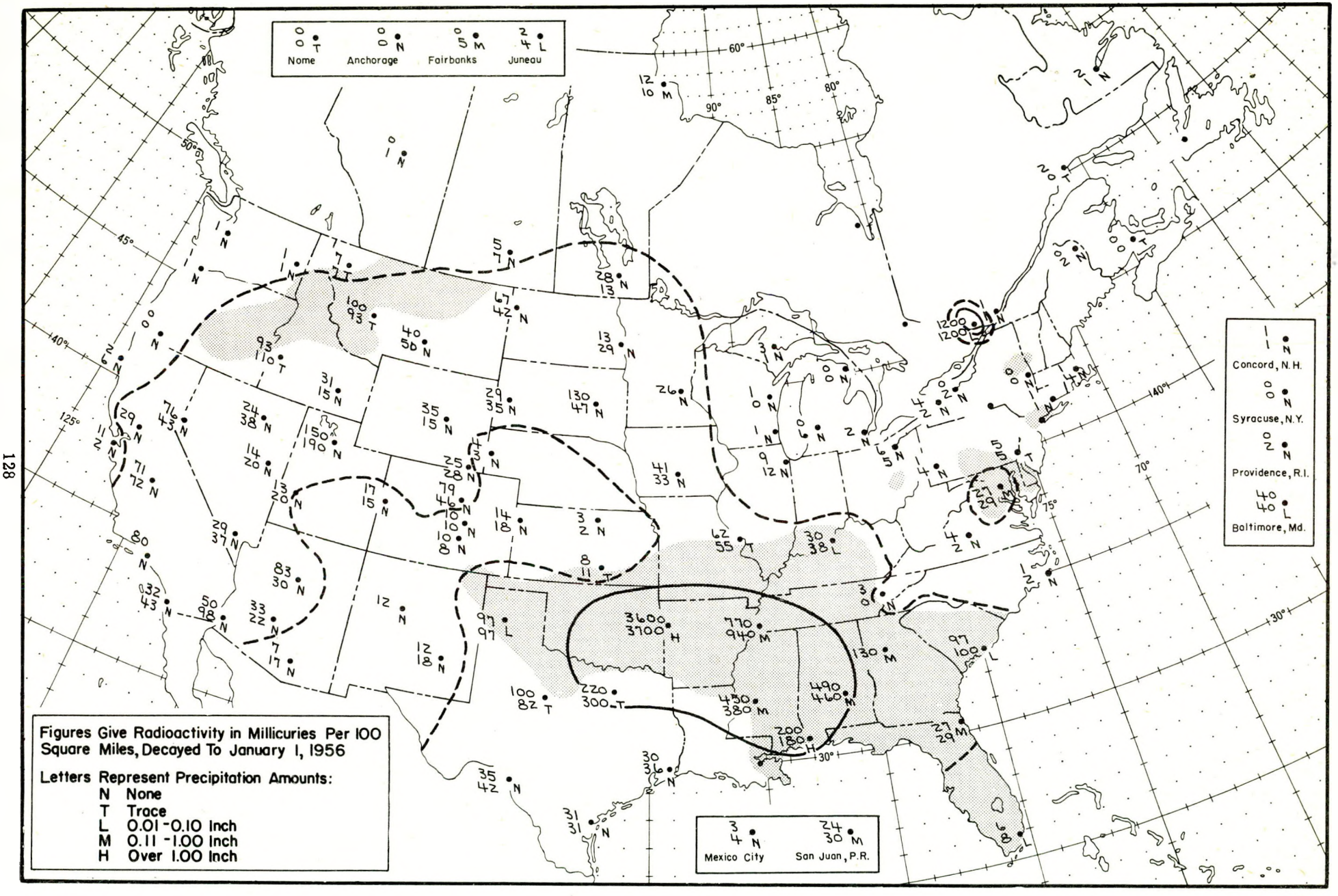

Figure A. 92 Radioactive fallout in the 24-hour period beginning 1230 G.C.T., May 20, 1955